

NATIONAL CENTRE FOR NUCLEAR RESEARCH

DOCTORAL THESIS

**Next-to-eikonal corrections in the
Color Glass Condensate**

Author:
Arantxa TYMOWSKA

Supervisor:
Tolga ALTINOLUK

*A thesis submitted in fulfillment of the requirements
for the degree of Doctor of Philosophy*

in the

BP2



May 16, 2023

Declaration of Authorship

I, Arantxa TYMOWSKA, declare that this thesis titled, "Next-to-eikonal corrections in the Color Glass Condensate" and the work presented in it are my own. I confirm that:

- This work was done wholly or mainly while in candidature for a research degree at the National Centre for Nuclear Research.
- Where any part of this thesis has previously been submitted for a degree or any other qualification at the National Centre for Nuclear Research or any other institution, this has been clearly stated.
- Where I have consulted the published work of others, this is always clearly attributed.
- Where I have quoted from the work of others, the source is always given. With the exception of such quotations, this thesis is entirely my own work.
- I have acknowledged all main sources of help.
- Where the thesis is based on work done by myself jointly with others, I have made clear exactly what was done by others and what I have contributed myself.

Signed:

Date:

NATIONAL CENTRE FOR NUCLEAR RESEARCH

Abstract

Next-to-eikonal corrections in the Color Glass Condensate

Arantxa TYMOWSKA

The high energy limit of Quantum Chromodynamics (QCD), in particular the Color Glass Condensate (CGC) effective theory is the framework used throughout this thesis. In CGC one of the most commonly used approximations is the eikonal approximation. This approximation amounts to taking into account only the contributions that are leading in energy, while systematically disregarding the energy suppressed corrections. The eikonal approximation is based on three assumptions. The first one takes the target as an infinitely thin 'shockwave', the second one is taking into consideration only the leading component of the background field, and, the third assumption is to disregard the dynamics of the target. The eikonal approximation is a very reliable one, specially in the high energy limits such as the energies reached at the Large Hadron Collider (LHC). However, when considering other experiments such as Relativistic Heavy Ion Collider (RHIC) or the future Electron Ion Collider (EIC), the scattering energies are lower compared to LHC.

The main goal of this work is, therefore, to provide the basis needed to compute the corrections to the eikonal approximation. These corrections are suppressed in energy with respect to the eikonal limit. This is the main motivation for the computation of such corrections, since the results obtained at this level of accuracy are expected to provide better precision for the phenomenology at the RHIC and EIC experiments. In order to obtain these corrections we relax the aforementioned eikonal assumptions.

After laying the basis of CGC and computing the Wilson line at the eikonal accuracy, the quark propagator at next-to-eikonal (NEik) accuracy in the gluon background field is computed. With the use of this propagator we compute different observables. The first observable computed is the forward quark-nucleus scattering at NEik accuracy, relaxing two out of the three assumptions in the eikonal approximation while the dynamics of the target is still neglected.

Finally, we relax the third assumption and take into account the dynamics of the target, thus obtaining the quark propagator at the full NEik accuracy in the gluon background field. With this propagator we compute two more observables, the DIS dijet production and the photon + jet production at NEik accuracy.

Streszczenie

Next-to-eikonal corrections in the Color Glass Condensate

Arantxa TYMOWSKA

Wysokoenergetyczny limit chromodynamiki kwantowej (QCD), a w szczególności efektywna teoria "Color Glass Condensate" (CGC), stanowią ramy teoretyczne wykorzystane w tej pracy. W CGC jednym z najczęściej stosowanych przybliżeń jest przybliżenie eikonalne. Polega ono na uwzględnieniu tylko tych składników, które są wiodące względem energii, podczas gdy wyrazy wyższego rzędu są systematycznie pomijane. Przybliżenie eikonalne opiera się na trzech założeniach. Pierwsze założenie zakłada, że tarcza jest nieskończenie cienką "falą uderzeniową", drugie założenie polega na uwzględnieniu tylko wiodącej składowej pola gluonowego tła, a trzecie założenie polega na zignorowaniu dynamiki jądra. Przybliżenie eikonalne jest bardzo dobrym przybliżeniem do opisu procesów rozproszeniowych, szczególnie w przypadku wysokich energii, takich jak te osiągnęte w Large Hadron Collider (LHC). Jednak, biorąc pod uwagę inne eksperymenty, takie jak prowadzone w Relativistic Heavy Ion Collider (RHIC) czy przyszły Electron Ion Collider (EIC), energie rozpraszania są niższe w porównaniu z LHC i efekty subeikonalne mogą być znaczące.

Głównym celem tej pracy jest przedstawianie formalizmu służącego do obliczania poprawek przybliżenia eikonalnego, oraz analiza procesów rozproszeniowych z ich uwzględnieniem. Te poprawki są tłumione energią w porównaniu z przybliżeniem eikonalnym. Przedstawienie wyników na tym poziomie dokładności jest główną motywacją tej pracy, ponieważ poprawiają one precyzję analiz fenomenologicznych do eksperymentów prowadzonych na RHIC i EIC. Aby uzyskać te poprawki, relaksujemy wcześniej wspomniane założenia przybliżenia eikonalnego.

Po przedstawieniu podstaw CGC i obliczeniu linii Wilsona z dokładnością eikonálną, obliczony zostaje propagator kwarków z dokładnością do następnego poziomu po eikonalnym (NEik) w tle pola gluonowego. Z wykorzystaniem tego propagatora obliczane są różne obserwowalne wielkości. Pierwszą obserwalną, którą obliczamy, jest przekrój czynny na rozpraszanie kwark-jądro na poziomie subeikonalnym, relaksując jednocześnie dwa z trzech założeń przybliżenia eikonalnego, podczas gdy dynamika tarczy wciąż jest pomijana.

Następnie, relaksujemy trzecie założenie i bierzemy pod uwagę dynamikę jądra, co pozwala na uzyskanie propagatora kwarkowego o pełnej dokładności NEik w polu tła gluonów. Z wykorzystaniem tego propagatora obliczamy jeszcze dwie obserwable, produkcję dwóch strumieni jetów w procesie głęboko nieelastycznego rozpraszania (DIS dijet) oraz produkcję fotonu i jetu z dokładnością NEik.

Acknowledgements

First, I want to show my most sincere gratitude to my supervisor Tolga, for helping me throughout all my PhD. Since my first year as PhD student he helped me to navigate the world of theoretical physics and introduced me to the world of research with great patience and advice. I would also like to thank deeply Guillaume, Alina, Nestor and Cyrille. Guillaume for always having time to help me when I was stuck in my calculations and solving my problems with an ease and speed most physicist only dream of, Alina for helping me during the long calculations of our joint papers and always being willing to lend a hand in anything I asked her. To Nestor for inviting me to stay and work alongside him in Santiago for two great months, where I learnt a lot and left inspired to continue in this world of research. And finally to Cyrille for inviting me to stay in Paris and work closely with him for a month, where I accidentally fell in love with the city, and where he was always ready to help me in any way he could.

Personalmente también quiero agradecerle estos años a mucha gente. Primero, a mi padre, sin él no estaría haciendo un doctorado ni hubiese llegado a ser física siquiera y eso es algo que no se puede agradecer con palabras. Desde pequeña ha sido y siempre será mi mejor amigo y mayor inspiración en la vida, y hoy soy física gracias a él y a las incontables discusiones sobre el "perpetuum mobile" y similares que tuvimos desde el día que entre a la carrera. También quiero agradecerle a mi menchu, por darme fuerza todos los días y un apoyo que no se puede describir ni agradecer en una sólo tesis, tendría que hacer 10 doctorados con sus 10 tesis para dedicárselas y acercarme un poco a expresar la gratitud y amor que siento.

Quiero también agradecer esta tesis a todas las personas que durante estos cuatro años han estado allí para mi y se han preocupado por mi y por mi aventura con la física. En primer lugar a mi hermana Sara, que pese a ser lingüista, me ha apoyado toda mi vida en esto de la física y ha estado allí en los peores momentos de julio en el centro de Murcia a 45 grados apoyándome en los exámenes, para poder ponerse la mayor cara de hermana orgullosa durante mis pequeños éxitos. Gracias Sara, porque pese a nuestros menos, que los hay, son muchos y pesan más nuestros más. Quiero agradecerle también estos años de aguantarme con mis estreses y mis quejas al físico que ha estado ya una década a mi lado, PJ, tus palabras de ánimo, y aún más las broncas, me han ayudado mucho a sobrellevar estos años. También quiero agradecerle al DIS2022 por haber conocido a Pedro, una de las personas que más me ha ayudado este tramo final del doctorado y sin el cual no hubiese podido afrontar muchos de los estresantes días de este último año, gracias por siempre querer lo mejor para mi y sacrificar tanto tu tiempo, y paciencia, en mí. A mi prima Kasia, que ha compartido estos años esta aventura conmigo y me ha sabido entender y aconsejar siempre, gracias por siempre mostrarme el orgullo que sientes por mi y que sabes que es recíproco. Quiero agradecerle a mi suegra Carmen todo el cariño y apoyo que me ha dado durante estos años, tanto que me he llevado alguna bronca por publicar un artículo y no avisarle. Finalmente, y no por ello menos importante, quiero darle las gracias también a toda mi familia, y en especial a mi madre, por todo el apoyo y cariño.

Contents

Declaration of Authorship	iii
Abstract	v
Streszczenie	vii
Acknowledgements	ix
1 Introduction to QCD	1
1.1 The QCD Lagrangian	1
1.2 Running coupling	3
1.3 Deep Inelastic Scattering	4
1.4 The DGLAP evolution equation	8
1.5 Gluon saturation	11
1.6 The McLerran-Venugopalan model	13
1.7 The Color Glass Condensate	15
2 Eikonal approximation and power counting beyond eikonal accuracy	17
2.1 The Eikonal approximation in physics	17
2.2 Eikonal approximation in Color Glass Condensate	18
2.3 Derivation of the quark propagator at eikonal accuracy	19
2.4 Power counting beyond the eikonal approximation	23
2.4.1 Scaling of the background field	23
2.4.2 Scaling of derivatives	24
2.4.3 Scaling of the width of the target	24
2.4.4 Eikonal and NEik contributions in propagators	25
3 NEik corrections: effects of finite width and transverse background field	27
3.1 Finite width effects	28
3.2 Including the interactions with the transverse component of the back- ground field	33
3.3 Quark propagator at next-to-eikonal accuracy	36
3.4 Forward quark-nucleus scattering	38
3.4.1 Quark-target scattering amplitude from the LSZ reduction	38
3.4.2 Unpolarized partonic cross section	41
3.4.3 Quark helicity asymmetry	44
3.5 Conclusions	46
4 DIS dijet production at NEik accuracy: including dynamics of the target	47
4.1 Reduction formula for the S-matrix and integrated propagators	48
4.2 Propagators at full NEik accuracy	50
4.2.1 Propagators from before to after the medium at NEik accuracy	51
4.2.2 Propagators from inside to after the medium at Eik accuracy	52
4.3 DIS-dijet production at NEik accuracy	54

4.3.1	Photon splitting inside the medium	55
4.3.2	Photon splitting before the medium	57
4.3.3	NEik DIS dijet production cross-section	70
4.4	Conclusions	82
5	Photon + jet production at next-to-eikonal accuracy	85
5.1	Quark propagators at NEik accuracy	85
5.2	S-matrix element	87
5.2.1	Photon emission after the medium	87
5.2.2	Photon emission before the medium	90
5.2.3	Photon emission inside the medium	93
5.2.4	Final expressions for the S-matrix	95
5.3	Photon + jet partonic cross-section	96
5.3.1	Generalized eikonal contribution to the cross-section	96
5.3.2	Explicit NEik contribution to the cross-section	98
5.4	Conclusions	102
6	Conclusions	105
	Bibliography	107
A	Light-Cone coordinates	111
B	Derivation of final expressions for the S-matrix in Photon+jet production	113

*Para mi compañero de vida Menchu y para el mejor amigo que
pude desear tener, y que coincidió con llamarse Papá*

1

Introduction to QCD

Before the introduction of the core of this thesis let us start with some important notions of quantum chromodynamics (QCD). This theory was first developed in the 1970s when the world of physics was trying to generalize the quantum theory of electrodynamics (QED) so we will see some characteristics of those theories being compared in this chapter. QCD is the theory that describes the behavior of strongly interacting particles that compose the hadrons. This chapter will lay the basics we need in order to study high energy collisions in the small- x regime, which will be the main focus of this thesis.

1.1 The QCD Lagrangian

Quantum chromodynamics is a non-Abelian gauge theory based on the symmetry transformation group $SU(N_c)$ with $N_c = 3$, as opposed to QED where we have an abelian gauge theory with the $U(1)$ symmetry group. What these theories do have in common is that their fundamental degrees of freedom are spin-1/2 particles and both have massless vector bosons with spin 1, photons for QED and gluons for QCD. In the case of QCD, the elementary massive particles are called quarks with their corresponding anti-particles called antiquarks. The fundamental representation of the $SU(3)$ group is the set of three dimensional matrices U that satisfy the conditions of unitarity, and where

$$\det(U) = 1.$$

In order to have a physical theory emerging from this symmetry group, one acts on some quantum fields which are the quark fields. The Lagrangian that remains unchanged while performing the $SU(3)$ transformations on these fields is the classical QCD Lagrangian and it is given by

$$\mathcal{L}_{QCD} = \bar{q}i(\gamma^\mu \mathcal{D}_\mu - m)q - \frac{1}{4}(F_{\mu\nu}^a)^2. \quad (1.1)$$

The first term with the quark and antiquark fields (q, \bar{q}) is the kinetic term. These quarks have six different flavors $q=u,d,s,c,b,t$. Each of these different quarks has a different quark mass associated to it. The kinetic term contains the covariant derivative

$$D_\mu = \partial_\mu + ig_s T^a A_{a\mu}. \quad (1.2)$$

The first term is the partial derivative and the second term is the needed addition in order to make the Lagrangian $SU(3)$ invariant (alongside with $\frac{1}{4}(F_{\mu\nu}^a)^2$). In this second term, there appears the new gauge field $A_{a\mu}$ representing the gluons, where the index a is the color index that takes values from 1 to $N_c^2 - 1 = 8$. Furthermore, g_s is the QCD coupling constant and T^a is the $SU(3)$ generator. Finally, the gluon field strength tensor is given by

$$F_{\mu\nu}^a = \partial_\mu A_\nu^a - \partial_\nu A_\mu^a + g_s f^{abc} A_\mu^b A_\nu^c \quad (1.3)$$

where f^{abc} are the structure constants that determine the Lie algebra of the group and they are the generators of the adjoint representation of $SU(3)$, the one defining gluons. When comparing QCD to QED one finds a crucial difference, since the mediating particle in QCD carries a color charge, as opposed to the electrically neutral photon. This property allows a shift in the color of a quark when it emits or absorbs a gluon (Fig.(1.1))

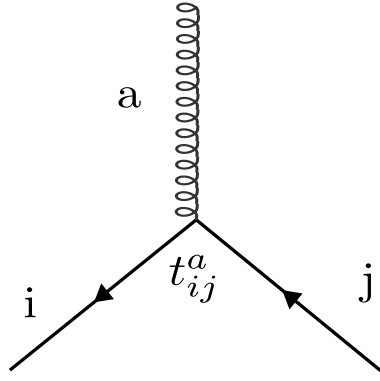


FIGURE 1.1: Representation of the color charge flow in a vertex through the emission/absorption of a gluon

This feature arises from the fact that QCD is a non-abelian theory, which is also responsible for the fact that gluons are allowed to self-interact with each other, unlike photons in QED. This self-interactions give rise to 3-gluon and 4-gluon vertices described by

$$g_s(\partial_\mu A_\nu^a - \partial_\nu A_\mu^a) f^{abc} A^{b\mu} A^{c\nu} \quad (1.4)$$

$$g_s^2 f^{abc} A^{b\mu} A^{c\nu} f^{ab'c'} A_\mu^{b'} A_\nu^{c'}, \quad (1.5)$$

where Eq.(1.4) corresponds to the 3-gluon vertex as represented in Fig.1.2 and Eq.(1.5) to the 4-gluon vertex, as represented in Fig.1.3.

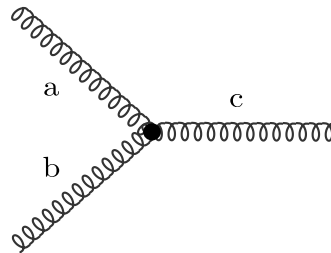


FIGURE 1.2: Representation of the self-interaction of three gluons

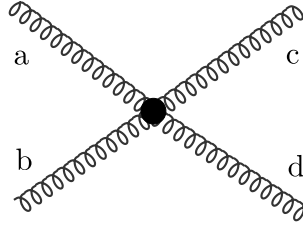


FIGURE 1.3: Representation of the self-interaction of four gluons

1.2 Running coupling

In the previous section g_s was introduced as a constant, but this statement is not complete and one can go beyond that to improve it. In this section the importance of g_s , or $\alpha_s = g_s^2/4\pi$ is discussed. In particular, we discuss how it changes with increasing energy. This is due to QCD being a renormalizable theory which makes the coupling constant, dependent on the momentum scale Q , or energy scale, of the interaction. The renormalization of the theory is determined by the renormalization scale μ_r , which helps in separating the high energy from the low energy regime, allowing one to treat these two regimes differently. However, this renormalization scale is artificial and as such one needs the physical observables to be independent of it, which is why one has to impose that the coupling constant depends on it, $g_s(\mu_r)$. In order to have a theory that leaves the physical observables invariant, it has to be described by a set of differential equations that depend on μ_r and are known as renormalization group equations (RGE) that encode the behavior of the β -function.

The solution of the RGE at first order is

$$\alpha_s(Q^2) = \frac{\alpha_s(\mu_r^2)}{1 + \alpha_s(\mu_r^2)\beta_0 \ln(Q^2/\mu_r^2)}. \quad (1.6)$$

One of the main differences between Abelian and non-Abelian theories lies precisely in the β -function.

In QED, for example, $\beta_0^{QED} = -4/3$ setting the behavior of the coupling in such a way that it goes towards zero when $\mu_r \rightarrow 0$ and towards infinity when $\mu_r \rightarrow \infty$. This implies that at high energies, or smaller distances, the attraction is stronger. However, for non-Abelian theories, such as QCD, one has

$$\beta_0 = \frac{11N_c - 2N_f}{12\pi} \quad (1.7)$$

and in the case of QCD, where $N_c = 3$ and $N_f = 6$, the coefficient is positive. This leads to a behavior of the coupling with μ_r such that it goes toward 0 at infinity and rises when $\mu_r \rightarrow 0$ (see figure Fig.1.4). This implies that when particles get closer and closer, the color attraction between them diminishes, that can be described as *asymptotic freedom* [1, 2]. To show an intuitive picture of this property one may consider two particles connected by a rubber band so that when you pull the particles apart, the band counteracts on this by increasing its tension. This is a simplified description of what is called in QCD *confinement*, which is the property that maintains the quarks bound to each other forming hadrons so that there are no 'free' quarks. Bringing back the previous example this would mean that the harder you pull the particles away, the harder gets the resistance to this action. Furthermore, if one pulls

too far away the quarks, this band would break in two pieces but the quarks do not appear free, instead, the gluon binding energy would break in two so we end up with two pairs of quarks coming from the original single pair.

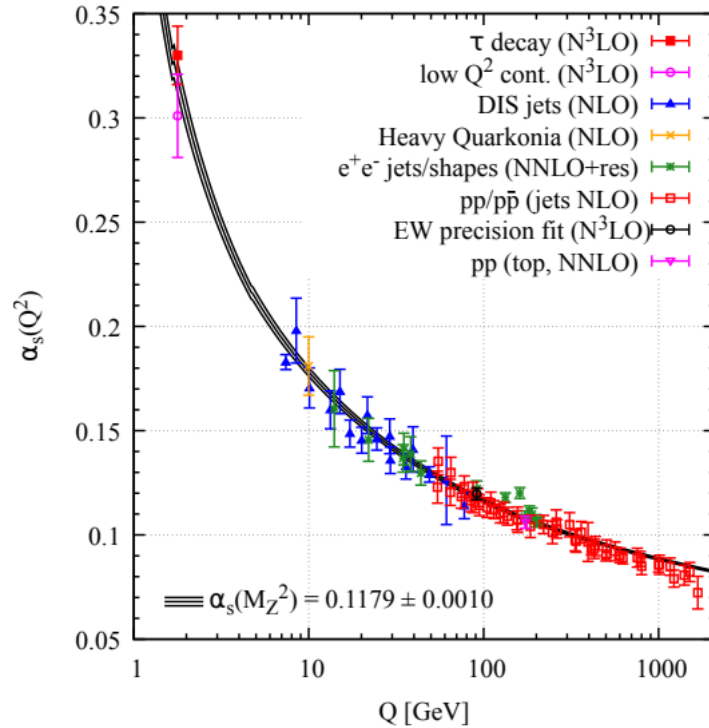


FIGURE 1.4: Measurements of α_s as a function of the energy scale Q . This figure has been taken from the Particle Data Group collaboration in [3]

A consequence of this renormalization mechanism at an energy scale that referred to as $\Lambda_{QCD} \approx 200$ MeV, the coupling constant α_s becomes larger than one and perturbation theory techniques can no longer be applied. This raises a problem since the energies at which perturbative techniques are not valid are energies very common in experiments. However the previously mentioned asymptotic freedom allows us to divide QCD in two frameworks, the first satisfying $\mu_r > \Lambda_{QCD}$ where one is still in the perturbative regime of QCD ($pQCD$) effectively, and a part that is not possible to apply these methods, relying then on experiments in order to extract the information. This plants the basis for factorization schemes, that are mainly applied in DIS processes.

1.3 Deep Inelastic Scattering

QCD is a theory that can be studied in two regimes: a perturbative one ($pQCD$) where we can use standard field theory methods, and a non-perturbative regime where these methods cannot be used to compute processes. However, as previously mentioned in section 1.2, real experiments are not restricted to hard processes, therefore, we need a reasonable combination of both regimes. This is how *factorization* is introduced and a scale is used to separate the regimes by energy. This scale is arbitrary so one must demand that the computation of observables does not depend on this scale.

However, in order to constrain the models that calculate the non-perturbative regime, we need experimental information from the structure of the hadron. For this reason, *Deep inelastic scattering (DIS)* is such an important process since experimental studies at the Hadron-Electron Ring Accelerator (HERA) have led to successfully probe the content of a hadron. In this process, a lepton with four momenta k^μ , mainly an electron, collides with a hadron with four-momentum P^μ and this interaction can be described as an exchange of a virtual vector boson, mainly photon, that carries a four-momentum q^μ , as illustrated in Fig.1.5. The result of this collision is a lepton with a four-momentum k'^μ and several partons.

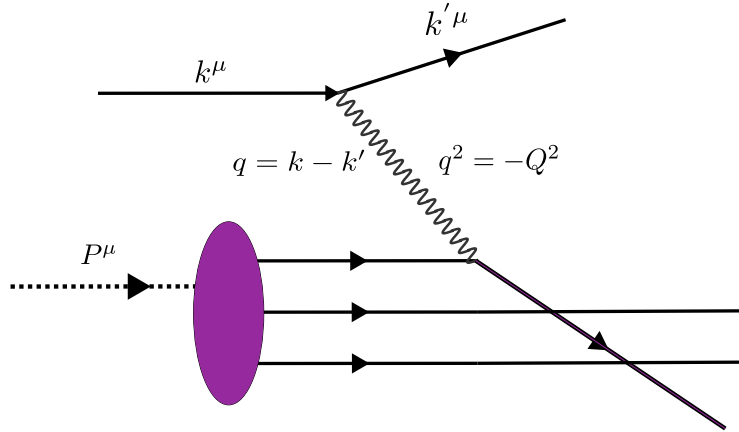


FIGURE 1.5: Representation of Deep Inelastic Scattering with a virtual photon probing the nucleus in the interaction with one parton

This process can be described by the following quantities that are Lorentz invariant

$$Q^2 = -q^2 \geq 0 \quad (1.8)$$

$$x = \frac{Q^2}{2P \cdot q} \quad (1.9)$$

$$y = \frac{P \cdot q}{P \cdot k} \quad (1.10)$$

where Q^2 is called the *virtuality* and in DIS this quantity exceeds the mass of the collided hadron. This is important because this virtuality also determines the spatial resolution scale of the probe, so for the energy range where deep inelastic scatterings occur, this allows us to resolve the partonic constituents of the hadron. Here x is also called the *Bjorken- x* variable, and it measures the inelasticity of the process. On the other hand y is the fractional energy loss of the incoming lepton.

Using the independent set of variables Q^2 and x , the DIS differential cross section can be written as

$$\frac{d^2\sigma}{dx dQ^2} = \frac{4\pi\alpha_s^2}{Q^4} \left[[1 + (1-y)^2]F_1(x, Q^2) + \frac{1-y}{x}[F_2(x, Q^2) - 2xF_1(x, Q^2)] \right] \quad (1.11)$$

where $F_1(x, Q^2), F_2(x, Q^2)$ are *structure functions* that are dimensionless and scalar, and they contain all the information about the initial hadron's structure. These structure functions were proposed to be Q^2 invariant at large energies by Bjorken [4] and

this was then experimentally confirmed by DIS experiments at SLAC-MIT [5].

$$\lim_{Q^2 \rightarrow \infty} F_{1,2}(x, Q^2) = F_{1,2}(x) \quad (1.12)$$

This is what is called Bjorken scaling and is one of the motivations that led to the formulation of the *parton model* [6] by Feynman, where the hadrons are seen in terms of point-like constituents. This means that the scattering in the DIS process does not occur with the proton or hadron as a whole, but with a parton inside of this hadron, as long as we restrict to the reference frame known as *Infinite Momentum Frame (IMF)* where we assume a very fast moving proton.

In this scenario, because of Lorentz time dilation, the interactions of the partons have large time scales compared to the interaction of the parton with the virtual photon, so that the partons look 'frozen' to the photon. For example, inside a hadron, a gluon cloud can fluctuate into a quark-antiquark pair, but the virtual photon would interact with one of these partons much faster than this recombination would happen. As a result, our 'probe' (the photon) sees the parton that it interacts with as if it was static. It is worth defining now the main differences among the constituents of a hadron, meaning the different types of partons we have: first we have *valence quarks* which are the quarks that usually compose the parent parton (3 valence quarks for the proton); secondly we have gluons that we already introduced in previous sections and they can be neglected at large values of x as valence quarks dominate that region, but they become more and more relevant as we approach the small- x region; finally we have sea quarks that form quark-antiquark pairs coming from a gluon.

Taking all of the above in consideration, we take the DIS process as the absorption of the virtual photon by one of the partons, where this parton carries just a fraction of the momentum of the hadron which is denoted by $p = \xi P$, with ξ the Bjorken- x assuming that the parton is on mass-shell. Now one can interpret the Bjorken- x as the momentum fraction that the struck quark carries from the initial parent hadron, so we work in the *quark parton model (QPM)* [7] where one also assumes the interactions among the partons are negligible when we consider short distances. The latter occurs when the time scales of the interactions among partons are much larger than the time scale of the scattering, as we previously explained for the struck parton to appear temporarily 'free'.

In the QPM we can use the factorisation in order to separate a process that contains hadrons, the hard interaction from the hadron content. This allows us to separate the perturbative interaction part (that we are able to compute) from the non-perturbative part, that is the hadron content. Since the last part is non computable, we need a parton density function in order to describe it, this gives us the probability to find the parton with a given momentum fraction ξ in the initial parent hadron, this probability is also known as the *parton distribution function (PDF)* represented by $f_i(\xi, Q^2)$ and it should be extracted from experiment. The number of quarks of a given flavour i and momentum fraction from ξ to $\xi + d\xi$ that one finds at a resolution Q^2 , is then $f_i(\xi, Q^2)d\xi$. With these ingredients the DIS cross section can be described as:

$$\frac{d^2\sigma^{e^-p \rightarrow e^-X}}{dxdq^2} = \int_0^1 d\xi f_i(\xi, Q^2) \hat{\sigma}_i(\xi, Q^2) \quad (1.13)$$

where at first non-trivial order we have

$$\hat{\sigma}_i = \frac{4\pi\alpha_s^2}{Q^4} \frac{e_i^2}{2} \delta(x_{Bj} - \xi) [1 + (1-y)^2]. \quad (1.14)$$

This is the cross section of the photon-parton scattering and is computable in perturbation theory and where x is the Bjorken- x , ζ is our momentum fraction and e_i the electric charge of the quark i . Notice that we only take into account the coupling of the quarks since gluons have no electric charge. Now if we compare 1.11 and 1.13 we obtain the following relation between the structure functions

$$F_2 = 2xF_1 = \sum_i e_i^2 x f(x, Q^2) \quad (1.15)$$

which is referred to as the Callan-Gross relation [8]. Results at the SLAC-MIT experiment pushed to identify Feynman's partons as the previously postulated by Gell-Mann quarks, a big accomplishment for the parton model.

Finally, we have seen that this parton model although successful for a description of the DIS process, lacks of theoretical description of the insight of the hadron, which stems from the factorization phenomena as one cannot provide analytical information for the non-perturbative region. Now, another issue arrives when one moves towards the small- x regime (high energies) where a violation of the of the Bjorken scaling that we previously described, can be seen. In this regime the structure function F_2 increases and one can expect an increase in the partonic density of the proton. This behavior can be seen in Fig.1.6

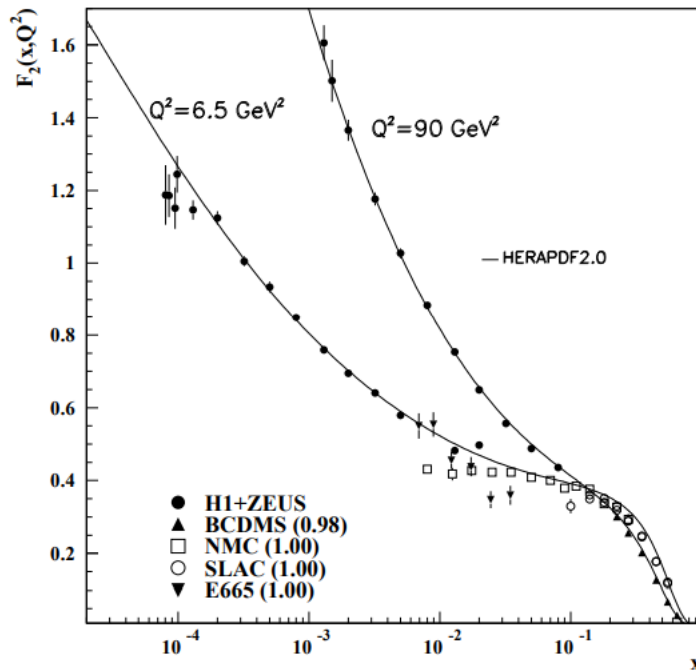


FIGURE 1.6: The proton structure function F_2 measured in DIS experiments with Bjorken scaling violation for values of Bjorken- x under 10^{-1} . This figure has been taken from the Particle Data Group collaboration in [9]

1.4 The DGLAP evolution equation

In the previous section we explained the QPM and the idea of separating the hard from soft parts by factorization, however this separation was not described rigorously. Due to the fact that we lack from taking all possible information into account, the parton model we described is only an approximation and we already saw in the previous section few of the problems we encounter within this model. One of these problems was the breakdown of Bjorken scaling for the structure functions which we face when going to larger energies, either when we go to small x and keep Q^2 fixed (Regge-Gribov limit) or to higher Q^2 and keep x fixed (Bjorken limit). The reason for this issue is precisely the lack of information we account for, since as for now we have only taken the interacting quarks into account and ignored corrections that come from the possible QCD interactions. Therefore, one can say that it is only the zeroth order of a perturbation expansion in α_s .

Introducing QCD corrections that come from the interaction among the partons gives us higher order computations, this is called next-to-leading order (NLO) in perturbation theory of QCD. It includes additional quantum fluctuations such as gluon emission before the interaction, interpreted as real corrections, and gluon fluctuation into itself as an emission-absorption, which is a virtual correction. These corrections can be seen in the figure below Fig.1.7. The data obtained from DIS processes becomes more and more sensitive to these corrections as one moves towards smaller x values where one no longer sees only the valence quarks but, as mentoined in the previous section, the sea quarks' presence is more and more noticeable.

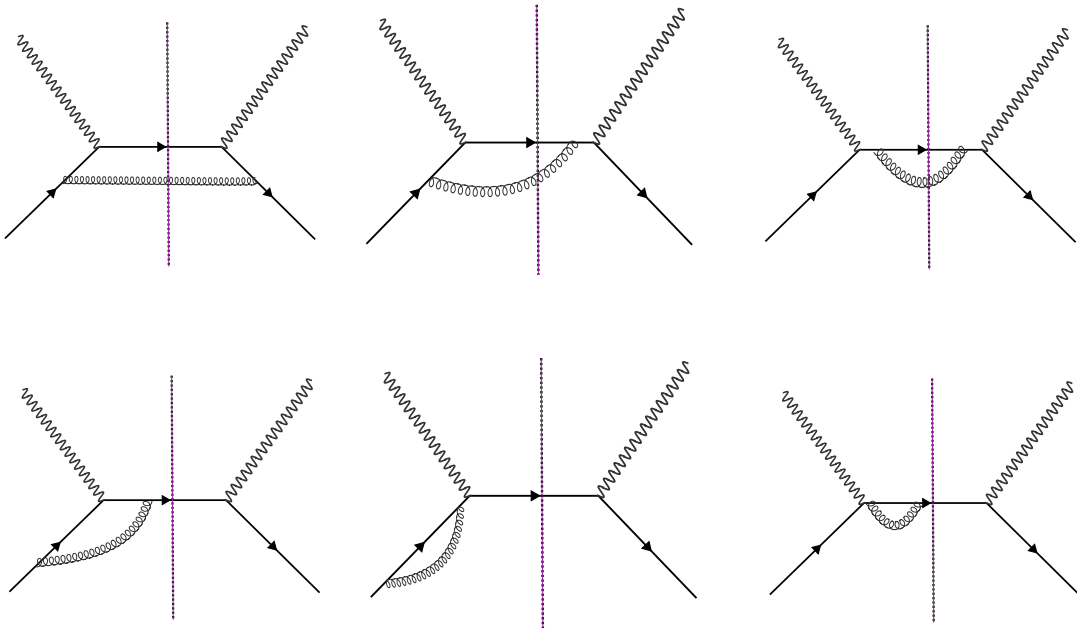


FIGURE 1.7: First order corrections to the Deep Inelastic Scattering process, with real correction on the upper line and virtual corrections in the lower line

Let us provide a simple picture on what happens in the nucleon at high energies to understand from a qualitative point of view why these corrections appear. Take first the nucleon as a bound state of valence quarks with gluon exchange between them and fluctuations that turn a quark into a gluon and a quark temporarily. However when probing this nucleon with the photon (for the case of DIS), one

needs to take into account the time and length scale of this photon, so it can resolve only the fluctuations that are larger and longer lived than the probe scales. Thus, for the Regge-Gribov limit, we can roughly interpret the x as the time resolution of the probe. Therefore, if one decreases its value, this photon is able to see shorter and shorter lived fluctuations that one needs to take into account as compared to lower energy values. On the other hand, for the Bjorken limit one has a higher space resolution of the probe (higher Q^2) allowing the photon to see a higher number of partons.

The corrections mentioned introduce, as discussed before, an artificial scale that needs to be taken care of in order to make our observables independent of this scale. This is done through RGEs that describe the evolution of the scale, and in our case we want to know the evolution of the PDFs as functions of the photon virtuality Q^2 . The RGEs that encode this behaviour are called the DGLAP evolution equations. They were proposed by Dokshitzer-Gribov-Lipatov-Altarelli-Parisi in [10–13]. The DGLAP evolution equation when perturbative schemes are valid ($Q^2 > \Lambda_{QCD}$) can be written as

$$\frac{\partial}{\partial \ln Q^2} \begin{pmatrix} \Sigma(x, Q^2) \\ G(x, Q^2) \end{pmatrix} = \frac{\alpha_s(Q^2)}{2\pi} \int_x^1 \frac{dz}{z} \begin{pmatrix} P_{qq}(z) & P_{qg}(z) \\ P_{gq}(z) & P_{gg}(z) \end{pmatrix} \times \begin{pmatrix} \Sigma(x/z, Q^2) \\ G(x/z, Q^2) \end{pmatrix} \quad (1.16)$$

where the sea quarks PDF are given by $\Sigma(x, Q^2) = f_q(x, Q^2) + f_{\bar{q}}(x, Q^2)$ and the gluon PDF by $G(x, Q^2)$. The $P_{ij}(z)$ are called the splitting functions and are represented diagrammatically in Fig. 1.8 at leading order (LO). They represent the probability functions for a parton i to emit a parton j carrying a z fraction of the longitudinal momentum from the parent parton. One needs to provide initial conditions in order to solve the DGLAP equation, meaning one needs an initial Q_0^2 that typically comes from experimental data and we can use in order to make predictions. Moving towards small- x values, an enhancement in the integrand of Eq.(1.16) by $P_{qg}, P_{gg} \sim 1/z$ appears. This translates as an enhancement of the evolution of the gluon PDFs with respect to the sea quark PDFs. This suggests that the small- x (or high energy) regime is dominated by gluons.

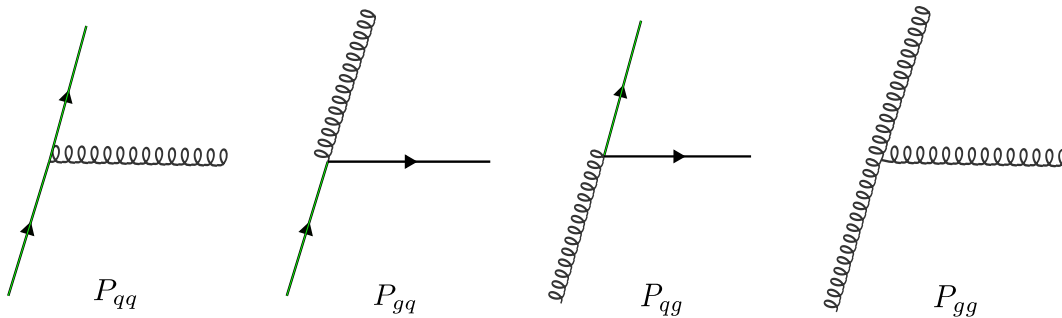


FIGURE 1.8: Representation for the diagrams of the four Leading Order splitting functions appearing in the DGLAP evolution equation

Let us now consider the probability of a gluon emitting another gluon with transverse¹ momentum k_{\perp} in the small- x and collinear ($|k_{\perp}| \rightarrow 0$) regimes.

¹Here, we introduce the light-coordinate notation that is explained in the Appendix A and will be used through the whole thesis.

$$P = \frac{\alpha_s N_c}{\pi} \frac{dx}{x} \frac{d^2 k_\perp}{k_\perp^2}, \quad (1.17)$$

we see that in this situation an additional logarithm of $1/x$ appears, and therefore this regime is referred to as the double logarithm approximation (DLA). One can interpret the solution to the DLA DGLAP [14] equation as a ladder diagram as shown in Fig.1.9. In this diagram one has on and on gluon emission that comes from another parent gluon. The transverse momentum of the gluons is ordered in such a way that it is lower as we go up in the ladder, while the longitudinal momentum goes in the opposite direction, with the highest value at the top of the ladder.

$$Q^2 \gg \mathbf{k}_n^2 \gg \mathbf{k}_{n-1}^2 \gg \dots \gg \mathbf{k}_1^2 \gg Q_0^2 \gg \Lambda_{QCD}^2 \quad (1.18)$$

$$P^+ \gg k_1^+ \gg k_2^+ \gg \dots \gg k_n^+ \gg k^+ \quad (1.19)$$

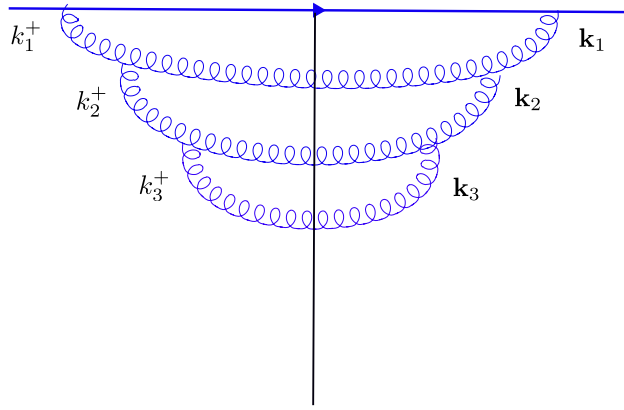


FIGURE 1.9: representation of the gluonic ladder-like diagram of one cascade

Taking into account everything that has been reviewed so far, one can write the probability of an ordered emission of a gluon in transverse and longitudinal momentum:

$$P_n = \int_{Q_0^2}^{Q^2} \frac{\bar{\alpha}_s d\mathbf{k}_1}{\mathbf{k}_1^2} \dots \int_{k_{n-1}}^{Q^2} \frac{\bar{\alpha}_s d\mathbf{k}_n}{\mathbf{k}_n^2} \int_{k^+}^{P^+} \frac{dk_1^+}{k_1^+} \dots \int_{k^+}^{k_{n-1}^+} \frac{dk_n^+}{k_n^+} \quad (1.20)$$

$$= \frac{1}{n!^2} \left[\bar{\alpha}_s \ln \frac{Q^2}{Q_0^2} \ln \frac{1}{x} \right]^n \quad (1.21)$$

with $\bar{\alpha}_s = \alpha_s N_c / \pi$.

Summing up the gluon emission probability for all orders of the cascade, one gets an estimation for the gluon distribution function

$$G(x, Q^2) \sim \sum_{n=0}^{\infty} P_n, \quad (1.22)$$

where one would get a prediction of the higher gluon distribution on lower x , making that region gluon dominated.

1.5 Gluon saturation

In the previous section we have seen the DGLAP evolution equations, which describe the dynamics of the hadrons for increasing value of Q^2 and keeping x fixed. However, in this section we are interested in the domain of small- x for fixed Q^2 , the Regge-Grobov limit, so we need a different picture from DGLAP. In this small- x limit, we resum powers of $\ln\frac{1}{x}$ instead of powers of $\ln Q^2$, which is the essential difference compared to DGLAP. The equation that is introduced in this section is therefore, an evolution in x instead of in Q^2 .

In this limit of small x and fixed Q^2 , the main mechanism for evolution is gluon radiation, and the gluonic content in a hadron evolve in this limit via cascades. Since we are only interested in resumming powers of $\ln\frac{1}{x}$, one only needs to impose strong ordering in the energy fractions of the radiated gluons. This ordering in the energy fraction is opposite when compared to the case of DGLAP, where the ordering is in transverse momenta. The transverse momenta in this limit is taken as a random walk in \mathbf{k}_\perp -space. The ordering in energy fractions is

$$x_1 \gg x_2 \dots \gg x_n, \quad (1.23)$$

x_1 being the energy fraction of the first emitted gluon, that then emits more gluons making the subsequent 'daughter' gluons have smaller energy fractions than the 'parent' gluon. This radiation process is described by the Balitsky-Fadin-Kuraev-Lipatov (BFKL) evolution equation ²:

$$\frac{\partial \phi(x, \mathbf{k}^2)}{\partial \ln(1/x)} = \frac{\alpha_s N_c}{\pi^2} \int \frac{d^2 \mathbf{q}}{(\mathbf{k} - \mathbf{q})} \left[\phi(x, \mathbf{q}^2) - \frac{\mathbf{k}^2}{2\mathbf{q}^2} \phi(x, \mathbf{k}^2) \right]. \quad (1.24)$$

that resums large logarithms of the type $\alpha_s \ln(1/x) \sim 1$. Here, $\phi(x, \mathbf{k}^2)$ is the *unintegrated gluon distribution (UGD)* that defines the number of gluons per unit phase space in a hadron with transverse momentum \mathbf{k} and longitudinal momentum fraction- x . The relation between the UGD and standard gluon PDF is

$$xG(x, Q^2) = \int_0^{Q^2} d^2 \mathbf{k} \phi(x, \mathbf{k}^2). \quad (1.25)$$

However in this equation, both PDFs and UGDs are non-perturbative quantities that can be extracted from data. Nevertheless, the solution of the BFKL equation (1.24), yields a gluon distribution that leads to a singular behavior in the small- x limit. The solution of Eq.(1.24) behaves as

$$\phi(x, \mathbf{k}^2) \sim x^{-\frac{4N_c \ln 2}{\pi} \alpha_s}. \quad (1.26)$$

which, violates unitarity. This is because the BFKL equation leads to an uninterrupted rise of the gluon distribution in the small- x limit and this violates unitarity. This is a fundamental requirement of any quantum field theory. The origin of this behavior is the fact that BFKL is a linear evolution equation.

Another problem the BFKL encounters is that in particle collisions experiments where the Froissart bound [18] is introduced, this bound is violated. The Froissart bound is given by

$$\sigma_{tot}(s) \leq \frac{1}{m_\pi^2} \ln^2 s. \quad (1.27)$$

²This evolution equation was first derived in [15, 16] and for a modern review of the derivation of the BFKL equations we refer to [17].

Here m_π is the pion mass and s the squared center of mass energy of the collision. The Froissart bound is a strong condition and it was derived in [17]. However, one can also derive this using the optical theorem and the black disk limit [14]. Using the BFKL solution, the small- x cross-section is roughly

$$\sigma_{tot}^{BFKL} \sim s^{\frac{4N_c \ln 2}{\pi} \alpha_s} \quad (1.28)$$

which violates the Froissart bound. This problem still remains to be solved in this saturated regime of QCD.

However, one can still restore unitarity by taking into account other evolution mechanisms beyond the gluon radiation. Consider a hadron with three valence quarks, each of these quarks yields the gluon cascade that was described previously. At one point, the gluon radiation from each of these cascades makes the nucleon to be densely packed, and the possible interactions between the gluons should be accounted for, as illustrated in Fig.1.10. The merging of the gluons from different cascades slows down the increase of the gluon distribution, it adds a term with negative coefficient and quadratic in gluon density to the BFKL equation. This effect is known as *gluon saturation*.

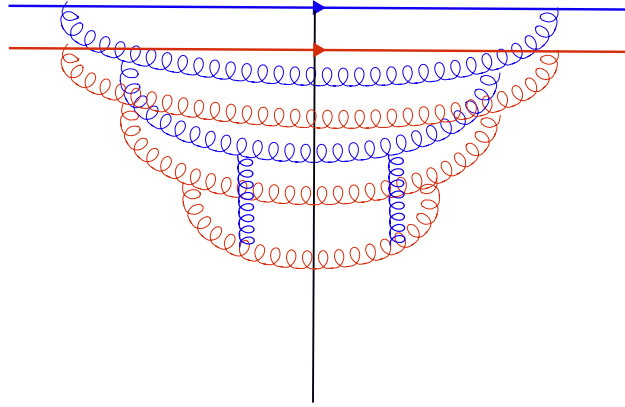


FIGURE 1.10: Interaction of the gluons coming from two different cascades, which ultimately gives rise to non-linear effects.

From the previous discussion one can see that at small- x BFKL cannot be used when non-linear effects become important. In DIS processes the virtual photon resolves only one parton at a time which makes the system dilute. The dilute scheme is not valid anymore at small- x and changes into a saturated system, where the recombination processes have to be taken into account, finally obtaining the non-linear terms. This description now agrees with the unitarity bound. This was first discussed in [19], where Gribov, Levin and Ryskin derived a non-linear evolution equation that is also an evolution in Q^2 . However, for our discussion it is sufficient to work with a schematic equation that contains the BFKL-like equation and looks like

$$\frac{\partial \phi(x, \mathbf{k})}{\partial \ln(1/x)} = a \frac{\partial^2 \phi}{\partial \mathbf{k}^2} + b \phi - c \alpha_s \phi^2, \quad (1.29)$$

where a, b and c are coefficients of order of unity and where we note that the new extra quadratic term has an extra power of α_s , thus the merging of two gluon cascades has two extra powers of the strong coupling g . Therefore, when the gluon density is of order $1/\alpha_s$, the non-linear terms should be taken into account.

In this regime, a boost in the longitudinal direction turns the nucleon into a ‘thin pancake’ due to Lorentz contraction. The probe, which is a virtual photon, does not resolve the gluon distribution in the longitudinal direction since it is larger than the ‘pancake’ nucleon. The probe sees only the number of gluons integrated over the z axis. Take then a nucleon of radius r_h , the surface density would be approximately

$$\rho_g \sim \frac{xG(x, \mathbf{k}^2)}{\pi r_h^2}, \quad (1.30)$$

which one should compare to the cross section for the recombination of two gluons. Since the probability of having two gluons recombine can be expressed as

$$\kappa = \rho_g \sigma_{gg} \sim \frac{xG(x, \mathbf{k}^2)}{\pi r_h^2} \frac{\alpha_s}{\mathbf{k}^2} \quad (1.31)$$

where the cross section for the recombination of two gluons is roughly $\sigma_{gg} \sim \alpha_s/\mathbf{k}^2$. In order to decide if it is large enough to account for that merging we apply the following condition $\rho_g \sigma_{gg} \geq 1$, and if this condition is met, recombination effects should be taken into account.

Let us now introduce a new quantity, the *saturation momentum* Q_s . This is defined in terms of the gluon distribution as

$$Q_s^2(x) \sim \frac{\alpha_s x G(x, Q_s^2)}{\pi r_h^2}. \quad (1.32)$$

and with this, the condition for taking into account the recombination effects can be rewritten as

$$\mathbf{k} \leq Q_s(x). \quad (1.33)$$

With this new quantity, Q_s , one can now separate the dilute regime from the saturated one. One can see in Fig.1.11 that $\ln Q_s^2$ separates the saturated regime from the dilute one.

Taking into account Eqs. (1.25) and (1.26), one can see that because $xG(x, Q_s^2) \sim x^{-\lambda}$, in Eq. (1.32) the saturation momentum depends on x as $Q_s^2 \sim x^{-\lambda}$ approximately, where $\lambda \approx 0.3$ [20, 21]. The discussion above can be also applied to a nucleus that contains A nucleons. Therefore, the UGD should be multiplied by A and taking into account that $\pi r_h^2 \sim A^{2/3}$. If one replaces in Q_s the factor $xG(x, Q_s^2) \sim x^{-\lambda}$. The saturation momentum would be proportional to

$$Q_{s,A}^2(x) \sim A^{1/3} \frac{1}{x^\lambda}. \quad (1.34)$$

The saturation momentum grows for larger nuclei because of the $A^{1/3}$ dependence. With all of the above in mind, we conclude this section with some numerical values. For RHIC kinematics (Gold nuclei at $x \approx 10^{-2}$) the saturation momentum is roughly $Q_s \approx 1.2\text{GeV}$ [22] while at LHC the value reaches $Q_s \approx 2\text{GeV}$ with $x \approx 10^{-4}$, where saturation effects would be even more present.

1.6 The McLerran-Venugopalan model

The main focus of this section is to introduce a model that sheds some light on the theoretical description of gluon saturation, the McLerran-Venugopalan (MV) model

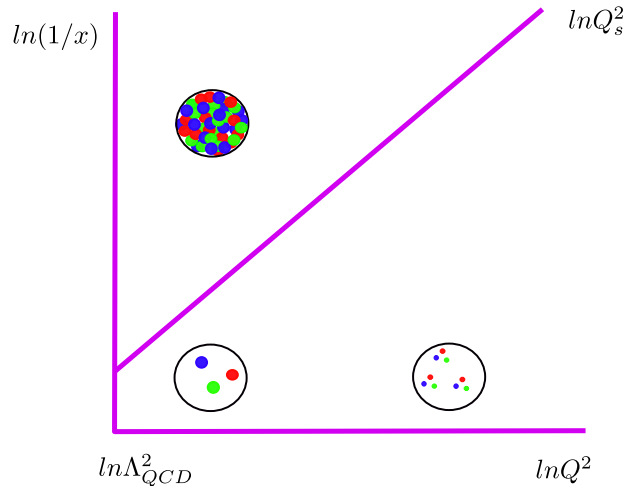


FIGURE 1.11: Evolution of the domains depending on x and Q^2 values. In the Bjorken limit with high Q^2 , we get the dilute regime, and in the Regge-Gribov limit with low- x , we get the saturated regime. Those regimes are separated by the saturation scale, Q_s .

[23–25]. As seen in previous sections, there are two main regions separated by their x values, the region of small- x where the saturation momentum is large and $Q_s^2 \gg \Lambda_{QCD}^2$. In this regime weak coupling methods can be used since $\alpha_s(Q_s) \ll 1$. The other region is a large- x region where weak coupling methods cannot be applied. The latter is also the region where the valence quarks dominate.

The MV model describes the parton content of a nucleus in the IMF, where the nucleus moves in the positive x_3 direction with a very large light-cone momentum $P^+ \gg \Lambda_{QCD}$. In the IMF the partons are separated as either *fast* or *slow* ones, based on their momentum fraction. The fast ones have a larger momentum fraction $p^+ = xP^+$ and are sharply localized around the light cone, roughly within the distance $\Delta x^- \sim 1/p^+$. The fast partons are also long-lived, with a mean lifetime $\Delta x^+ \propto p^+$. In the MV model these fast partons are quasi-static over the timescales relevant for the interaction and are identified with the valence quarks that act as radiative sources of the small- x gluons. Thus, we just need to specify the color current of the fast partons in order to compute the radiation of the slower gluons from the fast ones.

One needs to introduce a cutoff Λ^+ in the longitudinal momentum of the partons p^+ so that the fast partons with $p^+ > \Lambda^+$ can be replaced by a color current like

$$J_a^\mu(x) = \delta^{\mu+} \delta(x^-) \rho_a(\mathbf{x}), \quad (1.35)$$

with ρ_a the color charge density per unit of transverse area. The current, that sits at $x^- = 0$, has vanishing transverse component and only the + component in the light-cone coordinates is nonzero. As the current does not depend on x^+ , these new degrees of freedom are seen as static.

The slow partons, or gluons, that have $p^+ < \Lambda^+$ are described, as discussed in section 1.1, by the gauge fields A_a^μ and their action is the standard Yang-Mills action. The coupling between the fast and slow degrees of freedom is Eikonal and of the form

$$\int d^4x J_a^\mu(x) A_{\mu a}. \quad (1.36)$$

The action that encodes the dynamics of the gluon fields is

$$\mathcal{S} = \int d^4x \left(-\frac{1}{2} F_{\mu\nu}^a F^{\mu\nu,a} + J_\mu^a \mathcal{A}^{\mu,a} \right), \quad (1.37)$$

where the second term in Eq. (1.37) is identified as the interaction term and is the standard coupling between fields and sources defined in Eq. (1.36). The first term in Eq. (1.37) is the classical Yang-Mills action. Minimizing this action, the Yang-Mills equations of motion is obtained:

$$[D_\mu, F^{\mu\nu}] = J^{\nu,a} t^a = \delta^{\mu+} \rho^a(x^-, \mathbf{x}) t^a, \quad (1.38)$$

with ρ^a acting as the source of the classical gauge fields. In order to complete the theory, we have to find a model precisely for ρ^a , that describe the distribution of the fast partons. This distribution varies in time and so we can refer to the moment of the collision as just a snapshot of that distribution. Therefore, ρ^a should be seen as a stochastic variable that follows a statistical distribution $\mathcal{W}[\rho^a]$.

The MV model proposes a model for $\mathcal{W}[\rho^a]$ for the case of large nucleus. First, two color charges belonging to different nucleons are uncorrelated. In the MV model one assumes at two distinct points in the transverse plane, the values of the color charge densities are also uncorrelated. Secondly, take a tube in the longitudinal direction with cross section $d^2\mathbf{x}$ so that at one point \mathbf{x} , the amount $\rho_a(\mathbf{x})d^2\mathbf{x}$ is made up of all the color charges in that tube. These charges are also uncorrelated and random, and in a large nucleus one would have a large number of them ($\propto A^{1/3}$) so that ρ_a is an incoherent sum of many random variables. The statistical distribution for $\rho_a(\mathbf{x})$ is a Gaussian distribution and is characterized by a 2-point correlator as

$$\langle \rho_a(\mathbf{x}) \rho_b(\mathbf{y}) \rangle = \mu^2(x^-) \delta_{ab} \delta(\mathbf{x} - \mathbf{y}) \quad (1.39)$$

and the distribution is

$$\mathcal{W}[\rho_a] = \exp \left[- \int d^2\mathbf{x} \frac{\rho_a(\mathbf{x}) \rho_a(\mathbf{x})}{2\mu^2} \right]. \quad (1.40)$$

One is now able to compute the expectation value of an observable \mathcal{O} in the MV model by following the next steps. First one needs to obtain $\mathcal{O}[\rho_a]$, that is, the observable with an arbitrary ρ_a configuration of the color sources, assuming in the saturated regime $\rho_a \sim g^{-1}$. At Leading Order this model can describe gluon saturation, as the non-linearities in ρ_a have to be taken into account. Then one solves the classical Yang-Mills equation (1.38), and finally, average the observable over the distribution functional via

$$\langle \mathcal{O} \rangle = \int [D\rho_a] \mathcal{W}[\rho_a] \mathcal{O}[\rho_a]. \quad (1.41)$$

This final expectation value is gauge invariant as the distribution \mathcal{W} is invariant under gauge transformations, as well as the functional measure $[D\rho_a]$.

1.7 The Color Glass Condensate

The MV model presents a singular problem when going beyond the tree level calculations. Although it is sufficient for phenomenological calculations for processes like DIS, the factor $\delta(x^-)$ in the color current gives us singularities when going beyond tree level. One needs to assume then that the dependence on x^- comes as

$$\delta(x^-)\rho_a(\mathbf{x}) \rightarrow \rho_a(x^-, \mathbf{x}) \quad (1.42)$$

so this dependence is absorbed into ρ_a , yet still sitting at $x^- = 0$.

In the previous section we started out from imposing a momentum scale Λ^+ that separated the fast partons from the slow ones. This dependence of the artificial scale is taken into the functional weight $\mathcal{W}[\rho_a] \equiv \mathcal{W}_\Lambda[\rho_a]$, and gives the probability of observing a specific configuration of the color charge sources at this scale. However, the observables do not depend on this scale Λ^+ , so a new set of renormalization group equations are introduced. This RGE was derived by Jalilian-Marian, Iancu, McLerran, Weigert, Leonidov and Kovner (JIMWLK) in [26–30]. It describes the evolution of \mathcal{W}_{Λ^+} with changing momentum scale Λ^+ :

$$\frac{\partial \mathcal{W}_{\Lambda^+}[\rho]}{\partial \ln \Lambda^+} = \mathcal{H}_{JIMWLK} \mathcal{W}_{\Lambda^+}[\rho], \quad (1.43)$$

where \mathcal{H}_{JIMWLK} is the operator containing first and second derivatives with respect to ρ . We start at some initial scale Λ_0^+ that gives the initial condition $\mathcal{W}_{\Lambda_0^+}$ for which we would use (1.40) to model it. Thus, the JIMWLK evolution equation describes the evolution of this distribution as the cutoff decreases.

The *Color Glass Condensate* (CGC) is an effective theory that includes both, the separation of fast and slow partons according to the MV model, and the JIMWLK evolution equation. Breaking down the name of the theory, the *Color* stands for the fact that the gluons that govern the small- x regime, have color degrees of freedom. The word *Glass* comes from the time evolution of the degrees of freedom described by ρ_a . Due to Lorentz dilation this evolution is slow in comparison to the interaction time, like it is in glass systems. Finally the word *Condensate* stems from the saturated nature of the system in the small- x limit. The CGC may be also found in literature to stand for Color Gluon Cloud, but this is less common. A more complete review of theoretical and phenomenological aspects of CGC can be found in [31–33].

2

Eikonal approximation and power counting beyond eikonal accuracy

DISCLAIMER: The material presented in this chapter was originally published in Phys. Rev.D 104 (2021) 1, 014019 [34] and in Phys. Rev. D 107 (2023) 7, 074016 [35] of which I am a coauthor. More precisely, Section 2.2 and 2.3 was originally published in Phys. Rev.D 104 (2021) 1, 014019 and Section 2.4 was published in Phys. Rev. D 107 (2023) 7, 074016. This chapter only constitutes partial discussions of the original publications to give an introduction to eikonal approximation and the power counting beyond eikonal accuracy. The main results of these two publications will be presented in Chapters 3 and 4. At the beginning of each of these chapters I summarize my contributions to these publications as a disclaimer.

This chapter is dedicated to the Eikonal approximation since the bulk of the work throughout the Ph.D. was focused on computing the corrections to this approximation. In Section 2.1 one can find a brief introduction to the Eikonal approximation in different fields of physics. In Section 2.2 the Eikonal approximation in CGC is defined. In Section 2.3 we can find the derivation for the quark propagator at Eikonal accuracy and finally in section 2.4 there is a discussion about the power counting for eikonal and beyond eikonal approximation.

2.1 The Eikonal approximation in physics

In physics we find many areas where the Eikonal approximation is used like optics, seismology, quantum mechanics, QED or partial wave expansion. The word eikon (from Greek *eikenai*) means 'to resemble' or 'image' and this evolved ever since to what today is 'icon'. In physics, when one encounters a problem that is not possible to solve in an exact manner, one makes use of approximations. For the vast majority of the time, these approximations make good and reliable predictions.

In the mid XX-century, when high energy physics was being tested in experiments, it was soon realized the need for a new approximation that would give prediction in agreement with data. This is how the eikonal approximation came to life in quantum mechanics and quantum field theories. QCD was the main theory that benefited from this approximation, but we leave this discussion for the next section. However, the eikonal approximation was born many years before QFT or QM, and it was within the field of optics.

Optics, as we know today, is described in terms of waves that obey wave equations, and consequently behave according to Maxwell's equations. However, this set

of equations was not postulated until the XIX century, but we know that optics was able to describe a lot of phenomena many years before that, and to this day we can still admit the validity of some of these primitive explanations. This is due to taking the eikonal approximation, which allows us to treat the light as a 'ray light' in a way that we can approximate it by a straight line. With this approximation it was possible to describe how light works when it meets objects that are big enough, that is, large when compared with the wavelength of light. One example of a phenomena that was understood centuries ago precisely thanks to the eikonal approximation is reflection. However, when physicist tried to describe diffraction, they were forced to switch to the previously mentioned wave point of view for light, and with this they concluded that light, when treated in small scales, obeys Maxwell equations as every other type of wave.

Once one acknowledges that the light is a wave where the eikonal approximation works at a given scale, one realizes that this approximation may be valid for other fields in physics with a wave nature or where we find a diffusion equation.

Due to this, another domain of physics we should mention where the eikonal approximation has proven to be very useful is quantum mechanics. In QM this approximation works for scattering processes where incoming particles have a large momentum and the scattering angle is very small. When using the eikonal approximation in quantum mechanics, one ends up with a simplified set of differential equations that depend on only one variable, as a result of the straight line approximation. This is a big difference when comparing this approximation in quantum mechanics with the WKB approximation. The latter one, has as its objective to find approximate solutions to linear differential equations with coefficients that vary through space, however, this description with the trajectory is in general complicated when compared to the classical trajectory used in the eikonal approximation.

2.2 Eikonal approximation in Color Glass Condensate

Let us now focus on the Eikonal approximation within CGC. The CGC effective theory is used to describe processes at very high energies that are probed at the Relativistic Heavy Ion Collider (RHIC), Large Hadron Collider (LHC) or the future Electron Ion Collider (EIC). The validity of the eikonal approximation is then secured as it is an approximation for high energies. In this section the formulation for the eikonal approximation is shown within CGC, and we also discuss how it allows us to perform the calculations simpler in this saturated region.

Let us start with a reminder of what happens during a high energy collision, where relativistic kinematics are involved. The nucleon that appears at high energies is Lorentz contracted, therefore its geometry is modified to a two dimensional one in the laboratory frame. At the same time the internal timescales are also modified by the same Lorentz factor. While in the lower energy nucleon one has fluctuations among the partons that were short lived making very few of them probed by the photon, in a high energy nucleon the lifetimes of these fluctuations are dilated and more of them can be now probed. In these collisions several interactions among the constituents appear as well. When the duration of these interactions is boosted, the constituents appear as free in the collision and are rather unlikely to interact. These consequences are the reason for the increase of gluons probed during the process, and also the fact that now these gluons outnumber significantly other parton species such as valence and sea quarks.

In CGC there is another approximation apart from the eikonal one that need to be taken into account, that is the semi-classical approximation. As a consequence of this approximation the dense target is treated as a classical background field \mathcal{A}^μ , while the projectile is assumed to be dilute. This is why CGC is used for high energy dilute-dense systems, which can be achieved by boosting the dense target from their rest frames to the scattering energies. Boosting the target along the x^- direction leads to the following scaling of the background field \mathcal{A}^μ

$$\mathcal{A}_a^\mu(x) \rightarrow \begin{cases} \gamma_t \mathcal{A}_a^- (\gamma_t x^+, \frac{1}{\gamma_t} x^-, \mathbf{x}) \\ \frac{1}{\gamma_t} \mathcal{A}_a^+ (\gamma_t x^+, \frac{1}{\gamma_t} x^-, \mathbf{x}) \\ \mathcal{A}_a^i (\gamma_t x^+, \frac{1}{\gamma_t} x^-, \mathbf{x}) \end{cases}$$

the above shows two hierarchies that appear after the boost, one among the components of the background field, and one among the coordinates of this field. In the case of the components of the background field, the "-" component is power enhanced compared to the perpendicular and "+" component, which are left unchanged and suppressed, respectively. On the other hand, in the case of the coordinates, the opposite situation arises, being the "+" component enhanced and the "-" one suppressed, while the perpendicular component is still left unchanged.

The eikonal approximation in this configuration amounts to applying the following three assumptions. The first one states that the highly boosted background field that describes the target, is localized in the longitudinal direction around $x^+ = 0$ due to Lorentz contraction. This is also referred to as the *shockwave* approximation. The second assumption is to take into account only the leading component of the background field \mathcal{A}_a^- , neglecting then the subleading ones due to the hierarchy shown before. Finally the third assumption is to neglect the x^- dependence of the background field due to its slow dependence. In fact, this amounts to neglecting the dynamics of the target. Taking in all of the assumptions, one can describe the background field of the target as

$$\mathcal{A}_a^\mu(x^-, x^+, \mathbf{x}) \approx \delta^{\mu-} \delta(x^+) \mathcal{A}_a^-(\mathbf{x}). \quad (2.1)$$

Within the eikonal approximation, the projectile partons undergo multiple scatterings while propagating through the dense target and this information is encoded via Wilson lines. These Wilson lines are defined as path ordered exponentials of the leading component of the background field of the target. Finally, the eikonal approximation in CGC amounts to taking the contributions leading in energy and neglecting the power-suppressed ones in order to describe the scattering processes.

2.3 Derivation of the quark propagator at eikonal accuracy

Let us now derive the quark propagator at the pure eikonal level taking into consideration all the ingredients and assumptions that were discussed in section 2.2. The setup for this calculation includes the following definition for the quark propagator:

$$S_F(x, y)_{\beta\alpha} = S_{0,F}(x, y)_{\beta\alpha} + \delta S_F(x, y)_{\beta\alpha}, \quad (2.2)$$

where β and α are the fundamental color indices, $S_{0,F}(x, y)_{\beta\alpha}$ is the vacuum contribution to the propagator and $\delta S_F(x, y)_{\beta\alpha}$ is the medium correction. The vacuum

propagator is

$$S_{0,F}(x,y)_{\beta\alpha} = (\mathbf{1})_{\alpha\beta} \int \frac{d^4k}{(2\pi)^4} e^{-ik \cdot (x-y)} \frac{i(\not{k} + m)}{[k^2 - m^2 + i\epsilon]} \quad (2.3)$$

the Fourier transform is

$$S_F(x,y)_{\beta\alpha} = \int \frac{d^4q}{(2\pi)^4} \int \frac{d^4k}{(2\pi)^4} e^{-ix \cdot q} e^{iy \cdot k} \tilde{S}_F(q,k)_{\beta\alpha}. \quad (2.4)$$

The quark propagator that is computed in this section is in a background field taking only the pure $\mathcal{A}_a^-(x^+, \mathbf{x})$ component. The medium correction to the quark propagator in momentum space is obtained by summing multiple interaction diagrams of the type shown in Fig.2.1.

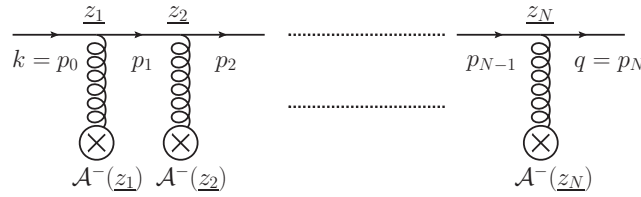


FIGURE 2.1: Multiple scattering of a quark on a pure \mathcal{A}^- background field.

This sum can be written as

$$\begin{aligned} \delta \tilde{S}_F(q,k)_{\beta\alpha} \Big|_{\text{pure } \mathcal{A}^-} &= \sum_{N=1}^{+\infty} \int \left[\prod_{n=1}^{N-1} \frac{d^4 p_n}{(2\pi)^4} \right] \int \left[\prod_{n=1}^N d^3 z_n e^{i z_n \cdot (p_n - p_{n-1})} 2\pi \delta(p_n^+ - p_{n-1}^+) \right] \\ &\times \left\{ \mathcal{P}_n \prod_{n=1}^N [-igt \cdot \mathcal{A}^-(z_n)] \right\}_{\beta\alpha} \frac{i(\not{q} + m)}{[q^2 - m^2 + i\epsilon]} \left\{ \mathcal{P}_n \prod_{n=0}^{N-1} \left[\gamma^+ \frac{i(\not{p}_n + m)}{[p_n^2 - m^2 + i\epsilon]} \right] \right\}, \end{aligned} \quad (2.5)$$

where $p_0 \equiv k$ and $p_N \equiv q$. The symbol \mathcal{P}_n shows the ordering of the matrix factors with increasing the value of n from right to left, for color matrices in the first bracket and Dirac matrices in the second one. From the equation Eq. (2.5) on, the notation $\mathcal{A}_\mu^a(x^+, \mathbf{x}) \equiv \mathcal{A}_\mu^a(\underline{x})$ is used for the leading coordinates. Noting that $\gamma^+ \gamma^+ = 0$, which comes from the fact that $g^{++} = 0$ in the light-cone coordinates. Using this one can get

$$\gamma^+(\not{p}_n + m)\gamma^+ = \{\gamma^+, \not{p}_n\} \gamma^+ = (2p_n^+) \gamma^+, \quad (2.6)$$

which simplifies the numerator in Eq. (2.5). One can perform the integration over p_n^- for each internal free fermion propagator as

$$\begin{aligned} &\int \frac{d p_n^-}{2\pi} e^{-i p_n^- (z_{n+1}^+ - z_n^+)} \frac{(2p_n^+) i}{[p_n^2 - m^2 + i\epsilon]} \\ &= \{\theta(p_n^+) \theta(z_{n+1}^+ - z_n^+) - \theta(-p_n^+) \theta(z_n^+ - z_{n+1}^+)\} e^{-i \not{p}_n^- (z_{n+1}^+ - z_n^+)}. \end{aligned} \quad (2.7)$$

where is on-shell, $\check{p}^- = (\mathbf{p}^2 + m^2)/(2p^+)$. Plugging in this result into Eq. (2.5), one gets

$$\begin{aligned} \delta\tilde{S}_F(q, k)_{\beta\alpha} \Big|_{\text{pure } \mathcal{A}^-} &= 2\pi\delta(q^+ - k^+) \frac{i(\check{q} + m)}{[q^2 - m^2 + i\epsilon]} \gamma^+ \frac{i(\check{k} + m)}{[k^2 - m^2 + i\epsilon]} \sum_{N=1}^{+\infty} \int \left[\prod_{n=1}^N d^3 z_n \right] \\ &\times \left\{ \theta(k^+) \left(\prod_{n=1}^{N-1} \theta(z_{n+1}^+ - z_n^+) \right) + (-1)^{N-1} \theta(-k^+) \left(\prod_{n=1}^{N-1} \theta(z_n^+ - z_{n+1}^+) \right) \right\} \\ &\times e^{iz_N \cdot q} e^{-iz_1 \cdot k} \left\{ \mathcal{P}_n \prod_{n=1}^N [-igt \cdot \mathcal{A}^-(z_n)] \right\}_{\beta\alpha} \\ &\times \int \left[\prod_{n=1}^{N-1} \frac{d^2 \mathbf{p}_n}{(2\pi)^2} e^{i\mathbf{p}_n \cdot (\mathbf{z}_{n+1} - \mathbf{z}_n)} e^{-i\check{p}_n^-(z_{n+1}^+ - z_n^+)} \right], \end{aligned} \quad (2.8)$$

Where the terms q^- and k^- are only present in the denominator and phase factor, while in the numerator q and k have been replaced by their on-shell counterparts \check{q} and \check{k} . Note also that in Eq. (2.8), $p_n^+ = k^+$ for n from 1 to $N-1$.

Here, we consider the background field with a finite support along the x^+ direction $[-L^+/2, L^+/2]$. In the eikonal limit, $L^+ \rightarrow 0$. This finite width L^+ is of order $O(1/\gamma)$ due to Lorentz contraction. Each vertex of interaction of the quark with the background field comes with an integration in x^+ over $[-L^+/2, L^+/2]$, thus bringing a suppression factor $1/\gamma$. In Eq. (2.8) one has $|z_{n+1}^+ - z_n^+| < L^+ \rightarrow 0$, thus the phase factors $\exp[-i\check{p}_n^-(z_{n+1}^+ - z_n^+)]$ can be replaced by 1 in first approximation. This approximation is possible only after taking the integral over p_n^- , otherwise one would not be able to recover the correct ordering in z^+ unambiguously. With this, one reduces the integrals in \mathbf{p}_n to $\delta^{(2)}(\mathbf{z}_{n+1} - \mathbf{z}_n)$ factors, leading then to the expression

$$\begin{aligned} \delta\tilde{S}_F(q, k)_{\beta\alpha} \Big|_{\text{pure } \mathcal{A}^-, \text{Eik.}} &= 2\pi\delta(q^+ - k^+) \frac{i(\check{q} + m)}{[q^2 - m^2 + i\epsilon]} \gamma^+ \frac{i(\check{k} + m)}{[k^2 - m^2 + i\epsilon]} \int d^2 \mathbf{z} e^{-iz \cdot (q - k)} \\ &\times \sum_{N=1}^{+\infty} \int \left[\prod_{n=1}^N dz_n^+ \right] e^{iz_N^+ q^-} e^{-iz_1^+ k^-} \left\{ \mathcal{P}_n \prod_{n=1}^N [-igt \cdot \mathcal{A}^-(z_n^+, \mathbf{z})] \right\}_{\beta\alpha} \\ &\times \left\{ \theta(k^+) \left(\prod_{n=1}^{N-1} \theta(z_{n+1}^+ - z_n^+) \right) + (-1)^{N-1} \theta(-k^+) \left(\prod_{n=1}^{N-1} \theta(z_n^+ - z_{n+1}^+) \right) \right\} \end{aligned} \quad (2.9)$$

Note that in Eq. (2.9) the $N = 1$ term has not been affected by the eikonal approximation therefore is still exact. Taking now the Fourier transform following the previously established convention, and performing the integrals over q^- and k^- thanks to Eq. (2.7), one gets

$$\begin{aligned}
 \delta S_F(x, y)_{\beta\alpha} \Big|_{\text{pure } \mathcal{A}^-, \text{Eik.}} &= \int \frac{d^3 q}{(2\pi)^3} \int \frac{d^3 k}{(2\pi)^3} 2\pi \delta(q^+ - k^+) e^{-ix \cdot \check{q} + iy \cdot \check{k}} \frac{(\check{q} + m)\gamma^+(\check{k} + m)}{(2k^+)^2} \\
 &\times \int d^2 \mathbf{z} e^{-iz \cdot (\mathbf{q} - \mathbf{k})} \sum_{N=1}^{+\infty} \int \left[\prod_{n=1}^N dz_n^+ \right] e^{iz_N^+ \check{q}^-} e^{-iz_1^+ \check{k}^-} \left\{ \mathcal{P}_n \prod_{n=1}^N [-igt \cdot \mathcal{A}^-(z_n^+, \mathbf{z})] \right\}_{\beta\alpha} \\
 &\times \left\{ \theta(k^+) \left(\prod_{n=0}^N \theta(z_{n+1}^+ - z_n^+) \right) + (-1)^{N+1} \theta(-k^+) \left(\prod_{n=0}^N \theta(z_n^+ - z_{n+1}^+) \right) \right\}, \tag{2.10}
 \end{aligned}$$

where $z_0^+ \equiv y^+$ and $z_{N+1}^+ \equiv x^+$. Since the integrals over q^- and k^- have already been performed, one can neglect the phase factors dependent on z_1^+ and z_N^+ , in the eikonal approximation. Using \mathcal{P}_+ and $\overline{\mathcal{P}}_+$ to indicate the ordering and anti-ordering of the color matrices along z^+ from right to left, one can recognize in Eq. (2.10) the series of expansion of the gauge link

$$\begin{aligned}
 \mathcal{U}_F(x^+, y^+; \mathbf{z}) &\equiv \mathbf{1} + \sum_{N=1}^{+\infty} \frac{1}{N!} \mathcal{P}_+ \left[-ig \int_{y^+}^{x^+} dz^+ t \cdot \mathcal{A}^-(z^+, \mathbf{z}) \right]^N \\
 &= \mathbf{1} + \sum_{N=1}^{+\infty} \int \left[\prod_{n=1}^N dz_n^+ \right] \left(\prod_{n=0}^N \theta(z_{n+1}^+ - z_n^+) \right) \left\{ \mathcal{P}_n \prod_{n=1}^N [-igt \cdot \mathcal{A}^-(z_n^+, \mathbf{z})] \right\} \tag{2.11}
 \end{aligned}$$

and of the conjugate gauge link

$$\begin{aligned}
 \mathcal{U}_F^\dagger(y^+, x^+; \mathbf{z}) &\equiv \mathbf{1} + \sum_{N=1}^{+\infty} \frac{1}{N!} \left\{ \overline{\mathcal{P}}_+ \left[-ig \int_{x^+}^{y^+} dz^+ t \cdot \mathcal{A}^-(z^+, \mathbf{z}) \right]^N \right\}^\dagger \\
 &= \mathbf{1} + \sum_{N=1}^{+\infty} \int \left[\prod_{n=1}^N dz_n^+ \right] \left(\prod_{n=0}^N \theta(z_n^+ - z_{n+1}^+) \right) \left\{ \mathcal{P}_n \prod_{n=1}^N [+igt \cdot \mathcal{A}^-(z_n^+, \mathbf{z})] \right\}, \tag{2.12}
 \end{aligned}$$

Thus, in the eikonal approximation, the complete \mathcal{A}^- medium correction to the quark propagator looks like

$$\begin{aligned}
 \delta S_F(x, y)_{\beta\alpha} \Big|_{\text{pure } \mathcal{A}^-, \text{Eik.}} &= \int \frac{d^3 q}{(2\pi)^3} \int \frac{d^3 k}{(2\pi)^3} 2\pi \delta(q^+ - k^+) e^{-ix \cdot \check{q} + iy \cdot \check{k}} \frac{(\check{q} + m)\gamma^+(\check{k} + m)}{(2k^+)^2} \\
 &\times \int d^2 \mathbf{z} e^{-iz \cdot (\mathbf{q} - \mathbf{k})} \left\{ \theta(k^+) \theta(x^+ - y^+) \left[\mathcal{U}_F(x^+, y^+; \mathbf{z}) - \mathbf{1} \right]_{\beta\alpha} \right. \\
 &\quad \left. - \theta(-k^+) \theta(y^+ - x^+) \left[\mathcal{U}_F^\dagger(y^+, x^+; \mathbf{z}) - \mathbf{1} \right]_{\beta\alpha} \right\}. \tag{2.13}
 \end{aligned}$$

which is valid for all values of x^+ and y^+ . In order to get the full propagator, one needs to combine the vacuum propagator Eq.(2.3) and the medium correction Eq.(2.13). This can be achieved by splitting the momentum space expression of the

vacuum propagator into a simple pole contribution in k^- and a non-pole contribution as follows

$$\frac{i(\not{k} + m)}{[k^2 - m^2 + i\epsilon]} = \frac{i \left[(\not{\check{k}} + m) + (k^- - \check{k}^-) \gamma^+ \right]}{[k^2 - m^2 + i\epsilon]} = \frac{i(\not{\check{k}} + m)}{[k^2 - m^2 + i\epsilon]} + \frac{i\gamma^+}{2k^+} \quad (2.14)$$

The simple pole contribution cancels identically the color identity matrix terms from Eq.(2.13) and one can use the identity

$$\int \frac{dk^+}{2\pi} \frac{i}{2k^+} e^{-ik^+(x^- - y^-)} = \frac{1}{4} \text{sgn}(x^- - y^-) \quad (2.15)$$

where the sign function is $\text{sgn}(x) \equiv \theta(x) - \theta(-x)$, thus we obtain

$$\begin{aligned} S_F(x, y)_{\beta\alpha} \Big|_{\text{pure } \mathcal{A}^-, \text{Eik.}} &= \mathbf{1}_{\alpha\beta} \delta^{(3)}(\underline{x} - \underline{y}) \text{sgn}(x^- - y^-) \frac{\gamma^+}{4} + \int \frac{d^3\mathbf{q}}{(2\pi)^3} \int \frac{d^3\mathbf{k}}{(2\pi)^3} \\ &\times 2\pi \delta(q^+ - k^+) e^{-ix \cdot \check{q} + iy \cdot \check{k}} \frac{(\not{\check{q}} + m) \gamma^+ (\not{\check{k}} + m)}{(2k^+)^2} \\ &\times \int d^2\mathbf{z} e^{-iz \cdot (\mathbf{q} - \mathbf{k})} \left\{ \theta(k^+) \theta(x^+ - y^+) \mathcal{U}_F(x^+, y^+; \mathbf{z})_{\beta\alpha} \right. \\ &\left. - \theta(-k^+) \theta(y^+ - x^+) \mathcal{U}_F^\dagger(y^+, x^+; \mathbf{z})_{\beta\alpha} \right\}. \end{aligned} \quad (2.16)$$

for the quark propagator in a pure \mathcal{A}^- background field, in the eikonal approximation valid for any x^+ and y^+ .

2.4 Power counting beyond the eikonal approximation

In this section we discuss the power counting beyond eikonal approximation since the actual purpose of this thesis is to show how one can get corrections beyond the eikonal order by relaxing the eikonal approximation described in section 2.2. These corrections are also called next-to-eikonal (NEik). In section 2.2 we discussed that the high-energy limit of a collision process can be understood in terms of the infinite Lorentz boost of the target, which introduced a hierarchy among both, the components of the background field and its coordinates. Thus, one can classify contributions according to their scaling with the Lorentz boost factor γ_t of the target.

2.4.1 Scaling of the background field

Under a large active boost of the target along the x^- direction, the components of the background field strength are transformed following the standard Lorentz transformation rules for tensors. In light-cone coordinates, the tensor components are enhanced by a factor γ_t for each upper “-” or lower “+” index under such a boost, and are suppressed by a factor $1/\gamma_t$ for each lower “-” or upper “+” index. The background field strength is defined as

$$\mathcal{F}_{ij}^a(\underline{z}) \equiv \partial_{\mathbf{z}^i} \mathcal{A}_j^a(\underline{z}) - \partial_{\mathbf{z}^j} \mathcal{A}_i^a(\underline{z}) - g f^{abc} \mathcal{A}_i^b(\underline{z}) \mathcal{A}_j^c(\underline{z}) \quad (2.17)$$

Hence, the components of the background field strength scale under a large boost of the target along x^- direction as

$$\mathcal{F}^{-j} \propto \gamma_t \gg 1 \quad (2.18)$$

$$\mathcal{F}^{ij} \propto (\gamma_t)^0 = 1 \quad (2.19)$$

$$\mathcal{F}^{-+} \propto (\gamma_t)^0 = 1 \quad (2.20)$$

$$\mathcal{F}^{+j} \propto \frac{1}{\gamma_t} \ll 1 \quad (2.21)$$

One can extend these rules to the background field of the target, thus obtaining the following scaling

$$\mathcal{A}^-(x) \propto \gamma_t \gg 1 \quad (2.22)$$

$$\mathcal{A}^i(x) \propto (\gamma_t)^0 = 1 \quad (2.23)$$

$$\mathcal{A}^+(x) \propto \frac{1}{\gamma_t} \ll 1. \quad (2.24)$$

from this scaling one can see that the NEik correction corresponds to taking into account the perpendicular component of the background field, while including $\mathcal{A}^+(x)$ would give us corrections of order next-to-next-to-eikonal, which is out of the scope of this thesis.

2.4.2 Scaling of derivatives

Let us now look at the scaling of the derivatives of the background field. These derivatives acting on the background field will appear when computing corrections to the eikonal approximation. The derivatives are with respect to any of the coordinates that the background field depends on. The scaling rules that these derivatives follow are the same ones based on the counting of "+" and "-" indices. A partial derivative on a tensor leads to a higher rank tensor, thus the following scaling rules apply

$$\partial_- \mathcal{F}^{\mu\nu} \propto \frac{1}{\gamma_t} \mathcal{F}^{\mu\nu} \ll \mathcal{F}^{\mu\nu} \quad (2.25)$$

$$\partial_+ \mathcal{F}^{\mu\nu} \propto \gamma_t \mathcal{F}^{\mu\nu} \gg \mathcal{F}^{\mu\nu} \quad (2.26)$$

$$\partial_i \mathcal{F}^{\mu\nu} \propto (\gamma_t)^0 \mathcal{F}^{\mu\nu} \quad (2.27)$$

in the case of partial derivatives acting on the background gauge field similar rules apply. Moreover, due to the scaling rules of the components of the background gauge field given in Eqs. (2.22), (2.23) and (2.24), background covariant derivatives follow the scaling rules as partial derivatives when acting on the background field.

2.4.3 Scaling of the width of the target

As we have seen in section 2.2, the eikonal approximation takes the width of the target as a infinitely thin shockwave, therefore in order to compute corrections that stem from relaxing this approximation one needs to introduce a finite width of the target.

Since the background field strength $\mathcal{F}^{\mu\nu}(x)$ represents a hadronic or nuclear target subject to confinement, it should decay faster than a power for $x^+ \rightarrow \pm\infty$. Hence, the profile of $\mathcal{F}^{\mu\nu}(x)$ along x^+ has a finite width, that we note L^+ . Due to Lorentz contraction under a large boost of the target along x^- direction, that width scales as

$$L^+ = O\left(\frac{1}{\gamma_t}\right) \quad (2.28)$$

In particular, in the limit of infinite boost, $\mathcal{F}^{\mu\nu}(x)$ becomes a shockwave of vanishing width along the x^+ direction. For the purpose of power counting, the finite width L^+ of $\mathcal{F}^{\mu\nu}(x)$ can be assimilated as a finite support for $\mathcal{F}^{\mu\nu}(x)$ along the x^+ . In a generic gauge where $A^-(x) \neq 0$ (for example the light-cone gauge $A^+(x) = 0$), the background gauge field $\mathcal{A}^\mu(x)$ has a finite width of $O(L^+)$ along the x^+ direction, which becomes a shockwave in the infinite boost limit. Therefore, each integration over the position x of a background field strength or gauge field insertion is effectively restricted to the small width L^+ along the x^+ direction, and can thus be counted as a suppression by a factor of L^+ or equivalently of $1/\gamma_t$ at large γ_t .

2.4.4 Eikonal and NEik contributions in propagators

As discussed in the previous sections, for the case of eikonal approximation, one takes only the leading contributions, or equivalently, the high-energy limit. Therefore only the leading component $\mathcal{A}^-(x)$ of the gauge field is kept and due to its enhancement with γ_t , each power of $\mathcal{A}^-(x)$ compensates the suppression due to the integration over its x^+ coordinate. Hence, multiple insertions of $\mathcal{A}^-(x)$ have to be resummed in the eikonal approximation, which as we have seen in section 2.3, lead to the Wilson lines describing the interaction of each parton in the projectile with the target in the CGC formalism in the eikonal approximation. Each $\mathcal{A}^-(x)$ insertion in a Wilson line has the same transverse position \mathbf{x} in the eikonal approximation, due to the parametrically small L^+ width of the target. As for scaling of the derivatives, they appear when one expands $\mathcal{A}^-(x)$ as a series in x^- , and each further term comes with an extra ∂_- acting on the background field. This term is suppressed by an extra $1/\gamma_t$ factor under large boosts. In the case of eikonal approximation, one needs to account only for the zeroth order term in this expansion, hence the x^- dependence of $\mathcal{A}^-(x)$ is neglected.

In order to compute a propagator at NEik accuracy, one needs to include contributions that are suppressed by one power of $1/\gamma_t$ at large γ_t compared to the eikonal contribution. These terms arise as follows:

- by replacing an enhanced $\mathcal{A}^-(x)$ insertion with a non-enhanced $\mathcal{A}^i(x)$ insertion,
- or by accounting for the transverse motion of the projectile parton over the duration L^+ of the interaction with the target,
- or by including terms with one ∂_{x^-} derivative acting on the background field in the gradient expansion of $\mathcal{A}^-(x)$ in x^- .

At the level of the cross-section, one has to square the amplitudes that contain these corrections, hence new technical difficulties may appear if the gradient expansion of all $\mathcal{A}^-(x)$ insertions is performed around a fixed value of x^- like $x^- = 0$. In order to bypass this issue, one can instead perform the gradient expansion of

all $\mathcal{A}^-(x)$ insertions around a common value of x^- and write the amplitude (or S-matrix) as integral over that variable. This amounts to resumming a subset of non-eikonal corrections together with the eikonal term and one obtains what we refer to as *generalized eikonal approximation*. In the second chapter, this generalized eikonal term does not appear but it is introduced in chapters 4 and 5. There, one can see which terms are kept and which ones are neglected in order to get both eikonal and NEik terms at the level of the cross-section.

Finally, we can find that there has been a lot of effort in the recent years to compute these NEik corrections. Initially, in Refs. [36, 37] subeikonal corrections that stem from considering a finite width target are computed for the gluon propagator and its application to single inclusive gluon production and various spin asymmetries in central pA collisions were studied at next-to-next-to-eikonal accuracy. In Refs. [38, 39], it was shown that these corrections can be attributed to the modifications of the Lipatov vertex in pp collisions. The effects of subeikonal corrections on the azimuthal harmonics for pp [40] and for pA [41, 42] collisions were also investigated. Recently, next-to-eikonal (NEik) corrections that are related with the transverse component of the background field [34] and the dynamics of the target [43] have been computed for scalar and quark propagators. Apart from the aforementioned works that focus on the derivation of the subeikonal corrections to the parton propagators and their applications to observables, in [44–55] quark and gluon helicity evolutions have been computed at next-to-eikonal accuracy. In [56, 57] helicity dependent extensions of the CGC at next-to-eikonal accuracy have been studied. In [58, 59] subeikonal corrections to both quark and gluon propagators have been calculated in the high-energy operator product expansion (OPE) formalism, and applied to study the polarized structure function g_1 at low x . Moreover, rapidity evolution of transverse momentum dependent parton distributions (TMDs) that interpolates between the low and moderate energies are studied in [60–64]. A similar idea is pursued in [65, 66] to study the interpolation between the low and moderate values of x for the unintegrated gluon distributions. Finally, an approach based on longitudinal momentum exchange between the projectile and the target during the interaction have been followed in [67–69] to study the subeikonal effects. The effects of subeikonal corrections are also studied in the context of orbital angular momentum in [70, 71].

3

NEik corrections: effects of finite width and transverse background field

DISCLAIMER: The material presented in this Chapter was originally published in *Phys. Rev. D* 104 (2021) 1, 014019 (which can be found as a the reference in this thesis [34]) of which I am a coauthor. My contributions to this publication can be summarized as follows. I have contributed to the derivation of the quark propagator at next-to-eikonal accuracy and also to the computation of the partonic cross section for the forward quark-nucleus scattering. I have also derived the antiquark propagator and computed the forward antiquark-nucleus cross section at NEik accuracy. I have presented these results in an invited (online) seminar in Centro de Investigación y de Estudios Avanzados del Instituto Politecnico Nacional de Mejiro, Mexico in December 2021.

The eikonal approximation that was reviewed in the previous chapter is a very successful and powerful tool when used to describe scatterings that are encountered in the asymptotically high energy regime. However, the energies that are reached in reality in scattering experiments are limited. Although for scattering energies that are achieved at the LHC, the eikonal approximation is still valid and gives reliable results when compared with the experimental data; subeikonal corrections are expected to be sizeable for RHIC and future EIC colliders phenomenology. One finds that it is of key importance to understand the applicability regions of the eikonal approximation and computing the corrections to this approximation in order to obtain a precise comparison of the experimental data with with the theoretical calculations.

In the previous section, the basis for computations at NEik order was laid down. In this chapter we calculate the quark propagator at NEik, which is then used to study an observable, the forward quark-nucleus scattering. In order to get corrections beyond the eikonal approximation one needs to relax the assumptions that were discussed in section 2.2. The idea of computing subeikonal correction for a better understanding of the lower energy regions in the experiments, triggered a lot of work in CGC to get these corrections, as we at the end of the previous chapter.

In this chapter, we focus on the quark propagator in a gluon background field and we compute the NEik corrections to it. These corrections originate from relaxing two of the assumptions stated in section 2.2. On one hand, in section 3.1, we consider a finite width of the target instead of the infinitely thin shockwave, obtaining thus NEik corrections due to finite longitudinal width that lead to the transverse motion

of the projectile parton during its interaction with the target. On the other hand, in section 3.2, we relax the fact that the target background field is defined only by its leading component, \mathcal{A}^- . We include the transverse component of the background field in the computations, since it is the next in order of the hierarchy among the components of the background field. Finally, in section 3.3 we combine both these results and obtain the quark propagator at NEik accuracy that will be used in section 3.4 in order to compute the forward quark-nucleus scattering cross-section.

3.1 Finite width effects

The first step in order to go beyond the eikonal approximation as we have said, is to relax the shockwave approximation. By doing so one gets a target with a finite longitudinal width that the projectile parton traverses. We adopt the same set up as in section 2.3, where we computed the quark propagator in the pure \mathcal{A}^- background at the eikonal level.

The support of the background field along the x^+ direction is $[-L^+/2, L^+/2]$. In order to derive the quark propagator in a at NEik in a pure \mathcal{A}^- background field, we start from Eq.(2.8). One can Fourier transform this into the position space using Eq.(2.4), and then integrate over \mathbf{p}_n (with n from 1 to $N-1$), and over q^- and k^- to arrive at

$$\begin{aligned} \delta S_F(x, y) \Big|_{\text{pure } \mathcal{A}^-} &= \int \frac{d^3 \underline{q}}{(2\pi)^3} \int \frac{d^3 \underline{k}}{(2\pi)^3} 2\pi \delta(q^+ - k^+) e^{-ix \cdot \underline{q}} e^{iy \cdot \underline{k}} \frac{(\not{q} + m)\gamma^+(\not{k} + m)}{(2k^+)^2} \\ &\times \sum_{N=1}^{+\infty} \int \left[\prod_{n=1}^N d^3 \underline{z}_n \right] e^{i \underline{z}_N \cdot \underline{q}} e^{-i \underline{z}_1 \cdot \underline{k}} \left\{ \mathcal{P}_N \prod_{n=1}^N [-igt \cdot \mathcal{A}^-(\underline{z}_n)] \right\} \\ &\times \left\{ \prod_{n=1}^{N-1} \left[\frac{(-i)k^+}{2\pi(z_{n+1}^+ - z_n^+)} e^{-i \frac{(z_{n+1}^+ - z_n^+)m^2}{2k^+}} e^{i \frac{k^+(z_{n+1}^+ - z_n^+)^2}{2(z_{n+1}^+ - z_n^+)}} \right] \right\} \\ &\times \left\{ \theta(k^+) \left(\prod_{n=0}^N \theta(z_{n+1}^+ - z_n^+) \right) + (-1)^{N+1} \theta(-k^+) \left(\prod_{n=0}^N \theta(z_n^+ - z_{n+1}^+) \right) \right\}, \quad (3.1) \end{aligned}$$

where we use the notation $z_0^+ \equiv y^+$ and $z_{N+1}^+ \equiv x^+$, and keeping fundamental color indices implicit. Applying the change of variables $\mathbf{z}_n \rightarrow \mathbf{u}_n$, defined as

$$\mathbf{z}_n \equiv \mathbf{u}_n + \frac{1}{2} \left(\frac{\mathbf{q}}{q^+} + \frac{\mathbf{k}}{k^+} \right) z_n^+ = \mathbf{u}_n + \frac{z_n^+ (\mathbf{q} + \mathbf{k})}{2k^+}. \quad (3.2)$$

one can simplify the phase factor. The interpretation for the change of variables is as follows. In the $2+1$ dimensional Galilean subgroup of the Poincaré group in light-cone coordinates, \mathbf{p}/p^+ plays the role of a transverse Galilean velocity, and z^+ the role of time. Hence, the change of variables Eq.(3.2) amounts to express the successive transverse positions of the quark in a transversely moving frame, with a Galilean velocity which is the average between the initial velocity of the quark \mathbf{k}/k^+

and the final one \mathbf{q}/q^+ . Eq.(3.1) then becomes

$$\begin{aligned}
\delta S_F(x, y) \Big|_{\text{pure } \mathcal{A}^-} &= \int \frac{d^3 \underline{q}}{(2\pi)^3} \int \frac{d^3 \underline{k}}{(2\pi)^3} 2\pi \delta(q^+ - k^+) e^{-ix \cdot \underline{q}} e^{iy \cdot \underline{k}} \frac{(\not{q} + m)\gamma^+(\not{k} + m)}{(2k^+)^2} \\
&\times \sum_{N=1}^{+\infty} \int \left[\prod_{n=1}^N dz_n^+ \right] \left\{ \theta(k^+) \left(\prod_{n=0}^N \theta(z_{n+1}^+ - z_n^+) \right) \right. \\
&+ (-1)^{N+1} \theta(-k^+) \left(\prod_{n=0}^N \theta(z_n^+ - z_{n+1}^+) \right) \left. \right\} \\
&\times e^{i(z_N^+ - z_1^+) \frac{(\mathbf{q}-\mathbf{k})^2}{8k^+}} \int \left[\prod_{n=1}^N d^2 \mathbf{u}_n \right] e^{-\frac{i}{2}(\mathbf{u}_N + \mathbf{u}_1) \cdot (\mathbf{q} - \mathbf{k})} \left\{ \prod_{n=1}^{N-1} \left[\frac{(-i)k^+}{2\pi(z_{n+1}^+ - z_n^+)} e^{i \frac{k^+(\mathbf{u}_{n+1} - \mathbf{u}_n)^2}{2(z_{n+1}^+ - z_n^+)}} \right] \right\} \\
&\times \left\{ \mathcal{P}_N \prod_{n=1}^N \left[-igt \cdot \mathcal{A}^- \left(z_n^+, \mathbf{u}_n + \frac{z_n^+(\mathbf{q} + \mathbf{k})}{2k^+} \right) \right] \right\}. \quad (3.3)
\end{aligned}$$

At this point one can perform the change of variables from \mathbf{u}_n (with n from 1 to N) to \mathbf{w}_n (with n from 1 to $N-1$) and \mathbf{z} defined as

$$\begin{aligned}
\mathbf{w}_n &\equiv \mathbf{u}_{n+1} - \mathbf{u}_n \\
\mathbf{z} &\equiv \frac{(\mathbf{u}_N + \mathbf{u}_1)}{2}. \quad (3.4)
\end{aligned}$$

finding thus,

$$\begin{aligned}
\delta S_F(x, y) \Big|_{\text{pure } \mathcal{A}^-} &= \int \frac{d^3 \underline{q}}{(2\pi)^3} \int \frac{d^3 \underline{k}}{(2\pi)^3} 2\pi \delta(q^+ - k^+) e^{-ix \cdot \underline{q}} e^{iy \cdot \underline{k}} \frac{(\not{q} + m)\gamma^+(\not{k} + m)}{(2k^+)^2} \\
&\times \sum_{N=1}^{+\infty} \int \left[\prod_{n=1}^N dz_n^+ \right] \left\{ \theta(k^+) \left(\prod_{n=0}^N \theta(z_{n+1}^+ - z_n^+) \right) \right. \\
&+ (-1)^{N+1} \theta(-k^+) \left(\prod_{n=0}^N \theta(z_n^+ - z_{n+1}^+) \right) \left. \right\} e^{i(z_N^+ - z_1^+) \frac{(\mathbf{q}-\mathbf{k})^2}{8k^+}} \int d^2 \mathbf{z} e^{-iz \cdot (\mathbf{q} - \mathbf{k})} \mathcal{E}, \quad (3.5)
\end{aligned}$$

where

$$\begin{aligned}
\mathcal{E} &\equiv \int \left\{ \prod_{n=1}^{N-1} \left[d^2 \mathbf{w}_n \frac{(-i)k^+}{2\pi(z_{n+1}^+ - z_n^+)} e^{i \frac{k^+ \mathbf{w}_n^2}{2(z_{n+1}^+ - z_n^+)}} \right] \right\} \\
&\times \left\{ \mathcal{P}_N \prod_{n=1}^N \left[-igt \cdot \mathcal{A}^- \left(z_n^+, \hat{\mathbf{z}}_n + \frac{1}{2} \sum_{n'=1}^{n-1} \mathbf{w}_{n'} - \frac{1}{2} \sum_{n'=n}^{N-1} \mathbf{w}_{n'} \right) \right] \right\}, \quad (3.6)
\end{aligned}$$

and using the notation $\hat{\mathbf{z}}_n \equiv \mathbf{z} + z_n^+(\mathbf{q} + \mathbf{k})/(2k^+)$ for the analog of the classical trajectory used in Refs. [36, 37]. The Taylor expansion of each background field insertion around its classical position $\hat{\mathbf{z}}_n$ allows us to go systematically beyond the Eikonal approximation. The integrations over \mathbf{w}_n can be performed analytically thanks to

$$\int d^2 \mathbf{w}_n \frac{(-i)k^+}{2\pi(z_{n+1}^+ - z_n^+)} e^{i \frac{k^+ \mathbf{w}_n^2}{2(z_{n+1}^+ - z_n^+)}} = 1 \quad (3.7)$$

$$\int d^2 \mathbf{w}_n \frac{(-i)k^+}{2\pi(z_{n+1}^+ - z_n^+)} e^{i \frac{k^+ \mathbf{w}_n^2}{2(z_{n+1}^+ - z_n^+)}} \mathbf{w}_n^i = 0 \quad (3.8)$$

$$\int d^2 \mathbf{w}_n \frac{(-i)k^+}{2\pi(z_{n+1}^+ - z_n^+)} e^{i \frac{k^+ \mathbf{w}_n^2}{2(z_{n+1}^+ - z_n^+)}} \mathbf{w}_n^i \mathbf{w}_n^j = \frac{i(z_{n+1}^+ - z_n^+)}{k^+} \delta^{ij}. \quad (3.9)$$

In order to account for the subeikonal corrections, one has to take into account all contributions quadratic in \mathbf{w}_n in the Taylor expansion, for each n separately. However, the two powers of \mathbf{w}_n do not necessarily come from the Taylor expansion of the same \mathcal{A}^- insertion. We thus find,

$$\begin{aligned} \mathcal{E} = & \left\{ 1 + \frac{i(z_N^+ - z_1^+)}{8k^+} \partial_{z_j} \partial_{z_i} \right\} \left\{ \mathcal{P}_n \prod_{n=1}^N [-igt \cdot \mathcal{A}^-(z_n^+, \hat{\mathbf{z}}_n)] \right\} \\ & - \frac{i}{2k^+} \sum_{n_1=1}^{N-1} \sum_{n_2=n_1+1}^N (z_{n_2}^+ - z_{n_1}^+) \\ & \times \left\{ \mathcal{P}_n [-igt \cdot \partial_j \mathcal{A}^-(z_{n_2}^+, \hat{\mathbf{z}}_{n_2})] [-igt \cdot \partial_j \mathcal{A}^-(z_{n_1}^+, \hat{\mathbf{z}}_{n_1})] \prod_{\substack{n=1 \\ n \neq n_1, n_2}}^N \right. \\ & \left. \times [-igt \cdot \mathcal{A}^-(z_n^+, \hat{\mathbf{z}}_n)] \right\} \\ & + \text{NNEik}. \end{aligned} \quad (3.10)$$

Then we obtain

$$\begin{aligned} e^{i(z_N^+ - z_1^+) \frac{(\mathbf{q}-\mathbf{k})^2}{8k^+}} \int d^2 \mathbf{z} e^{-iz \cdot (\mathbf{q}-\mathbf{k})} \mathcal{E} = & \int d^2 \mathbf{z} e^{-iz \cdot (\mathbf{q}-\mathbf{k})} \left\{ \mathcal{P}_n \prod_{n=1}^N [-igt \cdot \mathcal{A}^-(z_n^+, \hat{\mathbf{z}}_n)] \right\} \\ & - \frac{i}{2k^+} \int d^2 \mathbf{z} e^{-iz \cdot (\mathbf{q}-\mathbf{k})} \sum_{n_1=1}^{N-1} \sum_{n_2=n_1+1}^N (z_{n_2}^+ - z_{n_1}^+) \\ & \times \left\{ \mathcal{P}_n [-igt \cdot \partial_j \mathcal{A}^-(z_{n_2}^+, \hat{\mathbf{z}}_{n_2})] [-igt \cdot \partial_j \mathcal{A}^-(z_{n_1}^+, \hat{\mathbf{z}}_{n_1})] \prod_{\substack{n=1 \\ n \neq n_1, n_2}}^N \right. \\ & \left. \times [-igt \cdot \mathcal{A}^-(z_n^+, \hat{\mathbf{z}}_n)] \right\} \\ & + \text{NNEik}, \end{aligned} \quad (3.11)$$

where the correction obtained from the double integration by parts in \mathbf{z} cancels exactly the NEik correction that comes from expanding the phase factor.

Up to this point, we have performed the analog of what was called the expansion around the classical trajectory in Refs. [36, 37]. Now one has to perform the so called small angle expansion, in which the small parameters are $\hat{\mathbf{z}}_n - \mathbf{z}$. In order to reach

Next-to-Eikonal accuracy, it is sufficient to expand the leading term in Eq. (3.11) to first order in any $\hat{\mathbf{z}}_n - \mathbf{z}$, and make the replacement $\hat{\mathbf{z}}_n \mapsto \mathbf{z}$ in the subleading term in Eq. (3.11). One thus gets

$$\begin{aligned}
& e^{i(z_N^+ - z_1^+) \frac{(\mathbf{q}-\mathbf{k})^2}{8k^+}} \int d^2\mathbf{z} e^{-i\mathbf{z}\cdot(\mathbf{q}-\mathbf{k})} \mathcal{E} = \int d^2\mathbf{z} e^{-i\mathbf{z}\cdot(\mathbf{q}-\mathbf{k})} \left\{ \mathcal{P}_n \prod_{n=1}^N [-igt \cdot \mathcal{A}^-(z_n^+, \mathbf{z})] \right\} \\
& + \frac{(\mathbf{q}^j + \mathbf{k}^j)}{2k^+} \int d^2\mathbf{z} e^{-i\mathbf{z}\cdot(\mathbf{q}-\mathbf{k})} \sum_{n_1=1}^N z_{n_1}^+ \\
& \times \left\{ \mathcal{P}_n [-igt \cdot \partial_j \mathcal{A}^-(z_{n_1}^+, \mathbf{z})] \prod_{\substack{n=1 \\ n \neq n_1}}^N [-igt \cdot \mathcal{A}^-(z_n^+, \mathbf{z})] \right\} \\
& - \frac{i}{2k^+} \int d^2\mathbf{z} e^{-i\mathbf{z}\cdot(\mathbf{q}-\mathbf{k})} \sum_{n_1=1}^{N-1} \sum_{n_2=n_1+1}^N (z_{n_2}^+ - z_{n_1}^+) \\
& \times \left\{ \mathcal{P}_n [-igt \cdot \partial_j \mathcal{A}^-(z_{n_2}^+, \mathbf{z})] [-igt \cdot \partial_j \mathcal{A}^-(z_{n_1}^+, \mathbf{z})] \prod_{\substack{n=1 \\ n \neq n_1, n_2}}^N [-igt \cdot \mathcal{A}^-(z_n^+, \mathbf{z})] \right\} \\
& + \text{NNEik}. \tag{3.12}
\end{aligned}$$

Now one needs to insert this result into Eq. (3.5), and using the definitions we obtained for the Wilson lines in Eq.(2.11) and Eq.(2.12), we have

$$\begin{aligned}
& \delta S_F(x, y) \Big|_{\text{pure } \mathcal{A}^-} = \int \frac{d^3\mathbf{q}}{(2\pi)^3} \int \frac{d^3\mathbf{k}}{(2\pi)^3} 2\pi\delta(q^+ - k^+) e^{-ix\cdot\mathbf{q}} e^{iy\cdot\mathbf{k}} (\not{\mathbf{q}} + m)\gamma^+(\not{\mathbf{k}} + m) \\
& \times \frac{\theta(k^+)}{(2k^+)^2} \int d^2\mathbf{z} e^{-i\mathbf{z}\cdot(\mathbf{q}-\mathbf{k})} \left\{ [\mathcal{U}_F(x^+, y^+; \mathbf{z}) - \mathbf{1}] \right. \\
& + \frac{(\mathbf{q}^j + \mathbf{k}^j)}{2k^+} \int_{y^+}^{x^+} dv^+ v^+ \mathcal{U}_F(x^+, v^+; \mathbf{z}) [-igt \cdot \partial_j \mathcal{A}^-(v^+, \mathbf{z})] \mathcal{U}_F(v^+, y^+; \mathbf{z}) \\
& - \frac{i}{2k^+} \int_{y^+}^{x^+} dv^+ \int_{v^+}^{x^+} dw^+ (w^+ - v^+) \mathcal{U}_F(x^+, w^+; \mathbf{z}) [-igt \cdot \partial_j \mathcal{A}^-(w^+, \mathbf{z})] \\
& \left. \times \mathcal{U}_F(w^+, v^+; \mathbf{z}) [-igt \cdot \partial_j \mathcal{A}^-(v^+, \mathbf{z})] \mathcal{U}_F(v^+, y^+; \mathbf{z}) \right\} + \text{NNEik} \tag{3.13}
\end{aligned}$$

for $x^+ > y^+$, and

$$\begin{aligned}
\delta S_F(x, y) \Big|_{\text{pure } \mathcal{A}^-} &= \int \frac{d^3 \underline{q}}{(2\pi)^3} \int \frac{d^3 \underline{k}}{(2\pi)^3} 2\pi \delta(q^+ - k^+) e^{-ix \cdot \underline{q}} e^{iy \cdot \underline{k}} (\underline{q} + m) \gamma^+(\underline{k} + m) \\
&\times \frac{\theta(-k^+)}{(2k^+)^2} \int d^2 \mathbf{z} e^{-iz \cdot (\mathbf{q} - \mathbf{k})} \left\{ - [\mathcal{U}_F^\dagger(y^+, x^+; \mathbf{z}) - \mathbf{1}] \right. \\
&- \frac{(\mathbf{q}^j + \mathbf{k}^j)}{2k^+} \int_{x^+}^{y^+} dv^+ v^+ \mathcal{U}_F^\dagger(v^+, x^+; \mathbf{z}) [+igt \cdot \partial_j \mathcal{A}^-(v^+, \mathbf{z})] \mathcal{U}_F^\dagger(y^+, v^+; \mathbf{z}) \\
&- \frac{i}{2k^+} \int_{x^+}^{y^+} dv^+ \int_{x^+}^{v^+} dw^+ (v^+ - w^+) \mathcal{U}_F^\dagger(w^+, x^+; \mathbf{z}) [+igt \cdot \partial_j \mathcal{A}^-(w^+, \mathbf{z})] \\
&\times \left. \mathcal{U}_F^\dagger(v^+, w^+; \mathbf{z}) [+igt \cdot \partial_j \mathcal{A}^-(v^+, \mathbf{z})] \mathcal{U}_F^\dagger(y^+, v^+; \mathbf{z}) \right\} + \text{NNEik} \quad (3.14)
\end{aligned}$$

for $y^+ > x^+$.

From the following property of the Wilson line

$$\partial_{\mathbf{z}} \mathcal{U}_F(x^+, y^+; \mathbf{z}) = \int_{y^+}^{x^+} dz^+ \mathcal{U}_F(x^+, z^+; \mathbf{z}) [-igt \cdot \partial_{\mathbf{z}} \mathcal{A}^-(z^+, \mathbf{z})] \mathcal{U}_F(z^+, y^+; \mathbf{z}). \quad (3.15)$$

and taking $(w^+ - v^+) = \int_{v^+}^{w^+} dz^+$ one can rewrite the bilocal term in Eq. (3.13)

$$\begin{aligned}
&\int_{y^+}^{x^+} dv^+ \int_{v^+}^{x^+} dw^+ (w^+ - v^+) \mathcal{U}_F(x^+, w^+; \mathbf{z}) [-igt \cdot \partial_j \mathcal{A}^-(w^+, \mathbf{z})] \\
&\quad \times \mathcal{U}_F(w^+, v^+; \mathbf{z}) [-igt \cdot \partial_j \mathcal{A}^-(v^+, \mathbf{z})] \mathcal{U}_F(v^+, y^+; \mathbf{z}) \\
&= \int_{y^+}^{x^+} dz^+ \mathcal{U}_F(x^+, z^+; \mathbf{z}) \overleftarrow{\partial_{\mathbf{z}}}_j \overrightarrow{\partial_{\mathbf{z}}}_j \mathcal{U}_F(z^+, y^+; \mathbf{z}). \quad (3.16)
\end{aligned}$$

Here only for the overlap of the $[y^+, x^+]$ interval with the support $[-L^+/2, L^+/2]$ of the background field one gets nontrivial contributions in the integration over z^+ . The bilocal term in Eq. (3.14), can be written as

$$\begin{aligned}
&\int_{x^+}^{y^+} dv^+ \int_{x^+}^{v^+} dw^+ (v^+ - w^+) \mathcal{U}_F^\dagger(w^+, x^+; \mathbf{z}) [+igt \cdot \partial_j \mathcal{A}^-(w^+, \mathbf{z})] \\
&\quad \times \mathcal{U}_F^\dagger(v^+, w^+; \mathbf{z}) [+igt \cdot \partial_j \mathcal{A}^-(v^+, \mathbf{z})] \mathcal{U}_F^\dagger(y^+, v^+; \mathbf{z}) \\
&= \int_{x^+}^{y^+} dz^+ \mathcal{U}_F^\dagger(z^+, x^+; \mathbf{z}) \overleftarrow{\partial_{\mathbf{z}}}_j \overrightarrow{\partial_{\mathbf{z}}}_j \mathcal{U}_F^\dagger(y^+, z^+; \mathbf{z}). \quad (3.17)
\end{aligned}$$

Lastly, one can also rewrite the third line in both Eq. (3.13) and Eq. (3.14) using the previous discussion and also

$$v^+ = \frac{1}{2} \left[\int_{z_{\min}^+}^{v^+} dz^+ - \int_{v^+}^{z_{\max}^+} dz^+ \right] + \frac{(z_{\max}^+ + z_{\min}^+)}{2}. \quad (3.18)$$

for the case $x^+ > y^+$, and we get

$$\begin{aligned}
 & \int d^2\mathbf{z} e^{-iz\cdot(\mathbf{q}-\mathbf{k})} \int_{z_{\min}^+}^{z_{\max}^+} dv^+ v^+ \mathcal{U}_F(z_{\max}^+, v^+; \mathbf{z}) [-igt\cdot\partial_{z^j}\mathcal{A}^-(v^+, \mathbf{z})] \mathcal{U}_F(v^+, z_{\min}^+; \mathbf{z}) \\
 = & -\frac{1}{2} \int d^2\mathbf{z} e^{-iz\cdot(\mathbf{q}-\mathbf{k})} \int_{z_{\min}^+}^{z_{\max}^+} dz^+ \left[\mathcal{U}_F(z_{\max}^+, z^+; \mathbf{z}) \overset{\leftarrow}{\partial}_{z^j} \mathcal{U}_F(z^+, z_{\min}^+; \mathbf{z}) \right] \\
 & + \frac{i(z_{\max}^+ + z_{\min}^+)}{2} (\mathbf{q}^j - \mathbf{k}^j) \int d^2\mathbf{z} e^{-iz\cdot(\mathbf{q}-\mathbf{k})} \mathcal{U}_F(z_{\max}^+, z_{\min}^+; \mathbf{z}). \tag{3.19}
 \end{aligned}$$

In the particular case of the quark propagation through the whole medium, meaning $x^+ > L^+/2$ and $y^+ < -L^+/2$, we have $z_{\max}^+ = L^+/2$ and $z_{\min}^+ = -L^+/2$, so that $z_{\max}^+ + z_{\min}^+ = 0$, which implies that the extra term proportional to the eikonal contribution in Eq. (3.19) vanishes. All in all, we obtain the result for the case of the quark

$$\begin{aligned}
 S_F(x, y) \Big|_{\text{pure } \mathcal{A}^-} &= \int \frac{d^3q}{(2\pi)^3} \int \frac{d^3k}{(2\pi)^3} 2\pi\delta(q^+ - k^+) \frac{\theta(k^+)}{(2k^+)^2} e^{-ix\cdot\check{q} + iy\cdot\check{k}} (\check{q} + m)\gamma^+ \\
 &\times (\check{k} + m) \int d^2\mathbf{z} e^{-iz\cdot(\mathbf{q}-\mathbf{k})} \left\{ \mathcal{U}_F\left(\frac{L^+}{2}, -\frac{L^+}{2}; \mathbf{z}\right) \right. \\
 &\quad - \frac{(\mathbf{q}^j + \mathbf{k}^j)}{4k^+} \int_{-\frac{L^+}{2}}^{\frac{L^+}{2}} dz^+ \left[\mathcal{U}_F\left(\frac{L^+}{2}, z^+; \mathbf{z}\right) \overset{\leftarrow}{\partial}_{z^j} \mathcal{U}_F\left(z^+, -\frac{L^+}{2}; \mathbf{z}\right) \right] \\
 &\quad \left. - \frac{i}{2k^+} \int_{-\frac{L^+}{2}}^{\frac{L^+}{2}} dz^+ \left[\mathcal{U}_F\left(\frac{L^+}{2}, z^+; \mathbf{z}\right) \overset{\leftarrow}{\partial}_{z^j} \overset{\rightarrow}{\partial}_{z^j} \mathcal{U}_F\left(z^+, -\frac{L^+}{2}; \mathbf{z}\right) \right] \right\} + \text{NNEik}. \tag{3.20}
 \end{aligned}$$

For $x^+ < y^+$, the situation is analog. In particular, for $y^+ > L^+/2$ and $x^+ < -L^+/2$, one finds the result for the antiquark:

$$\begin{aligned}
 S_F(x, y) \Big|_{\text{pure } \mathcal{A}^-} &= \int \frac{d^3q}{(2\pi)^3} \int \frac{d^3k}{(2\pi)^3} 2\pi\delta(q^+ - k^+) \frac{\theta(-k^+)}{(2k^+)^2} e^{-ix\cdot\check{q} + iy\cdot\check{k}} (\check{q} + m)\gamma^+ \\
 &\times (\check{k} + m) \int d^2\mathbf{z} e^{-iz\cdot(\mathbf{q}-\mathbf{k})} \left\{ -\mathcal{U}_F^\dagger\left(\frac{L^+}{2}, -\frac{L^+}{2}; \mathbf{z}\right) \right. \\
 &\quad - \frac{(\mathbf{q}^j + \mathbf{k}^j)}{4k^+} \int_{-\frac{L^+}{2}}^{\frac{L^+}{2}} dz^+ \left[\mathcal{U}_F^\dagger\left(z^+, -\frac{L^+}{2}; \mathbf{z}\right) \overset{\leftarrow}{\partial}_{z^j} \mathcal{U}_F^\dagger\left(\frac{L^+}{2}, z^+; \mathbf{z}\right) \right] \\
 &\quad \left. - \frac{i}{2k^+} \int_{-\frac{L^+}{2}}^{\frac{L^+}{2}} dz^+ \left[\mathcal{U}_F^\dagger\left(z^+, -\frac{L^+}{2}; \mathbf{z}\right) \overset{\leftarrow}{\partial}_{z^j} \overset{\rightarrow}{\partial}_{z^j} \mathcal{U}_F^\dagger\left(\frac{L^+}{2}, z^+; \mathbf{z}\right) \right] \right\} + \text{NNEik}. \tag{3.21}
 \end{aligned}$$

Thus, we have the final result for a quark propagator with a finite width of the target in Eq (3.20), and Eq(3.21) for the antiquark propagator.

3.2 Including the interactions with the transverse component of the background field

Let us now concentrate on the corrections beyond the eikonal approximation that stem from relaxing the assumption that neglects all components of the background field except \mathcal{A}^- . We include the interaction with the perpendicular component, \mathcal{A}_\perp .

We use the results of the previous section 3.1 and we compute the interactions with the perpendicular component via perturbation theory in position space. Thus, for a single insertion of \mathcal{A}_j , the contribution is computed via

$$\delta S_F(x, y) \Big|_{\text{single } \mathcal{A}_\perp} = \int d^4 z S_F(x, z) \Big|_{\text{pure } \mathcal{A}^-} [-ig \gamma^j t^a] \mathcal{A}_j^a(\underline{z}) S_F(z, y) \Big|_{\text{pure } \mathcal{A}^-}. \quad (3.22)$$

In Eq. (3.22), the integration in z^+ gives a L^+ factor for $L^+ \rightarrow 0$, whereas \mathcal{A}_j^a is independent of L^+ in that limit. One may think that this contribution would then start already at NEik order, however this naive power counting fails due to the instantaneous contribution to the quark propagator, see Eq. (2.16). The delta distribution gives a trivial contribution when integrating over z^+ . In that case, the transverse field $\mathcal{A}_j^a(\underline{z})$ is taken at $z^+ = x^+$ or at $z^+ = y^+$, which is possible only if x^+ or y^+ belong to the support $[-L^+/2, L^+/2]$.

In order to avoid these complications, we focus on the case in which neither x^+ nor y^+ belong to the support $[-L^+/2, L^+/2]$ of the background field and the naive power counting in L^+ applies. Then, Eq. (3.22) starts at NEik accuracy, with a term obtained by using the eikonal expression Eq.(2.16) for both propagators in \mathcal{A}^- background.

For $x^+ > L^+/2$ and $y^+ < -L^+/2$, one obtains

$$\begin{aligned} \delta S_F(x, y) \Big|_{\text{single } \mathcal{A}_\perp} &= \int d^4 z \int \frac{d^3 q}{(2\pi)^3} \int \frac{d^3 p_2}{(2\pi)^3} 2\pi \delta(q^+ - p_2^+) e^{-ix \cdot \not{q} + iz \cdot \not{p}_2} \frac{(\not{q} + m) \gamma^+}{(2q^+)^2} \\ &\times (\not{p}_2 + m) \int d^2 \mathbf{v} e^{-iv \cdot (\mathbf{q} - \mathbf{p}_2)} \theta(q^+) \mathcal{U}_F \left(\frac{L^+}{2}, z^+; \mathbf{v} \right) [-ig \gamma^j t^a] \mathcal{A}_j^a(\underline{z}) \\ &\times \int \frac{d^3 p_1}{(2\pi)^3} \int \frac{d^3 k}{(2\pi)^3} 2\pi \delta(p_1^+ - k^+) e^{-iz \cdot \not{p}_1 + iy \cdot \not{k}} \frac{(\not{p}_1 + m) \gamma^+ (\not{k} + m)}{(2k^+)^2} \\ &\times \int d^2 \mathbf{u} e^{-iu \cdot (\mathbf{p}_1 - \mathbf{k})} \theta(k^+) \mathcal{U}_F \left(z^+, -\frac{L^+}{2}; \mathbf{u} \right) + \text{NNEik}, \end{aligned} \quad (3.23)$$

due to the ordering $x^+ > z^+ > y^+$, only the terms with positive light-cone momentum q^+ or k^+ from Eq. (2.16) survive. Then, the integration over z^- yields $p_1^+ = p_2^+ = k^+ = q^+$. The Dirac algebra in Eq. (3.23) can then be performed as

$$\begin{aligned} &(\not{q} + m) \gamma^+ (\not{p}_2 + m) \gamma^j (\not{p}_1 + m) \gamma^+ (\not{k} + m) \\ &= (2k^+) (\not{q} + m) \left[\gamma^j \gamma^+ \gamma^i \mathbf{p}_1^i + \mathbf{p}_2^i \gamma^i \gamma^+ \gamma^j \right] (\not{k} + m). \end{aligned} \quad (3.24)$$

where we can write \mathbf{p}_1^i and \mathbf{p}_2^i in the numerator (3.24) as derivatives with respect to \mathbf{u}^i or \mathbf{v}^i acting on the phase factor in Eq. (3.23), then one finally gets the expression

$$\begin{aligned} \delta S_F(x, y) \Big|_{\text{single } \mathcal{A}_\perp} &= \int \frac{d^3 q}{(2\pi)^3} \int \frac{d^3 k}{(2\pi)^3} 2\pi \delta(q^+ - k^+) \frac{\theta(k^+)}{(2k^+)^3} e^{-ix \cdot \not{q}} e^{iy \cdot \not{k}} \\ &\times (\not{q} + m) \gamma^j \gamma^+ \gamma^i (\not{k} + m) \int d^3 \underline{z} \left[e^{-iz \cdot \mathbf{q}} \mathcal{U}_F \left(\frac{L^+}{2}, z^+; \mathbf{z} \right) \right] \\ &\times \left[\overleftarrow{\partial}_{z^i} [gt \cdot \mathcal{A}_i(\underline{z})] - [gt \cdot \mathcal{A}_j(\underline{z})] \overrightarrow{\partial}_{z^i} \right] \left[\mathcal{U}_F \left(z^+, -\frac{L^+}{2}; \mathbf{z} \right) e^{iz \cdot \mathbf{k}} \right] + \text{NNEik} \end{aligned} \quad (3.25)$$

Note that the transverse derivatives here act on both the Wilson lines and the phase factors.

The result for the case of the antiquark propagating through a shockwave, that is, $y^+ > L^+/2$ and $x^+ < -L^+/2$, can be computed in a similar manner only keeping terms with negative q^+ or k^+ from Eq. (2.16) this time. This result is

$$\begin{aligned} \delta S_F(x, y) \Big|_{\text{single } \mathcal{A}_\perp} &= \int \frac{d^3 \underline{q}}{(2\pi)^3} \int \frac{d^3 \underline{k}}{(2\pi)^3} 2\pi \delta(q^+ - k^+) \frac{\theta(-k^+)}{(2k^+)^3} e^{-ix \cdot \underline{\check{q}}} e^{iy \cdot \underline{\check{k}}} \\ &\times (\not{\check{q}} + m) \gamma^j \gamma^+ \gamma^i (\not{\check{k}} + m) \int d^3 \underline{z} \left[e^{-iz \cdot \mathbf{q}} \mathcal{U}_F^+(z^+, -\frac{L^+}{2}; \mathbf{z}) \right] \\ &\times \left[\overleftarrow{\partial}_{z^j} [gt \cdot \mathcal{A}_i(\underline{z})] - [gt \cdot \mathcal{A}_j(\underline{z})] \overrightarrow{\partial}_{z^i} \right] \left[\mathcal{U}_F^+\left(\frac{L^+}{2}, z^+; \mathbf{z}\right) e^{iz \cdot \mathbf{k}} \right] + \text{NNEik}. \end{aligned} \quad (3.26)$$

At this point, in order to compute the full NEik corrections that stem from including the transverse field insertions, one needs to include the insertions of two such fields. In this case, the contribution looks like

$$\begin{aligned} \delta S_F(x, y) \Big|_{\text{double } \mathcal{A}_\perp} &= \int d^4 z \int d^4 z' S_F(x, z') \Big|_{\text{pure } \mathcal{A}^-} [-ig \gamma^j t^b] \mathcal{A}_j^b(\underline{z}') S_F(z', z) \Big|_{\text{pure } \mathcal{A}^-} \\ &\times [-ig \gamma^i t^a] \mathcal{A}_i^a(\underline{z}) S_F(z, y) \Big|_{\text{pure } \mathcal{A}^-}. \end{aligned} \quad (3.27)$$

Following the previous discussion at the beginning of this section about power counting, one realises that due to the extra integration, each extra insertion would bring an extra power of L^+ for $L^+ \rightarrow 0$ naively. However, due to the instantaneous contribution to the quark propagator, see Eq. (2.16), this naive power counting fails as discussed previously. Let us focus on the cases in which neither x^+ nor y^+ belong to the support $[-L^+/2, L^+/2]$ of the background field and the instantaneous term in Eq. (2.16) does not contribute to the external legs in Eq. (3.27). By contrast, the instantaneous term contributes to the internal line, giving the dominant contribution to Eq. (3.27), which is at NEik accuracy.

For $x^+ > L^+/2$ and $y^+ < -L^+/2$, one obtains

$$\begin{aligned} \delta S_F(x, y) \Big|_{\text{double } \mathcal{A}_\perp} &= \int d^4 z \int d^4 z' \int \frac{d^3 \underline{q}}{(2\pi)^3} \int \frac{d^3 \underline{p}_2}{(2\pi)^3} 2\pi \delta(q^+ - p_2^+) e^{-ix \cdot \underline{\check{q}} + iz' \cdot \underline{\check{p}}_2} \\ &\times \frac{(\not{\check{q}} + m) \gamma^+ (\not{\check{p}}_2 + m)}{(2q^+)^2} \int d^2 \mathbf{v} e^{-iv \cdot (\mathbf{q} - \mathbf{p}_2)} \theta(q^+) \mathcal{U}_F\left(\frac{L^+}{2}, z'^+; \mathbf{v}\right) \\ &\times [-ig \gamma^j t^b] \mathcal{A}_j^b(\underline{z}') \delta^{(3)}(\underline{z}' - \underline{z}) \gamma^+ \int \frac{dp^+}{2\pi} \frac{i}{2p^+} e^{-ip^+(z'^- - z^-)} [-ig \gamma^i t^a] \mathcal{A}_i^a(\underline{z}) \\ &\times \int \frac{d^3 \underline{p}_1}{(2\pi)^3} \int \frac{d^3 \underline{k}}{(2\pi)^3} 2\pi \delta(p_1^+ - k^+) e^{-iz \cdot \underline{\check{p}}_1 + iy \cdot \underline{\check{k}}} \frac{(\not{\check{p}}_1 + m) \gamma^+ (\not{\check{k}} + m)}{(2k^+)^2} \\ &\times \int d^2 \mathbf{u} e^{-iu \cdot (\mathbf{p}_1 - \mathbf{k})} \theta(k^+) \mathcal{U}_F\left(z^+, -\frac{L^+}{2}; \mathbf{u}\right) + \text{NNEik}, \end{aligned} \quad (3.28)$$

using Eq.(2.15) for the sign function. Finally for the case of the quark going through the whole shockwave is given by:

$$\begin{aligned}
\delta S_F(x, y) \Big|_{\text{double } \mathcal{A}_\perp} &= \int \frac{d^3 q}{(2\pi)^3} \int \frac{d^3 k}{(2\pi)^3} 2\pi \delta(q^+ - k^+) \frac{\theta(k^+)}{(2k^+)^3} e^{-ix \cdot \check{q}} e^{iy \cdot \check{k}} \\
&\times (\not{\check{q}} + m) \gamma^j \gamma^+ \gamma^i (\not{\check{k}} + m) \int d^3 \underline{z} e^{-iz \cdot (\mathbf{q} - \mathbf{k})} \\
&\times (-i) \mathcal{U}_F\left(\frac{L^+}{2}, z^+; \mathbf{z}\right) [gt \cdot \mathcal{A}_j(\underline{z})] [gt \cdot \mathcal{A}_i(\underline{z})] \mathcal{U}_F\left(z^+, -\frac{L^+}{2}; \mathbf{z}\right) + \text{NNEik}
\end{aligned} \tag{3.29}$$

A similar computation corresponding to the case of an antiquark going through the whole shockwave, where $y^+ > L^+/2$ and $x^+ < -L^+/2$, leads to the final result:

$$\begin{aligned}
\delta S_F(x, y) \Big|_{\text{double } \mathcal{A}_\perp} &= \int \frac{d^3 q}{(2\pi)^3} \int \frac{d^3 k}{(2\pi)^3} 2\pi \delta(q^+ - k^+) \frac{\theta(-k^+)}{(2k^+)^3} e^{-ix \cdot \check{q}} e^{iy \cdot \check{k}} \\
&\times (\not{\check{q}} + m) \gamma^j \gamma^+ \gamma^i (\not{\check{k}} + m) \int d^3 \underline{z} e^{-iz \cdot (\mathbf{q} - \mathbf{k})} \\
&\times (-i) \mathcal{U}_F^\dagger\left(z^+, -\frac{L^+}{2}; \mathbf{z}\right) [gt \cdot \mathcal{A}_j(\underline{z})] [gt \cdot \mathcal{A}_i(\underline{z})] \mathcal{U}_F^\dagger\left(\frac{L^+}{2}, z^+; \mathbf{z}\right) + \text{NNEik}.
\end{aligned} \tag{3.30}$$

Finally, one could naively generalize such results to the case of higher number of insertions of the transverse components of the background field. Keeping only the instantaneous term in the internal quark lines, only one integration in z^+ would survive, thus giving a Next-to-Eikonal contribution. However, that contribution vanishes, because the instantaneous term is proportional to γ^+ , which anticommutes with the transverse γ^j . Hence, there is no non-vanishing contribution with two successive instantaneous quark lines separated only by an \mathcal{A}_\perp insertion.

3.3 Quark propagator at next-to-eikonal accuracy

In sections 3.1 and 3.2, we have computed up to next-to-eikonal accuracy the quark (and antiquark) propagator considering both the finite width of the target and the interaction with the perpendicular component of the background field. For the case of the quark, our final expressions is given in Eq.(3.20) for the propagator through a pure \mathcal{A}^- field at NEik, and Eqs. (3.25) and (3.29) provide the corrections due to single and double \mathcal{A}_\perp insertions, respectively. One finds a difference in these expressions in the spinor structure since, the one in the pure \mathcal{A}^- background at eikonal and NEik accuracy differ from the spinor structure resulting from single and double \mathcal{A}_\perp insertions. Therefore one can separate the spinor structure into symmetric and antisymmetric terms in i, j as

$$\gamma^j \gamma^+ \gamma^i = -\gamma^+ \gamma^j \gamma^i = -\gamma^+ \left(\frac{\{\gamma^j, \gamma^i\}}{2} + \frac{[\gamma^j, \gamma^i]}{2} \right) = \delta^{ij} \gamma^+ + \gamma^+ \frac{[\gamma^i, \gamma^j]}{2}, \tag{3.31}$$

now the pure \mathcal{A}^- contributions, $(\not{\check{q}} + m) \gamma^+ (\not{\check{k}} + m)$, can be combined with the symmetric part in Eq.(3.31). We propose to split the propagator contributions at NEik as

$$S_F(x, y) = S_F(x, y) \Big|_{\text{unpol.}} + S_F(x, y) \Big|_{\text{h. dep.}} \quad (3.32)$$

where the first term corresponds to an unpolarized piece and the second one to an helicity-dependent piece, since $[\gamma^i, \gamma^j]$ is proportional to the quark helicity when acting on a u or v spinor.

Combining the contributions from Eqs. (3.20), (3.25) and (3.29), we get the expressions for the quark propagator through the medium, for $x^+ > L^+/2$ and $y^+ < -L^+/2$,

$$\begin{aligned} S_F(x, y) \Big|_{\text{unpol.}} &= \int \frac{d^3 \underline{q}}{(2\pi)^3} \int \frac{d^3 \underline{k}}{(2\pi)^3} 2\pi \delta(q^+ - k^+) \frac{\theta(k^+)}{(2k^+)^2} e^{-ix \cdot \underline{q}} e^{iy \cdot \underline{k}} (\not{q} + m) \gamma^+ (\not{k} + m) \\ &\times \int d^2 \mathbf{z} e^{-iz \cdot (\mathbf{q} - \mathbf{k})} \left\{ \mathcal{U}_F \left(\frac{L^+}{2}, -\frac{L^+}{2}; \mathbf{z} \right) \right. \\ &\quad - \frac{(\mathbf{q}^j + \mathbf{k}^j)}{4k^+} \int_{-\frac{L^+}{2}}^{\frac{L^+}{2}} dz^+ \left[\mathcal{U}_F \left(\frac{L^+}{2}, z^+; \mathbf{z} \right) \overleftrightarrow{\mathcal{D}}_{z^j} \mathcal{U}_F \left(z^+, -\frac{L^+}{2}; \mathbf{z} \right) \right] \\ &\quad \left. - \frac{i}{2k^+} \int_{-\frac{L^+}{2}}^{\frac{L^+}{2}} dz^+ \left[\mathcal{U}_F \left(\frac{L^+}{2}, z^+; \mathbf{z} \right) \overleftarrow{\mathcal{D}}_{z^j} \overrightarrow{\mathcal{D}}_{z^j} \mathcal{U}_F \left(z^+, -\frac{L^+}{2}; \mathbf{z} \right) \right] \right\} + \text{NNEik} \quad (3.33) \end{aligned}$$

and

$$\begin{aligned} S_F(x, y) \Big|_{\text{h. dep.}} &= \int \frac{d^3 \underline{q}}{(2\pi)^3} \int \frac{d^3 \underline{k}}{(2\pi)^3} 2\pi \delta(q^+ - k^+) \frac{\theta(k^+)}{(2k^+)^3} e^{-ix \cdot \underline{q}} e^{iy \cdot \underline{k}} \\ &\times (\not{q} + m) \gamma^+ \frac{[\gamma^i, \gamma^j]}{4} (\not{k} + m) \int d^2 \mathbf{z} e^{-iz \cdot (\mathbf{q} - \mathbf{k})} \\ &\times \int_{-\frac{L^+}{2}}^{\frac{L^+}{2}} dz^+ \mathcal{U}_F \left(\frac{L^+}{2}, z^+; \mathbf{z} \right) g t \cdot \mathcal{F}_{ij}(\underline{z}) \mathcal{U}_F \left(z^+, -\frac{L^+}{2}; \mathbf{z} \right) + \text{NNEik}, \quad (3.34) \end{aligned}$$

where we used the following notation for the covariant derivatives and field strength tensor:

$$\overrightarrow{\mathcal{D}}_{z^\mu} \equiv \partial_{z^\mu} + i g t \cdot \mathcal{A}_\mu(\underline{z}) \quad (3.35)$$

$$\overleftarrow{\mathcal{D}}_{z^\mu} \equiv \partial_{z^\mu} - i g t \cdot \mathcal{A}_\mu(\underline{z}) \quad (3.36)$$

$$\overleftrightarrow{\mathcal{D}}_{z^\mu} \equiv \overrightarrow{\mathcal{D}}_{z^\mu} - \overleftarrow{\mathcal{D}}_{z^\mu} = \overleftrightarrow{\partial}_{z^\mu} + 2i g t \cdot \mathcal{A}_\mu(\underline{z}) \quad (3.37)$$

$$\mathcal{F}_{ij}^a(\underline{z}) \equiv \partial_{z^i} \mathcal{A}_j^a(\underline{z}) - \partial_{z^j} \mathcal{A}_i^a(\underline{z}) - g f^{abc} \mathcal{A}_i^b(\underline{z}) \mathcal{A}_j^c(\underline{z}). \quad (3.38)$$

Note that in Eq.(3.33) the transverse covariant derivatives act only on the Wilson lines, not on the phase factors. Since no explicit gauge condition has been imposed on the background field, the results Eq.(3.33) and Eq.(3.34) are written in terms of gauge-covariant building blocks as expected. In Eq.(3.33), the first term corresponds to the typical eikonal contribution, whereas the remaining two terms and the helicity dependent contribution given in Eq.(3.34) are the NEik corrections to the quark propagator passing through medium.

Similar arguments hold for the antiquark propagator given in Eqs. (3.21), (3.26) and (3.30), leading to the following two separate contributions for the case of $y^+ > L^+/2$ and $x^+ < -L^+/2$:

$$\begin{aligned}
 S_F(x, y) \Big|_{\text{unpol.}} &= \int \frac{d^3 q}{(2\pi)^3} \int \frac{d^3 k}{(2\pi)^3} 2\pi \delta(q^+ - k^+) \frac{\theta(-k^+)}{(2k^+)^2} e^{-ix \cdot \check{q}} e^{iy \cdot \check{k}} (\check{q} + m) \gamma^+ (\check{k} + m) \\
 &\times \int d^2 \mathbf{z} e^{-iz \cdot (\mathbf{q} - \mathbf{k})} \left\{ -\mathcal{U}_F^\dagger \left(\frac{L^+}{2}, -\frac{L^+}{2}; \mathbf{z} \right) \right. \\
 &\quad - \frac{(\mathbf{q}^i + \mathbf{k}^j)}{4k^+} \int_{-\frac{L^+}{2}}^{\frac{L^+}{2}} dz^+ \left[\mathcal{U}_F^\dagger \left(z^+, -\frac{L^+}{2}; \mathbf{z} \right) \overleftrightarrow{\mathcal{D}}_{z^j} \mathcal{U}_F^\dagger \left(\frac{L^+}{2}, z^+; \mathbf{z} \right) \right] \\
 &\quad \left. - \frac{i}{2k^+} \int_{-\frac{L^+}{2}}^{\frac{L^+}{2}} dz^+ \left[\mathcal{U}_F^\dagger \left(z^+, -\frac{L^+}{2}; \mathbf{z} \right) \overleftrightarrow{\mathcal{D}}_{z^i} \overrightarrow{\mathcal{D}}_{z^j} \mathcal{U}_F^\dagger \left(\frac{L^+}{2}, z^+; \mathbf{z} \right) \right] \right\} + \text{NNEik} \quad (3.39)
 \end{aligned}$$

and

$$\begin{aligned}
 S_F(x, y) \Big|_{\text{h. dep.}} &= \int \frac{d^3 q}{(2\pi)^3} \int \frac{d^3 k}{(2\pi)^3} 2\pi \delta(q^+ - k^+) \frac{\theta(-k^+)}{(2k^+)^3} e^{-ix \cdot \check{q}} e^{iy \cdot \check{k}} \\
 &\times (\check{q} + m) \gamma^+ \frac{[\gamma^i, \gamma^j]}{4} (\check{k} + m) \int d^2 \mathbf{z} e^{-iz \cdot (\mathbf{q} - \mathbf{k})} \\
 &\times \int_{-\frac{L^+}{2}}^{\frac{L^+}{2}} dz^+ \mathcal{U}_F^\dagger \left(z^+, -\frac{L^+}{2}; \mathbf{z} \right) g^t \cdot \mathcal{F}_{ij}(\underline{z}) \mathcal{U}_F^\dagger \left(\frac{L^+}{2}, z^+; \mathbf{z} \right) + \text{NNEik}. \quad (3.40)
 \end{aligned}$$

These final expressions summarize the result for the quark and antiquark propagators at NEik accuracy going through the whole medium, where we take into account corrections that stem from both, considering a finite width of the target and the interactions with the transverse component of the background field. The final results are written in a gauge-covariant form.

3.4 Forward quark-nucleus scattering

In this final section, we apply the obtained results to study the inclusive forward quark-nucleus scattering in pA collisions. Although forward quark production occurs at high energies and therefore one may suggest that these NEik corrections, that are energy suppressed, can be neglected in this case, for moderate energies these corrections can improve the description of experimental data. This is the case for experiments such as at RHIC and at the future EIC, where the NEik corrections are expected to give more precise information.

In the rest of this section, first we compute the quark-nucleus scattering amplitude by using the LSZ reduction formula and then use the computed amplitude to calculate the unpolarized forward quark production cross section as well as the quark helicity asymmetry at NEik accuracy.

3.4.1 Quark-target scattering amplitude from the LSZ reduction

Let us start from the definition of the free fermion fields:

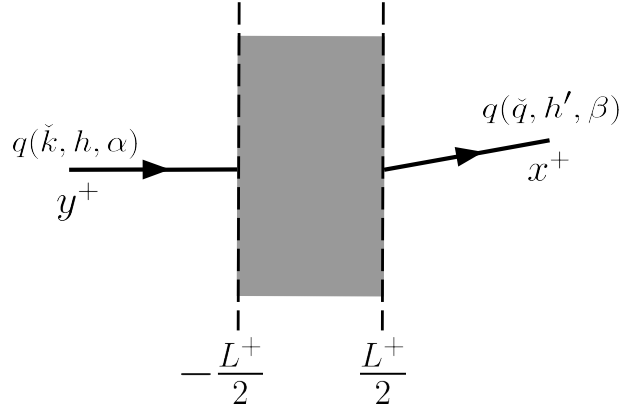


FIGURE 3.1: Elastic scattering of a quark on a strong background field.

$$\Psi_\alpha(x) = \int_0^\infty \frac{dp^+}{2\pi} \int \frac{d^2\mathbf{p}}{(2\pi)^2} \frac{1}{2p^+} \sum_h \left[\hat{b}(\check{p}, h, \alpha) u(\check{p}, h) e^{-i\check{p}\cdot x} + \hat{d}^\dagger(\check{p}, h, \alpha) v(\check{p}, h) e^{i\check{p}\cdot x} \right] \quad (3.41)$$

$$\bar{\Psi}_\alpha(x) = \int_0^\infty \frac{dp^+}{2\pi} \int \frac{d^2\mathbf{p}}{(2\pi)^2} \frac{1}{2p^+} \sum_h \left[\hat{d}(\check{p}, h, \alpha) \bar{v}(\check{p}, h) e^{-i\check{p}\cdot x} + \hat{b}^\dagger(\check{p}, h, \alpha) \bar{u}(\check{p}, h) e^{i\check{p}\cdot x} \right] \quad (3.42)$$

where \check{p} is the on-shell momentum defined in section 2.3 and $h = \pm 1/2$ is helicity. \hat{b} and \hat{b}^\dagger (\hat{d} and \hat{d}^\dagger) are the annihilation and creation operators, respectively, of a quark (antiquark). Using the following property of the spinors

$$\bar{u}(\check{p}, h) \gamma^+ u(\check{k}, h') = \sqrt{2p^+} \sqrt{2k^+} \delta_{hh'}, \quad (3.43)$$

Eqs. (3.41) and (3.42) can be inverted in order to express the annihilation and creation operators for a quark in terms of the free quark field as

$$\hat{b}(\check{k}, h, \alpha) = \int d^2\mathbf{x} \int dx^- e^{ix\cdot\check{k}} \bar{u}(\check{k}, h) \gamma^+ \Psi_\alpha(x), \quad (3.44)$$

$$\hat{b}^\dagger(\check{k}, h, \alpha) = \int d^2\mathbf{x} \int dx^- e^{-ix\cdot\check{k}} \bar{\Psi}_\alpha(x) \gamma^+ u(\check{k}, h). \quad (3.45)$$

Our process is a quark that undergoes multiple scatterings while it propagates through the target, that is, the strong background field. The quark is considered free in the asymptotic past and future. Thus, one can build the corresponding "in" and "out" Fock space. The annihilation operator of a quark in the "out" Fock space and creation operator of a quark in the "in" Fock space with the interacting quark field $\Psi_\beta(x)$ can be written as

$$\hat{b}_{\text{out}}(\check{q}, h', \beta) = \lim_{x^+ \rightarrow +\infty} \int d^2\mathbf{x} \int dx^- e^{ix\cdot\check{q}} \bar{u}(\check{q}, h') \gamma^+ \Psi_\beta(x), \quad (3.46)$$

$$\hat{b}_{\text{in}}^\dagger(\check{k}, h, \alpha) = \lim_{y^+ \rightarrow -\infty} \int d^2\mathbf{y} \int dy^- e^{-iy\cdot\check{k}} \bar{\Psi}_\alpha(y) \gamma^+ u(\check{k}, h) \quad (3.47)$$

The S-matrix element for quark scattering on the background field (see Fig. 3.1) is defined as

$$S_{q(\check{q},h',\beta)\leftarrow q(\check{k},h,\alpha)} = \langle 0|\hat{b}_{\text{out}}(\check{q},h,\beta)\hat{b}_{\text{in}}^\dagger(\check{k},h,\alpha)|0\rangle \quad (3.48)$$

with the vacuum states $\langle 0| = \langle 0|_{\text{in}} = \langle 0|_{\text{out}}$. Using Eqs. (3.46) and (3.47), the S-matrix element can be rewritten as

$$S_{q(\check{q},h',\beta)\leftarrow q(\check{k},h,\alpha)} = \lim_{x^+\rightarrow+\infty} \lim_{y^+\rightarrow-\infty} \int d^2\mathbf{x} \int dx^- \int d^2\mathbf{y} \int dy^- e^{ix\cdot\check{q}-iy\cdot\check{k}} \times \bar{u}(\check{q},h')\gamma^+ S_F(x,y)_{\beta\alpha}\gamma^+ u(\check{k},h) \quad (3.49)$$

with the following definition for the Feynman propagator

$$S_F(x,y)_{\beta\alpha} = \langle 0|\hat{T}[\Psi_\beta(x)\bar{\Psi}_\alpha(y)]|0\rangle \quad (3.50)$$

where \hat{T} is the time ordering operator. Finally, the quark Feynman propagator in background field, $S_F(x,y)_{\alpha\beta}$, is written in Eq. (3.32) with the explicit expressions of the unpolarized piece given in Eq. (3.33) and the helicity dependent piece given in Eq. (3.34) at NEik accuracy. Let us first define the scattering amplitude:

$$\mathcal{M}_{q(\check{q},h',\beta)\leftarrow q(\check{k},h,\alpha)} \equiv \mathcal{M}_{\alpha\beta}^{hh'}(\underline{k}, \mathbf{q}) \quad (3.51)$$

which appears in the S-matrix as

$$S_{q(\check{q},h',\beta)\leftarrow q(\check{k},h,\alpha)} = (2k^+)2\pi\delta(q^+ - k^+)i\mathcal{M}_{\alpha\beta}^{hh'}(\underline{k}, \mathbf{q}). \quad (3.52)$$

In order to extract this amplitude, one needs to compare the expressions Eq. (3.49) and Eq. (3.52), where the first one can be computed inserting into the definition the Eqs. (3.32), (3.33) and (3.34). After performing these calculations one obtains the following scattering amplitude at NEik accuracy:

$$i\mathcal{M}_{\alpha\beta}^{hh'}(\underline{k}, \mathbf{q}) = \frac{1}{2k^+} \int d^2\mathbf{z} e^{-iz\cdot(\mathbf{q}-\mathbf{k})} \bar{u}(\check{q},h')\gamma^+ \left\{ \mathcal{U}_F\left(\frac{L^+}{2}, -\frac{L^+}{2}; \mathbf{z}\right) \right. \quad (3.53) \\ + \frac{i[\gamma^i, \gamma^j]}{8k^+} \int_{-\frac{L^+}{2}}^{\frac{L^+}{2}} dz^+ \left[\mathcal{U}_F\left(\frac{L^+}{2}, z^+; \mathbf{z}\right) \left(-igt \cdot \mathcal{F}_{ij}(\underline{z}) \right) \mathcal{U}_F\left(z^+, -\frac{L^+}{2}; \mathbf{z}\right) \right] \\ - \frac{i}{2k^+} \int_{-\frac{L^+}{2}}^{\frac{L^+}{2}} dz^+ \left[\mathcal{U}_F\left(\frac{L^+}{2}, z^+; \mathbf{z}\right) \overleftarrow{\mathcal{D}}_{z^j} \overrightarrow{\mathcal{D}}_{z^j} \mathcal{U}_F\left(z^+, -\frac{L^+}{2}; \mathbf{z}\right) \right] \\ \left. - \frac{(\mathbf{q}^j + \mathbf{k}^j)}{4k^+} \int_{-\frac{L^+}{2}}^{\frac{L^+}{2}} dz^+ \left[\mathcal{U}_F\left(\frac{L^+}{2}, z^+; \mathbf{z}\right) \overleftrightarrow{\mathcal{D}}_{z^j} \mathcal{U}_F\left(z^+, -\frac{L^+}{2}; \mathbf{z}\right) \right] \right\}_{\alpha\beta} u(\check{k},h)$$

We would like to emphasize that the second term in Eq. (3.53) which is proportional to $[\gamma^i, \gamma^j]$ introduces the helicity dependence on the scattering amplitude at NEik order and it governs the polarization effects during the scattering process. This helicity dependent term can be further simplified by using the helicity operator S^3 , which acts on spinors as

$$S^3 u(\check{k},h) = hu(\check{k},h), \quad (3.54)$$

$$S^3 v(\check{k},h) = -hv(\check{k},h). \quad (3.55)$$

Since $[\gamma^i, \gamma^j] = -4i\epsilon^{ij}S^3$, the spinor structure of the helicity dependent term in the scattering amplitude given in Eq. (3.53) can be simplified to

$$\bar{u}(\check{q}, h') \gamma^+ \frac{[\gamma^i, \gamma^j]}{4} u(\check{k}, h) = -i\epsilon^{ij}h \bar{u}(\check{q}, h') \gamma^+ u(\check{k}, h) \quad (3.56)$$

where ϵ^{ij} is the antisymmetric tensor with $\epsilon^{12} = +1$. By using this simplification for the helicity dependent term and the relation in Eq. (3.43), the scattering amplitude can be written at NEik accuracy as

$$\begin{aligned} i\mathcal{M}_{\alpha\beta}^{hh'}(\underline{k}, \mathbf{q}) &= \delta_{hh'} \int d^2\mathbf{z} e^{-i\mathbf{z}\cdot(\mathbf{q}-\mathbf{k})} \left\{ \mathcal{U}_F\left(\frac{L^+}{2}, -\frac{L^+}{2}; \mathbf{z}\right) \right. \\ &+ \frac{\epsilon^{ij}h}{2k^+} \int_{-\frac{L^+}{2}}^{\frac{L^+}{2}} dz^+ \left[\mathcal{U}_F\left(\frac{L^+}{2}, z^+; \mathbf{z}\right) \left(-igt \cdot \mathcal{F}_{ij}(\underline{z}) \right) \mathcal{U}_F\left(z^+, -\frac{L^+}{2}; \mathbf{z}\right) \right] \\ &- \frac{i}{2k^+} \int_{-\frac{L^+}{2}}^{\frac{L^+}{2}} dz^+ \left[\mathcal{U}_F\left(\frac{L^+}{2}, z^+; \mathbf{z}\right) \overleftarrow{\mathcal{D}}_{\mathbf{z}j} \overrightarrow{\mathcal{D}}_{\mathbf{z}i} \mathcal{U}_F\left(z^+, -\frac{L^+}{2}; \mathbf{z}\right) \right] \\ &\left. - \frac{(\mathbf{q}^j + \mathbf{k}^j)}{4k^+} \int_{-\frac{L^+}{2}}^{\frac{L^+}{2}} dz^+ \left[\mathcal{U}_F\left(\frac{L^+}{2}, z^+; \mathbf{z}\right) \overleftarrow{\mathcal{D}}_{\mathbf{z}j} \mathcal{U}_F\left(z^+, -\frac{L^+}{2}; \mathbf{z}\right) \right] \right\}_{\alpha\beta} \quad (3.57) \end{aligned}$$

3.4.2 Unpolarized partonic cross section

According to the hybrid factorization ansatz [72], in order to compute the hadronic cross section one first computes the partonic cross section. In our case this corresponds to the projectile quark (or antiquark) scattering on the dense target. Then, the partonic cross section is convoluted with the quark distribution function in the proton and with the fragmentation function. Nevertheless, our goal is simply to understand qualitatively the effects of the quark propagator computed at NEik accuracy. Therefore, we restrict ourselves to the computation of the partonic cross section.

At the partonic level, the differential cross section of the quark traversing the target and undergoing multiple scatterings with the strong background field is given as

$$d^3\sigma_{q(\check{k}, h, \alpha) \rightarrow q(\check{q}, h', \beta)} = (2q^+) 2\pi \delta(q^+ - k^+) \mathcal{M}_{\alpha\beta}^{hh'}(\underline{k}, \mathbf{q})^\dagger \mathcal{M}_{\alpha\beta}^{hh'}(\underline{k}, \mathbf{q}) \frac{\theta(q^+)}{2q^+} \frac{d^2\mathbf{q}}{(2\pi)^2} \frac{dq^+}{2\pi} \quad (3.58)$$

After performing the trivial integration over the outgoing quark longitudinal momentum q^+ , the partonic cross section can be cast into

$$\frac{d^2\sigma^{qA \rightarrow q+X}}{d^2\mathbf{q}} = \frac{1}{(2\pi)^2} \frac{1}{2N_c} \sum_{h, h'} \sum_{\alpha, \beta} \mathcal{M}_{\alpha\beta}^{hh'}(\underline{k}, \mathbf{q})^\dagger \mathcal{M}_{\alpha\beta}^{hh'}(\underline{k}, \mathbf{q}) \Big|_{q^+=k^+}. \quad (3.59)$$

Here, the factor 2 in the denominator originates from averaging over the initial state quark helicity and the factor N_c from averaging over the color, while summing over the final state helicity and color. Using the explicit expression for the forward quark scattering amplitude given in Eq. (3.57), the partonic level production cross section

at NEik accuracy yields

$$\begin{aligned}
 \frac{d^2\sigma^{qA\rightarrow q+X}}{d^2\mathbf{q}} &= \frac{1}{N_c} \frac{1}{(2\pi)^2} \int d^2\mathbf{z}' \int d^2\mathbf{z} e^{-i(\mathbf{q}-\mathbf{k})\cdot(\mathbf{z}-\mathbf{z}')} \text{tr} \left\{ \mathcal{U}_F^\dagger(\mathbf{z}') \mathcal{U}_F(\mathbf{z}) \right. \\
 &+ \frac{1}{2k^+} \int_{-\frac{L^+}{2}}^{\frac{L^+}{2}} dz^+ \mathcal{U}_F^\dagger(\mathbf{z}') \mathcal{U}_F\left(\frac{L^+}{2}, z^+; \mathbf{z}\right) \left[-i \overleftarrow{\mathcal{D}}_{z^+} \overrightarrow{\mathcal{D}}_{z^+} - \frac{(\mathbf{q}^j + \mathbf{k}^j)}{2} \overleftarrow{\mathcal{D}}_{z^+} \right] \mathcal{U}_F\left(z^+, -\frac{L^+}{2}; \mathbf{z}\right) \\
 &+ \frac{1}{2k^+} \int_{-\frac{L^+}{2}}^{\frac{L^+}{2}} dz^+ \mathcal{U}_F^\dagger\left(z^+, -\frac{L^+}{2}; \mathbf{z}'\right) \left[i \overleftarrow{\mathcal{D}}_{z^+} \overrightarrow{\mathcal{D}}_{z^+} + \frac{(\mathbf{q}^j + \mathbf{k}^j)}{2} \overleftarrow{\mathcal{D}}_{z^+} \right] \\
 &\left. \times \mathcal{U}_F^\dagger\left(\frac{L^+}{2}, z^+; \mathbf{z}'\right) \mathcal{U}_F(\mathbf{z}) \right\} \quad (3.60)
 \end{aligned}$$

where we used $\mathcal{U}_F(\mathbf{z}) \equiv \mathcal{U}_F\left(\frac{L^+}{2}, -\frac{L^+}{2}; \mathbf{z}\right)$ for the Wilson lines. Thus Eq. (3.60) represents the case of unpolarized target and projectile, where the trace arises from the summation over the initial and final color indices α and β ¹.

Let us now discuss the symmetry properties for the unpolarized cross-section. After introducing the target averaging, the unpolarized cross section reads

$$\begin{aligned}
 \left\langle \frac{d^2\sigma^{qA\rightarrow q+X}}{d^2\mathbf{q}} \right\rangle_A &= \frac{1}{(2\pi)^2} \int d^2\mathbf{r} e^{-i(\mathbf{q}-\mathbf{k})\cdot\mathbf{r}} \left\{ d_F(\mathbf{r}) - \frac{1}{2k^+} \frac{(\mathbf{q}^j + \mathbf{k}^j)}{2} \right. \\
 &\left. \times \left[\mathcal{O}_{(1)}^j(\mathbf{r}) + \mathcal{O}_{(1)}^{tj}(-\mathbf{r}) \right] - \frac{i}{2k^+} \left[\mathcal{O}_{(2)}(\mathbf{r}) - \mathcal{O}_{(2)}^\dagger(-\mathbf{r}) \right] \right\} \quad (3.61)
 \end{aligned}$$

where we introduced the new variables $(\mathbf{z} - \mathbf{z}') \equiv \mathbf{r}$ and $(\mathbf{z} + \mathbf{z}') \equiv 2\mathbf{b}$. In Eq. (3.61) we introduced the following dipole and decorated dipole operators:

$$d_F(\mathbf{r}) = \frac{1}{N_c} \int d^2\mathbf{b} \left\langle \text{tr} \left[\mathcal{U}_F^\dagger\left(\frac{L^+}{2}, -\frac{L^+}{2}; \mathbf{b} - \frac{\mathbf{r}}{2}\right) \mathcal{U}_F\left(\frac{L^+}{2}, -\frac{L^+}{2}; \mathbf{b} + \frac{\mathbf{r}}{2}\right) \right] \right\rangle_A \quad (3.62)$$

$$\begin{aligned}
 \mathcal{O}_{(1)}^j(\mathbf{r}) &= \frac{1}{N_c} \int d^2\mathbf{b} \int_{-\frac{L^+}{2}}^{\frac{L^+}{2}} dz^+ \left\langle \text{tr} \left[\mathcal{U}_F^\dagger\left(\mathbf{b} - \frac{\mathbf{r}}{2}\right) \right. \right. \\
 &\left. \left. \times \mathcal{U}_F\left(\frac{L^+}{2}, z^+; \mathbf{b} + \frac{\mathbf{r}}{2}\right) \overleftarrow{\mathcal{D}}_{\mathbf{b} + \frac{\mathbf{r}}{2}} \overrightarrow{\mathcal{D}}_{\mathbf{b} + \frac{\mathbf{r}}{2}} \mathcal{U}_F\left(z^+, -\frac{L^+}{2}; \mathbf{b} + \frac{\mathbf{r}}{2}\right) \right] \right\rangle_A, \quad (3.63)
 \end{aligned}$$

$$\begin{aligned}
 \mathcal{O}_{(2)}(\mathbf{r}) &= \frac{1}{N_c} \int d^2\mathbf{b} \int_{-L^+/2}^{L^+/2} dz^+ \left\langle \text{tr} \left[\mathcal{U}_F^\dagger\left(\mathbf{b} - \frac{\mathbf{r}}{2}\right) \right. \right. \\
 &\left. \left. \times \mathcal{U}_F\left(\frac{L^+}{2}, z^+; \mathbf{b} + \frac{\mathbf{r}}{2}\right) \overleftarrow{\mathcal{D}}_{\mathbf{b} + \frac{\mathbf{r}}{2}} \overrightarrow{\mathcal{D}}_{\mathbf{b} + \frac{\mathbf{r}}{2}} \mathcal{U}_F\left(z^+, -\frac{L^+}{2}; \mathbf{b} + \frac{\mathbf{r}}{2}\right) \right] \right\rangle_A. \quad (3.64)
 \end{aligned}$$

The operator $\mathcal{O}_{(1)}^j(\mathbf{r})$ behaves as a vector quantity under rotations in the transverse plane, thus satisfying

$$\mathcal{O}_{(1)}^j(-\mathbf{r}) = -\mathcal{O}_{(1)}^j(\mathbf{r}) \quad (3.65)$$

$$\mathcal{O}_{(1)}^{tj}(-\mathbf{r}) = -\mathcal{O}_{(1)}^{tj}(\mathbf{r}) \quad (3.66)$$

¹Note that helicity dependent term in the forward quark scattering amplitude given in Eq. (3.57) vanishes at the level of the cross section after summing over incoming and outgoing quark helicities.

On the contrary, the operator $\mathcal{O}_{(2)}(\mathbf{r})$ behaves as a scalar quantity under rotations in the transverse plane, so that

$$\mathcal{O}_{(2)}(-\mathbf{r}) = \mathcal{O}_{(2)}(\mathbf{r}) \quad (3.67)$$

$$\mathcal{O}_{(2)}^\dagger(-\mathbf{r}) = \mathcal{O}_{(2)}^\dagger(\mathbf{r}) \quad (3.68)$$

Using the above symmetry properties, target-averaged unpolarized cross section can be written as

$$\begin{aligned} \left\langle \frac{d^2\sigma^{qA \rightarrow q+X}}{d^2\mathbf{q}} \right\rangle_A &= \frac{1}{(2\pi)^2} \int d^2\mathbf{r} e^{-i(\mathbf{q}-\mathbf{k})\cdot\mathbf{r}} \left\{ d_F(\mathbf{r}) - \frac{1}{2k^+} \frac{(\mathbf{q}^j+\mathbf{k}^j)}{2} \right. \\ &\quad \left. \times \left[\mathcal{O}_{(1)}^j(\mathbf{r}) - \mathcal{O}_{(1)}^{\dagger j}(\mathbf{r}) \right] - \frac{i}{2k^+} \left[\mathcal{O}_{(2)}(\mathbf{r}) - \mathcal{O}_{(2)}^\dagger(\mathbf{r}) \right] \right\} \quad (3.69) \end{aligned}$$

Let us rewrite now the NEik corrections to the unpolarized cross-section in terms of the known operators Pomeron and Odderon. These operators are defined in terms of the fundamental dipole and its hermitian conjugate:

$$P(\mathbf{x}, \mathbf{y}) = \frac{1}{2} \left[2 - d_F(\mathbf{x}, \mathbf{y}) - d_F^\dagger(\mathbf{x}, \mathbf{y}) \right] \quad (3.70)$$

$$O(\mathbf{x}, \mathbf{y}) = \frac{1}{2} \left[d_F(\mathbf{x}, \mathbf{y}) - d_F^\dagger(\mathbf{x}, \mathbf{y}) \right] \quad (3.71)$$

with the fundamental dipole operator defined in Eq. (3.62). In order to preserve the consistency, we introduce the same change of variables (\mathbf{r} and \mathbf{b}) in Eqs. (3.70) and (3.71), and define the following new operators which are integrated expressions of the Pomeron and Odderon operators over \mathbf{b} :

$$\bar{P}(\mathbf{r}) \equiv \int d^2\mathbf{b} P\left(\mathbf{b} + \frac{\mathbf{r}}{2}, \mathbf{b} - \frac{\mathbf{r}}{2}\right) = \frac{1}{2} \left[2 - d_F(\mathbf{r}) - d_F^\dagger(\mathbf{r}) \right] \quad (3.72)$$

$$\bar{O}(\mathbf{r}) \equiv \int d^2\mathbf{b} O\left(\mathbf{b} + \frac{\mathbf{r}}{2}, \mathbf{b} - \frac{\mathbf{r}}{2}\right) = \frac{1}{2} \left[d_F(\mathbf{r}) - d_F^\dagger(\mathbf{r}) \right]. \quad (3.73)$$

Using these definitions, the target-averaged unpolarized partonic cross section for a quark can be written as

$$\begin{aligned} \left\langle \frac{d^2\sigma^{qA \rightarrow q+X}}{d^2\mathbf{q}} \right\rangle_A &= \frac{1}{(2\pi)^2} \int d^2\mathbf{r} e^{-i(\mathbf{q}-\mathbf{k})\cdot\mathbf{r}} \left\{ 1 - \bar{P}(\mathbf{r}) \right. \\ &\quad \left. + \left[\bar{O}(\mathbf{r}) - \frac{1}{2k^+} \frac{(\mathbf{q}^j+\mathbf{k}^j)}{2} \left[\mathcal{O}_{(1)}^j(\mathbf{r}) - \mathcal{O}_{(1)}^{\dagger j}(\mathbf{r}) \right] - \frac{i}{2k^+} \left[\mathcal{O}_{(2)}(\mathbf{r}) - \mathcal{O}_{(2)}^\dagger(\mathbf{r}) \right] \right] \right\} \\ &= \frac{1}{(2\pi)^2} \int d^2\mathbf{r} \left\{ \cos [(\mathbf{q}-\mathbf{k})\cdot\mathbf{r}] \left[1 - \bar{P}(\mathbf{r}) \right] \right. \\ &\quad \left. + \sin [(\mathbf{q}-\mathbf{k})\cdot\mathbf{r}] \left[\text{Im}\bar{O}(\mathbf{r}) - \frac{(\mathbf{q}^j+\mathbf{k}^j)}{2k^+} \text{Im}\mathcal{O}_{(1)}^j(\mathbf{r}) \right] + \cos [(\mathbf{q}-\mathbf{k})\cdot\mathbf{r}] \frac{1}{k^+} \text{Im}\mathcal{O}_{(2)}(\mathbf{r}) \right\}. \quad (3.74) \end{aligned}$$

The analogous expression for antiquark-nucleus scattering reads

$$\begin{aligned}
\left\langle \frac{d^2 \sigma^{qA \rightarrow q+X}}{d^2 \mathbf{q}} \right\rangle_A &= \frac{1}{(2\pi)^2} \int d^2 \mathbf{r} e^{-i(\mathbf{q}-\mathbf{k}) \cdot \mathbf{r}} \left\{ 1 - \bar{P}(\mathbf{r}) \right. \\
&- \left. \left(\bar{O}(\mathbf{r}) - \frac{1}{2k^+} \frac{(\mathbf{q}^i + \mathbf{k}^i)}{2} \left[\mathcal{O}_{(1)}^j(\mathbf{r}) - \mathcal{O}_{(1)}^{\dagger j}(\mathbf{r}) \right] - \frac{i}{2k^+} \left[\mathcal{O}_{(2)}(\mathbf{r}) - \mathcal{O}_{(2)}^{\dagger}(\mathbf{r}) \right] \right) \right\} \\
&= \frac{1}{(2\pi)^2} \int d^2 \mathbf{r} \left\{ \cos [(\mathbf{q} - \mathbf{k}) \cdot \mathbf{r}] \left[1 - \bar{P}(\mathbf{r}) \right] \right. \\
&- \left. \sin [(\mathbf{q} - \mathbf{k}) \cdot \mathbf{r}] \left[\text{Im} \bar{O}(\mathbf{r}) - \frac{(\mathbf{q}^i + \mathbf{k}^i)}{2k^+} \text{Im} \mathcal{O}_{(1)}^j(\mathbf{r}) \right] - \cos [(\mathbf{q} - \mathbf{k}) \cdot \mathbf{r}] \frac{1}{k^+} \text{Im} \mathcal{O}_{(2)}(\mathbf{r}) \right\}. \tag{3.75}
\end{aligned}$$

The Pomeron is even under both signature transformation ($\mathcal{U}(\mathbf{x}) \rightarrow \mathcal{U}^{\dagger}(\mathbf{x})$) and charge conjugation (quark \rightarrow antiquark) while the Odderon is odd under both transformations. If one compares Eqs.(3.74) and (3.75), one realises that NEik corrections in the unpolarized partonic cross section couple to the Odderon, since they are also odd under these transformations. However, for the unpolarized cross section, a Pomeron type contribution is seen at the strict eikonal order. Moreover, we also expect to see such contributions at NNEik (next-to-next-to-eikonal) accuracy just like the analogue contributions for gluon propagator computed in [37]. Finally, Odderon type contributions are seen both at eikonal and NEik orders.

3.4.3 Quark helicity asymmetry

The other application considered here for our background quark propagator at NEik accuracy concerns the quark helicity asymmetry. Here, we again restrict ourselves to the partonic level.

We consider the difference between the cross sections for a quark of positive and negative helicity scattering on the nucleus target

$$\frac{d^2 \Delta \sigma^{qA \rightarrow q+X}}{d^2 \mathbf{q}} \equiv \frac{d^2 \sigma^{q^{(+)}A \rightarrow q+X}}{d^2 \mathbf{q}} - \frac{d^2 \sigma^{q^{(-)}A \rightarrow q+X}}{d^2 \mathbf{q}} \tag{3.76}$$

that we call the quark helicity asymmetry.² This asymmetry, when written in terms of the forward quark scattering amplitude $\mathcal{M}_{\alpha\beta}^{hh'}(\underline{k}, \mathbf{q})$ (keeping the conventions from Fig. 3.1), reads

$$\frac{d^2 \Delta \sigma^{qA \rightarrow q+X}}{d^2 \mathbf{q}} = \frac{1}{(2\pi)^2} \frac{1}{2N_c} \sum_{h,h'} \sum_{\alpha,\beta} (2h) \mathcal{M}_{\alpha\beta}^{hh'}(\underline{k}, \mathbf{q})^{\dagger} \mathcal{M}_{\alpha\beta}^{hh'}(\underline{k}, \mathbf{q}) \Big|_{q^+ = k^+} \tag{3.77}$$

since $h = \pm 1/2$. Now we insert the definition of the forward quark scattering amplitude Eq. (3.57) into the definition of the quark helicity asymmetry Eq.(3.77) and

²In principle an asymmetry is defined as the ratio of difference over the sum of positive and negative helicity contributions. Here, we focus on the numerator for simplicity and still call it as asymmetry with a small abuse of language.

get

$$\begin{aligned} \frac{d^2 \Delta \sigma^{qA \rightarrow q+X}}{d^2 \mathbf{q}} &= \frac{1}{N_c} \frac{1}{(2\pi)^2} \int d^2 \mathbf{z}' \int d^2 \mathbf{z} e^{-i(\mathbf{q}-\mathbf{k}) \cdot (\mathbf{z}-\mathbf{z}')} \frac{1}{4k^+} \\ &\times \text{tr} \left\{ \int_{-\frac{L^+}{2}}^{\frac{L^+}{2}} dz^+ \mathcal{U}_F^\dagger(\mathbf{z}') \mathcal{U}_F\left(\frac{L^+}{2}, z^+; \mathbf{z}\right) [\epsilon^{ij} (-igt \cdot \mathcal{F}_{ij}(\underline{z}))] \mathcal{U}_F\left(z^+, -\frac{L^+}{2}; \mathbf{z}\right) \right. \\ &\left. + \int_{-\frac{L^+}{2}}^{\frac{L^+}{2}} dz^+ \mathcal{U}_F^\dagger\left(z^+, -\frac{L^+}{2}; \mathbf{z}'\right) [\epsilon^{ij} (igt \cdot \mathcal{F}_{ij}(z^+, \mathbf{z}'))] \mathcal{U}_F^\dagger\left(\frac{L^+}{2}, z^+; \mathbf{z}'\right) \mathcal{U}_F(\mathbf{z}) \right\}. \end{aligned} \quad (3.78)$$

Note that in this case, only the helicity dependent piece of the quark scattering amplitude contributes to the quark helicity asymmetry. Moreover, the quark helicity asymmetry starts already at NEik order, unlike the unpolarized partonic cross-section, which contained an eikonal part as well.

As in the previous case, let us now look at the symmetry properties of the quark helicity asymmetry. Following the same logic as before, we introduce the variables \mathbf{b} and \mathbf{r} , and we average over the target. The quark helicity asymmetry thus can be written as

$$\left\langle \frac{d^2 \Delta \sigma^{qA \rightarrow q+X}}{d^2 \mathbf{q}} \right\rangle_A = \frac{1}{(2\pi)^2} \int d^2 \mathbf{r} e^{-i(\mathbf{q}-\mathbf{k}) \cdot \mathbf{r}} \frac{(-i)}{4k^+} [O_{(3)}(\mathbf{r}) - O_{(3)}^\dagger(-\mathbf{r})] \quad (3.79)$$

where we define the new decorated dipole operator $O_{(3)}(\mathbf{r})$ as

$$\begin{aligned} O_{(3)}(\mathbf{r}) &= \frac{1}{N_c} \int d^2 \mathbf{b} \int_{-L^+/2}^{L^+/2} dz^+ \left\langle \text{tr} \left[\mathcal{U}_F^\dagger\left(\mathbf{b} - \frac{\mathbf{r}}{2}\right) \mathcal{U}_F\left(\frac{L^+}{2}, z^+; \mathbf{b} + \frac{\mathbf{r}}{2}\right) \right. \right. \\ &\left. \left. \times \left\{ \epsilon^{ij} [gt \cdot \mathcal{F}_{ij}(z^+, \mathbf{b} + \frac{\mathbf{r}}{2})] \right\} \mathcal{U}_F\left(z^+, -\frac{L^+}{2}; \mathbf{b} + \frac{\mathbf{r}}{2}\right) \right] \right\rangle_A. \end{aligned} \quad (3.80)$$

Since in $O_{(3)}(\mathbf{r})$, the antisymmetric tensor ϵ^{ij} is already contracted with the ij component of the field strength tensor, this operator $O_{(3)}(\mathbf{r})$ behaves as a scalar quantity under rotations within the transverse plane, and therefore

$$O_{(3)}(-\mathbf{r}) = O_{(3)}(\mathbf{r}) \quad (3.81)$$

$$O_{(3)}^\dagger(-\mathbf{r}) = O_{(3)}^\dagger(\mathbf{r}) \quad (3.82)$$

and the target-averaged quark helicity asymmetry reads

$$\begin{aligned} \left\langle \frac{d^2 \Delta \sigma^{qA \rightarrow q+X}}{d^2 \mathbf{q}} \right\rangle_A &= \frac{1}{(2\pi)^2} \int d^2 \mathbf{r} e^{-i(\mathbf{q}-\mathbf{k}) \cdot \mathbf{r}} \frac{(-i)}{4k^+} [O_{(3)}(\mathbf{r}) - O_{(3)}^\dagger(\mathbf{r})] \\ &= \frac{1}{(2\pi)^2} \frac{1}{2k^+} \int d^2 \mathbf{r} \cos [(\mathbf{q}-\mathbf{k}) \cdot \mathbf{r}] \text{Im} O_{(3)}(\mathbf{r}). \end{aligned} \quad (3.83)$$

Following the similar path in order to compute the antiquark helicity asymmetry, one gets

$$\begin{aligned} \left\langle \frac{d^2 \Delta \sigma^{\bar{q}A \rightarrow \bar{q}+X}}{d^2 \mathbf{q}} \right\rangle_A &= \frac{1}{(2\pi)^2} \int d^2 \mathbf{r} e^{-i(\mathbf{q}-\mathbf{k}) \cdot \mathbf{r}} \frac{(-i)}{4k^+} [O_{(3)}(\mathbf{r}) - O_{(3)}^\dagger(\mathbf{r})] \\ &= \frac{1}{(2\pi)^2} \frac{1}{2k^+} \int d^2 \mathbf{r} \cos [(\mathbf{q}-\mathbf{k}) \cdot \mathbf{r}] \text{Im} O_{(3)}(\mathbf{r}). \end{aligned} \quad (3.84)$$

The form of the target-averaged helicity asymmetries given in Eqs.(3.83) and (3.84) suggests that it is odd under signature transformation but even under charge conjugation which is compatible with neither Pomeron nor Odderon type of behavior. These quantum numbers are instead observed in higher order Reggeons [73, 74].

3.5 Conclusions

Thus, in this chapter we have computed the quark and antiquark propagator at NEik accuracy by relaxing two assumptions from the eikonal approximation. Therefore, we have taken into account both, a finite width of the target and the interaction with the transverse component of the background field. It is also worth mentioning that we have taken into account the cases of not only one insertion of the transverse component of the background field, but also two such insertions in order to get the full result at NEik accuracy that stems from this correction. The quark propagator as well as the antiquark propagator have been divided into two different contributions, the unpolarized and the helicity dependent one.

With these propagators at NEik accuracy, we have computed the quark-nucleus scattering and the antiquark-nucleus scattering. The results of these observables are divided into unpolarized partonic cross-section and quark-helicity asymmetry. Finally, the target-averaged unpolarized partonic cross-section is expressed in terms of Pomeron and Odderon operators, while the quark helicity asymmetry behaviour is instead observed in higher order Reggeons.

4

DIS dijet production at NEik accuracy: including dynamics of the target

DISCLAIMER: The material presented in this Chapter was originally published in Phys. Rev. D 107 (2023) 7, 074016 (which corresponds to the reference [35] in this thesis) of which I am a coauthor. My contributions to this publication can be summarized as follows. I have contributed to the derivation of the quark propagators from before to after the medium and the propagator from inside to after the medium. I have also contributed to the computation of the NEik DIS dijet production cross section both via longitudinal and via transverse photon. I have given talks presenting these results in the “DIS2022: XXIX International Workshop on Deep-Inelastic Scattering and Related Subjects” (Santiago de Compostela, Spain in May 2022), in the summer school “GDR-QCD HIC in the QCD phase diagram” (Nantes, France in July 2022) and in the “XXIX Cracow Epiphany Meeting: on Physics at the Electron-Ion Collider and in Future Facilities” (Cracow, Poland in January 2023).

In this chapter we introduce a new type of NEik correction to the quark propagator in addition to the two types of corrections studied in sections 3.1, 3.2. This new contribution stems from relaxing the third assumption presented in section 2.2, that is, including the dependence of the gluon background field on the coordinate x^- . This new effect takes into account the dynamics of the gluon background field.

In this chapter we present the full quark (and antiquark) propagator at next-to-eikonal accuracy in the gluon background field, where we include all the possible corrections that stem from relaxing the eikonal approximation. We use this propagator to compute the DIS dijet production at NEik accuracy. In fact, within the CGC effective theory, gluon saturation effects in DIS on a dense target is one of the most frequently used observables. This is due to the fact that it provides a clean environment to probe gluon saturation. Furthermore, computing this observable at NEik accuracy is of great importance since it is one of the focus for the future EIC, where the energies are lower compared to LHC. Since NEik corrections are suppressed in power of energy, computing these corrections for an observable that planned to be studied at lower energies, was the main motivation behind this work.

This chapter is organized as follows, in section 4.1 we lay out the reduction formula for the S-matrix element. In section 4.2 we compute the propagators that will

then contribute to the cross section for DIS dijet production and the production cross-section is presented in section 4.3.

4.1 Reduction formula for the S-matrix and integrated propagators

Let us consider the process in which a virtual photon of momentum q and polarization λ splits into a quark of momentum k_1 and an antiquark of momentum k_2 , in the presence of a gluon background field $\mathcal{A}^\mu(x)$ representing the target. The S-matrix element for that process can be obtained following the LSZ approach. Due to the photon splitting vertex, the first non-zero contribution to the S-matrix is at order e in QED. We are interested in the lowest order contribution in perturbation theory in a possibly strong background field, which is then of order $e g^0$ at the S-matrix level, with $g \mathcal{A}^\mu(x)$ resummed to all orders. At this order, the S-matrix can be written as¹

$$S_{q_1 \bar{q}_2 \leftarrow \gamma^*} = \int d^4z \epsilon_\mu^\lambda(q) e^{-iq \cdot z} \langle 0 | d_{\text{out}}(2) b_{\text{out}}(1) : \bar{\Psi}(z) (-ie e_f \gamma^\mu) \Psi(z) : | 0 \rangle. \quad (4.1)$$

In Eq. (4.1), $b_{\text{out}}(1)$ and $d_{\text{out}}(2)$ are the annihilation operators for the outgoing quark and antiquark in the asymptotic free Fock space, whereas $\epsilon_\mu^\lambda(q) e^{-iq \cdot z}$ accounts for the incoming virtual photon, and the normal-ordered current operator comes from the photon splitting vertex. The quark field $\Psi(z)$ in Eq. (4.1) is a quantum field in a modified interaction picture, in such a way that the evolution of $\Psi(z)$ is generated by a Hamiltonian quadratic in the quantum fields, but with terms of any order in the background field. Hence, not only the free limit of the theory but also the interactions of quantum particles with the background field contributes to the evolution of $\Psi(z)$. Only the interactions between quantum particles are removed from the evolution of $\Psi(z)$ in this picture with respect to the Heisenberg picture. Moreover, we assume that the background field alone cannot lead to pair creation or pair annihilation of quantum particles. Then, the only possible contribution to the expectation value in Eq. (4.1) factorizes as

$$\begin{aligned} & \langle 0 | d_{\text{out}}(2) b_{\text{out}}(1) : \bar{\Psi}(z) (-ie e_f \gamma^\mu) \Psi(z) : | 0 \rangle \\ &= \langle 0 | b_{\text{out}}(1) \bar{\Psi}(z) | 0 \rangle (-ie e_f \gamma^\mu) \langle 0 | d_{\text{out}}(2) \Psi(z) | 0 \rangle. \end{aligned} \quad (4.2)$$

the annihilation operators $b_{\text{out}}(1)$ and $d_{\text{out}}(2)$ can be expressed as in the previous chapter

$$b_{\text{out}}(1) = \lim_{x^+ \rightarrow +\infty} \int d^2\mathbf{x} \int dx^- e^{ik_1 \cdot x} \bar{u}(1) \gamma^+ \Psi(x) \quad (4.3)$$

$$d_{\text{out}}(2) = \lim_{y^+ \rightarrow +\infty} \int d^2\mathbf{y} \int dy^- e^{ik_2 \cdot y} \bar{\Psi}(y) \gamma^+ v(2). \quad (4.4)$$

The Feynman quark propagator in the gluon background field is defined as

¹See Appendix A for the notation on the light-cone coordinates and on-shell momenta. We also use the condensed notations $u(1) \equiv u(k_1, h_1)$ and $v(2) \equiv v(k_2, h_2)$ for the Dirac spinors, where h_1 or h_2 is the light-front helicity.

$$\begin{aligned}
S_F(x, y) &= \langle 0 | T(\Psi(x) \bar{\Psi}(y)) | 0 \rangle \\
&= \theta(x^0 - y^0) \langle 0 | \Psi(x) \bar{\Psi}(y) | 0 \rangle - \theta(y^0 - x^0) \langle 0 | \bar{\Psi}(y) \Psi(x) | 0 \rangle. \quad (4.5)
\end{aligned}$$

Here the implicit spinor and color indices of the fields are not contracted. The minus sign in the second term is because of the Fermi-Dirac statistics for fermions (quarks). We thus have

$$\begin{aligned}
\langle 0 | \Psi(x) \bar{\Psi}(z) | 0 \rangle &= S_F(x, z) \quad \text{for } x^+ \rightarrow +\infty \\
\langle 0 | \bar{\Psi}(y) \Psi(z) | 0 \rangle &= -S_F(z, y) \quad \text{for } y^+ \rightarrow +\infty. \quad (4.6)
\end{aligned}$$

With these ingredients, the S-matrix element at lowest order $e g^0$ but with the interactions with the background field resummed to all orders, can be written as

$$\begin{aligned}
S_{q_1 \bar{q}_2 \leftarrow \gamma^*} &= \lim_{x^+, y^+ \rightarrow +\infty} \int d^2 \mathbf{x} \int dx^- \int d^2 \mathbf{y} \int dy^- e^{i\mathbf{k}_1 \cdot \mathbf{x}} e^{i\mathbf{k}_2 \cdot \mathbf{y}} \\
&\times \epsilon_\mu^\lambda(q) \int d^4 z e^{-iq \cdot z} \bar{u}(1) \gamma^+ S_F(x, z) (-iee_f \gamma^\mu) (-S_F(z, y)) \gamma^+ v(2). \quad (4.7)
\end{aligned}$$

Defining the integrated quark and antiquark propagators as

$$\tilde{S}_F^q(z) = \lim_{x^+ \rightarrow +\infty} \int d^2 \mathbf{x} \int dx^- e^{i\mathbf{k}_1 \cdot \mathbf{x}} \bar{u}(1) \gamma^+ S_F(x, z) \quad (4.8)$$

$$\tilde{S}_F^{\bar{q}}(z) = \lim_{y^+ \rightarrow +\infty} \int d^2 \mathbf{y} \int dy^- e^{i\mathbf{k}_2 \cdot \mathbf{y}} (-1) S_F(z, y) \gamma^+ v(2). \quad (4.9)$$

the S-matrix can be once again, rewritten as

$$S_{q_1 \bar{q}_2 \leftarrow \gamma^*} = -iee_f \epsilon_\mu^\lambda(q) \int d^4 z e^{-iq \cdot z} \tilde{S}_F^q(z) \gamma^\mu \tilde{S}_F^{\bar{q}}(z). \quad (4.10)$$

Let us now consider the process of DIS dijet production. We assume that the background field strength has a finite support of length L^+ along z^+ . Then the range $[-\infty, -L^+/2]$ is before the target, and $[L^+/2, +\infty]$ is after the target. The region $[-L^+/2, L^+/2]$ is inside the target. We also choose the light-cone gauge $A^+ = 0$, where not only the field strength but also the gauge field vanishes outside the target. The S-matrix element can be split into the three contributions corresponding to each region as

$$\begin{aligned}
S_{q_1 \bar{q}_2 \leftarrow \gamma^*} &= -iee_f \epsilon_\mu^\lambda(q) \int d^2 \mathbf{z} \int dz^- \int_{-\infty}^{-L^+/2} dz^+ e^{-iq \cdot z} \tilde{S}_F^q(z)_{\alpha\delta} \gamma^\mu \tilde{S}_F^{\bar{q}}(z)_{\delta\beta} \\
&-iee_f \epsilon_\mu^\lambda(q) \int d^2 \mathbf{z} \int dz^- \int_{-L^+/2}^{L^+/2} dz^+ e^{-iq \cdot z} \tilde{S}_F^q(z)_{\alpha\delta} \gamma^\mu \tilde{S}_F^{\bar{q}}(z)_{\delta\beta} \\
&-iee_f \epsilon_\mu^\lambda(q) \int d^2 \mathbf{z} \int dz^- \int_{L^+/2}^{+\infty} dz^+ e^{-iq \cdot z} \tilde{S}_{0,F}^q(z)_{\alpha\delta} \gamma^\mu \tilde{S}_{0,F}^{\bar{q}}(z)_{\delta\beta} \quad (4.11)
\end{aligned}$$

The third term corresponds to the photon crossing the medium and splitting after, however, the photon does not interact with the gluon field at LO in QED. Thus, the third term corresponds to the vacuum contribution, which vanishes in our configuration. This vacuum contribution vanishes because the condition in a DIS process ($q^2 < 0$) is not compatible with the 4-momentum conservation $\check{k}_1^\mu + \check{k}_2^\mu = q^\mu$ and

other requirements that one obtains in this configuration. The first two terms contain medium-induced contributions as well as the vacuum contribution, however, since the latter is zero, we can rewrite it as

$$S_{q_1\bar{q}_2\leftarrow\gamma^*} = S_{q_1\bar{q}_2\leftarrow\gamma^*}^{\text{bef}} + S_{q_1\bar{q}_2\leftarrow\gamma^*}^{\text{in}} \quad (4.12)$$

where

$$S_{q_1\bar{q}_2\leftarrow\gamma^*}^{\text{bef}} = -iee_f \epsilon_\mu^\lambda(q) \int d^2\mathbf{z} \int dz^- \int_{-\infty}^{-L^+/2} dz^+ e^{-iq\cdot z} \times \left[\tilde{S}_F^q(z) \gamma^\mu \tilde{S}_F^{\bar{q}}(z) - e^{i(\check{k}_1+\check{k}_2)\cdot z} \bar{u}(1) \gamma^\mu v(2) \right] \quad (4.13)$$

$$S_{q_1\bar{q}_2\leftarrow\gamma^*}^{\text{in}} = -iee_f \epsilon_\mu^\lambda(q) \int d^2\mathbf{z} \int dz^- \int_{-L^+/2}^{L^+/2} dz^+ e^{-iq\cdot z} \times \left[\tilde{S}_F^q(z) \gamma^\mu \tilde{S}_F^{\bar{q}}(z) - e^{i(\check{k}_1+\check{k}_2)\cdot z} \bar{u}(1) \gamma^\mu v(2) \right] \quad (4.14)$$

that are the medium-induced contributions corresponding to the photon splitting before (see Fig. 4.1 left panel) or inside (see Fig. 4.1 right panel) the target, respectively.

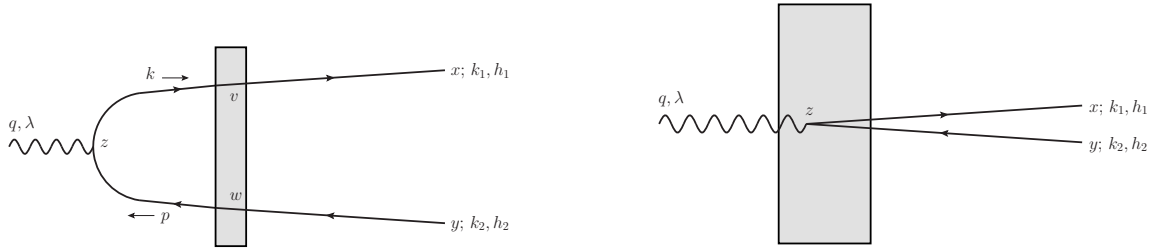


FIGURE 4.1: Contributions to dijet production in DIS at next-to-eikonal accuracy: photon splitting into a $q\bar{q}$ pair before reaching the target (left panel) and photon splitting inside the target (right panel).

4.2 Propagators at full NEik accuracy

In this chapter, our goal is to compute the cross-section for DIS dijet production at NEik accuracy. In order to compute this, one needs the expressions for the quark propagators contributing to this process at full NEik order in the gluon background field. There are two such kinds of propagators, one where the splitting of the photon into a quark-antiquark pair occurs before the medium, and one when this splitting happens inside of it. The propagators derived in this section are at full NEik accuracy because they contain not only the corrections to the eikonal approximation computed in the previous chapter, but also take into account the dynamics of the target by considering the dependence of the Wilson line on the z^- coordinate.

In the contribution Eq.(4.13) to the S-matrix element, the photon splits at light-cone time z^+ before the medium. The integration over z^+ does not bring a suppression at large γ_t in that case. In order to calculate both the eikonal and NEik terms in the contribution Eq.(4.13) to the S-matrix element, one should thus include both eikonal and NEik terms in the reduced propagators $\tilde{S}_F^q(z)$ and $\tilde{S}_F^{\bar{q}}(z)$.

By contrast, in the contribution Eq.(4.14) to the S-matrix element, the photon splits at light-cone time z^+ inside the medium, so that the integration over z^+ brings a suppression by a factor L^+ , and thus is of order $1/\gamma_t$. Hence, the expression Eq.(4.14) does not contribute at eikonal accuracy, and starts contributing only at NEik accuracy. One should thus restrict to the eikonal expression for the reduced propagators $\tilde{S}_F^q(z)$ and $\tilde{S}_F^{\bar{q}}(z)$.

Let us first show the quark propagator in a background field with only the leading \mathcal{A}^- component

$$\begin{aligned}
S_F(x, y)_{\beta\alpha} \Big|_{\text{pure } \mathcal{A}^-, \text{Eik.}} &= \mathbf{1}_{\beta\alpha} \delta^{(3)}(\underline{x}-\underline{y}) \gamma^+ \int \frac{dk^+}{2\pi} \frac{i}{2k^+} e^{-ik^+(x^- - y^-)} \\
&+ \int \frac{d^3\mathbf{p}}{(2\pi)^3} \int \frac{d^3\mathbf{k}}{(2\pi)^3} e^{-ix \cdot \mathbf{p} + iy \cdot \mathbf{k}} \int dz^- e^{iz^-(p^+ - k^+)} \int d^2\mathbf{z} e^{-iz \cdot (\mathbf{p} - \mathbf{k})} \frac{(\not{\mathbf{p}} + m)}{2p^+} \gamma^+ \\
&\times \left\{ \theta(x^+ - y^+) \theta(p^+) \theta(k^+) \mathcal{U}_F(x^+, y^+; \mathbf{z}, z^-)_{\beta\alpha} \right. \\
&\left. - \theta(y^+ - x^+) \theta(-p^+) \theta(-k^+) \mathcal{U}_F^{\dagger}(y^+, x^+; \mathbf{z}, z^-)_{\beta\alpha} \right\} \frac{(\not{\mathbf{k}} + m)}{2k^+}. \tag{4.15}
\end{aligned}$$

This propagator is at eikonal order up to the z^- dependence on the Wilson lines. This is what we call generalized eikonal since it recovers the strict eikonal form upon setting $z^- = 0$. The first term on the right hand side of Eq. (4.15) corresponds to an instantaneous quark exchange. By contrast, the two terms in the bracket correspond respectively to the propagation of a quark or of an antiquark in the background field. The Wilson line appearing in the expression above is defined as

$$\mathcal{U}_F(x^+, y^+; \mathbf{z}, z^-) \equiv \mathcal{P}_+ \exp \left\{ -ig \int_{y^+}^{x^+} dz^+ \mathcal{A}^-(z) \right\} \tag{4.16}$$

with \mathcal{P}_+ denoting the ordering of color matrices along z^+ direction. This Wilson line goes back to its standard eikonal definition if one sets $z^- = 0$.

4.2.1 Propagators from before to after the medium at NEik accuracy

In order to compute the contribution of the photon splitting into a quark-antiquark pair before the medium, one needs the expression for the quark propagator that traverses the whole medium. In this case, y is before and x after the support of the background field, the transverse components \mathcal{A}_j only matter at NEik accuracy, and the first term in the bracket in Eq. (4.15) gives the entire result at Eikonal accuracy. For this configuration, the NEik corrections were computed in chapter 3 where the z^- dependence was neglected. The quark propagator including all NEik effects in a gluon background field in the region $x^+ > L^+/2$ and $y^+ < -L^+/2$, can be written as ²

²In the case of Wilson lines traversing the whole medium, in order to avoid unnecessary cluttering, we adopt the compact notation $\mathcal{U}_F(\mathbf{z}, z^-) \equiv \mathcal{U}_F\left(\frac{L^+}{2}, -\frac{L^+}{2}; \mathbf{z}, z^-\right)$, and similarly we will use the notation $\mathcal{U}_F(\mathbf{z}) \equiv \mathcal{U}_F\left(\frac{L^+}{2}, -\frac{L^+}{2}; \mathbf{z}\right)$.

$$\begin{aligned}
 S_F(x, y) &= \int \frac{d^3 p}{(2\pi)^3} \int \frac{d^3 k}{(2\pi)^3} \theta(p^+) \theta(k^+) e^{-ix \cdot \not{p}} e^{iy \cdot \not{k}} \int dz^- e^{iz^-(p^+ - k^+)} \int d^2 \mathbf{z} e^{-iz \cdot (\mathbf{p} - \mathbf{k})} \\
 &\times \frac{(\not{p} + m)}{2p^+} \gamma^+ \left\{ \mathcal{U}_F(\mathbf{z}, z^-) \right. \\
 &- \frac{(\mathbf{p}^j + \mathbf{k}^j)}{2(p^+ + k^+)} \int_{-\frac{L^+}{2}}^{\frac{L^+}{2}} dz^+ \left[\mathcal{U}_F\left(\frac{L^+}{2}, z^+; \mathbf{z}, z^-\right) \overleftarrow{\mathcal{D}}_{\mathbf{z}^j} \mathcal{U}_F\left(z^+, -\frac{L^+}{2}; \mathbf{z}, z^-\right) \right] \\
 &- \frac{i}{(p^+ + k^+)} \int_{-\frac{L^+}{2}}^{\frac{L^+}{2}} dz^+ \left[\mathcal{U}_F\left(\frac{L^+}{2}, z^+; \mathbf{z}, z^-\right) \overleftarrow{\mathcal{D}}_{\mathbf{z}^j} \overrightarrow{\mathcal{D}}_{\mathbf{z}^j} \mathcal{U}_F\left(z^+, -\frac{L^+}{2}; \mathbf{z}, z^-\right) \right] \\
 &+ \frac{[\gamma^i, \gamma^j]}{4(p^+ + k^+)} \int_{-\frac{L^+}{2}}^{\frac{L^+}{2}} dz^+ \mathcal{U}_F\left(\frac{L^+}{2}, z^+; \mathbf{z}, z^-\right) g^t \cdot \mathcal{F}_{ij}(z) \mathcal{U}_F\left(z^+, -\frac{L^+}{2}; \mathbf{z}, z^-\right) \left. \right\} \frac{(\not{k} + m)}{2k^+} \\
 &+ O(\text{NNEik}), \tag{4.17}
 \end{aligned}$$

and for the case of antiquark propagating through the whole medium, meaning $y^+ > L^+/2$ and $x^+ < -L^+/2$, one has

$$\begin{aligned}
 S_F(x, y) &= \int \frac{d^3 p}{(2\pi)^3} \int \frac{d^3 k}{(2\pi)^3} \theta(-p^+) \theta(-k^+) e^{-ix \cdot \not{p}} e^{iy \cdot \not{k}} \int dz^- e^{iz^-(p^+ - k^+)} \int d^2 \mathbf{z} \\
 &\times e^{-iz \cdot (\mathbf{p} - \mathbf{k})} \frac{(\not{p} + m)}{2p^+} \gamma^+ \left\{ -\mathcal{U}_F^\dagger(\mathbf{z}, z^-) \right. \\
 &- \frac{(\mathbf{p}^j + \mathbf{k}^j)}{2(p^+ + k^+)} \int_{-\frac{L^+}{2}}^{\frac{L^+}{2}} dz^+ \left[\mathcal{U}_F^\dagger\left(z^+, -\frac{L^+}{2}; \mathbf{z}, z^-\right) \overleftarrow{\mathcal{D}}_{\mathbf{z}^j} \mathcal{U}_F^\dagger\left(\frac{L^+}{2}, z^+; \mathbf{z}, z^-\right) \right] \\
 &- \frac{i}{(p^+ + k^+)} \int_{-\frac{L^+}{2}}^{\frac{L^+}{2}} dz^+ \left[\mathcal{U}_F^\dagger\left(z^+, -\frac{L^+}{2}; \mathbf{z}, z^-\right) \overleftarrow{\mathcal{D}}_{\mathbf{z}^j} \overrightarrow{\mathcal{D}}_{\mathbf{z}^j} \mathcal{U}_F^\dagger\left(\frac{L^+}{2}, z^+; \mathbf{z}, z^-\right) \right] \\
 &+ \frac{[\gamma^i, \gamma^j]}{4(p^+ + k^+)} \int_{-\frac{L^+}{2}}^{\frac{L^+}{2}} dz^+ \mathcal{U}_F^\dagger\left(z^+, -\frac{L^+}{2}; \mathbf{z}, z^-\right) g^t \cdot \mathcal{F}_{ij}(z) \mathcal{U}_F^\dagger\left(\frac{L^+}{2}, z^+; \mathbf{z}, z^-\right) \left. \right\} \frac{(\not{k} + m)}{2k^+} \\
 &+ O(\text{NNEik}). \tag{4.18}
 \end{aligned}$$

where we used the same notation as in Eqs. (3.35), (3.36), (3.37) and (3.38) for the covariant derivatives and field strength.

4.2.2 Propagators from inside to after the medium at Eik accuracy

In this subsection we compute the propagator for the case when the splitting of the photon occurs inside the medium, which corresponds to the outgoing quark kinematics $x^+ > L^+/2$ and $-L^+/2 < y^+ < L^+/2$ as well as to the outgoing antiquark kinematics $y^+ > L^+/2$ and $-L^+/2 < x^+ < L^+/2$. The diagrammatical representation for this case corresponds to the right panel in Fig.4.1. First, we compute the quark propagator. From Eq. (4.15), one can read off the quark propagator in pure A^- background at Eikonal accuracy in the inside-after quark kinematics and find

$$\begin{aligned}
 S_F(x, y)_{\beta\alpha} \Big|_{\text{pure } A^-, \text{Eik.}}^{\text{IA}, q} &= \int \frac{d^3 p}{(2\pi)^3} \int \frac{d^3 k}{(2\pi)^3} \theta(p^+) \theta(k^+) e^{-ix \cdot \not{p}} e^{iy \cdot \not{k} - iy \cdot \mathbf{k}} \frac{(\not{p} + m)}{2p^+} \gamma^+ \frac{(\not{k} + m)}{2k^+} \\
 &\times \int dz^- e^{iz^-(p^+ - k^+)} \int d^2 \mathbf{z} e^{-iz \cdot (\mathbf{p} - \mathbf{k})} \mathcal{U}_F(x^+, y^+; \mathbf{z}, z^-)_{\beta\alpha}. \tag{4.19}
 \end{aligned}$$

where the phase $e^{iy^+\check{k}^-}$ was dropped, since it contributes only at beyond eikonal accuracy as $|y^+| < L^+/2$. The Dirac structure can be expressed as

$$\begin{aligned} (\not{\check{p}} + m)\gamma^+(\not{\check{k}} + m) &= (\not{\check{p}} + m) \left[\{\gamma^+, \not{\check{k}}\} - (\not{\check{k}} - m)\gamma^+ \right] \\ &= (\not{\check{p}} + m) \left[2k^+ - (\not{\check{p}} - m)\gamma^+ - (\not{\check{k}} - \not{\check{p}})\gamma^+ \right] \\ &= (\not{\check{p}} + m) \left[2k^+ - (k^+ - p^+)\gamma^- \gamma^+ + (\mathbf{k}^i - \mathbf{p}^i)\gamma^i \gamma^+ \right]. \end{aligned} \quad (4.20)$$

We plug this in the propagator and obtain

$$\begin{aligned} S_F(x, y)_{\beta\alpha} \Big|_{\text{pure } \mathcal{A}^-, \text{Eik.}}^{\text{IA, } q} &= \int \frac{d^3 p}{(2\pi)^3} \int \frac{d^3 k}{(2\pi)^3} \frac{\theta(p^+)}{2p^+} \theta(k^+) e^{-ix \cdot \check{p}} e^{iy^- k^+ - iy \cdot \mathbf{k}} \int dz^- \int d^2 \mathbf{z} \\ &\times e^{iz^-(p^+ - k^+)} e^{-iz \cdot (\mathbf{p} - \mathbf{k})} (\not{\check{p}} + m) \left[1 + \frac{\gamma^- \gamma^+}{2k^+} i\overrightarrow{\partial}_{z^-} - \frac{\gamma^+ \gamma^i}{2k^+} i\overrightarrow{\partial}_{z^i} \right] \mathcal{U}_F(x^+, y^+; \mathbf{z}, z^-)_{\beta\alpha}. \end{aligned} \quad (4.21)$$

The z^- dependence of the background field and of $\mathcal{U}_F(x^+, y^+; \mathbf{z}, z^-)$ is parametrically slow for a highly boosted target due to Lorentz time dilation. For that reason, the term in $\partial_{z^-} \mathcal{U}_F(x^+, y^+; \mathbf{z}, z^-)$ is a NEik correction. In order to evaluate Eq.(4.14) at NEik accuracy, we need the propagator Eq.(4.21) only at strict Eikonal accuracy. In Eq.(4.21), it is thus safe to neglect the term in $\partial_{z^-} \mathcal{U}_F(x^+, y^+; \mathbf{z}, z^-)$. Moreover, the whole dependence of $\mathcal{U}_F(x^+, y^+; \mathbf{z}, z^-)$ on z^- can be neglected as well. The integral over z^- is then straightforward to perform and we also integrate over \mathbf{k} and then k^+ . One finds

$$\begin{aligned} S_F(x, y)_{\beta\alpha} \Big|_{\text{pure } \mathcal{A}^-, \text{Eik.}}^{\text{IA, } q} &= \int \frac{d^3 p}{(2\pi)^3} \frac{\theta(p^+)}{2p^+} e^{-ix \cdot \check{p}} e^{iy^- p^+} e^{-iy \cdot \mathbf{p}} \\ &\times (\not{\check{p}} + m) \left[1 - \frac{\gamma^+ \gamma^i}{2p^+} i\overrightarrow{\partial}_{y^i} \right] \mathcal{U}_F(x^+, y^+; \mathbf{y})_{\beta\alpha}. \end{aligned} \quad (4.22)$$

We also need to compute the contribution coming from the interaction with the transverse component of the background field. We compute this using the expression

$$\delta S_F(x, y) \Big|_{\text{single } \mathcal{A}_\perp} = \int d^4 w S_F(x, w) \Big|_{\text{pure } \mathcal{A}^-} [-ig \gamma^j t^a] \mathcal{A}_j^a(w) S_F(w, y) \Big|_{\text{pure } \mathcal{A}^-}. \quad (4.23)$$

By naive counting, one may think that due to the integration over w^+ in this region, where $\mathcal{A}_j^a(w)$ is non-trivial, the contribution Eq.(4.23) seems to be a NEik correction. However, due to the instantaneous term present in the propagator in pure \mathcal{A}^- field Eq.(4.15), this integration can be removed, and an Eikonal contribution can indeed be obtained³ with the transverse gauge field inserted either at $w^+ = x^+$ or at $w^+ = y^+$. In the inside-after kinematics $x^+ > L^+/2$ and $-L^+/2 < y^+ < L^+/2$ under consideration, the gauge field vanishes at x^+ but not at y^+ , so that Eq. (4.23) provides

³Because the Dirac structure of the instantaneous contribution to the propagator is simply γ^+ , we would get $\gamma^+ \gamma^j \gamma^+ = 0$ in the case of two instantaneous propagators separated by a transverse field insertion. Because of this observation, there is no Eikonal contribution to the quark propagator in inside-after kinematics with more than one transverse gauge field insertion.

an Eikonal contribution

$$\begin{aligned}
 \delta S_F(x, y) \Big|_{\text{single } \mathcal{A}_\perp, \text{Eik.}}^{\text{IA}, q} &= \int d^4 w S_F(x, w) \Big|_{\text{pure } \mathcal{A}^-, \text{Eik.}}^{\text{IA}, q} [-ig \gamma^j t^a] \mathcal{A}_j^a(w) S_F(w, y) \Big|_{\text{pure } \mathcal{A}^-, \text{instant.}} \\
 &= \int d^4 w \int \frac{d^3 p}{(2\pi)^3} \frac{\theta(p^+)}{2p^+} e^{-ix \cdot \not{p}} e^{iw^- p^+} e^{-i\mathbf{w} \cdot \mathbf{p}} (\not{p} + m) \\
 &\times \left\{ \left[1 - \frac{\gamma^+ \gamma^i}{2p^+} i \overrightarrow{\partial}_{\mathbf{w}^i} \right] \mathcal{U}_F(x^+, w^+; \mathbf{w}) \right\} \\
 &\times [-ig \gamma^j t^a] \mathcal{A}_j^a(\underline{w}) \delta^{(3)}(\underline{w} - \underline{y}) \gamma^+ \int \frac{dq^+}{2\pi} \frac{i}{2q^+} e^{-iq^+(w^- - y^-)}, \tag{4.24}
 \end{aligned}$$

where we have neglected the dependence on the w^- coordinate of \mathcal{A}_j^a . In the above expression the term with the derivative ∂_{w^i} vanishes, since it comes with the Dirac structure $\gamma^+ \gamma^i \gamma^j \gamma^+ = \gamma^+ \gamma^+ \gamma^i \gamma^j = 0$. Performing the integration over w , and then over q^+ , we get

$$\begin{aligned}
 \delta S_F(x, y) \Big|_{\text{single } \mathcal{A}_\perp, \text{Eik.}}^{\text{IA}, q} &= \int \frac{d^3 p}{(2\pi)^3} \frac{\theta(p^+)}{2p^+} e^{-ix \cdot \not{p}} e^{iy^- p^+} e^{-iy \cdot \mathbf{p}} (\not{p} + m) \\
 &\times (-1) \frac{\gamma^+ \gamma^j}{2p^+} \mathcal{U}_F(x^+, y^+; \mathbf{y}) [gt \cdot \mathcal{A}_j(\underline{y})]. \tag{4.25}
 \end{aligned}$$

One can obtain the full quark propagator at NEik order for the case of the photon splitting inside the medium by summing the expressions Eq.(4.22) and Eq.(4.25). One then finds

$$\begin{aligned}
 S_F(x, y) \Big|_{\text{Eik.}}^{\text{IA}, q} &= \int \frac{d^3 p}{(2\pi)^3} \frac{\theta(p^+)}{2p^+} e^{-ix \cdot \not{p}} \\
 &\times (\not{p} + m) \mathcal{U}_F(x^+, y^+; \mathbf{y}) \left[1 - \frac{\gamma^+ \gamma^i}{2p^+} i \overleftarrow{\mathcal{D}}_{\mathbf{y}^i} \right] e^{iy^- p^+} e^{-iy \cdot \mathbf{p}}. \tag{4.26}
 \end{aligned}$$

In a similar manner, one can compute the propagator for the antiquark at Eikonal accuracy in the inside-after kinematics, that is, $y^+ > L^+/2$ and $-L^+/2 < x^+ < L^+/2$. One finds

$$\begin{aligned}
 S_F(x, y) \Big|_{\text{Eik.}}^{\text{IA}, \bar{q}} &= \int \frac{d^3 k}{(2\pi)^3} (-1) \frac{\theta(-k^+)}{2k^+} e^{iy \cdot \not{k}} \\
 &\times e^{-ix^- k^+} e^{ix \cdot \mathbf{k}} \left[1 - \frac{\gamma^+ \gamma^i}{2k^+} i \overrightarrow{\mathcal{D}}_{\mathbf{x}^i} \right] \mathcal{U}_F^+(y^+, x^+; \mathbf{x}) (\not{k} + m). \tag{4.27}
 \end{aligned}$$

4.3 DIS-dijet production at NEik accuracy

In this section we compute the S-matrix elements and then the cross-section for the DIS dijet production. We can split this computation into two contributions according to the two types of diagrams for this process, as in Fig. 4.1.

4.3.1 Photon splitting inside the medium

Let us first discuss the contributions coming from the diagram with splitting inside. We need the expressions for the reduced propagators $\tilde{S}_F^q(z)$ and $\tilde{S}_F^{\bar{q}}(z)$ at Eikonal accuracy when the vertex location z^μ is inside the target, meaning $-L^+/2 < z^+ < L^+/2$. In the case of the reduced quark propagator $\tilde{S}_F^q(z)$, it simply amounts to insert the expression Eq.(4.26) into the definition Eq.(4.8), as

$$\begin{aligned} \tilde{S}_F^q(z) \Big|_{\text{Eik.}}^{\text{In}} &= \lim_{x^+ \rightarrow +\infty} \int d^2\mathbf{x} \int dx^- e^{i\mathbf{k}_1 \cdot \mathbf{x}} \bar{u}(1) \gamma^+ S_F(x, z) \Big|_{\text{Eik.}}^{\text{IA, } q} \\ &= \frac{\theta(k_1^+)}{2k_1^+} \bar{u}(1) \gamma^+ (\not{k}_1 + m) \mathcal{U}_F(+\infty, z^+; \mathbf{z}) \left[1 - \frac{\gamma^+ \gamma^i}{2k_1^+} i \overleftarrow{\mathcal{D}}_{\mathbf{z}^i} \right] e^{iz^- k_1^+} e^{-i\mathbf{z} \cdot \mathbf{k}_1} \\ &= \mathcal{U}_F\left(\frac{L^+}{2}, z^+; \mathbf{z}\right) \bar{u}(1) \left[1 - \frac{\gamma^+ \gamma^i}{2k_1^+} i \overleftarrow{\mathcal{D}}_{\mathbf{z}^i} \right] e^{iz^- k_1^+} e^{-i\mathbf{z} \cdot \mathbf{k}_1}, \end{aligned} \quad (4.28)$$

where it does not matter if the end point of the Wilson line is taken at $+\infty$ or at $+L^+/2$, since the gauge field vanishes outside the target.

Similarly, inserting the expression Eq.(4.27) into the definition Eq.(4.9), one finds the reduced antiquark propagator at Eikonal accuracy from z^μ inside the target as

$$\begin{aligned} \tilde{S}_F^{\bar{q}}(z) \Big|_{\text{Eik.}}^{\text{In}} &= \lim_{y^+ \rightarrow +\infty} \int d^2\mathbf{y} \int dy^- e^{i\mathbf{k}_2 \cdot \mathbf{y}} (-1) S_F(z, y) \Big|_{\text{Eik.}}^{\text{IA, } \bar{q}} \gamma^+ v(2) \\ &= e^{iz^- k_2^+} e^{-i\mathbf{z} \cdot \mathbf{k}_2} \left[1 + \frac{\gamma^+ \gamma^j}{2k_2^+} i \overrightarrow{\mathcal{D}}_{\mathbf{z}^j} \right] v(2) \mathcal{U}_F^\dagger\left(\frac{L^+}{2}, z^+; \mathbf{z}\right). \end{aligned} \quad (4.29)$$

Inserting the expressions Eq.(4.28) and Eq.(4.29) into the S-matrix expression, Eq. (4.14), and dropping the z^+ dependent phase factors, since they would contribute only at NNEik accuracy in the S-matrix and cross section, one gets

$$\begin{aligned} S_{q_1 \bar{q}_2 \leftarrow \gamma^*}^{\text{in}} &= -iee_f e_\mu^\lambda(q) 2\pi\delta(k_1^+ + k_2^+ - q^+) \int d^2\mathbf{z} \int_{-L^+/2}^{L^+/2} dz^+ \bar{u}(1) \mathcal{U}_F\left(\frac{L^+}{2}, z^+; \mathbf{z}\right) \\ &\quad \times \left\{ -\frac{\gamma^+ \gamma^i \gamma^\mu}{2k_1^+} i \overleftarrow{\mathcal{D}}_{\mathbf{z}^i} e^{-i(\mathbf{k}_1 + \mathbf{k}_2 - \mathbf{q}) \cdot \mathbf{z}} + e^{-i(\mathbf{k}_1 + \mathbf{k}_2 - \mathbf{q}) \cdot \mathbf{z}} \frac{\gamma^\mu \gamma^+ \gamma^j}{2k_2^+} i \overrightarrow{\mathcal{D}}_{\mathbf{z}^j} \right. \\ &\quad \left. + \frac{\gamma^+ \gamma^i \gamma^\mu \gamma^+ \gamma^j}{(2k_1^+)(2k_2^+)} \overleftarrow{\mathcal{D}}_{\mathbf{z}^i} e^{-i(\mathbf{k}_1 + \mathbf{k}_2 - \mathbf{q}) \cdot \mathbf{z}} \overrightarrow{\mathcal{D}}_{\mathbf{z}^j} \right\} \mathcal{U}_F^\dagger\left(\frac{L^+}{2}, z^+; \mathbf{z}\right) v(2). \end{aligned} \quad (4.30)$$

The color structure in the first term can be simplified as

$$\left[\mathcal{U}_F\left(\frac{L^+}{2}, z^+; \mathbf{z}\right) \overleftarrow{\mathcal{D}}_{\mathbf{z}^i} \mathcal{U}_F^\dagger\left(\frac{L^+}{2}, z^+; \mathbf{z}\right) \right] = -\frac{1}{2} \left[\mathcal{U}_F\left(\frac{L^+}{2}, z^+; \mathbf{z}\right) \overleftrightarrow{\mathcal{D}}_{\mathbf{z}^i} \mathcal{U}_F^\dagger\left(\frac{L^+}{2}, z^+; \mathbf{z}\right) \right] \quad (4.31)$$

and similarly the second one

$$\left[\mathcal{U}_F\left(\frac{L^+}{2}, z^+; \mathbf{z}\right) \overrightarrow{\mathcal{D}}_{\mathbf{z}^j} \mathcal{U}_F^\dagger\left(\frac{L^+}{2}, z^+; \mathbf{z}\right) \right] = \frac{1}{2} \left[\mathcal{U}_F\left(\frac{L^+}{2}, z^+; \mathbf{z}\right) \overleftrightarrow{\mathcal{D}}_{\mathbf{z}^j} \mathcal{U}_F^\dagger\left(\frac{L^+}{2}, z^+; \mathbf{z}\right) \right] \quad (4.32)$$

Using these expressions the "in" contribution to the S-matrix reads:

$$\begin{aligned}
S_{q_1 \bar{q}_2 \leftarrow \gamma^*}^{\text{in}} &= -iee_f \epsilon_\mu^\lambda(q) 2\pi\delta(k_1^+ + k_2^+ - q^+) \int d^2\mathbf{z} e^{-i(\mathbf{k}_1 + \mathbf{k}_2 - \mathbf{q}) \cdot \mathbf{z}} \int_{-L^+/2}^{L^+/2} dz^+ \\
&\times \left\{ \left[\frac{i}{4k_1^+} \bar{u}(1) \gamma^+ \gamma^j \gamma^\mu v(2) + \frac{i}{4k_2^+} \bar{u}(1) \gamma^\mu \gamma^+ \gamma^j v(2) \right] \right. \\
&\times \left[\mathcal{U}_F\left(\frac{L^+}{2}, z^+; \mathbf{z}\right) \overleftrightarrow{\mathcal{D}}_{\mathbf{z}^i} \mathcal{U}_F^\dagger\left(\frac{L^+}{2}, z^+; \mathbf{z}\right) \right] \\
&\left. + \frac{g^{\mu+}}{2k_1^+ k_2^+} \bar{u}(1) \gamma^+ \gamma^i \gamma^j v(2) \left[\mathcal{U}_F\left(\frac{L^+}{2}, z^+; \mathbf{z}\right) \overleftrightarrow{\mathcal{D}}_{\mathbf{z}^i} \overleftrightarrow{\mathcal{D}}_{\mathbf{z}^j} \mathcal{U}_F^\dagger\left(\frac{L^+}{2}, z^+; \mathbf{z}\right) \right] \right\}, \quad (4.33)
\end{aligned}$$

where now the covariant derivatives act only on the Wilson lines and not on the phases.

At this point, before computing the cross-section, one can evaluate the S-matrix for the two possible polarization of the photon in this process. We have both transverse and longitudinal polarization, but the last term in Eq.(4.33) does not contribute to the scattering processes, since in the light-cone gauge $\epsilon_\lambda^+(q) = 0$.

Longitudinal photon case :

In light-cone gauge, the longitudinal polarization vector can be chosen as

$$\epsilon_\mu^\lambda(q) \rightarrow \epsilon_\mu^L(q) \equiv \frac{Q}{q^+} g_\mu^+ . \quad (4.34)$$

Upon inserting this in Eq. (4.33), the first two Dirac structures vanish as well due to $\gamma^+ \gamma^+ = 0$ and $\{\gamma^+, \gamma^i\} = 0$. Therefore, in the case of longitudinally polarized photon, the inside contribution to the S-matrix element vanishes at NEik order:

$$S_{q_1 \bar{q}_2 \leftarrow \gamma_L^*}^{\text{in}} = 0 + O(\text{NNEik}) . \quad (4.35)$$

Transverse photon case :

For a transverse photon, the two possible polarization vectors in light-cone gauge can be written as

$$\begin{aligned}
\epsilon_\lambda^+(q) &= 0 \\
\epsilon_\lambda^i(q) &= \epsilon_\lambda^i \\
\epsilon_\lambda^-(q) &= \frac{\mathbf{q}^i \epsilon_\lambda^i}{q^+}
\end{aligned} \quad (4.36)$$

inserting these polarization vectors in Eq. (4.33), one gets

$$\begin{aligned}
S_{q_1 \bar{q}_2 \leftarrow \gamma_T^*}^{\text{in}} &= ee_f \epsilon_\lambda^i 2\pi\delta(k_1^+ + k_2^+ - q^+) \left[-\frac{1}{4k_1^+} \bar{u}(1) \gamma^+ \gamma^j \gamma^i v(2) - \frac{1}{4k_2^+} \bar{u}(1) \gamma^i \gamma^+ \gamma^j v(2) \right] \\
&\times \int d^2\mathbf{z} e^{-i(\mathbf{k}_1 + \mathbf{k}_2 - \mathbf{q}) \cdot \mathbf{z}} \int_{-L^+/2}^{L^+/2} dz^+ \left[\mathcal{U}_F\left(\frac{L^+}{2}, z^+; \mathbf{z}\right) \overleftrightarrow{\mathcal{D}}_{\mathbf{z}^i} \mathcal{U}_F^\dagger\left(\frac{L^+}{2}, z^+; \mathbf{z}\right) \right]. \quad (4.37)
\end{aligned}$$

It is convenient to separate the parts of the Dirac structures into symmetric and antisymmetric under the exchange of i and j . Then, one finds

$$\begin{aligned}
S_{q_1 \bar{q}_2 \leftarrow \gamma_T^*}^{\text{in}} &= e e_f \varepsilon_\lambda^i 2\pi \delta(k_1^+ + k_2^+ - q^+) \frac{q^+}{4k_1^+ k_2^+} \bar{u}(1) \gamma^+ \left(\frac{(k_2^+ - k_1^+)}{q^+} \delta^{ij} + \frac{1}{2} [\gamma^i, \gamma^j] \right) v(2) \\
&\times \int d^2 \mathbf{z} e^{-i(\mathbf{k}_1 + \mathbf{k}_2 - \mathbf{q}) \cdot \mathbf{z}} \int_{-L^+/2}^{L^+/2} dz^+ \left[\mathcal{U}_F \left(\frac{L^+}{2}, z^+; \mathbf{z} \right) \overleftrightarrow{\mathcal{D}}_{\mathbf{z}} \mathcal{U}_F^+ \left(\frac{L^+}{2}, z^+; \mathbf{z} \right) \right].
\end{aligned} \tag{4.38}$$

4.3.2 Photon splitting before the medium

We now focus on the contribution Eq.(4.13) to the S-matrix, in which the photon splits before the target, at NEik accuracy. The first step is then to calculate the reduced quark and antiquark propagators $\tilde{S}_F^q(z)$ and $\tilde{S}_F^{\bar{q}}(z)$ at NEik accuracy. When the photon splits before the target, we use, for the quark propagator in the formula Eq.(4.8), the expression Eq.(4.17). Then we get

$$\begin{aligned}
\tilde{S}_F^q(z) &= \lim_{x^+ \rightarrow +\infty} \int d^2 \mathbf{x} \int dx^- e^{ik_1 \cdot x} \bar{u}(1) \gamma^+ \int \frac{d^3 \underline{p}}{(2\pi)^3} \int \frac{d^3 \underline{k}}{(2\pi)^3} \int dv^- e^{iv \cdot (p^+ - k^+)} \\
&\times \theta(k^+) \theta(p^+) e^{-ix \cdot \check{p}} e^{iz \cdot \check{k}} \frac{(\check{p} + m)}{2p^+} \gamma^+ \int d^2 \mathbf{v} e^{-iv \cdot (\mathbf{p} - \mathbf{k})} \left\{ \mathcal{U}_F(\mathbf{v}, v^-) + \frac{1}{p^+ + k^+} \int_{-\frac{L^+}{2}}^{\frac{L^+}{2}} dv^+ \right. \\
&\times \left[\mathcal{U}_F \left(\frac{L^+}{2}, v^+; \mathbf{v}, v^- \right) \left(\frac{[\gamma^i, \gamma^j]}{4} g t \cdot \mathcal{F}_{ij}(v) - \frac{(\mathbf{p}^j + \mathbf{k}^j)}{2} \overleftrightarrow{\mathcal{D}}_{\mathbf{v}^j} - i \overleftarrow{\mathcal{D}}_{\mathbf{v}^j} \overrightarrow{\mathcal{D}}_{\mathbf{v}^j} \right) \right. \\
&\left. \left. \times \mathcal{U}_F \left(v^+, -\frac{L^+}{2}; \mathbf{v}, v^- \right) \right] \right\} \frac{(\check{k} + m)}{2k^+}
\end{aligned} \tag{4.39}$$

using $\gamma^+(\check{p} + m)\gamma^+ = 2p^+\gamma^+$ and integrating first over \mathbf{x} and x^- and then over \underline{p} we obtain

$$\begin{aligned}
\tilde{S}_F^q(z) &= \bar{u}(1) \gamma^+ \int \frac{d^3 \underline{k}}{(2\pi)^3} \theta(k^+) e^{iz \cdot \check{k}} \int dv^- e^{iv \cdot (k_1^+ - k^+)} \int d^2 \mathbf{v} e^{-iv \cdot (\mathbf{k}_1 - \mathbf{k})} \left\{ \mathcal{U}_F(\mathbf{v}, v^-) \right. \\
&+ \frac{1}{k_1^+ + k^+} \int_{-\frac{L^+}{2}}^{\frac{L^+}{2}} dv^+ \left[\mathcal{U}_F \left(\frac{L^+}{2}, v^+; \mathbf{v}, v^- \right) \left(\frac{[\gamma^i, \gamma^j]}{4} g t \cdot \mathcal{F}_{ij}(v) - \frac{(\mathbf{k}_1^j + \mathbf{k}^j)}{2} \overleftrightarrow{\mathcal{D}}_{\mathbf{v}^j} - i \overleftarrow{\mathcal{D}}_{\mathbf{v}^j} \overrightarrow{\mathcal{D}}_{\mathbf{v}^j} \right) \right. \\
&\left. \left. \times \mathcal{U}_F \left(v^+, -\frac{L^+}{2}; \mathbf{v}, v^- \right) \right] \right\} \frac{(\check{k} + m)}{2k^+}.
\end{aligned} \tag{4.40}$$

where we used $e^{ix^+(\check{k}_1^- - \check{p}^-)} \rightarrow e^{ix^+(\check{k}_1^- - \check{k}_1^-)} = 1$.

For the anti-quark propagator in the formula Eq.(4.9) we use the expression Eq.(4.18). We have

$$\begin{aligned}
 \tilde{S}_F^{\bar{q}}(z) &= \lim_{y^+ \rightarrow +\infty} \int d^2\mathbf{y} \int dy^- e^{ik_2 \cdot y} \int \frac{d^3\mathbf{p}}{(2\pi)^3} \int \frac{d^3\mathbf{k}}{(2\pi)^3} \int dw^- e^{iw^-(p^+ - k^+)} \\
 &\times \theta(-p^+) \theta(-k^+) e^{-iz \cdot \check{p}} e^{iy \cdot \check{k}} \frac{(\check{p} + m)}{2p^+} \gamma^+ \int d^2\mathbf{w} e^{-i\mathbf{w} \cdot (\mathbf{p} - \mathbf{k})} \left\{ \mathcal{U}_F^+(\mathbf{w}, w^-) \right. \\
 &- \frac{1}{p^+ + k^+} \int_{-\frac{L^+}{2}}^{\frac{L^+}{2}} dw^+ \left[\mathcal{U}_F^+(w^+, -\frac{L^+}{2}; \mathbf{w}, w^-) \right. \\
 &\times \left. \left. \left(\frac{[\gamma^i, \gamma^j]}{4} gt \cdot \mathcal{F}_{ij}(w) - \frac{(\mathbf{p}^j + \mathbf{k}^j)}{2} \overleftarrow{\mathcal{D}}_{\mathbf{w}^j} - i \overleftarrow{\mathcal{D}}_{\mathbf{w}^j} \overrightarrow{\mathcal{D}}_{\mathbf{w}^j} \right) \mathcal{U}_F^+\left(\frac{L^+}{2}, w^+; \mathbf{w}, w^-\right) \right] \right\} \\
 &\times \frac{(\check{k} + m)}{2k^+} \gamma^+ v(2) \tag{4.41}
 \end{aligned}$$

Since γ^+ commutes with $[\gamma^i, \gamma^j]$ we can use $\gamma^+(\check{k} + m)\gamma^+ = 2k^+\gamma^+$. We also integrate first over \mathbf{y} and y^- and then over \mathbf{k} and obtain

$$\begin{aligned}
 \tilde{S}_F^{\bar{q}}(z) &= \int \frac{d^3\mathbf{p}}{(2\pi)^3} \theta(-p^+) \theta(k_2^+) \int dw^- e^{iw^-(p^+ + k_2^+)} e^{-iz \cdot \check{p}} \frac{(\check{p} + m)}{2p^+} \int d^2\mathbf{w} e^{-i\mathbf{w} \cdot (\mathbf{p} + \mathbf{k}_2)} \\
 &\times \left\{ \mathcal{U}_F^+(\mathbf{w}, w^-) \left[\mathcal{U}_F^+(w^+, -\frac{L^+}{2}; \mathbf{w}, w^-) \right. \right. \\
 &\times \left. \left. \left(\frac{[\gamma^i, \gamma^j]}{4} gt \cdot \mathcal{F}_{ij}(w) - \frac{(\mathbf{p}^j - \mathbf{k}_2^j)}{2} \overleftarrow{\mathcal{D}}_{\mathbf{w}^j} - i \overleftarrow{\mathcal{D}}_{\mathbf{w}^j} \overrightarrow{\mathcal{D}}_{\mathbf{w}^j} \right) \mathcal{U}_F^+\left(\frac{L^+}{2}, w^+; \mathbf{w}, w^-\right) \right] \right\} \gamma^+ v(2) \tag{4.42}
 \end{aligned}$$

where we used $e^{iy^+(\check{k}^- + \check{k}_2^-)} \rightarrow e^{iy^+(-\check{k}_2^- + \check{k}_2^-)} = 1$.

Inserting now the propagators Eq.(4.40) and Eq.(4.42) to Eq.(4.13) we get

$$\begin{aligned}
 S_{q_1 \bar{q}_2 \leftarrow \gamma^*}^{\text{bef}} &= -ie e_f \epsilon_\mu^\lambda(q) \int \frac{d^3\mathbf{k}}{(2\pi)^3} \theta(k^+) \int \frac{d^3\mathbf{p}}{(2\pi)^3} \theta(-p^+) \int d^2\mathbf{z} \int dz^- \int_{-\infty}^{-L^+/2} dz^+ \\
 &\times e^{-iz \cdot (q - \check{k} + \check{p})} \int dv^- e^{iv^-(k_1^+ - k^+)} \int dw^- e^{iw^-(k_2^+ + p^+)} \int d^2\mathbf{v} e^{-i\mathbf{v} \cdot (\mathbf{k}_1 - \mathbf{k})} \\
 &\times \int d^2\mathbf{w} e^{-i\mathbf{w} \cdot (\mathbf{p} + \mathbf{k}_2)} \bar{u}(1) \gamma^+ \left\{ \mathcal{U}_F(\mathbf{v}, v^-) + \frac{1}{k_1^+ + k^+} \int_{-\frac{L^+}{2}}^{\frac{L^+}{2}} dv^+ \mathcal{U}_F\left(\frac{L^+}{2}, v^+; \mathbf{v}, v^-\right) \right. \\
 &\times \left. \left(\frac{[\gamma^i, \gamma^j]}{4} gt \cdot \mathcal{F}_{ij}(v) - \frac{(\mathbf{k}_1^j + \mathbf{k}^j)}{2} \overleftarrow{\mathcal{D}}_{\mathbf{v}^j} - i \overleftarrow{\mathcal{D}}_{\mathbf{v}^j} \overrightarrow{\mathcal{D}}_{\mathbf{v}^j} \right) \mathcal{U}_F\left(v^+, -\frac{L^+}{2}; \mathbf{v}, v^-\right) \right\} \frac{(\check{k} + m)}{2k^+} \\
 &\times \gamma^\mu \frac{(\check{p} + m)}{2p^+} \left\{ \mathcal{U}_F^+(\mathbf{w}, w^-) + \frac{1}{k_2^+ - p^+} \int_{-\frac{L^+}{2}}^{\frac{L^+}{2}} dw^+ \mathcal{U}_F^+(w^+, -\frac{L^+}{2}; \mathbf{w}, w^-) \right. \\
 &\times \left. \left(\frac{[\gamma^i, \gamma^j]}{4} gt \cdot \mathcal{F}_{i'j'}(w) - \frac{(\mathbf{p}^{j'} - \mathbf{k}_2^{j'})}{2} \overleftarrow{\mathcal{D}}_{\mathbf{w}^{j'}} - i \overleftarrow{\mathcal{D}}_{\mathbf{w}^{j'}} \overrightarrow{\mathcal{D}}_{\mathbf{w}^{j'}} \right) \mathcal{U}_F^+\left(\frac{L^+}{2}, w^+; \mathbf{w}, w^-\right) \right\} \\
 &\times \gamma^+ v(2) + i e e_f \epsilon_\mu^\lambda(q) \bar{u}(1) \gamma^\mu v(2) \int d^2\mathbf{z} \int dz^- \int_{-\infty}^{-L^+/2} dz^+ e^{-iz \cdot (q - \check{k}_1 - \check{k}_2)} \tag{4.43}
 \end{aligned}$$

The integrals over the location z^μ of the photon splitting vertex before the target can be performed explicitly: the unrestricted integrations over \mathbf{z} and z^- enforce the conservation of the transverse and $+$ components of the momentum at the vertex, whereas the integrations over z^+ are of the form

$$\int_{-\infty}^{-L^+/2} dz^+ e^{-iz^+E^-} = \frac{i}{(E^- + i\epsilon)} e^{i\frac{L^+}{2}E^-}, \quad (4.44)$$

with $E^- = (q^- - \check{k}^- + \check{p}^-)$, except in the vacuum subtraction term, in which $E^- = (q^- - \check{k}_1^- - \check{k}_2^-)$. We thus obtain

$$\begin{aligned} S_{q_1\bar{q}_2\leftarrow\gamma^*}^{\text{bef}} &= -iee_f \epsilon_\mu^\lambda(q) \int \frac{d^3\mathbf{k}}{(2\pi)^3} \theta(k^+) \int \frac{d^3\mathbf{p}}{(2\pi)^3} \theta(-p^+) (2\pi)^3 \delta^{(3)}(\underline{q} - \underline{k} + \underline{p}) \\ &\times \frac{ie^{i\frac{L^+}{2}(q^- - \check{k}^- + \check{p}^-)}}{(q^- - \check{k}^- + \check{p}^- + i\epsilon)} \int dv^- e^{iv^-(k_1^+ - k^+)} \int dw^- e^{iw^-(k_2^+ + p^+)} \int d^2\mathbf{v} e^{-i\mathbf{v}\cdot(\mathbf{k}_1 - \mathbf{k})} \\ &\times \int d^2\mathbf{w} e^{-i\mathbf{w}\cdot(\mathbf{p} + \mathbf{k}_2)} \bar{u}(1)\gamma^+ \left\{ \mathcal{U}_F(\mathbf{v}, v^-) + \frac{1}{k_1^+ + k^+} \int_{-\frac{L^+}{2}}^{\frac{L^+}{2}} dv^+ \mathcal{U}_F\left(\frac{L^+}{2}, v^+; \mathbf{v}, v^-\right) \right. \\ &\times \left. \left(\frac{[\gamma^i, \gamma^j]}{4} g t \cdot \mathcal{F}_{ij}(v) - \frac{(\mathbf{k}_1^j + \mathbf{k}^j)}{2} \overleftrightarrow{\mathcal{D}}_{\mathbf{v}j} - i \overleftrightarrow{\mathcal{D}}_{\mathbf{v}j} \overrightarrow{\mathcal{D}}_{\mathbf{v}j} \right) \mathcal{U}_F\left(v^+, -\frac{L^+}{2}; \mathbf{v}, v^-\right) \right\} \\ &\times \frac{(\check{k}^- + m)}{2k^+} \gamma^\mu \frac{(\check{p}^- + m)}{2p^+} \left\{ \mathcal{U}_F^\dagger(\mathbf{w}, w^-) + \frac{1}{k_2^+ - p^+} \int_{-\frac{L^+}{2}}^{\frac{L^+}{2}} dw^+ \mathcal{U}_F^\dagger\left(w^+, -\frac{L^+}{2}; \mathbf{w}, w^-\right) \right. \\ &\times \left. \left(\frac{[\gamma^i, \gamma^j]}{4} g t \cdot \mathcal{F}_{ij}(w) - \frac{(\mathbf{p}^j - \mathbf{k}_2^j)}{2} \overleftrightarrow{\mathcal{D}}_{\mathbf{w}j} - i \overleftrightarrow{\mathcal{D}}_{\mathbf{w}j} \overrightarrow{\mathcal{D}}_{\mathbf{w}j} \right) \mathcal{U}_F^\dagger\left(\frac{L^+}{2}, w^+; \mathbf{w}, w^-\right) \right\} \\ &\times \gamma^+ v(2) + iee_f \epsilon_\mu^\lambda(q) \bar{u}(1)\gamma^\mu v(2) (2\pi)^3 \delta^{(3)}(\underline{q} - \underline{k}_1 - \underline{k}_2) \frac{ie^{i\frac{L^+}{2}(q^- - \check{k}_1^- - \check{k}_2^-)}}{(q^- - \check{k}_1^- - \check{k}_2^- + i\epsilon)}. \end{aligned} \quad (4.45)$$

In Eq.(4.45) one can find contributions at both generalized eikonal and subeikonal order. The latter can be split into different types of contributions that are at NEik order: decorations on the Wilson line associated with the quark or with the antiquark and phase factor dependent on the target width L^+ . The generalized eikonal term is represented by the dependence on v^- or w^- of the background field and Wilson lines. However, we only account for one of these NEik terms at a time, since taking two such corrections together would yield terms that are at NNEik accuracy at the level of the S-matrix and cross-section.

Let us consider the contribution to the expression Eq.(4.45) with decorations inserted on the quark Wilson line. This contribution only starts at NEik accuracy due to the integration over the v^+ at which the decorations are inserted. We can thus neglect in that contribution any further non-Eikonal effect: the phase factor dependent on L^+ , and the dependence on v^- and w^- of the background field and Wilson lines. The latter allows us to perform the integrations over v^- and w^- analytically, and to obtain⁴

⁴Note that in this case $\theta(k^+) = \theta(k_1^+) = 1$ and $\theta(-p^+) = \theta(k_2^+) = 1$, since $k_1^+ > 0$ and $k_2^+ > 0$ by definition for the produced particles.

$$\begin{aligned}
 S_{q_1 \bar{q}_2 \leftarrow \gamma^*}^{\text{bef}} \Big|_{\text{dec. on } q} &= 2\pi\delta(k_1^+ + k_2^+ - q^+) (-i) e e_f \epsilon_\mu^\lambda(q) \int \frac{d^3 \underline{k}}{(2\pi)^3} 2\pi\delta(k^+ - k_1^+) \int \frac{d^3 \underline{p}}{(2\pi)^3} \\
 &\times (2\pi)^3 \delta^{(3)}(\underline{q} - \underline{k} + \underline{p}) \frac{1}{2k_1^+} \frac{i}{(q^- - \check{k}^- + \check{p}^- + i\epsilon)} \int d^2 \underline{\mathbf{v}} e^{-i\mathbf{v} \cdot (\mathbf{k}_1 - \mathbf{k})} \int d^2 \underline{\mathbf{w}} e^{-i\mathbf{w} \cdot (\mathbf{p} + \mathbf{k}_2)} \bar{u}(1) \\
 &\times \int_{-\frac{L^+}{2}}^{\frac{L^+}{2}} dv^+ \left[\mathcal{U}_F\left(\frac{L^+}{2}, v^+; \mathbf{v}\right) \left(\frac{[\gamma^i, \gamma^j]}{4} g t \cdot \mathcal{F}_{ij}(\underline{v}) - \frac{(\mathbf{k}_1^j + \mathbf{k}^j)}{2} \overleftarrow{\mathcal{D}}_{\mathbf{v}^j} - i \overleftarrow{\mathcal{D}}_{\mathbf{v}^j} \overrightarrow{\mathcal{D}}_{\mathbf{v}^j} \right) \right. \\
 &\left. \times \mathcal{U}_F\left(v^+, -\frac{L^+}{2}; \mathbf{v}\right) \mathcal{U}_F^\dagger(\mathbf{w}) \right] \gamma^+ \frac{(\check{k}^+ + m)}{2k^+} \gamma^\mu \frac{(\check{p}^+ + m)}{2p^+} \gamma^+ v(2). \tag{4.46}
 \end{aligned}$$

Similarly, one can extract from Eq. (4.45) the NEik contribution associated with decorations inserted on the antiquark Wilson line, and simplify it into

$$\begin{aligned}
 S_{q_1 \bar{q}_2 \leftarrow \gamma^*}^{\text{bef}} \Big|_{\text{dec. on } \bar{q}} &= 2\pi\delta(k_1^+ + k_2^+ - q^+) (-i) e e_f \epsilon_\mu^\lambda(q) \int \frac{d^3 \underline{k}}{(2\pi)^3} 2\pi\delta(k^+ - k_1^+) \int \frac{d^3 \underline{p}}{(2\pi)^3} \\
 &\times (2\pi)^3 \delta^{(3)}(\underline{q} - \underline{k} + \underline{p}) \frac{1}{2k_2^+} \frac{i}{(q^- - \check{k}^- + \check{p}^- + i\epsilon)} \bar{u}(1) \gamma^+ \frac{(\check{k}^+ + m)}{2k^+} \gamma^\mu \\
 &\times \frac{(\check{p}^+ + m)}{2p^+} \gamma^+ \int d^2 \underline{\mathbf{v}} e^{-i\mathbf{v} \cdot (\mathbf{k}_1 - \mathbf{k})} \int d^2 \underline{\mathbf{w}} e^{-i\mathbf{w} \cdot (\mathbf{p} + \mathbf{k}_2)} \int_{-\frac{L^+}{2}}^{\frac{L^+}{2}} dw^+ \left[\mathcal{U}_F(\mathbf{v}) \mathcal{U}_F^\dagger\left(w^+, -\frac{L^+}{2}; \mathbf{w}\right) \right. \\
 &\left. \times \left(\frac{[\gamma^i, \gamma^j]}{4} g t \cdot \mathcal{F}_{ij}(\underline{w}) - \frac{(\mathbf{p}^j - \mathbf{k}_2^j)}{2} \overleftarrow{\mathcal{D}}_{\mathbf{w}^j} - i \overleftarrow{\mathcal{D}}_{\mathbf{w}^j} \overrightarrow{\mathcal{D}}_{\mathbf{w}^j} \right) \mathcal{U}_F^\dagger\left(\frac{L^+}{2}, w^+; \mathbf{w}\right) \right] v(2). \tag{4.47}
 \end{aligned}$$

After extracting from Eq. (4.45) the contributions Eq.(4.46) and Eq.(4.47) of decorations on the quark or antiquark Wilson lines, the leftover is

$$\begin{aligned}
 S_{q_1 \bar{q}_2 \leftarrow \gamma^*}^{\text{bef}} - S_{q_1 \bar{q}_2 \leftarrow \gamma^*}^{\text{bef}} \Big|_{\text{dec. on } q} - S_{q_1 \bar{q}_2 \leftarrow \gamma^*}^{\text{bef}} \Big|_{\text{dec. on } \bar{q}} &= -i e e_f \epsilon_\mu^\lambda(q) \int \frac{d^3 \underline{k}}{(2\pi)^3} \theta(k^+) \int \frac{d^3 \underline{p}}{(2\pi)^3} \\
 &\times \theta(-p^+) (2\pi)^3 \delta^{(3)}(\underline{q} - \underline{k} + \underline{p}) \frac{i}{(q^- - \check{k}^- + \check{p}^- + i\epsilon)} e^{i\frac{L^+}{2}(q^- - \check{k}^- + \check{p}^-)} \bar{u}(1) \gamma^+ \\
 &\times \frac{(\check{k}^+ + m)}{2k^+} \gamma^\mu \frac{(\check{p}^+ + m)}{2p^+} \gamma^+ v(2) \int d^2 \underline{\mathbf{v}} e^{-i\mathbf{v} \cdot (\mathbf{k}_1 - \mathbf{k})} \int d^2 \underline{\mathbf{w}} e^{-i\mathbf{w} \cdot (\mathbf{p} + \mathbf{k}_2)} \\
 &\times \int dv^- e^{iv^-(k_1^+ - k^+)} \int dw^- e^{iw^-(k_2^+ + p^+)} \mathcal{U}_F(\mathbf{v}, v^-) \mathcal{U}_F^\dagger(\mathbf{w}, w^-) \\
 &+ i e e_f \epsilon_\mu^\lambda(q) \bar{u}(1) \gamma^\mu v(2) (2\pi)^3 \delta^{(3)}(\underline{q} - \underline{k}_1 - \underline{k}_2) \frac{i}{(q^- - \check{k}_1^- - \check{k}_2^- + i\epsilon)} e^{i\frac{L^+}{2}(q^- - \check{k}_1^- - \check{k}_2^-)}. \tag{4.48}
 \end{aligned}$$

Noting that

$$\begin{aligned}
& \int \frac{d^3 \underline{k}}{(2\pi)^3} \theta(k^+) \int \frac{d^3 \underline{p}}{(2\pi)^3} \theta(-p^+) (2\pi)^3 \delta^{(3)}(\underline{q} - \underline{k} + \underline{p}) \frac{i}{(q^- - \check{k}^- + \check{p}^- + i\epsilon)} \\
& \times e^{i\frac{L^+}{2}(q^- - \check{k}^- + \check{p}^-)} \bar{u}(1) \gamma^+ \frac{(\check{\mathbf{k}} + m)}{2k^+} \gamma^\mu \frac{(\check{\mathbf{p}} + m)}{2p^+} \gamma^+ v(2) \int d^2 \mathbf{v} e^{-i\mathbf{v} \cdot (\mathbf{k}_1 - \mathbf{k})} \int d^2 \mathbf{w} e^{-i\mathbf{w} \cdot (\mathbf{p} + \mathbf{k}_2)} \\
& \times \int dv^- e^{iv^-(k_1^+ - k^+)} \int dw^- e^{iw^-(k_2^+ + p^+)} \\
& = \int \frac{d^3 \underline{k}}{(2\pi)^3} \theta(k^+) \int \frac{d^3 \underline{p}}{(2\pi)^3} \theta(-p^+) (2\pi)^3 \delta^{(3)}(\underline{q} - \underline{k} + \underline{p}) \frac{i}{(q^- - \check{k}^- + \check{p}^- + i\epsilon)} e^{i\frac{L^+}{2}(q^- - \check{k}^- + \check{p}^-)} \\
& \times \bar{u}(1) \gamma^+ \frac{(\check{\mathbf{k}} + m)}{2k^+} \gamma^\mu \frac{(\check{\mathbf{p}} + m)}{2p^+} \gamma^+ v(2) (2\pi)^3 \delta^{(3)}(\underline{k} - \underline{k}_1) (2\pi)^3 \delta^{(3)}(\underline{p} + \underline{k}_2) \\
& = (2\pi)^3 \delta^{(3)}(\underline{q} - \underline{k}_1 - \underline{k}_2) \frac{i}{(q^- - \check{k}_1^- - \check{k}_2^- + i\epsilon)} e^{i\frac{L^+}{2}(q^- - \check{k}_1^- - \check{k}_2^-)} \bar{u}(1) \gamma^\mu v(2) , \tag{4.49}
\end{aligned}$$

it is possible to rewrite Eq. (4.48) as

$$\begin{aligned}
& S_{q_1 \bar{q}_2 \leftarrow \gamma^*}^{\text{bef}} - S_{q_1 \bar{q}_2 \leftarrow \gamma^*}^{\text{bef}} \Big|_{\text{dec. on } q} - S_{q_1 \bar{q}_2 \leftarrow \gamma^*}^{\text{bef}} \Big|_{\text{dec. on } \bar{q}} = -iee_f \epsilon_\mu^\lambda(q) \int \frac{d^3 \underline{k}}{(2\pi)^3} \theta(k^+) \\
& \times \int \frac{d^3 \underline{p}}{(2\pi)^3} \theta(-p^+) (2\pi)^3 \delta^{(3)}(\underline{q} - \underline{k} + \underline{p}) \frac{i}{(q^- - \check{k}^- + \check{p}^- + i\epsilon)} e^{i\frac{L^+}{2}(q^- - \check{k}^- + \check{p}^-)} \bar{u}(1) \gamma^+ \\
& \times \frac{(\check{\mathbf{k}} + m)}{2k^+} \gamma^\mu \frac{(\check{\mathbf{p}} + m)}{2p^+} \gamma^+ v(2) \int d^2 \mathbf{v} e^{-i\mathbf{v} \cdot (\mathbf{k}_1 - \mathbf{k})} \int d^2 \mathbf{w} e^{-i\mathbf{w} \cdot (\mathbf{p} + \mathbf{k}_2)} \int dv^- e^{iv^-(k_1^+ - k^+)} \\
& \times \int dw^- e^{iw^-(k_2^+ + p^+)} \left[\mathcal{U}_F(\mathbf{v}, v^-) \mathcal{U}_F^\dagger(\mathbf{w}, w^-) - 1 \right] . \tag{4.50}
\end{aligned}$$

Expanding the L^+ dependent phase factor at small target width L^+ , one finds the contribution linear in L^+ to be ⁵

$$\begin{aligned}
& S_{q_1 \bar{q}_2 \leftarrow \gamma^*}^{\text{bef}} \Big|_{L^+ \text{ phase}} = 2\pi \delta(k_1^+ + k_2^+ - q^+) (-i) ee_f \epsilon_\mu^\lambda(q) \int \frac{d^3 \underline{k}}{(2\pi)^3} 2\pi \delta(k^+ - k_1^+) \int \frac{d^3 \underline{p}}{(2\pi)^3} \\
& \times (2\pi)^3 \delta^{(3)}(\underline{q} - \underline{k} + \underline{p}) (-1) \frac{L^+}{2} \bar{u}(1) \gamma^+ \frac{(\check{\mathbf{k}} + m)}{2k^+} \gamma^\mu \frac{(\check{\mathbf{p}} + m)}{2p^+} \gamma^+ v(2) \\
& \times \int d^2 \mathbf{v} e^{-i\mathbf{v} \cdot (\mathbf{k}_1 - \mathbf{k})} \int d^2 \mathbf{w} e^{-i\mathbf{w} \cdot (\mathbf{p} + \mathbf{k}_2)} \left[\mathcal{U}_F(\mathbf{v}) \mathcal{U}_F^\dagger(\mathbf{w}) - 1 \right] . \tag{4.51}
\end{aligned}$$

⁵here we neglect the dependence of the Wilson lines on v^- or w^- since due to the overall L^+ factor, this contribution already starts at NEik order

Subtracting the contribution Eq.(4.51) as well from Eq. (4.50), one has, at NEik accuracy

$$\begin{aligned}
& S_{q_1\bar{q}_2\leftarrow\gamma^*}^{\text{bef}} - S_{q_1\bar{q}_2\leftarrow\gamma^*}^{\text{bef}} \Big|_{\text{dec. on } q} - S_{q_1\bar{q}_2\leftarrow\gamma^*}^{\text{bef}} \Big|_{\text{dec. on } \bar{q}} - S_{q_1\bar{q}_2\leftarrow\gamma^*}^{\text{bef}} \Big|_{L^+ \text{ phase}} = -iee_f \epsilon_\mu^\lambda(q) \\
& \int \frac{d^3\mathbf{k}}{(2\pi)^3} \theta(k^+) \int \frac{d^3\mathbf{p}}{(2\pi)^3} \theta(-p^+) (2\pi)^3 \delta^{(3)}(\underline{q} - \underline{k} + \underline{p}) \frac{i}{(q^- - \check{k}^- + \check{p}^- + i\epsilon)} \\
& \times \bar{u}(1) \gamma^+ \frac{(\check{\mathbf{k}} + m)}{2k^+} \gamma^\mu \frac{(\check{\mathbf{p}} + m)}{2p^+} \gamma^+ v(2) \int d^2\mathbf{v} e^{-iv \cdot (\mathbf{k}_1 - \mathbf{k})} \int d^2\mathbf{w} e^{-iw \cdot (\mathbf{p} + \mathbf{k}_2)} \\
& \times \int dv^- e^{iv^-(k_1^+ - k^+)} \int dw^- e^{iw^-(k_2^+ + p^+)} \left[\mathcal{U}_F(\mathbf{v}, v^-) \mathcal{U}_F^\dagger(\mathbf{w}, w^-) - 1 \right]. \quad (4.52)
\end{aligned}$$

In Eq. (4.52), the only leftover effect beyond the Eikonal approximation is the dependence on v^- or w^- of the Wilson lines. Using the change of variables $(v^-, w^-) \mapsto (b^-, r^-)$ defined as

$$b^- = \frac{(v^- + w^-)}{2}, \quad r^- = (w^- - v^-) \quad (4.53)$$

so that

$$w^- = b^- + \frac{r^-}{2}, \quad v^- = b^- - \frac{r^-}{2}, \quad (4.54)$$

By Taylor-expanding the Wilson lines around b^- , one finds that two separate NEik contributions come out. The first one is the generalized eikonal contribution that contains the the dependence of the Wilson lines on a common b^- as the only leftover effect beyond the strict Eikonal approximation

$$\begin{aligned}
& S_{q_1\bar{q}_2\leftarrow\gamma^*}^{\text{bef}} \Big|_{\text{Gen. Eik}} = -iee_f \epsilon_\mu^\lambda(q) \int d^2\mathbf{v} \int d^2\mathbf{w} \int db^- e^{ib^-(k_1^+ + k_2^+ - q^+)} \\
& \times \left[\mathcal{U}_F(\mathbf{v}, b^-) \mathcal{U}_F^\dagger(\mathbf{w}, b^-) - 1 \right] \int \frac{d^3\mathbf{k}}{(2\pi)^3} \theta(k^+) 2\pi \delta \left(k^+ - \frac{1}{2}(k_1^+ - k_2^+ + q^+) \right) \\
& \times \int \frac{d^3\mathbf{p}}{(2\pi)^3} \theta(-p^+) (2\pi)^3 \delta^{(3)}(\underline{q} - \underline{k} + \underline{p}) \\
& \times e^{-iv \cdot (\mathbf{k}_1 - \mathbf{k})} e^{-iw \cdot (\mathbf{p} + \mathbf{k}_2)} \frac{i}{(q^- - \check{k}^- + \check{p}^- + i\epsilon)} \bar{u}(1) \gamma^+ \frac{(\check{\mathbf{k}} + m)}{2k^+} \gamma^\mu \frac{(\check{\mathbf{p}} + m)}{2p^+} \gamma^+ v(2), \quad (4.55)
\end{aligned}$$

Second, we have an explicit NEik correction⁶

$$\begin{aligned}
S_{q_1\bar{q}_2\leftarrow\gamma^*}^{\text{bef}} \Big|_{\text{dyn. target}} &= 2\pi\delta(k_1^+ + k_2^+ - q^+) (-i)ee_f \epsilon_\mu^\lambda(q) \int d^2\mathbf{v} \int d^2\mathbf{w} \\
&\times \left[\mathcal{U}_F(\mathbf{v}, b^-) \overleftrightarrow{\partial}_{b^-} \mathcal{U}_F^\dagger(\mathbf{w}, b^-) \right] \Big|_{b^-=0} \\
&\times \int \frac{d^3\mathbf{k}}{(2\pi)^3} \theta(k^+) (-1) \frac{i}{2} 2\pi\delta'(k^+ - k_1^+) \int \frac{d^3\mathbf{p}}{(2\pi)^3} \theta(-p^+) (2\pi)^3 \delta^{(3)}(\underline{q} - \underline{k} + \underline{p}) \\
&\times e^{-i\mathbf{v}\cdot(\mathbf{k}_1 - \mathbf{k})} e^{-i\mathbf{w}\cdot(\mathbf{p} + \mathbf{k}_2)} \frac{i}{(q^- - \check{k}^- + \check{p}^- + i\epsilon)} \bar{u}(1)\gamma^+ \frac{(\check{\mathbf{k}} + m)}{2k^+} \gamma^\mu \frac{(\check{\mathbf{p}} + m)}{2p^+} \gamma^+ v(2). \quad (4.56)
\end{aligned}$$

The $-$ axis in light-cone coordinates can be interpreted as the longitudinal direction for the right-moving projectile and as the time direction for the left-moving target. If the target background field is dynamical, meaning z^- dependent, the quark and antiquark from the projectile will probe a different value of the field not only because of their transverse separation $\mathbf{w} - \mathbf{v}$ but also because of their longitudinal separation $r^- = w^- - v^-$. The contribution Eq.(4.56) is then the NEik correction induced by the tidal-like force exerted by the dynamical background field on the quark and antiquark due to their longitudinal separation r^- .

All in all, we have written the S-matrix element for the before diagram at NEik accuracy as

$$\begin{aligned}
S_{q_1\bar{q}_2\leftarrow\gamma^*}^{\text{bef}} &= S_{q_1\bar{q}_2\leftarrow\gamma^*}^{\text{bef}} \Big|_{\text{Gen. Eik}} + S_{q_1\bar{q}_2\leftarrow\gamma^*}^{\text{bef}} \Big|_{\text{dec. on } q} + S_{q_1\bar{q}_2\leftarrow\gamma^*}^{\text{bef}} \Big|_{\text{dec. on } \bar{q}} + S_{q_1\bar{q}_2\leftarrow\gamma^*}^{\text{bef}} \Big|_{L^+ \text{ phase}} \\
&+ S_{q_1\bar{q}_2\leftarrow\gamma^*}^{\text{bef}} \Big|_{\text{dyn. target}} + O(NNEik), \quad (4.57)
\end{aligned}$$

Most of these contributions contain the same energy denominator:

$$(q^- - \check{k}^- + \check{p}^- + i\epsilon) = \frac{(\mathbf{q}^2 - Q^2)}{2q^+} - \frac{(\mathbf{k}^2 + m^2)}{2k^+} + \frac{(\mathbf{p}^2 + m^2)}{2p^+} + i\epsilon, \quad (4.58)$$

Introducing the photon virtuality $Q^2 \equiv -q^\mu q_\mu$ and using the momentum conservation constraint $\underline{p} = \underline{k} - \underline{q}$ at the photon splitting vertex, one finds

$$(q^- - \check{k}^- + \check{p}^- + i\epsilon) = -\frac{Q^2}{2q^+} - \frac{q^+}{2k^+(q^+ - k^+)} \left[\left(\mathbf{k} - \frac{k^+}{q^+} \mathbf{q} \right)^2 + m^2 \right] + i\epsilon. \quad (4.59)$$

Since the real part of this energy denominator cannot change sign, the $+i\epsilon$ has no effect and can be always dropped. Using the expression Eq.(4.59) in the Generalized

⁶Note that due to the choice of the light cone gauge $A^+ = 0$, the ordinary derivative $\overleftrightarrow{\partial}_{b^-}$ can equivalently be written as a covariant derivative $\overleftrightarrow{D}_{b^-}$.

Eikonal contribution Eq.(4.55), one has

$$\begin{aligned}
 S_{q_1 \bar{q}_2 \leftarrow \gamma^*}^{\text{bef}} \Big|_{\text{Gen. Eik}} &= ee_f \epsilon_\mu^\lambda(q) \int d^2 \mathbf{v} \int d^2 \mathbf{w} \int db^- e^{ib^-(k_1^+ + k_2^+ - q^+)} \\
 &\times \left[\mathcal{U}_F(\mathbf{v}, b^-) \mathcal{U}_F^\dagger(\mathbf{w}, b^-) - 1 \right] \frac{2\pi}{2q^+} \int \frac{d^3 \mathbf{k}}{(2\pi)^3} \theta(k^+) \theta(q^+ - k^+) \delta \left(k^+ - \frac{1}{2}(k_1^+ - k_2^+ + q^+) \right) \\
 &\times e^{-iv \cdot (\mathbf{k}_1 - \mathbf{k})} e^{-i\mathbf{w} \cdot (\mathbf{k}_2 + \mathbf{k} - \mathbf{q})} \frac{\bar{u}(1) \gamma^+ (\not{\mathbf{k}} + m) \gamma^\mu (\not{\mathbf{k}} - \not{\mathbf{q}} + m) \gamma^+ v(2)}{\left[\left(\mathbf{k} - \frac{k^+}{q^+} \mathbf{q} \right)^2 + m^2 + \frac{k^+(q^+ - k^+)}{(q^+)^2} Q^2 \right]}. \quad (4.60)
 \end{aligned}$$

Similarly, one obtains

$$\begin{aligned}
 S_{q_1 \bar{q}_2 \leftarrow \gamma^*}^{\text{bef}} \Big|_{\text{dyn. target}} &= 2\pi \delta(k_1^+ + k_2^+ - q^+) ee_f \epsilon_\mu^\lambda(q) \int d^2 \mathbf{v} \int d^2 \mathbf{w} \\
 &\times \left[\mathcal{U}_F(\mathbf{v}, b^-) \overleftrightarrow{\partial}_{b^-} \mathcal{U}_F^\dagger(\mathbf{w}, b^-) \right] \Big|_{b^- = 0} \frac{(-i)}{4q^+} \int \frac{d^3 \mathbf{k}}{(2\pi)^3} \theta(k^+) \theta(q^+ - k^+) 2\pi \delta'(k^+ - k_1^+) \\
 &\times e^{-iv \cdot (\mathbf{k}_1 - \mathbf{k})} e^{-i\mathbf{w} \cdot (\mathbf{k}_2 + \mathbf{k} - \mathbf{q})} \frac{\bar{u}(1) \gamma^+ (\not{\mathbf{k}} + m) \gamma^\mu (\not{\mathbf{k}} - \not{\mathbf{q}} + m) \gamma^+ v(2)}{\left[\left(\mathbf{k} - \frac{k^+}{q^+} \mathbf{q} \right)^2 + m^2 + \frac{k^+(q^+ - k^+)}{(q^+)^2} Q^2 \right]}. \quad (4.61)
 \end{aligned}$$

from Eq. (4.56) and

$$\begin{aligned}
 S_{q_1 \bar{q}_2 \leftarrow \gamma^*}^{\text{bef}} \Big|_{L^+ \text{ phase}} &= 2\pi \delta(k_1^+ + k_2^+ - q^+) ee_f \epsilon_\mu^\lambda(q) \int d^2 \mathbf{v} \int d^2 \mathbf{w} \left[\mathcal{U}_F(\mathbf{v}) \mathcal{U}_F^\dagger(\mathbf{w}) - 1 \right] \\
 &\times \frac{(-i)L^+}{8k_1^+ k_2^+} \int \frac{d^3 \mathbf{k}}{(2\pi)^3} 2\pi \delta(k^+ - k_1^+) e^{-iv \cdot (\mathbf{k}_1 - \mathbf{k})} e^{-i\mathbf{w} \cdot (\mathbf{k}_2 + \mathbf{k} - \mathbf{q})} \\
 &\times \bar{u}(1) \gamma^+ (\not{\mathbf{k}} + m) \gamma^\mu (\not{\mathbf{k}} - \not{\mathbf{q}} + m) \gamma^+ v(2) \quad (4.62)
 \end{aligned}$$

from Eq. (4.51). Then, from Eq. (4.46) and choosing to trade \mathbf{k} for a derivative in \mathbf{w} for the extra contribution of \mathbf{k} as compared to the rest of the S-matrix contributions, one finds

$$\begin{aligned}
 S_{q_1 \bar{q}_2 \leftarrow \gamma^*}^{\text{bef}} \Big|_{\text{dec. on } q} &= 2\pi \delta(k_1^+ + k_2^+ - q^+) ee_f \epsilon_\mu^\lambda(q) \int d^2 \mathbf{v} \int d^2 \mathbf{w} \frac{1}{4q^+ k_1^+} \int_{-\frac{L^+}{2}}^{\frac{L^+}{2}} dv^+ \int \frac{d^3 \mathbf{k}}{(2\pi)^3} \\
 &\times 2\pi \delta(k^+ - k_1^+) \bar{u}(1) \left\{ \left[\mathcal{U}_F\left(\frac{L^+}{2}, v^+; \mathbf{v}\right) \right. \right. \\
 &\times \left(\frac{[\gamma^i, \gamma^j]}{4} g t \cdot \mathcal{F}_{ij}(v) - \frac{(\mathbf{k}_1^i - \mathbf{k}_2^j + \mathbf{q}^j)}{2} \overleftrightarrow{\mathcal{D}}_{\mathbf{v}^j} - i \overleftarrow{\mathcal{D}}_{\mathbf{v}^j} \overrightarrow{\mathcal{D}}_{\mathbf{v}^j} \right) \\
 &\times \left. \left. \mathcal{U}_F\left(v^+, -\frac{L^+}{2}; \mathbf{v}\right) \mathcal{U}_F^\dagger(\mathbf{w}) \right] + \frac{i}{2} \left[\mathcal{U}_F\left(\frac{L^+}{2}, v^+; \mathbf{v}\right) \overleftrightarrow{\mathcal{D}}_{\mathbf{v}^j} \mathcal{U}_F\left(v^+, -\frac{L^+}{2}; \mathbf{v}\right) (\partial_{\mathbf{w}^j} \mathcal{U}_F^\dagger(\mathbf{w})) \right] \right\} \\
 &\times \frac{\gamma^+ (\not{\mathbf{k}} + m) \gamma^\mu (\not{\mathbf{k}} - \not{\mathbf{q}} + m) \gamma^+ v(2)}{\left[\left(\mathbf{k} - \frac{k^+}{q^+} \mathbf{q} \right)^2 + m^2 + \frac{k^+(q^+ - k^+)}{(q^+)^2} Q^2 \right]} e^{-iv \cdot (\mathbf{k}_1 - \mathbf{k})} e^{-i\mathbf{w} \cdot (\mathbf{k}_2 + \mathbf{k} - \mathbf{q})}. \quad (4.63)
 \end{aligned}$$

In order to obtain more compact expressions, let us introduce the notations

$$\mathcal{U}_{F;j}^{(1)}(\mathbf{v}) = \int_{-\frac{L^+}{2}}^{\frac{L^+}{2}} dv^+ \mathcal{U}_F\left(\frac{L^+}{2}, v^+; \mathbf{v}\right) \overleftrightarrow{\mathcal{D}}_{\mathbf{v}j} \mathcal{U}_F\left(v^+, -\frac{L^+}{2}; \mathbf{v}\right) \quad (4.64)$$

$$\mathcal{U}_F^{(2)}(\mathbf{v}) = \int_{-\frac{L^+}{2}}^{\frac{L^+}{2}} dv^+ \mathcal{U}_F\left(\frac{L^+}{2}, v^+; \mathbf{v}\right) \overleftrightarrow{\mathcal{D}}_{\mathbf{v}j} \overrightarrow{\mathcal{D}}_{\mathbf{v}j} \mathcal{U}_F\left(v^+, -\frac{L^+}{2}; \mathbf{v}\right) \quad (4.65)$$

$$\mathcal{U}_{F;jj}^{(3)}(\mathbf{v}) = \int_{-\frac{L^+}{2}}^{\frac{L^+}{2}} dv^+ \mathcal{U}_F\left(\frac{L^+}{2}, v^+; \mathbf{v}\right) g t \cdot \mathcal{F}_{ij}(\underline{v}) \mathcal{U}_F\left(v^+, -\frac{L^+}{2}; \mathbf{v}\right) \quad (4.66)$$

for the decorated Wilson lines appearing at NEik accuracy. Their Hermitian conjugate is

$$\mathcal{U}_{F;j}^{(1)\dagger}(\mathbf{v}) = - \int_{-\frac{L^+}{2}}^{\frac{L^+}{2}} dv^+ \mathcal{U}_F^\dagger\left(v^+, -\frac{L^+}{2}; \mathbf{v}\right) \overleftrightarrow{\mathcal{D}}_{\mathbf{v}j} \mathcal{U}_F^\dagger\left(\frac{L^+}{2}, v^+; \mathbf{v}\right) \quad (4.67)$$

$$\mathcal{U}_F^{(2)\dagger}(\mathbf{v}) = \int_{-\frac{L^+}{2}}^{\frac{L^+}{2}} dv^+ \mathcal{U}_F^\dagger\left(v^+, -\frac{L^+}{2}; \mathbf{v}\right) \overleftrightarrow{\mathcal{D}}_{\mathbf{v}j} \overrightarrow{\mathcal{D}}_{\mathbf{v}j} \mathcal{U}_F^\dagger\left(\frac{L^+}{2}, v^+; \mathbf{v}\right) \quad (4.68)$$

$$\mathcal{U}_{F;jj}^{(3)\dagger}(\mathbf{v}) = \int_{-\frac{L^+}{2}}^{\frac{L^+}{2}} dv^+ \mathcal{U}_F^\dagger\left(v^+, -\frac{L^+}{2}; \mathbf{v}\right) g t \cdot \mathcal{F}_{ij}(\underline{v}) \mathcal{U}_F^\dagger\left(\frac{L^+}{2}, v^+; \mathbf{v}\right). \quad (4.69)$$

With these notations, the expression Eq.(4.63) becomes

$$\begin{aligned} S_{q_1 \bar{q}_2 \leftarrow \gamma^*}^{\text{bef}} \Big|_{\text{dec. on } q} &= 2\pi \delta(k_1^+ + k_2^+ - q^+) e e_f \epsilon_\mu^\lambda(q) \frac{1}{4q^+ k_1^+} \int d^2 \mathbf{v} \int d^2 \mathbf{w} \int \frac{d^3 \mathbf{k}}{(2\pi)^3} \\ &\times 2\pi \delta(k^+ - k_1^+) e^{-i\mathbf{v} \cdot (\mathbf{k}_1 - \mathbf{k})} e^{-i\mathbf{w} \cdot (\mathbf{k}_2 + \mathbf{k} - \mathbf{q})} \bar{u}(1) \left[\frac{[\gamma^i, \gamma^j]}{4} \mathcal{U}_{F;jj}^{(3)}(\mathbf{v}) - i \mathcal{U}_F^{(2)}(\mathbf{v}) \right. \\ &\left. + \mathcal{U}_{F;j}^{(1)}(\mathbf{v}) \left(-\frac{(\mathbf{k}_1^j - \mathbf{k}_2^j + \mathbf{q}^j)}{2} + \frac{i}{2} \partial_{\mathbf{w}j} \right) \right] \mathcal{U}_F^\dagger(\mathbf{w}) \frac{\gamma^+(\check{\mathbf{k}} + m) \gamma^\mu (\check{\mathbf{k}} - \mathbf{q} + m) \gamma^+ v(2)}{\left[\left(\mathbf{k} - \frac{k^+}{q^+} \mathbf{q} \right)^2 + m^2 + \frac{k^+(q^+ - k^+)}{(q^+)^2} Q^2 \right]}. \end{aligned} \quad (4.70)$$

Following the same steps, one can rewrite the contribution with decoration on the antiquark Wilson line Eq.(4.47) as

$$\begin{aligned} S_{q_1 \bar{q}_2 \leftarrow \gamma^*}^{\text{bef}} \Big|_{\text{dec. on } \bar{q}} &= 2\pi \delta(k_1^+ + k_2^+ - q^+) e e_f \epsilon_\mu^\lambda(q) \frac{1}{4q^+ k_2^+} \int d^2 \mathbf{v} \int d^2 \mathbf{w} \\ &\times \int \frac{d^3 \mathbf{k}}{(2\pi)^3} 2\pi \delta(k^+ - k_1^+) \frac{\bar{u}(1) \gamma^+(\check{\mathbf{k}} + m) \gamma^\mu (\check{\mathbf{k}} - \mathbf{q} + m) \gamma^+}{\left[\left(\mathbf{k} - \frac{k^+}{q^+} \mathbf{q} \right)^2 + m^2 + \frac{k^+(q^+ - k^+)}{(q^+)^2} Q^2 \right]} e^{-i\mathbf{w} \cdot (\mathbf{k}_2 + \mathbf{k} - \mathbf{q})} \\ &\times \left[\mathcal{U}_F(\mathbf{v}) \left(\frac{[\gamma^i, \gamma^j]}{4} \mathcal{U}_{F;jj}^{(3)\dagger}(\mathbf{w}) - i \mathcal{U}_F^{(2)\dagger}(\mathbf{w}) + \left(\frac{i}{2} \overleftarrow{\partial}_{\mathbf{v}j} - \frac{(\mathbf{k}_2^j - \mathbf{k}_1^j + \mathbf{q}^j)}{2} \right) \mathcal{U}_{F;j}^{(1)\dagger}(\mathbf{w}) \right) \right] \\ &\times v(2) e^{-i\mathbf{v} \cdot (\mathbf{k}_1 - \mathbf{k})}, \end{aligned} \quad (4.71)$$

Let us now consider specific polarizations of the photon in the S-matrix expressions.

Longitudinal photon case :

Introducing the longitudinal polarization vector in LC gauge given in Eq.(4.34), one finds

$$\begin{aligned} \epsilon_\mu^L(q) \gamma^+ (\check{k}+m) \gamma^\mu (\check{k}-q+m) \gamma^+ &= \frac{Q}{q^+} \gamma^+ (\check{k}+m) \gamma^+ (\check{k}-q+m) \gamma^+ \\ &= \frac{Q}{q^+} \{ \gamma^+, \check{k} \} \gamma^+ \{ \check{k}-q, \gamma^+ \} = -\frac{4k^+(q^+-k^+)}{q^+} Q \gamma^+. \end{aligned} \quad (4.72)$$

Inserting this result into Eq.(4.62)

$$\begin{aligned} S_{q_1 \bar{q}_2 \leftarrow \gamma_L^*}^{\text{bef}} \Big|_{L^+ \text{ phase}} &= 2\pi \delta(k_1^+ + k_2^+ - q^+) e e_f Q \bar{u}(1) \gamma^+ v(2) \frac{iL^+}{2q^+} \int d^2\mathbf{v} \int d^2\mathbf{w} \\ &\times \left[\mathcal{U}_F(\mathbf{v}) \mathcal{U}_F^\dagger(\mathbf{w}) - 1 \right] \delta^{(2)}(\mathbf{v}-\mathbf{w}) e^{-i\mathbf{v}\cdot(\mathbf{k}_1+\mathbf{k}_2-\mathbf{q})} = 0. \end{aligned} \quad (4.73)$$

In order to calculate the cross section, it is sufficient to know the S-matrix element for $\mathbf{q} = 0$. Hence, we will assume $\mathbf{q} = 0$ from now on, for simplicity. Then, inserting the expression Eq.(4.72) into Eq.(4.60) and taking $\mathbf{q} = 0$, one obtains

$$\begin{aligned} S_{q_1 \bar{q}_2 \leftarrow \gamma_L^*}^{\text{bef}} \Big|_{\text{Gen. Eik}} &= -2Q \frac{e e_f}{2\pi} \bar{u}(1) \gamma^+ v(2) \frac{(q^+ + k_1^+ - k_2^+)(q^+ + k_2^+ - k_1^+)}{4(q^+)^2} \\ &\times \theta(q^+ + k_1^+ - k_2^+) \theta(q^+ + k_2^+ - k_1^+) \int d^2\mathbf{v} e^{-i\mathbf{v}\cdot\mathbf{k}_1} \int d^2\mathbf{w} e^{-i\mathbf{w}\cdot\mathbf{k}_2} \\ &\times K_0(\hat{Q}|\mathbf{w}-\mathbf{v}|) \int db^- e^{ib^-(k_1^+ + k_2^+ - q^+)} \left[\mathcal{U}_F(\mathbf{v}, b^-) \mathcal{U}_F^\dagger(\mathbf{w}, b^-) - 1 \right], \end{aligned} \quad (4.74)$$

where we used the relation

$$\int \frac{d^2\mathbf{k}}{(2\pi)^2} \frac{e^{-i\mathbf{k}\cdot\mathbf{r}}}{(\mathbf{k}^2 + \Delta)} = \frac{1}{2\pi} K_0(\sqrt{\Delta}|\mathbf{r}|), \quad (4.75)$$

where $K_\alpha(z)$ is the modified Bessel function of the second kind. In Eq. (4.74), we have introduced the notation

$$\hat{Q} = \sqrt{m^2 + \frac{(q^+ + k_1^+ - k_2^+)(q^+ - k_1^+ + k_2^+)}{4(q^+)^2} Q^2}. \quad (4.76)$$

Similarly, in the longitudinal photon case, Eq. (4.70) becomes

$$\begin{aligned} S_{q_1 \bar{q}_2 \leftarrow \gamma_L^*}^{\text{bef}} \Big|_{\text{dec. on } q} &= 2\pi \delta(k_1^+ + k_2^+ - q^+) \frac{e e_f}{2\pi} (-1) Q \frac{k_2^+}{(q^+)^2} \\ &\times \int d^2\mathbf{v} e^{-i\mathbf{v}\cdot\mathbf{k}_1} \int d^2\mathbf{w} e^{-i\mathbf{w}\cdot\mathbf{k}_2} K_0(\bar{Q}|\mathbf{w}-\mathbf{v}|) \bar{u}(1) \gamma^+ \\ &\times \left[\frac{[\gamma^i, \gamma^j]}{4} \mathcal{U}_{F;ij}^{(3)}(\mathbf{v}) - i \mathcal{U}_F^{(2)}(\mathbf{v}) + \mathcal{U}_{F;ij}^{(1)}(\mathbf{v}) \left(\frac{(\mathbf{k}_2^j - \mathbf{k}_1^j)}{2} + \frac{i}{2} \partial_{\mathbf{w}^j} \right) \right] \mathcal{U}_F^\dagger(\mathbf{w}) v(2) \end{aligned} \quad (4.77)$$

and Eq. (4.71)

$$\begin{aligned}
S_{q_1\bar{q}_2\leftarrow\gamma_L^*}^{\text{bef}} \Big|_{\text{dec. on } \bar{q}} &= 2\pi\delta(k_1^+ + k_2^+ - q^+) \frac{ee_f}{2\pi} (-1)Q \frac{k_1^+}{(q^+)^2} \\
&\times \int d^2\mathbf{v} e^{-i\mathbf{v}\cdot\mathbf{k}_1} \int d^2\mathbf{w} e^{-i\mathbf{w}\cdot\mathbf{k}_2} K_0(\bar{Q}|\mathbf{w}-\mathbf{v}|) \bar{u}(1)\gamma^+ \\
&\times \left[\mathcal{U}_F(\mathbf{v}) \left(\frac{[\gamma^i, \gamma^j]}{4} \mathcal{U}_{F:ij}^{(3)\dagger}(\mathbf{w}) - i\mathcal{U}_F^{(2)\dagger}(\mathbf{w}) + \left(\frac{i}{2} \overleftrightarrow{\partial}_{\mathbf{v}j} - \frac{(\mathbf{k}_2^j - \mathbf{k}_1^j)}{2} \right) \mathcal{U}_{F:ij}^{(1)\dagger}(\mathbf{w}) \right) \right] v(2),
\end{aligned} \tag{4.78}$$

where \bar{Q} is defined as⁷

$$\bar{Q} \equiv \sqrt{m^2 + Q^2 \frac{k_1^+ k_2^+}{(q^+)^2}}. \tag{4.79}$$

Finally, integrating by part in k^+ , Eq. (4.61) leads to

$$\begin{aligned}
S_{q_1\bar{q}_2\leftarrow\gamma_L^*}^{\text{bef}} \Big|_{\text{dyn. target}} &= 2\pi\delta(k_1^+ + k_2^+ - q^+) iQ \frac{ee_f}{2\pi} \bar{u}(1)\gamma^+ v(2) \frac{(k_1^+ - k_2^+)}{(q^+)^2} \int d^2\mathbf{v} e^{-i\mathbf{v}\cdot\mathbf{k}_1} \\
&\times \int d^2\mathbf{w} e^{-i\mathbf{w}\cdot\mathbf{k}_2} \left[K_0(\bar{Q}|\mathbf{w}-\mathbf{v}|) - \frac{(\bar{Q}^2 - m^2)}{2\bar{Q}} |\mathbf{w}-\mathbf{v}| K_1(\bar{Q}|\mathbf{w}-\mathbf{v}|) \right] \\
&\times \left[\mathcal{U}_F(\mathbf{v}, b^-) \overleftrightarrow{\partial}_b \mathcal{U}_F^\dagger(\mathbf{w}, b^-) \right] \Big|_{b^-=0},
\end{aligned} \tag{4.80}$$

where we have discarded zero mode contributions at $k_1^+ = 0$ or $k_2^+ = 0$, which would not contribute to the cross section of dijet production in the experimentally meaningful range. We also have used both the relation Eq.(4.75) and

$$\int \frac{d^2\mathbf{k}}{(2\pi)^2} \frac{e^{-i\mathbf{k}\cdot\mathbf{r}}}{(\mathbf{k}^2 + \Delta)^2} = \frac{1}{4\pi} \frac{|\mathbf{r}|}{\sqrt{\Delta}} K_1(\sqrt{\Delta}|\mathbf{r}|). \tag{4.81}$$

Collecting all the results for the longitudinal polarization of the photon in the S-matrix element, at NEik accuracy this is given by

$$S_{q_1\bar{q}_2\leftarrow\gamma_L^*} = S_{q_1\bar{q}_2\leftarrow\gamma_L^*}^{\text{bef}} \Big|_{\text{Gen. Eik}} + S_{q_1\bar{q}_2\leftarrow\gamma_L^*}^{\text{bef}} \Big|_{\text{dec. on } q} + S_{q_1\bar{q}_2\leftarrow\gamma_L^*}^{\text{bef}} \Big|_{\text{dec. on } \bar{q}} + S_{q_1\bar{q}_2\leftarrow\gamma_L^*}^{\text{bef}} \Big|_{\text{dyn. target}} \tag{4.82}$$

where explicit expressions for each contribution are given in Eqs. (4.74), (4.77), (4.78) and (4.80). We would like to remind that the contribution Eq.(4.73) vanishes, as well as the contribution from photon splitting inside the target Eq.(4.35).

By contrast, the strict Eikonal approximation for the S-matrix element can be obtained from the Generalized Eikonal contribution Eq.(4.74) by setting the $b^- = 0$

⁷Note that \hat{Q} , as defined in Eq. (4.76), collapses to \bar{Q} if $k_1^+ + k_2^+ = q^+$, which is the case in most terms, apart from the generalized eikonal contribution (4.74). Still, we keep a separate notation for \bar{Q} , since that quantity is the one commonly used in the literature about dipole factorization for DIS processes in the eikonal limit.

dependence of the Wilson lines. In such a way, one recovers the standard result

$$\begin{aligned} S_{q_1 \bar{q}_2 \leftarrow \gamma_L^*}^{\text{bef}} \Big|_{\text{Strict Eik}} &= 2\pi \delta(k_1^+ + k_2^+ - q^+) (-2) Q \frac{ee_f}{2\pi} \bar{u}(1) \gamma^+ v(2) \frac{k_1^+ k_2^+}{(q^+)^2} \int d^2 \mathbf{v} e^{-i\mathbf{v} \cdot \mathbf{k}_1} \\ &\times \int d^2 \mathbf{w} e^{-i\mathbf{w} \cdot \mathbf{k}_2} K_0(\bar{Q} |\mathbf{w} - \mathbf{v}|) \left[\mathcal{U}_F(\mathbf{v}) \mathcal{U}_F^\dagger(\mathbf{w}) - 1 \right]. \end{aligned} \quad (4.83)$$

Transverse photon case :

Let us now consider the case of transverse photon polarization, with polarization vectors as given in Eq.(4.36). The part of the Dirac structure associated with the photon splitting before the target, is then

$$\begin{aligned} &\gamma^+ (\not{\mathbf{k}} + m) \not{\epsilon}_\lambda(q) (\not{\mathbf{k}} - \not{q} + m) \gamma^+ \\ &= \gamma^+ \left[k^+ \gamma^- - \mathbf{k}^j \gamma^j + m \right] \left[-\epsilon_\lambda^i \gamma^i + \epsilon_\lambda^i \frac{\mathbf{q}^i}{q^+} \gamma^+ \right] \left[(k^+ - q^+) \gamma^- - (\mathbf{k}^l - \mathbf{q}^l) \gamma^l + m \right] \gamma^+ \\ &= \gamma^+ \left[-\mathbf{k}^j \gamma^j + m \right] \left[-\epsilon_\lambda^i \gamma^i \right] (k^+ - q^+) \gamma^- \gamma^+ + \gamma^+ k^+ \gamma^- \left[-\epsilon_\lambda^i \gamma^i \right] \left[-(\mathbf{k}^l - \mathbf{q}^l) \gamma^l + m \right] \gamma^+ \\ &\quad + \gamma^+ k^+ \gamma^- \left[\epsilon_\lambda^i \frac{\mathbf{q}^i}{q^+} \gamma^+ \right] (k^+ - q^+) \gamma^- \gamma^+ \\ &= \epsilon_\lambda^i \gamma^+ \left\{ 2(q^+ - k^+) \left[-\mathbf{k}^j \gamma^j + m \right] \gamma^i + 2k^+ \gamma^i \left[(\mathbf{k}^j - \mathbf{q}^j) \gamma^j + m \right] - \frac{4k^+(q^+ - k^+)}{q^+} \mathbf{q}^i \right\} \\ &= 2q^+ \epsilon_\lambda^i \gamma^+ \left\{ \left[\frac{(q^+ - 2k^+)}{q^+} \delta^{ij} + \frac{[\gamma^i, \gamma^j]}{2} \right] \left[\mathbf{k}^j - \frac{k^+}{q^+} \mathbf{q}^j \right] + m \gamma^i \right\}. \end{aligned} \quad (4.84)$$

Inserting this into the expression Eq. (4.60) for the generalized eikonal contribution, taking $\mathbf{q} = 0$, and using the identities Eq.(4.75) and

$$\int \frac{d^2 \mathbf{k}}{(2\pi)^2} \frac{e^{-i\mathbf{k} \cdot \mathbf{r}}}{(\mathbf{k}^2 + \Delta)} \mathbf{k}^j = \frac{(-i)}{2\pi} \frac{\mathbf{r}^j}{|\mathbf{r}|} \sqrt{\Delta} K_1(\sqrt{\Delta} |\mathbf{r}|). \quad (4.85)$$

one finds

$$\begin{aligned} S_{q_1 \bar{q}_2 \leftarrow \gamma_T^*}^{\text{bef}} \Big|_{\text{Gen. Eik}} &= \frac{ee_f}{2\pi} \epsilon_\lambda^i \theta(q^+ + k_1^+ - k_2^+) \theta(q^+ + k_2^+ - k_1^+) \int d^2 \mathbf{v} e^{-i\mathbf{v} \cdot \mathbf{k}_1} \int d^2 \mathbf{w} e^{-i\mathbf{w} \cdot \mathbf{k}_2} \\ &\times \left\{ -i \frac{(\mathbf{w}^j - \mathbf{v}^j)}{|\mathbf{w} - \mathbf{v}|} \hat{Q} K_1(\hat{Q} |\mathbf{w} - \mathbf{v}|) \bar{u}(1) \gamma^+ \left[\frac{(k_2^+ - k_1^+)}{q^+} \delta^{ij} + \frac{[\gamma^i, \gamma^j]}{2} \right] v(2) \right. \\ &\left. + K_0(\hat{Q} |\mathbf{w} - \mathbf{v}|) m \bar{u}(1) \gamma^+ \gamma^i v(2) \right\} \int db^- e^{ib^-(k_1^+ + k_2^+ - q^+)} \left[\mathcal{U}_F(\mathbf{v}, b^-) \mathcal{U}_F^\dagger(\mathbf{w}, b^-) - 1 \right], \end{aligned} \quad (4.86)$$

In the same way, in the transverse photon case and for $\mathbf{q} = 0$, the contribution Eq.(4.70) becomes

$$\begin{aligned}
S_{q_1\bar{q}_2\leftarrow\gamma_T^*}^{\text{bef}} \Big|_{\text{dec. on } q} &= 2\pi\delta(k_1^+ + k_2^+ - q^+) \frac{ee_f}{2\pi} \varepsilon_\lambda^i \frac{1}{2k_1^+} \int d^2\mathbf{v} e^{-i\mathbf{v}\cdot\mathbf{k}_1} \int d^2\mathbf{w} e^{-i\mathbf{w}\cdot\mathbf{k}_2} \bar{u}(1)\gamma^+ \\
&\times \left[\frac{[\gamma^l, \gamma^m]}{4} \mathcal{U}_{F;lm}^{(3)}(\mathbf{v}) - i\mathcal{U}_F^{(2)}(\mathbf{v}) + \mathcal{U}_{F;l}^{(1)}(\mathbf{v}) \left(\frac{(\mathbf{k}_2^l - \mathbf{k}_1^l)}{2} + \frac{i}{2} \partial_{\mathbf{w}^l} \right) \right] \mathcal{U}_F^\dagger(\mathbf{w}) \\
&\times \left\{ -i \frac{(\mathbf{w}^j - \mathbf{v}^j)}{|\mathbf{w} - \mathbf{v}|} \bar{Q} K_1(\bar{Q}|\mathbf{w} - \mathbf{v}|) \left[\frac{(k_2^+ - k_1^+)}{q^+} \delta^{ij} + \frac{[\gamma^i, \gamma^j]}{2} \right] + K_0(\bar{Q}|\mathbf{w} - \mathbf{v}|) m \gamma^i \right\} v(2)
\end{aligned} \tag{4.87}$$

and the contribution Eq.(4.71) becomes

$$\begin{aligned}
S_{q_1\bar{q}_2\leftarrow\gamma_T^*}^{\text{bef}} \Big|_{\text{dec. on } \bar{q}} &= 2\pi\delta(k_1^+ + k_2^+ - q^+) \frac{ee_f}{2\pi} \varepsilon_\lambda^i \frac{1}{2k_2^+} \int d^2\mathbf{v} e^{-i\mathbf{v}\cdot\mathbf{k}_1} \int d^2\mathbf{w} e^{-i\mathbf{w}\cdot\mathbf{k}_2} \\
&\times \bar{u}(1)\gamma^+ \left\{ -i \frac{(\mathbf{w}^j - \mathbf{v}^j)}{|\mathbf{w} - \mathbf{v}|} \bar{Q} K_1(\bar{Q}|\mathbf{w} - \mathbf{v}|) \left[\frac{(k_2^+ - k_1^+)}{q^+} \delta^{ij} + \frac{[\gamma^i, \gamma^j]}{2} \right] + K_0(\bar{Q}|\mathbf{w} - \mathbf{v}|) m \gamma^i \right\} \\
&\times \left[\mathcal{U}_F(\mathbf{v}) \left(\frac{[\gamma^l, \gamma^m]}{4} \mathcal{U}_{F;lm}^{(3)\dagger}(\mathbf{w}) - i\mathcal{U}_F^{(2)\dagger}(\mathbf{w}) + \left(\frac{i}{2} \overleftarrow{\partial}_{\mathbf{v}^l} - \frac{(\mathbf{k}_2^l - \mathbf{k}_1^l)}{2} \right) \mathcal{U}_{F;l}^{(1)\dagger}(\mathbf{w}) \right) \right] v(2).
\end{aligned} \tag{4.88}$$

Using the expression Eq.(4.84), the contribution Eq.(4.62) can be simplified for transverse photon and $\mathbf{q} = 0$, as

$$\begin{aligned}
S_{q_1\bar{q}_2\leftarrow\gamma_T^*}^{\text{bef}} \Big|_{L^+ \text{ phase}} &= 2\pi\delta(k_1^+ + k_2^+ - q^+) ee_f \varepsilon_\lambda^i \frac{(-1)L^+ q^+}{8k_1^+ k_2^+} \bar{u}(1)\gamma^+ \left[\frac{(k_2^+ - k_1^+)}{q^+} \delta^{ij} + \frac{[\gamma^i, \gamma^j]}{2} \right] v(2) \\
&\times \int d^2\mathbf{v} e^{-i\mathbf{v}\cdot(\mathbf{k}_1 + \mathbf{k}_2)} \left[\mathcal{U}_F(\mathbf{v}) \overleftrightarrow{\partial}_{\mathbf{v}^j} \mathcal{U}_F^\dagger(\mathbf{v}) \right],
\end{aligned} \tag{4.89}$$

where, in all the final expressions, the derivatives act only within the square bracket, on the Wilson lines.

Using Eq. (4.84) and taking $\mathbf{q} = 0$, the contribution Eq.(4.61) associated with the dynamics of the target can be evaluated as

$$\begin{aligned}
S_{q_1\bar{q}_2\leftarrow\gamma_T^*}^{\text{bef}} \Big|_{\text{dyn. target}} &= 2\pi\delta(k_1^+ + k_2^+ - q^+) \frac{ee_f}{2\pi} \varepsilon_\lambda^i \int d^2\mathbf{v} e^{-i\mathbf{v}\cdot\mathbf{k}_1} \int d^2\mathbf{w} e^{-i\mathbf{w}\cdot\mathbf{k}_2} \\
&\times \left[\mathcal{U}_F(\mathbf{v}, b^-) \overleftrightarrow{\partial}_{b^-} \mathcal{U}_F^\dagger(\mathbf{w}, b^-) \right] \Big|_{b^-=0} \bar{u}(1)\gamma^+ \\
&\times \left\{ -\frac{(\mathbf{w}^j - \mathbf{v}^j)}{|\mathbf{w} - \mathbf{v}| q^+} \bar{Q} K_1(\bar{Q}|\mathbf{w} - \mathbf{v}|) - \frac{i(k_2^+ - k_1^+) Q^2 |\mathbf{w} - \mathbf{v}|}{4(q^+)^2 \bar{Q}} K_1(\bar{Q}|\mathbf{w} - \mathbf{v}|) m \gamma^i \right. \\
&\quad \left. - \frac{(k_2^+ - k_1^+) Q^2}{4(q^+)^2} (\mathbf{w}^j - \mathbf{v}^j) K_0(\bar{Q}|\mathbf{w} - \mathbf{v}|) \left[\frac{(k_2^+ - k_1^+)}{q^+} \delta^{ij} + \frac{[\gamma^i, \gamma^j]}{2} \right] \right\} v(2),
\end{aligned} \tag{4.90}$$

where we used the identities Eqs.(4.81), (4.85) and

$$\int \frac{d^2\mathbf{k}}{(2\pi)^2} \frac{e^{-i\mathbf{k}\cdot\mathbf{r}}}{(\mathbf{k}^2 + \Delta)^2} \mathbf{k}^j = \frac{(-i)}{4\pi} \mathbf{r}^j K_0(\sqrt{\Delta}|\mathbf{r}|). \tag{4.91}$$

All in all, at NEik accuracy, the S-matrix element for $q\bar{q}$ production from a transverse photon is given by

$$S_{q_1\bar{q}_2\leftarrow\gamma_T^*} = S_{q_1\bar{q}_2\leftarrow\gamma_T^*}\Big|_{\text{Gen. Eik}} + S_{q_1\bar{q}_2\leftarrow\gamma_T^*}\Big|_{\text{dec. on } q} + S_{q_1\bar{q}_2\leftarrow\gamma_T^*}\Big|_{\text{dec. on } \bar{q}} + S_{q_1\bar{q}_2\leftarrow\gamma_T^*}\Big|_{L^+ \text{ phase}} + S_{q_1\bar{q}_2\leftarrow\gamma_T^*}\Big|_{\text{dyn. target}} + S_{q_1\bar{q}_2\leftarrow\gamma_T^*}^{\text{in}} \quad (4.92)$$

where explicit expressions for each contribution coming from the photon splitting before reaching the target are given in Eqs. (4.86), (4.87), (4.88), (4.89), and (4.90). The expression for the contribution coming from the photon splitting inside the target is given in Eq. (4.38).

Again, the strict Eikonal approximation for the S-matrix element is obtained from the Generalized Eikonal contribution Eq.(4.86) by neglecting the b^- dependence of the Wilson lines. In such a way, one recovers the standard result

$$S_{q_1\bar{q}_2\leftarrow\gamma_T^*}\Big|_{\text{Strict Eik}} = 2\pi\delta(k_1^+ + k_2^+ - q^+) \frac{ee_f}{2\pi} \varepsilon_\lambda^i \int d^2\mathbf{v} e^{-i\mathbf{v}\cdot\mathbf{k}_1} \int d^2\mathbf{w} e^{-i\mathbf{w}\cdot\mathbf{k}_2} \times \left[\mathcal{U}_F(\mathbf{v})\mathcal{U}_F^\dagger(\mathbf{w}) - 1 \right] \left\{ -i \frac{(\mathbf{w}^j - \mathbf{v}^j)}{|\mathbf{w} - \mathbf{v}|} \bar{Q} K_1(\bar{Q}|\mathbf{w} - \mathbf{v}|) \bar{u}(1)\gamma^+ \left[\frac{(k_2^+ - k_1^+)}{q^+} \delta^{ij} + \frac{[\gamma^i, \gamma^j]}{2} \right] \times v(2) + K_0(\bar{Q}|\mathbf{w} - \mathbf{v}|) m \bar{u}(1)\gamma^+ \gamma^i v(2) \right\}. \quad (4.93)$$

4.3.3 NEik DIS dijet production cross-section

In this subsection we compute the cross-section for the DIS dijet production at NEik from the expressions for the S-matrix elements computed previously in this section for both the longitudinal and the transverse polarization of the photon.

In the standard CGC framework, where the eikonal limit is adopted, the background field is independent of x^- . Therefore, the light-cone "+" momentum cannot be exchanged with the target. The scattering amplitude in this case is defined as

$$S_{q_1\bar{q}_2\leftarrow\gamma_L^*}\Big|_{x^- \text{ indep.}} = (2q^+) 2\pi \delta(k_1^+ + k_2^+ - q^+) i\mathcal{M}_{q_1\bar{q}_2\leftarrow\gamma_L^*}, \quad (4.94)$$

and the cross-section yields

$$\frac{d\sigma_{\gamma_L^* \rightarrow q_1\bar{q}_2}}{d\text{P.S.}}\Big|_{x^- \text{ indep.}} = (2q^+) 2\pi \delta(k_1^+ + k_2^+ - q^+) \sum_{\text{hel., col.}} |\mathcal{M}_{q_1\bar{q}_2\leftarrow\gamma_L^*}|^2, \quad (4.95)$$

with

$$d\text{P.S.} = \frac{d^2\mathbf{k}_1}{(2\pi)^2} \frac{dk_1^+}{2k_1^+} \frac{d^2\mathbf{k}_2}{(2\pi)^2} \frac{dk_2^+}{2k_2^+} (2\pi), \quad (4.96)$$

and the summation in Eq. (4.95) is over the colors and light-front helicities of the produced quark and anti-quark.

When performing a strict expansion of the S-matrix element into Eikonal contribution, NEik contribution and so on, the gradient expansion of the background field

with respect to x^- would be performed entirely. In that case, not all the terms would be of the form Eq.(4.94): some NEik corrections would include $\delta'(k_1^+ + k_2^+ - q^+)$ instead. It is not possible to calculate the contribution of such terms to the cross section without introducing wave-packets, which is a major inconvenience. This is the motivation which has led us to introduce the Generalized Eikonal approximation, in which the dependence of the Wilson lines on a common x^- is kept at the S-matrix level.

We would like to mention that, at the accuracy considered in the present study, this modified procedure is necessary only to compute the contribution of the squared Generalized Eikonal amplitude to the cross section. For the rest of the contributions that are explicitly NEik order, the x^- dependence of the background field can be neglected, and one can go back to the standard procedure from eikonal CGC to obtain the cross section.

Following this argument, the cross section at NEik accuracy for DIS dijet for longitudinal photon can be written as

$$\frac{d\sigma_{\gamma_L^* \rightarrow q_1 \bar{q}_2}}{d\text{P.S.}} = \left. \frac{d\sigma_{\gamma_L^* \rightarrow q_1 \bar{q}_2}}{d\text{P.S.}} \right|_{\text{Gen. Eik}} + \left. \frac{d\sigma_{\gamma_L^* \rightarrow q_1 \bar{q}_2}}{d\text{P.S.}} \right|_{\text{NEik corr.}} + O(\text{NNEik}). \quad (4.97)$$

The Generalized Eikonal contribution to the cross section that depends on a common Δb^- is then given by

$$\begin{aligned} \left. \frac{d\sigma_{\gamma_L^* \rightarrow q_1 \bar{q}_2}}{d\text{P.S.}} \right|_{\text{Gen. Eik}} &= 2q^+ \int d(\Delta b^-) e^{i\Delta b^- (k_1^+ + k_2^+ - q^+)} \\ &\times \sum_{\text{hel., col.}} \left\langle \left(\mathbf{M}_{q_1 \bar{q}_2 \leftarrow \gamma_L^*}^{\text{Gen. Eik}} \left(-\frac{\Delta b^-}{2} \right) \right)^\dagger \mathbf{M}_{q_1 \bar{q}_2 \leftarrow \gamma_L^*}^{\text{Gen. Eik}} \left(\frac{\Delta b^-}{2} \right) \right\rangle \end{aligned} \quad (4.98)$$

where we average over the background field of the target. The relation between the S-matrix and the scattering amplitude b^- -dependent is

$$S_{q_1 \bar{q}_2 \leftarrow \gamma_L^*} \Big|_{\text{Gen. Eik}} = 2q^+ \int db^- e^{ib^- (k_1^+ + k_2^+ - q^+)} i \mathbf{M}_{q_1 \bar{q}_2 \leftarrow \gamma_L^*}^{\text{Gen. Eik}}(b^-). \quad (4.99)$$

The NEik correction terms in the cross-section Eq. (4.97), are computed by multiplying the amplitudes for generalized eikonal and explicit NEik ones. This is due to the fact that squaring two NEik amplitudes would yield a cross-section at NNEik order instead of NEik. Thus, the revised Generalized Eikonal contribution is Eq.(4.74) and the NEik corrections Eqs.(4.77), (4.78) and (4.80) in the longitudinal photon case). In that case, and at the NEik accuracy, the Generalized Eikonal contribution Eq.(4.74) can be replaced by the strict Eikonal contribution Eq.(4.83) in order to obtain a final result at NEik accuracy. Then, the x^- -dependence of the background field can be dropped, and relations of the type Eqs. (4.94) and (4.95) can be used, leading to

$$\left. \frac{d\sigma_{\gamma_L^* \rightarrow q_1 \bar{q}_2}}{d\text{P.S.}} \right|_{\text{NEik corr.}} = (2q^+) 2\pi \delta(k_1^+ + k_2^+ - q^+) \sum_{\text{hel., col.}} 2\text{Re} \left\langle \left(\mathcal{M}_{q_1 \bar{q}_2 \leftarrow \gamma_L^*}^{\text{strict Eik}} \right)^\dagger \mathcal{M}_{q_1 \bar{q}_2 \leftarrow \gamma_L^*}^{\text{NEik corr.}} \right\rangle. \quad (4.100)$$

Generalized eikonal cross-section via longitudinal photon :

By comparing Eqs. (4.74) and (4.99), one can read off the b^- -dependent amplitude

$$i\mathbf{M}_{q_1\bar{q}_2\leftarrow\gamma_L^*}^{\text{Gen.Eik}}(b^-) = -Q \frac{ee_f}{2\pi} \bar{u}(1)\gamma^+v(2) \frac{(q^++k_1^+-k_2^+)(q^++k_2^+-k_1^+)}{4(q^+)^3} \theta(q^++k_1^+-k_2^+) \\ \times \theta(q^++k_2^+-k_1^+) \int d^2\mathbf{v} e^{-i\mathbf{v}\cdot\mathbf{k}_1} \int d^2\mathbf{w} e^{-i\mathbf{w}\cdot\mathbf{k}_2} K_0(\hat{Q}|\mathbf{w}-\mathbf{v}|) \left[\mathcal{U}_F(\mathbf{v}, b^-) \mathcal{U}_F^\dagger(\mathbf{w}, b^-) - 1 \right]. \quad (4.101)$$

Inserting Eq. (4.101) into Eq. (4.98), one arrives at⁸

$$\frac{d\sigma_{\gamma_L^*\rightarrow q_1\bar{q}_2}}{d\text{P.S.}} \Bigg|_{\text{Gen.Eik}} = 2q^+ \int d(\Delta b^-) e^{i\Delta b^-(k_1^++k_2^+-q^+)} \left(\frac{ee_f Q}{2\pi} \right)^2 \theta(q^++k_1^+-k_2^+) \\ \times \theta(q^+-k_1^++k_2^+) \frac{k_1^+k_2^+}{2(q^+)^6} (q^++k_1^+-k_2^+)^2 (q^+-k_1^++k_2^+)^2 \int_{\mathbf{v},\mathbf{v}',\mathbf{w},\mathbf{w}'} e^{i\mathbf{k}_1\cdot(\mathbf{v}'-\mathbf{v})} \\ \times e^{i\mathbf{k}_2\cdot(\mathbf{w}'-\mathbf{w})} K_0(\hat{Q}|\mathbf{w}'-\mathbf{v}'|) K_0(\hat{Q}|\mathbf{w}-\mathbf{v}|) \left\langle \text{Tr} \left[\left(\mathcal{U}_F(\mathbf{w}', -\frac{\Delta b^-}{2}) \mathcal{U}_F^\dagger(\mathbf{v}', -\frac{\Delta b^-}{2}) - 1 \right) \right. \right. \\ \left. \left. \times \left(\mathcal{U}_F(\mathbf{v}, \frac{\Delta b^-}{2}) \mathcal{U}_F^\dagger(\mathbf{w}, \frac{\Delta b^-}{2}) - 1 \right) \right] \right\rangle. \quad (4.102)$$

where we used for the Dirac numerator:

$$\mathcal{N}_{1L} \equiv \sum_{h_1, h_2 = \pm\frac{1}{2}} (\bar{u}(1)\gamma^+v(2))^\dagger \bar{u}(1)\gamma^+v(2) \\ = (2k_1^+) \text{Tr}_D \left[\frac{\{\gamma^+, \not{k}_2\}}{2} \right] = (2k_1^+) \frac{(2k_2^+)}{2} \text{Tr}_D [1] = 8k_1^+k_2^+ \quad (4.103)$$

Splitting the color operators, one can define the following dipole and quadrupole operators

$$d(\mathbf{v}, \mathbf{w}) = \left\langle \frac{1}{N_c} \text{Tr} [\mathcal{U}_F(\mathbf{v}) \mathcal{U}_F^\dagger(\mathbf{w})] \right\rangle \quad (4.104)$$

$$Q\left(\mathbf{w}', \mathbf{v}', \mathbf{v}, \mathbf{w}, \frac{\Delta b^-}{2}\right) = \left\langle \frac{1}{N_c} \text{Tr} \left[\mathcal{U}_F\left(\mathbf{w}', \frac{\Delta b^-}{2}\right) \mathcal{U}_F^\dagger\left(\mathbf{v}', \frac{\Delta b^-}{2}\right) \right. \right. \\ \left. \left. \times \mathcal{U}_F\left(\mathbf{v}, -\frac{\Delta b^-}{2}\right) \mathcal{U}_F^\dagger\left(\mathbf{w}, -\frac{\Delta b^-}{2}\right) \right] \right\rangle, \quad (4.105)$$

and we rewrite the expression Eq. (4.102) as

$$\frac{d\sigma_{\gamma_L^*\rightarrow q_1\bar{q}_2}}{d\text{P.S.}} \Bigg|_{\text{Gen.Eik}} = N_c \frac{\alpha_{em}}{\pi} e_f^2 Q^2 \theta(q^++k_1^+-k_2^+) \theta(q^+-k_1^++k_2^+) \frac{k_1^+k_2^+}{(q^+)^5} (q^++k_1^+-k_2^+)^2 \\ \times (q^+-k_1^++k_2^+)^2 \int_{\mathbf{v},\mathbf{v}',\mathbf{w},\mathbf{w}'} e^{i\mathbf{k}_1\cdot(\mathbf{v}'-\mathbf{v})} e^{i\mathbf{k}_2\cdot(\mathbf{w}'-\mathbf{w})} K_0(\hat{Q}|\mathbf{w}'-\mathbf{v}'|) K_0(\hat{Q}|\mathbf{w}-\mathbf{v}|) \\ \times \int d(\Delta b^-) e^{i\Delta b^-(k_1^++k_2^+-q^+)} \left\{ Q\left(\mathbf{w}', \mathbf{v}', \mathbf{v}, \mathbf{w}, \frac{\Delta b^-}{2}\right) - d(\mathbf{w}', \mathbf{v}') - d(\mathbf{v}, \mathbf{w}) + 1 \right\} \quad (4.106)$$

⁸Here we introduce a compact notation for the transverse coordinate integrals $\int_x \dots \equiv \int d^2\mathbf{x} \dots$

with $\alpha_{\text{em}} = e^2/(4\pi)$.

Explicit NEik cross-section via longitudinal photon :

The strict eikonal and full NEik correction amplitudes are related to their corresponding S-matrix elements as in Eq. (4.94). From Eq. (4.83). The strict Eikonal amplitude is

$$i\mathcal{M}_{q_1\bar{q}_2\leftarrow\gamma_L^*}^{\text{strict Eik}} = -Q \frac{ee_f}{2\pi} \bar{u}(1)\gamma^+v(2) \frac{k_1^+k_2^+}{(q^+)^3} \int d^2\mathbf{v} e^{-i\mathbf{v}\cdot\mathbf{k}_1} \times \int d^2\mathbf{w} e^{-i\mathbf{w}\cdot\mathbf{k}_2} K_0(\bar{Q}|\mathbf{w}-\mathbf{v}|) \left[\mathcal{U}_F(\mathbf{v})\mathcal{U}_F^\dagger(\mathbf{w}) - 1 \right]. \quad (4.107)$$

The NEik correction to the amplitude can be written as

$$i\mathcal{M}_{q_1\bar{q}_2\leftarrow\gamma_L^*}^{\text{NEik corr.}} = i\mathcal{M}_{q_1\bar{q}_2\leftarrow\gamma_L^*}^{\text{dec. on } q} + i\mathcal{M}_{q_1\bar{q}_2\leftarrow\gamma_L^*}^{\text{dec. on } \bar{q}} + i\mathcal{M}_{q_1\bar{q}_2\leftarrow\gamma_L^*}^{\text{dyn. target}}, \quad (4.108)$$

with the three terms obtained from Eqs. (4.77), (4.78) and (4.80) as

$$i\mathcal{M}_{q_1\bar{q}_2\leftarrow\gamma_L^*}^{\text{dec. on } q} = -Q \frac{ee_f}{2\pi} \frac{k_2^+}{2(q^+)^3} \int d^2\mathbf{v} e^{-i\mathbf{v}\cdot\mathbf{k}_1} \int d^2\mathbf{w} e^{-i\mathbf{w}\cdot\mathbf{k}_2} K_0(\bar{Q}|\mathbf{w}-\mathbf{v}|) \times \bar{u}(1)\gamma^+ \left[\frac{[\gamma^i, \gamma^j]}{4} \mathcal{U}_{F;ij}^{(3)}(\mathbf{v}) - i\mathcal{U}_F^{(2)}(\mathbf{v}) + \mathcal{U}_{F;j}^{(1)}(\mathbf{v}) \left(\frac{(\mathbf{k}_2^j - \mathbf{k}_1^j)}{2} + \frac{i}{2} \partial_{\mathbf{w}^i} \right) \right] \times \mathcal{U}_F^\dagger(\mathbf{w})v(2), \quad (4.109)$$

$$i\mathcal{M}_{q_1\bar{q}_2\leftarrow\gamma_L^*}^{\text{dec. on } \bar{q}} = -Q \frac{ee_f}{2\pi} \frac{k_1^+}{2(q^+)^3} \int d^2\mathbf{v} e^{-i\mathbf{v}\cdot\mathbf{k}_1} \int d^2\mathbf{w} e^{-i\mathbf{w}\cdot\mathbf{k}_2} K_0(\bar{Q}|\mathbf{w}-\mathbf{v}|) \times \bar{u}(1)\gamma^+ \left[\mathcal{U}_F(\mathbf{v}) \left(\frac{[\gamma^i, \gamma^j]}{4} \mathcal{U}_{F;ij}^{(3)\dagger}(\mathbf{w}) - i\mathcal{U}_F^{(2)\dagger}(\mathbf{w}) + \left(\frac{i}{2} \overleftarrow{\partial}_{\mathbf{v}^i} - \frac{(\mathbf{k}_2^j - \mathbf{k}_1^j)}{2} \right) \mathcal{U}_{F;j}^{(1)\dagger}(\mathbf{w}) \right) \right] \times v(2), \quad (4.110)$$

and

$$i\mathcal{M}_{q_1\bar{q}_2\leftarrow\gamma_L^*}^{\text{dyn. target}} = iQ \frac{ee_f}{2\pi} \bar{u}(1)\gamma^+v(2) \frac{(k_1^+ - k_2^+)}{2(q^+)^3} \int d^2\mathbf{v} e^{-i\mathbf{v}\cdot\mathbf{k}_1} \int d^2\mathbf{w} e^{-i\mathbf{w}\cdot\mathbf{k}_2} \times \left[K_0(\bar{Q}|\mathbf{w}-\mathbf{v}|) - \frac{(\bar{Q}^2 - m^2)}{2\bar{Q}} |\mathbf{w}-\mathbf{v}| K_1(\bar{Q}|\mathbf{w}-\mathbf{v}|) \right] \times \left[\mathcal{U}_F(\mathbf{v}, b^-) \overleftrightarrow{\partial}_{b^-} \mathcal{U}_F^\dagger(\mathbf{w}, b^-) \right] \Big|_{b^-=0}. \quad (4.111)$$

In these NEik amplitudes, we encounter that the terms with a \mathcal{F}_{ij} decoration lead at the cross-section level to a Dirac structure that ends up vanishing, therefore they

do not contribute at the cross-section level. This vanishing Dirac structure is

$$\begin{aligned}
 \mathcal{N}_{2L} &\equiv \sum_{h_1, h_2 = \pm \frac{1}{2}} (\bar{u}(1)\gamma^+v(2))^\dagger \bar{u}(1)\gamma^+[\gamma^i, \gamma^j]v(2) \\
 &= \sum_{h_1, h_2 = \pm \frac{1}{2}} \bar{v}(2)\gamma^+u(1)\bar{u}(1)\gamma^+[\gamma^i, \gamma^j]v(2) = \text{Tr}_D \left[\gamma^+(\check{\mathbf{k}}_1 + m)\gamma^+[\gamma^i, \gamma^j](\check{\mathbf{k}}_2 - m) \right] \\
 &= \text{Tr}_D \left[\gamma^+ \left\{ \check{\mathbf{k}}_1, \gamma^+ \right\} [\gamma^i, \gamma^j] \check{\mathbf{k}}_2 \right] = (2k_1^+) \text{Tr}_D \left[\gamma^+[\gamma^i, \gamma^j] \check{\mathbf{k}}_2 \right] \\
 &= (2k_1^+) \text{Tr}_D \left[\frac{\{\gamma^+, \check{\mathbf{k}}_2\}}{2} [\gamma^i, \gamma^j] \right] = (2k_1^+) \frac{(2k_2^+)}{2} \text{Tr}_D \left[[\gamma^i, \gamma^j] \right] = 0 \quad (4.112)
 \end{aligned}$$

where $\text{Tr}_D [[\gamma^i, \gamma^j]] = 0$.

The rest of the terms at NEik have the same Dirac algebra as the one performed in Eq. (4.103) and contribute to the cross-section as follows. From Eq. (4.109) we encounter, after multiplying with the eikonal amplitude

$$\begin{aligned}
 \frac{d\sigma_{\gamma_L^* \rightarrow q_1 \bar{q}_2}}{d\text{P.S.}} \Bigg|_{\text{NEik corr.}}^{\text{dec. on } q} &= (2q^+) 2\pi\delta(k_1^+ + k_2^+ - q^+) 8k_1^+ k_2^+ Q^2 \left(\frac{ee_f}{2\pi} \right)^2 \frac{k_1^+ k_2^+}{(q^+)^3} \frac{k_2^+}{2(q^+)^3} \\
 &\times 2\text{Re} \int_{\mathbf{v}, \mathbf{v}', \mathbf{w}, \mathbf{w}'} e^{i\mathbf{k}_1 \cdot (\mathbf{v}' - \mathbf{v})} e^{i\mathbf{k}_2 \cdot (\mathbf{w}' - \mathbf{w})} \text{K}_0(\bar{Q}|\mathbf{w}' - \mathbf{v}'|) \text{K}_0(\bar{Q}|\mathbf{w} - \mathbf{v}|) \\
 &\times \text{Tr} \left\langle \left[\mathcal{U}_F(\mathbf{w}') \mathcal{U}_F^\dagger(\mathbf{v}') - 1 \right] \left[-i\mathcal{U}_F^{(2)}(\mathbf{v}) + \mathcal{U}_{F;j}^{(1)}(\mathbf{v}) \left(\frac{(\mathbf{k}_2^j - \mathbf{k}_1^j)}{2} + \frac{i}{2} \partial_{\mathbf{w}j} \right) \right] \mathcal{U}_F^\dagger(\mathbf{w}) \right\rangle. \quad (4.113)
 \end{aligned}$$

Similarly, the contribution from Eq. (4.110) at cross section level is

$$\begin{aligned}
 \frac{d\sigma_{\gamma_L^* \rightarrow q_1 \bar{q}_2}}{d\text{P.S.}} \Bigg|_{\text{NEik corr.}}^{\text{dec. on } \bar{q}} &= (2q^+) 2\pi\delta(k_1^+ + k_2^+ - q^+) 8k_1^+ k_2^+ Q^2 \left(\frac{ee_f}{2\pi} \right)^2 \frac{k_1^+ k_2^+}{(q^+)^3} \frac{k_1^+}{2(q^+)^3} \\
 &\times 2\text{Re} \int_{\mathbf{v}, \mathbf{v}', \mathbf{w}, \mathbf{w}'} e^{i\mathbf{k}_1 \cdot (\mathbf{v}' - \mathbf{v})} e^{i\mathbf{k}_2 \cdot (\mathbf{w}' - \mathbf{w})} \text{K}_0(\bar{Q}|\mathbf{w}' - \mathbf{v}'|) \text{K}_0(\bar{Q}|\mathbf{w} - \mathbf{v}|) \\
 &\times \text{Tr} \left\langle \left[\mathcal{U}_F(\mathbf{w}') \mathcal{U}_F^\dagger(\mathbf{v}') - 1 \right] \left[\mathcal{U}_F(\mathbf{v}) \left(-i\mathcal{U}_F^{(2)\dagger}(\mathbf{w}) + \left(\frac{i}{2} \overleftarrow{\partial}_{\mathbf{v}i} - \frac{(\mathbf{k}_2^j - \mathbf{k}_1^j)}{2} \right) \mathcal{U}_{F;j}^{(1)\dagger}(\mathbf{w}) \right) \right] \right\rangle. \quad (4.114)
 \end{aligned}$$

Finally, the contribution from Eq. (4.111) at cross section level is

$$\begin{aligned}
 \frac{d\sigma_{\gamma_L^* \rightarrow q_1 \bar{q}_2}}{d\text{P.S.}} \Bigg|_{\text{NEik corr.}}^{\text{dyn. target}} &= (2q^+) 2\pi\delta(k_1^+ + k_2^+ - q^+) 8k_1^+ k_2^+ Q^2 \left(\frac{ee_f}{2\pi} \right)^2 \\
 &\times \frac{k_1^+ k_2^+}{(q^+)^3} \frac{(k_1^+ - k_2^+)}{2(q^+)^3} 2\text{Re} (-i) \int_{\mathbf{v}, \mathbf{v}', \mathbf{w}, \mathbf{w}'} e^{i\mathbf{k}_1 \cdot (\mathbf{v}' - \mathbf{v})} e^{i\mathbf{k}_2 \cdot (\mathbf{w}' - \mathbf{w})} \\
 &\times \left[\text{K}_0(\bar{Q}|\mathbf{w} - \mathbf{v}|) - \frac{(\bar{Q}^2 - m^2)}{2\bar{Q}} |\mathbf{w} - \mathbf{v}| \text{K}_1(\bar{Q}|\mathbf{w} - \mathbf{v}|) \right] \\
 &\times \text{K}_0(\bar{Q}|\mathbf{w}' - \mathbf{v}'|) \text{Tr} \left\langle \left[\mathcal{U}_F(\mathbf{w}') \mathcal{U}_F^\dagger(\mathbf{v}') - 1 \right] \left[\mathcal{U}_F(\mathbf{v}, b^-) \overleftrightarrow{\partial}_b \mathcal{U}_F^\dagger(\mathbf{w}, b^-) \right] \Big|_{b^- = 0} \right\rangle. \quad (4.115)
 \end{aligned}$$

As in the previous case for generalized eikonal cross-section, we introduce the different types of decorated dipole and quadrupole operators.

$$d_j^{(1)}(\mathbf{v}_*, \mathbf{w}) = \left\langle \frac{1}{N_c} \text{Tr} \left[\mathcal{U}_{F;j}^{(1)}(\mathbf{v}) \mathcal{U}_F^\dagger(\mathbf{w}) \right] \right\rangle \quad (4.116)$$

$$d^{(2)}(\mathbf{v}_*, \mathbf{w}) = \left\langle \frac{1}{N_c} \text{Tr} \left[\mathcal{U}_F^{(2)}(\mathbf{v}) \mathcal{U}_F^\dagger(\mathbf{w}) \right] \right\rangle \quad (4.117)$$

$$Q_j^{(1)}(\mathbf{w}', \mathbf{v}', \mathbf{v}_*, \mathbf{w}) = \left\langle \frac{1}{N_c} \text{Tr} \left[\mathcal{U}_F(\mathbf{w}') \mathcal{U}_F^\dagger(\mathbf{v}') \mathcal{U}_{F;j}^{(1)}(\mathbf{v}) \mathcal{U}_F^\dagger(\mathbf{w}) \right] \right\rangle \quad (4.118)$$

$$Q^{(2)}(\mathbf{w}', \mathbf{v}', \mathbf{v}_*, \mathbf{w}) = \left\langle \frac{1}{N_c} \text{Tr} \left[\mathcal{U}_F(\mathbf{w}') \mathcal{U}_F^\dagger(\mathbf{v}') \mathcal{U}_F^{(2)}(\mathbf{v}) \mathcal{U}_F^\dagger(\mathbf{w}) \right] \right\rangle \quad (4.119)$$

$$\tilde{d}(\mathbf{v}_*, \mathbf{w}_*) = \left\langle \frac{1}{N_c} \text{Tr} \left[\left(\mathcal{U}_F(\mathbf{v}, b^-) \overset{\leftarrow}{\partial}_- \mathcal{U}_F^\dagger(\mathbf{w}, b^-) \right) \Big|_{b^-=0} \right] \right\rangle, \quad (4.120)$$

$$\tilde{Q}(\mathbf{w}', \mathbf{v}', \mathbf{v}_*, \mathbf{w}_*) = \left\langle \frac{1}{N_c} \text{Tr} \left[\mathcal{U}_F(\mathbf{w}') \mathcal{U}_F^\dagger(\mathbf{v}') \left(\mathcal{U}_F(\mathbf{v}, b^-) \overset{\leftarrow}{\partial}_- \mathcal{U}_F^\dagger(\mathbf{w}, b^-) \right) \Big|_{b^-=0} \right] \right\rangle. \quad (4.121)$$

where the star indicates the position of the decoration.

$$\begin{aligned} \frac{d\sigma_{\gamma_L^* \rightarrow q_1 \bar{q}_2}}{d\text{P.S.}} \Big|_{\text{NEik corr.}}^{\text{dec. on } q} &= 2\pi \delta(k_1^+ + k_2^+ - q^+) 8N_c \frac{\alpha_{\text{em}}}{\pi} e_f^2 Q^2 \frac{(k_1^+)^2 (k_2^+)^3}{(q^+)^5} \\ &\times 2\text{Re} \int_{\mathbf{v}, \mathbf{v}', \mathbf{w}, \mathbf{w}'} e^{i\mathbf{k}_1 \cdot (\mathbf{v}' - \mathbf{v})} e^{i\mathbf{k}_2 \cdot (\mathbf{w}' - \mathbf{w})} \text{K}_0(\bar{Q} |\mathbf{w}' - \mathbf{v}'|) \text{K}_0(\bar{Q} |\mathbf{w} - \mathbf{v}|) \\ &\times \left\{ \left[\frac{(\mathbf{k}_2^j - \mathbf{k}_1^j)}{2} + \frac{i}{2} \partial_{\mathbf{w}^j} \right] \left[Q_j^{(1)}(\mathbf{w}', \mathbf{v}', \mathbf{v}_*, \mathbf{w}) - d_j^{(1)}(\mathbf{v}_*, \mathbf{w}) \right] \right. \\ &\left. - i \left[Q^{(2)}(\mathbf{w}', \mathbf{v}', \mathbf{v}_*, \mathbf{w}) - d^{(2)}(\mathbf{v}_*, \mathbf{w}) \right] \right\}, \end{aligned} \quad (4.122)$$

$$\begin{aligned} \frac{d\sigma_{\gamma_L^* \rightarrow q_1 \bar{q}_2}}{d\text{P.S.}} \Big|_{\text{NEik corr.}}^{\text{dec. on } \bar{q}} &= 2\pi \delta(k_1^+ + k_2^+ - q^+) 8N_c \frac{\alpha_{\text{em}}}{\pi} e_f^2 Q^2 \frac{(k_1^+)^3 (k_2^+)^2}{(q^+)^5} \\ &\times 2\text{Re} \int_{\mathbf{v}, \mathbf{v}', \mathbf{w}, \mathbf{w}'} e^{i\mathbf{k}_1 \cdot (\mathbf{v}' - \mathbf{v})} e^{i\mathbf{k}_2 \cdot (\mathbf{w}' - \mathbf{w})} \text{K}_0(\bar{Q} |\mathbf{w}' - \mathbf{v}'|) \text{K}_0(\bar{Q} |\mathbf{w} - \mathbf{v}|) \\ &\times \left\{ \left[-\frac{(\mathbf{k}_2^j - \mathbf{k}_1^j)}{2} + \frac{i}{2} \partial_{\mathbf{v}^j} \right] \right. \\ &\left. \left[Q_j^{(1)}(\mathbf{v}', \mathbf{w}', \mathbf{w}_*, \mathbf{v})^\dagger - d_j^{(1)}(\mathbf{w}_*, \mathbf{v})^\dagger \right] - i \left[Q^{(2)}(\mathbf{v}', \mathbf{w}', \mathbf{w}_*, \mathbf{v})^\dagger - d^{(2)}(\mathbf{w}_*, \mathbf{v})^\dagger \right] \right\} \end{aligned} \quad (4.123)$$

and

$$\begin{aligned}
 \left. \frac{d\sigma_{\gamma_L^* \rightarrow q_1 \bar{q}_2}}{d\text{P.S.}} \right|_{\text{NEik corr.}}^{\text{dyn. target}} &= 2\pi\delta(k_1^+ + k_2^+ - q^+) 8N_c \frac{\alpha_{\text{em}}}{\pi} e_f^2 Q^2 \frac{(k_1^+)^2 (k_2^+)^2 (k_1^+ - k_2^+)}{(q^+)^5} \\
 &\times 2\text{Re}(-i) \int_{\mathbf{v}, \mathbf{v}', \mathbf{w}, \mathbf{w}'} e^{i\mathbf{k}_1 \cdot (\mathbf{v}' - \mathbf{v})} e^{i\mathbf{k}_2 \cdot (\mathbf{w}' - \mathbf{w})} \left[\tilde{Q}(\mathbf{w}', \mathbf{v}', \mathbf{v}_*, \mathbf{w}_*) - \tilde{d}(\mathbf{v}_*, \mathbf{w}_*) \right] \\
 &\times K_0(\bar{Q}|\mathbf{w}' - \mathbf{v}'|) \left[K_0(\bar{Q}|\mathbf{w} - \mathbf{v}|) - \frac{(\bar{Q}^2 - m^2)}{2\bar{Q}} |\mathbf{w} - \mathbf{v}| K_1(\bar{Q}|\mathbf{w} - \mathbf{v}|) \right]. \quad (4.124)
 \end{aligned}$$

All in all, the NEik correction to the cross section for longitudinal photon beyond the generalized Eikonal contribution Eq. (4.106) is given by the sum of the contributions Eqs. (4.122), (4.123) and (4.124).

Generalized eikonal cross-section via transverse photon :

For the case of the transverse polarization of the photon, we proceed in the same manner as in the last two cases. The generalized eikonal contribution is obtained as

$$\begin{aligned}
 \left. \frac{d\sigma_{\gamma_T^* \rightarrow q_1 \bar{q}_2}}{d\text{P.S.}} \right|_{\text{Gen. Eik}} &= 2q^+ \int d(\Delta b^-) e^{i\Delta b^- (k_1^+ + k_2^+ - q^+)} \\
 &\times \frac{1}{2} \sum_{\lambda} \sum_{\text{hel., col.}} \left\langle \left(\mathbf{M}_{q_1 \bar{q}_2 \leftarrow \gamma_T^*}^{\text{Gen. Eik}} \left(-\frac{\Delta b^-}{2} \right) \right)^\dagger \mathbf{M}_{q_1 \bar{q}_2 \leftarrow \gamma_T^*}^{\text{Gen. Eik}} \left(\frac{\Delta b^-}{2} \right) \right\rangle, \quad (4.125)
 \end{aligned}$$

which includes an averaging over the polarization λ of the incoming transverse photon. The b^- dependent amplitude involved in Eq. (4.125) is defined in the same way as in Eq. (4.99), and can be read off from the generalized eikonal expression from the S-matrix Eq. (4.86) in the transverse photon case. In such a way, one finds

$$\begin{aligned}
 i\mathbf{M}_{q_1 \bar{q}_2 \leftarrow \gamma_T^*}^{\text{Gen. Eik}}(b^-) &= \frac{ee_f}{2\pi} \varepsilon_\lambda^i \frac{1}{2q^+} \theta(q^+ + k_1^+ - k_2^+) \theta(q^+ + k_2^+ - k_1^+) \int d^2\mathbf{v} e^{-i\mathbf{v} \cdot \mathbf{k}_1} \int d^2\mathbf{w} \\
 &\times e^{-i\mathbf{w} \cdot \mathbf{k}_2} \left\{ -i \frac{(\mathbf{w}^j - \mathbf{v}^j)}{|\mathbf{w} - \mathbf{v}|} \hat{Q} K_1(\hat{Q}|\mathbf{w} - \mathbf{v}|) \bar{u}(1) \gamma^+ \left[\frac{(k_2^+ - k_1^+)}{q^+} \delta^{ij} + \frac{[\gamma^i, \gamma^j]}{2} \right] v(2) \right. \\
 &\left. + K_0(\hat{Q}|\mathbf{w} - \mathbf{v}|) m \bar{u}(1) \gamma^+ \gamma^i v(2) \right\} \left[\mathcal{U}_F(\mathbf{v}, b^-) \mathcal{U}_F^\dagger(\mathbf{w}, b^-) - 1 \right]. \quad (4.126)
 \end{aligned}$$

This yields the following generalized eikonal cross-section

$$\begin{aligned}
\left. \frac{d\sigma_{\gamma_T^* \rightarrow q_1 \bar{q}_2}}{d\text{P.S.}} \right|_{\text{Gen. Eik}} &= 2q^+ \int d(\Delta b^-) e^{i\Delta b^- (k_1^+ + k_2^+ - q^+)} \left(\frac{ee_f}{2\pi} \right)^2 \frac{1}{(2q^+)^2} \theta(q^+ + k_1^+ - k_2^+) \\
&\times \theta(q^+ + k_2^+ - k_1^+) \int_{\mathbf{v}, \mathbf{v}', \mathbf{w}, \mathbf{w}'} e^{i\mathbf{k}_1 \cdot (\mathbf{v}' - \mathbf{v})} e^{i\mathbf{k}_2 \cdot (\mathbf{w}' - \mathbf{w})} \\
&\times \left\{ 8k_1^+ k_2^+ m^2 K_0(\hat{Q} |\mathbf{w}' - \mathbf{v}'|) K_0(\hat{Q} |\mathbf{w} - \mathbf{v}|) + 4k_1^+ k_2^+ \left[1 + \left(\frac{k_2^+ - k_1^+}{q^+} \right)^2 \right] \right. \\
&\times \left. \hat{Q}^2 \frac{(\mathbf{w}' - \mathbf{v}') \cdot (\mathbf{w} - \mathbf{v})}{|\mathbf{w}' - \mathbf{v}'| |\mathbf{w} - \mathbf{v}|} K_1(\hat{Q} |\mathbf{w}' - \mathbf{v}'|) K_1(\hat{Q} |\mathbf{w} - \mathbf{v}|) \right\} \\
&\times \left\langle \text{Tr} \left[\left(\mathcal{U}_F(\mathbf{w}', -\frac{\Delta b^-}{2}) \mathcal{U}_F^\dagger(\mathbf{v}', -\frac{\Delta b^-}{2}) - \mathbf{1} \right) \left(\mathcal{U}_F(\mathbf{v}, \frac{\Delta b^-}{2}) \mathcal{U}_F^\dagger(\mathbf{w}, \frac{\Delta b^-}{2}) - \mathbf{1} \right) \right] \right\rangle.
\end{aligned} \tag{4.127}$$

simplifying as in the case of the longitudinal polarization of the photon, we finally obtain

$$\begin{aligned}
\left. \frac{d\sigma_{\gamma_T^* \rightarrow q_1 \bar{q}_2}}{d\text{P.S.}} \right|_{\text{Gen. Eik}} &= N_c \frac{\alpha_{\text{em}}}{\pi} e_f^2 \frac{2k_1^+ k_2^+}{q^+} \theta(q^+ + k_1^+ - k_2^+) \theta(q^+ + k_2^+ - k_1^+) \\
&\times \int_{\mathbf{v}, \mathbf{v}', \mathbf{w}, \mathbf{w}'} e^{i\mathbf{k}_1 \cdot (\mathbf{v}' - \mathbf{v})} e^{i\mathbf{k}_2 \cdot (\mathbf{w}' - \mathbf{w})} \left\{ 2m^2 K_0(\hat{Q} |\mathbf{w}' - \mathbf{v}'|) K_0(\hat{Q} |\mathbf{w} - \mathbf{v}|) \right. \\
&+ \left. \left[1 + \left(\frac{k_2^+ - k_1^+}{q^+} \right)^2 \right] \hat{Q}^2 \frac{(\mathbf{w}' - \mathbf{v}') \cdot (\mathbf{w} - \mathbf{v})}{|\mathbf{w}' - \mathbf{v}'| |\mathbf{w} - \mathbf{v}|} K_1(\hat{Q} |\mathbf{w}' - \mathbf{v}'|) K_1(\hat{Q} |\mathbf{w} - \mathbf{v}|) \right\} \\
&\times \int d(\Delta b^-) e^{i\Delta b^- (k_1^+ + k_2^+ - q^+)} \left\{ Q(\mathbf{w}', \mathbf{v}', \mathbf{v}, \mathbf{w}, \frac{\Delta b^-}{2}) - d(\mathbf{w}', \mathbf{v}') - d(\mathbf{v}, \mathbf{w}) + 1 \right\}.
\end{aligned} \tag{4.128}$$

Explicit NEik cross-section via transverse photon :

The NEik correction to the transverse photon cross-section, up to the averaging over λ , as

$$\begin{aligned}
\left. \frac{d\sigma_{\gamma_T^* \rightarrow q_1 \bar{q}_2}}{d\text{P.S.}} \right|_{\text{NEik corr.}} &= (2q^+) 2\pi \delta(k_1^+ + k_2^+ - q^+) \\
&\times \frac{1}{2} \sum_{\lambda} \sum_{\text{hel., col.}} 2\text{Re} \left\langle \left(\mathcal{M}_{q_1 \bar{q}_2 \leftarrow \gamma_T^*}^{\text{strict Eik}} \right)^\dagger \mathcal{M}_{q_1 \bar{q}_2 \leftarrow \gamma_T^*}^{\text{NEik corr.}} \right\rangle.
\end{aligned} \tag{4.129}$$

It amounts to calculating the interference between the strict Eikonal amplitude and the NEik correction to the amplitude, normalized as in Eq. (4.94). From Eq. (4.93),

the strict eikonal amplitude for transverse photon is found to be

$$\begin{aligned}
 i\mathcal{M}_{q_1\bar{q}_2\leftarrow\gamma_T^*}^{\text{strict Eik}} &= \frac{ee_f}{2\pi} \varepsilon_\lambda^i \frac{1}{2q^+} \int d^2\mathbf{v} e^{-i\mathbf{v}\cdot\mathbf{k}_1} \int d^2\mathbf{w} e^{-i\mathbf{w}\cdot\mathbf{k}_2} \left[\mathcal{U}_F(\mathbf{v})\mathcal{U}_F^\dagger(\mathbf{w}) - 1 \right] \\
 &\times \left\{ -i \frac{(\mathbf{w}^j - \mathbf{v}^j)}{|\mathbf{w} - \mathbf{v}|} \bar{Q} K_1 (\bar{Q} |\mathbf{w} - \mathbf{v}|) \bar{u}(1)\gamma^+ \left[\frac{(k_2^+ - k_1^+)}{q^+} \delta^{ij} + \frac{[\gamma^i, \gamma^j]}{2} \right] v(2) \right. \\
 &\left. \times + K_0 (\bar{Q} |\mathbf{w} - \mathbf{v}|) m \bar{u}(1)\gamma^+ \gamma^i v(2) \right\}. \tag{4.130}
 \end{aligned}$$

By contrast, the NEik correction to the amplitude is the sum of five contributions

$$i\mathcal{M}_{q_1\bar{q}_2\leftarrow\gamma_T^*}^{\text{NEik corr.}} = i\mathcal{M}_{q_1\bar{q}_2\leftarrow\gamma_T^*}^{\text{in}} + i\mathcal{M}_{q_1\bar{q}_2\leftarrow\gamma_T^*}^{\text{dec. on } q} + i\mathcal{M}_{q_1\bar{q}_2\leftarrow\gamma_T^*}^{\text{dec. on } \bar{q}} + i\mathcal{M}_{q_1\bar{q}_2\leftarrow\gamma_T^*}^{L^+ \text{ phase}} + i\mathcal{M}_{q_1\bar{q}_2\leftarrow\gamma_T^*}^{\text{dyn. target}}, \tag{4.131}$$

corresponding to the contributions Eqs. (4.38), (4.87), (4.88), (4.89) and (4.90) to the S-matrix element respectively. We thus have

$$\begin{aligned}
 i\mathcal{M}_{q_1\bar{q}_2\leftarrow\gamma_T^*}^{\text{in}} &= ee_f \varepsilon_\lambda^i \frac{1}{8k_1^+ k_2^+} \bar{u}(1)\gamma^+ \left[\frac{(k_2^+ - k_1^+)}{q^+} \delta^{ij} + \frac{1}{2} [\gamma^i, \gamma^j] \right] v(2) \\
 &\times \int d^2\mathbf{z} e^{-i(\mathbf{k}_1 + \mathbf{k}_2)\cdot\mathbf{z}} \int_{-L^+/2}^{L^+/2} dz^+ \left[\mathcal{U}_F\left(\frac{L^+}{2}, z^+; \mathbf{z}\right) \overleftrightarrow{\mathcal{D}}_{\mathbf{z}} \mathcal{U}_F^\dagger\left(\frac{L^+}{2}, z^+; \mathbf{z}\right) \right], \tag{4.132}
 \end{aligned}$$

$$\begin{aligned}
 i\mathcal{M}_{q_1\bar{q}_2\leftarrow\gamma_T^*}^{\text{dec. on } q} &= \frac{ee_f}{2\pi} \varepsilon_\lambda^i \frac{1}{2q^+} \frac{1}{2k_1^+} \int d^2\mathbf{v} e^{-i\mathbf{v}\cdot\mathbf{k}_1} \int d^2\mathbf{w} e^{-i\mathbf{w}\cdot\mathbf{k}_2} \bar{u}(1)\gamma^+ \\
 &\times \left[\left(\frac{[\gamma^l, \gamma^m]}{4} \mathcal{U}_{F;lm}^{(3)}(\mathbf{v}) - i\mathcal{U}_F^{(2)}(\mathbf{v}) + \mathcal{U}_{F;l}^{(1)}(\mathbf{v}) \left(\frac{(\mathbf{k}_2^l - \mathbf{k}_1^l)}{2} + \frac{i}{2} \overrightarrow{\partial_{\mathbf{w}^l}} \right) \right) \mathcal{U}_F^\dagger(\mathbf{w}) \right] \\
 &\times \left\{ -i \frac{(\mathbf{w}^j - \mathbf{v}^j)}{|\mathbf{w} - \mathbf{v}|} \bar{Q} K_1 (\bar{Q} |\mathbf{w} - \mathbf{v}|) \left[\frac{(k_2^+ - k_1^+)}{q^+} \delta^{ij} + \frac{[\gamma^i, \gamma^j]}{2} \right] \right. \\
 &\left. + K_0 (\bar{Q} |\mathbf{w} - \mathbf{v}|) m \gamma^i \right\} v(2), \tag{4.133}
 \end{aligned}$$

$$\begin{aligned}
 i\mathcal{M}_{q_1\bar{q}_2\leftarrow\gamma_T^*}^{\text{dec. on } \bar{q}} &= \frac{ee_f}{2\pi} \varepsilon_\lambda^i \frac{1}{2q^+} \frac{1}{2k_2^+} \int d^2\mathbf{v} e^{-i\mathbf{v}\cdot\mathbf{k}_1} \int d^2\mathbf{w} e^{-i\mathbf{w}\cdot\mathbf{k}_2} \bar{u}(1)\gamma^+ \\
 &\times \left\{ -i \frac{(\mathbf{w}^j - \mathbf{v}^j)}{|\mathbf{w} - \mathbf{v}|} \bar{Q} K_1 (\bar{Q} |\mathbf{w} - \mathbf{v}|) \left[\frac{(k_2^+ - k_1^+)}{q^+} \delta^{ij} + \frac{[\gamma^i, \gamma^j]}{2} \right] + K_0 (\bar{Q} |\mathbf{w} - \mathbf{v}|) m \gamma^i \right\} \\
 &\times \left[\mathcal{U}_F(\mathbf{v}) \left(\frac{[\gamma^l, \gamma^m]}{4} \mathcal{U}_{F;lm}^{(3)\dagger}(\mathbf{w}) - i\mathcal{U}_F^{(2)\dagger}(\mathbf{w}) + \left(\frac{i}{2} \overleftarrow{\partial_{\mathbf{v}^l}} - \frac{(\mathbf{k}_2^l - \mathbf{k}_1^l)}{2} \right) \mathcal{U}_{F;l}^{(1)\dagger}(\mathbf{w}) \right) \right] v(2), \tag{4.134}
 \end{aligned}$$

$$\begin{aligned}
 i\mathcal{M}_{q_1\bar{q}_2\leftarrow\gamma_T^*}^{L^+ \text{ phase}} &= ee_f \varepsilon_\lambda^i \frac{(-1)^{L^+}}{16k_1^+ k_2^+} \bar{u}(1)\gamma^+ \left[\frac{(k_2^+ - k_1^+)}{q^+} \delta^{ij} + \frac{[\gamma^i, \gamma^j]}{2} \right] v(2) \\
 &\times \int d^2\mathbf{z} e^{-i\mathbf{z}\cdot(\mathbf{k}_1 + \mathbf{k}_2)} \left[\mathcal{U}_F(\mathbf{z}) \overleftrightarrow{\mathcal{D}}_{\mathbf{z}} \mathcal{U}_F^\dagger(\mathbf{z}) \right] \tag{4.135}
 \end{aligned}$$

and

$$\begin{aligned}
i\mathcal{M}_{q_1\bar{q}_2\leftarrow\gamma_T^*}^{\text{dyn. target}} &= \frac{ee_f}{2\pi} \varepsilon_\lambda^i \frac{1}{2(q^+)^2} \int d^2\mathbf{v} e^{-i\mathbf{v}\cdot\mathbf{k}_1} \int d^2\mathbf{w} e^{-i\mathbf{w}\cdot\mathbf{k}_2} \\
&\times \left[\mathcal{U}_F(\mathbf{v}, b^-) \overset{\leftarrow}{\partial}_{b^-} \mathcal{U}_F^\dagger(\mathbf{w}, b^-) \right] \Big|_{b^-=0} \\
&\times \bar{u}(1)\gamma^+ \left\{ -\frac{(\mathbf{w}^i - \mathbf{v}^i)\bar{Q}}{|\mathbf{w} - \mathbf{v}|} \mathbf{K}_1(\bar{Q}|\mathbf{w} - \mathbf{v}|) - \frac{i(k_2^+ - k_1^+)Q^2|\mathbf{w} - \mathbf{v}|}{4q^+\bar{Q}} \mathbf{K}_1(\bar{Q}|\mathbf{w} - \mathbf{v}|) m\gamma^i \right. \\
&\left. - \frac{(k_2^+ - k_1^+)Q^2}{4q^+} (\mathbf{w}^j - \mathbf{v}^j)\mathbf{K}_0(\bar{Q}|\mathbf{w} - \mathbf{v}|) \left[\frac{(k_2^+ - k_1^+)}{q^+} \delta^{ij} + \frac{[\gamma^i, \gamma^j]}{2} \right] \right\} v(2). \quad (4.136)
\end{aligned}$$

After computing the cross-sections and introducing the following notation for the remaining decorated dipole and quadrupole

$$d_{ij}^{(3)}(\mathbf{v}_*, \mathbf{w}) = \left\langle \frac{1}{N_c} \text{Tr} \left[\mathcal{U}_{F;ij}^{(3)}(\mathbf{v}) \mathcal{U}_F^\dagger(\mathbf{w}) \right] \right\rangle \quad (4.137)$$

$$Q_{ij}^{(3)}(\mathbf{w}', \mathbf{v}', \mathbf{v}_*, \mathbf{w}) = \left\langle \frac{1}{N_c} \text{Tr} \left[\mathcal{U}_F(\mathbf{w}') \mathcal{U}_F^\dagger(\mathbf{v}') \mathcal{U}_{F;ij}^{(3)}(\mathbf{v}) \mathcal{U}_F^\dagger(\mathbf{w}) \right] \right\rangle. \quad (4.138)$$

At the cross-section level one finds the following Dirac structures

$$\begin{aligned}
\mathcal{N}_{1T} &\equiv \frac{1}{2} \sum_\lambda \sum_{h_1, h_2 = \pm\frac{1}{2}} \varepsilon_\lambda^{i'*} \varepsilon_\lambda^i \left(\bar{u}(1)\gamma^+ \right. \\
&\times \left. \left[\frac{(k_2^+ - k_1^+)}{q^+} \delta^{i'j'} + \frac{[\gamma^{i'}, \gamma^{j'}]}{2} \right] v(2) \right)^\dagger \bar{u}(1)\gamma^+ \left[\frac{(k_2^+ - k_1^+)}{q^+} \delta^{ij} + \frac{[\gamma^i, \gamma^j]}{2} \right] v(2) \quad (4.139)
\end{aligned}$$

$$\mathcal{N}_{2T} \equiv \frac{1}{2} \sum_\lambda \sum_{h_1, h_2 = \pm\frac{1}{2}} \varepsilon_\lambda^{i'*} \varepsilon_\lambda^i \left(\bar{u}(1)\gamma^+ \gamma^{i'} v(2) \right)^\dagger \bar{u}(1)\gamma^+ \gamma^i v(2) \quad (4.140)$$

$$\begin{aligned}
\mathcal{N}_{3T} &\equiv \frac{1}{2} \sum_\lambda \sum_{h_1, h_2 = \pm\frac{1}{2}} \varepsilon_\lambda^{i'*} \varepsilon_\lambda^i \left(\bar{u}(1)\gamma^+ \gamma^{i'} v(2) \right)^\dagger \bar{u}(1)\gamma^+ \left[\frac{(k_2^+ - k_1^+)}{q^+} \delta^{ij} + \frac{[\gamma^i, \gamma^j]}{2} \right] v(2) \\
&\quad (4.141)
\end{aligned}$$

$$\begin{aligned}
\mathcal{N}_{4T} &\equiv \frac{1}{2} \sum_\lambda \sum_{h_1, h_2 = \pm\frac{1}{2}} \varepsilon_\lambda^{i'*} \varepsilon_\lambda^i \left(\bar{u}(1)\gamma^+ \left[\frac{(k_2^+ - k_1^+)}{q^+} \delta^{i'j'} + \frac{[\gamma^{i'}, \gamma^{j'}]}{2} \right] v(2) \right)^\dagger \bar{u}(1)\gamma^+ \gamma^i v(2). \\
&\quad (4.142)
\end{aligned}$$

and in the case of the \mathcal{F}_{lm} decoration inserted on the antiquark line, at \mathbf{w} , we have

$$\begin{aligned} \mathcal{N}_{1''T} &\equiv \frac{1}{2} \sum_{\lambda} \sum_{h_1, h_2 = \pm \frac{1}{2}} \varepsilon_{\lambda}^{i'*} \varepsilon_{\lambda}^i \left(\bar{u}(1) \gamma^+ \left[\frac{(k_2^+ - k_1^+)}{q^+} \delta^{i'j'} + \frac{[\gamma^{i'}, \gamma^{j'}]}{2} \right] v(2) \right)^{\dagger} \\ &\quad \times \bar{u}(1) \gamma^+ \left[\frac{(k_2^+ - k_1^+)}{q^+} \delta^{ij} + \frac{[\gamma^i, \gamma^j]}{2} \right] [\gamma^l, \gamma^m] v(2) \end{aligned} \quad (4.143)$$

$$\mathcal{N}_{2''T} \equiv \frac{1}{2} \sum_{\lambda} \sum_{h_1, h_2 = \pm \frac{1}{2}} \varepsilon_{\lambda}^{i'*} \varepsilon_{\lambda}^i \left(\bar{u}(1) \gamma^+ \gamma^{i'} v(2) \right)^{\dagger} \bar{u}(1) \gamma^+ \gamma^i [\gamma^l, \gamma^m] v(2) \quad (4.144)$$

$$\begin{aligned} \mathcal{N}_{3''T} &\equiv \frac{1}{2} \sum_{\lambda} \sum_{h_1, h_2 = \pm \frac{1}{2}} \varepsilon_{\lambda}^{i'*} \varepsilon_{\lambda}^i \left(\bar{u}(1) \gamma^+ \gamma^{i'} v(2) \right)^{\dagger} \bar{u}(1) \gamma^+ \\ &\quad \times \left[\frac{(k_2^+ - k_1^+)}{q^+} \delta^{ij} + \frac{[\gamma^i, \gamma^j]}{2} \right] [\gamma^l, \gamma^m] v(2) \end{aligned} \quad (4.145)$$

$$\begin{aligned} \mathcal{N}_{4''T} &\equiv \frac{1}{2} \sum_{\lambda} \sum_{h_1, h_2 = \pm \frac{1}{2}} \varepsilon_{\lambda}^{i'*} \varepsilon_{\lambda}^i \left(\bar{u}(1) \gamma^+ \left[\frac{(k_2^+ - k_1^+)}{q^+} \delta^{i'j'} + \frac{[\gamma^{i'}, \gamma^{j'}]}{2} \right] v(2) \right)^{\dagger} \\ &\quad \times \bar{u}(1) \gamma^+ \gamma^i [\gamma^l, \gamma^m] v(2). \end{aligned} \quad (4.146)$$

The transverse polarization vectors obey the completeness relation

$$\sum_{\lambda} \varepsilon_{\lambda}^{i'*} \varepsilon_{\lambda}^i = \delta^{i'i}. \quad (4.147)$$

and after computing all this Dirac algebra we arrive at

$$\mathcal{N}_{1T} = 4k_1^+ k_2^+ \delta^{j'j} \left[1 + \frac{(k_2^+ - k_1^+)^2}{(q^+)^2} \right]. \quad (4.148)$$

$$\mathcal{N}_{2T} = 8k_1^+ k_2^+. \quad (4.149)$$

$$\mathcal{N}_{3T} = 0 \quad (4.150)$$

$$\mathcal{N}_{4T} = 0 \quad (4.151)$$

and also

$$\mathcal{N}_{1''T} = \frac{16k_1^+ k_2^+ (k_1^+ - k_2^+)}{q^+} \left[\delta^{j'l} \delta^{jm} - \delta^{jl} \delta^{j'm} \right] \quad (4.152)$$

$$\mathcal{N}_{2''T} = 0 \quad (4.153)$$

$$\mathcal{N}_{3''T} = 0 \quad (4.154)$$

$$\mathcal{N}_{4''T} = 0. \quad (4.155)$$

In the calculation of the contribution of Eq. (4.134) at cross section level, the Dirac algebra can be performed using the relations Eqs. (4.148), (4.149), (4.150) and (4.151), apart from the terms involving the longitudinal chromomagnetic background field \mathcal{F}_{lm} , which lead to the Dirac structures calculated in Eqs. (4.153), (4.154), (4.155), (4.152).

$$\begin{aligned}
\frac{d\sigma_{\gamma_T^* \rightarrow q_1 \bar{q}_2}}{d\text{P.S.}} \Big|_{\text{NEik corr.}}^{\text{in}} &= 2\pi\delta(k_1^+ + k_2^+ - q^+) N_c \alpha_{\text{em}} e_f^2 \left[1 + \left(\frac{k_2^+ - k_1^+}{q^+} \right)^2 \right] \\
&\times 2\text{Re} (i) \int_{\mathbf{z}, \mathbf{v}', \mathbf{w}'} e^{i\mathbf{k}_1 \cdot (\mathbf{v}' - \mathbf{z})} e^{i\mathbf{k}_2 \cdot (\mathbf{w}' - \mathbf{z})} \\
&\times \frac{(\mathbf{w}'^j - \mathbf{v}'^j)}{|\mathbf{w}' - \mathbf{v}'|} \bar{Q} K_1 (\bar{Q} |\mathbf{w}' - \mathbf{v}'|) \int_{-L^+/2}^{L^+/2} dz^+ \left\langle \frac{1}{N_c} \text{Tr} [\mathcal{U}_F(\mathbf{w}') \mathcal{U}_F^\dagger(\mathbf{v}') - 1] \right. \\
&\times \left. \left[\mathcal{U}_F\left(\frac{L^+}{2}, z^+; \mathbf{z}\right) \overleftrightarrow{\mathcal{D}}_{\mathbf{z}} \mathcal{U}_F^\dagger\left(\frac{L^+}{2}, z^+; \mathbf{z}\right) \right] \right\rangle, \tag{4.156}
\end{aligned}$$

$$\begin{aligned}
\frac{d\sigma_{\gamma_T^* \rightarrow q_1 \bar{q}_2}}{d\text{P.S.}} \Big|_{\text{NEik corr.}}^{L^+ \text{ phase}} &= 2\pi\delta(k_1^+ + k_2^+ - q^+) N_c \alpha_{\text{em}} e_f^2 \left[1 + \left(\frac{k_2^+ - k_1^+}{q^+} \right)^2 \right] \\
&\times 2\text{Re} (-i) \frac{L^+}{2} \int_{\mathbf{z}, \mathbf{v}', \mathbf{w}'} e^{i\mathbf{k}_1 \cdot (\mathbf{v}' - \mathbf{z})} e^{i\mathbf{k}_2 \cdot (\mathbf{w}' - \mathbf{z})} \\
&\times \frac{(\mathbf{w}'^j - \mathbf{v}'^j)}{|\mathbf{w}' - \mathbf{v}'|} \bar{Q} K_1 (\bar{Q} |\mathbf{w}' - \mathbf{v}'|) \left\langle \frac{1}{N_c} \text{Tr} [\mathcal{U}_F(\mathbf{w}') \mathcal{U}_F^\dagger(\mathbf{v}') - 1] \left[\mathcal{U}_F(\mathbf{z}) \overleftrightarrow{\mathcal{D}}_{\mathbf{z}} \mathcal{U}_F^\dagger(\mathbf{z}) \right] \right\rangle, \tag{4.157}
\end{aligned}$$

$$\begin{aligned}
\frac{d\sigma_{\gamma_T^* \rightarrow q_1 \bar{q}_2}}{d\text{P.S.}} \Big|_{\text{NEik corr.}}^{\text{dec. on } q} &= 2\pi\delta(k_1^+ + k_2^+ - q^+) N_c \frac{\alpha_{\text{em}}}{\pi} e_f^2 \frac{2k_2^+}{q^+} 2\text{Re} \int_{\mathbf{v}, \mathbf{v}', \mathbf{w}, \mathbf{w}'} e^{i\mathbf{k}_1 \cdot (\mathbf{v}' - \mathbf{v})} \\
&\times e^{i\mathbf{k}_2 \cdot (\mathbf{w}' - \mathbf{w})} \left\{ \left[\left(\frac{(\mathbf{k}_2^j - \mathbf{k}_1^j)}{2} + \frac{i}{2} \partial_{\mathbf{w}^j} \right) (Q_j^{(1)}(\mathbf{w}', \mathbf{v}', \mathbf{v}_*, \mathbf{w}) - d_j^{(1)}(\mathbf{v}_*, \mathbf{w})) \right. \right. \\
&- i (Q^{(2)}(\mathbf{w}', \mathbf{v}', \mathbf{v}_*, \mathbf{w}) - d^{(2)}(\mathbf{v}_*, \mathbf{w})) \left. \right] \\
&\times \left[\frac{1}{2} \left(1 + \left(\frac{k_2^+ - k_1^+}{q^+} \right)^2 \right) \frac{(\mathbf{w}' - \mathbf{v}') \cdot (\mathbf{w} - \mathbf{v})}{|\mathbf{w}' - \mathbf{v}'| |\mathbf{w} - \mathbf{v}|} \bar{Q}^2 K_1 (\bar{Q} |\mathbf{w}' - \mathbf{v}'|) K_1 (\bar{Q} |\mathbf{w} - \mathbf{v}|) \right. \\
&+ m^2 K_0 (\bar{Q} |\mathbf{w}' - \mathbf{v}'|) K_0 (\bar{Q} |\mathbf{w} - \mathbf{v}|) \left. \right] + \frac{(k_1^+ - k_2^+)}{q^+} \frac{(\mathbf{w}'^i - \mathbf{v}'^i)(\mathbf{w}^j - \mathbf{v}^j)}{|\mathbf{w}' - \mathbf{v}'| |\mathbf{w} - \mathbf{v}|} \\
&\times \bar{Q}^2 K_1 (\bar{Q} |\mathbf{w}' - \mathbf{v}'|) K_1 (\bar{Q} |\mathbf{w} - \mathbf{v}|) (Q_{ij}^{(3)}(\mathbf{w}', \mathbf{v}', \mathbf{v}_*, \mathbf{w}) - d_{ij}^{(3)}(\mathbf{v}_*, \mathbf{w})) \left. \right\}, \tag{4.158}
\end{aligned}$$

$$\begin{aligned}
 \left. \frac{d\sigma_{\gamma_T^* \rightarrow q_1 \bar{q}_2}}{d\text{P.S.}} \right|_{\text{NEik corr.}}^{\text{dec. on } \bar{q}} &= 2\pi\delta(k_1^+ + k_2^+ - q^+) N_c \frac{\alpha_{\text{em}}}{\pi} e_f^2 \frac{2k_1^+}{q^+} 2\text{Re} \int_{\mathbf{v}, \mathbf{v}', \mathbf{w}, \mathbf{w}'} \\
 &\times e^{i\mathbf{k}_1 \cdot (\mathbf{v}' - \mathbf{v})} e^{i\mathbf{k}_2 \cdot (\mathbf{w}' - \mathbf{w})} \left\{ \left[\frac{1}{2} \left[1 + \left(\frac{k_2^+ - k_1^+}{q^+} \right)^2 \right] \frac{(\mathbf{w}' - \mathbf{v}') \cdot (\mathbf{w} - \mathbf{v})}{|\mathbf{w}' - \mathbf{v}'| |\mathbf{w} - \mathbf{v}|} \bar{Q}^2 \right. \right. \\
 &\times \left. \left. \text{K}_1(\bar{Q} |\mathbf{w}' - \mathbf{v}'|) \text{K}_1(\bar{Q} |\mathbf{w} - \mathbf{v}|) + m^2 \text{K}_0(\bar{Q} |\mathbf{w}' - \mathbf{v}'|) \text{K}_0(\bar{Q} |\mathbf{w} - \mathbf{v}|) \right] \right. \\
 &\times \left\{ \left[-\frac{(\mathbf{k}_2^j - \mathbf{k}_1^j)}{2} + \frac{i}{2} \partial_{\mathbf{v}^j} \right] \left[Q_j^{(1)}(\mathbf{v}', \mathbf{w}', \mathbf{w}_*, \mathbf{v})^\dagger - d_j^{(1)}(\mathbf{w}_*, \mathbf{v})^\dagger \right] \right. \\
 &\left. \left. - i \left[Q^{(2)}(\mathbf{v}', \mathbf{w}', \mathbf{w}_*, \mathbf{v})^\dagger - d^{(2)}(\mathbf{w}_*, \mathbf{v})^\dagger \right] \right\} + \frac{(k_1^+ - k_2^+)}{q^+} \frac{(\mathbf{w}'^i - \mathbf{v}'^i)(\mathbf{w}^j - \mathbf{v}^j)}{|\mathbf{w}' - \mathbf{v}'| |\mathbf{w} - \mathbf{v}|} \right. \\
 &\left. \times \bar{Q}^2 \text{K}_1(\bar{Q} |\mathbf{w}' - \mathbf{v}'|) \text{K}_1(\bar{Q} |\mathbf{w} - \mathbf{v}|) \left[Q_{ij}^{(3)}(\mathbf{v}', \mathbf{w}', \mathbf{w}_*, \mathbf{v})^\dagger - d_{ij}^{(3)}(\mathbf{w}_*, \mathbf{v})^\dagger \right] \right\}. \tag{4.159}
 \end{aligned}$$

and finally

$$\begin{aligned}
 \left. \frac{d\sigma_{\gamma_T^* \rightarrow q_1 \bar{q}_2}}{d\text{P.S.}} \right|_{\text{NEik corr.}}^{\text{dyn. target}} &= 2\pi\delta(k_1^+ + k_2^+ - q^+) N_c \frac{\alpha_{\text{em}}}{\pi} e_f^2 \frac{k_1^+ k_2^+ (k_2^+ - k_1^+)}{(q^+)^3} \\
 &\times 2\text{Re} (-i) \int_{\mathbf{v}, \mathbf{v}', \mathbf{w}, \mathbf{w}'} e^{i\mathbf{k}_1 \cdot (\mathbf{v}' - \mathbf{v})} e^{i\mathbf{k}_2 \cdot (\mathbf{w}' - \mathbf{w})} \left[\tilde{Q}(\mathbf{w}', \mathbf{v}', \mathbf{v}_*, \mathbf{w}_*) - \tilde{d}(\mathbf{v}_*, \mathbf{w}_*) \right] \\
 &\times \left\{ \frac{1}{2} \left[1 + \left(\frac{k_2^+ - k_1^+}{q^+} \right)^2 \right] \frac{(\mathbf{w}' - \mathbf{v}') \cdot (\mathbf{w} - \mathbf{v})}{|\mathbf{w}' - \mathbf{v}'|} \right. \\
 &\times \bar{Q} \text{K}_1(\bar{Q} |\mathbf{w}' - \mathbf{v}'|) Q^2 \text{K}_0(\bar{Q} |\mathbf{w} - \mathbf{v}|) + m^2 Q^2 \text{K}_0(\bar{Q} |\mathbf{w}' - \mathbf{v}'|) \frac{|\mathbf{w} - \mathbf{v}|}{\bar{Q}} \\
 &\left. \times \text{K}_1(\bar{Q} |\mathbf{w} - \mathbf{v}|) + 2 \frac{(\mathbf{w}' - \mathbf{v}') \cdot (\mathbf{w} - \mathbf{v})}{|\mathbf{w}' - \mathbf{v}'| |\mathbf{w} - \mathbf{v}|} \bar{Q}^2 \text{K}_1(\bar{Q} |\mathbf{w}' - \mathbf{v}'|) \text{K}_1(\bar{Q} |\mathbf{w} - \mathbf{v}|) \right\}, \tag{4.160}
 \end{aligned}$$

4.4 Conclusions

To sum up, in this chapter we computed the DIS dijet production cross section at full next-to-eikonal accuracy in a dynamical gluon background field in the Color Glass Condensate framework. In order to achieve this level of accuracy we have relaxed all the eikonal assumptions and computed first the quark and antiquark propagators at full NEik accuracy in the gluon background field, and taking these results we computed the cross-section. This cross-section is computed for both polarizations of the photon, longitudinal and transverse.

The cross sections for both transverse and longitudinal photon are written as a generalized eikonal contribution and explicit NEik corrections. The generalized eikonal contribution includes the average z^- dependence of the background gluon

field at the amplitude level. Therefore, it goes beyond the strict eikonal approximation by including “+” - momentum exchange with the target. On the other hand, explicit NEik contributions are independent of this effect since it brings further power suppression at high energy.

Beyond the generalized eikonal approximation, the z^- dependence of the background field provides a new type of explicit NEik correction (Eq. (4.124) for longitudinal and Eq. (4.160) for transverse photon polarization) that encodes the relative z^- dependence of the quark and antiquark at amplitude level. This correction gives a new type of decorated dipole Eq. (4.120) and quadrupole Eq. (4.121) operators that include a derivative of the Wilson lines along the “-” light-cone direction.

5

Photon + jet production at next-to-eikonal accuracy

DISCLAIMER: The material presented in this Chapter is a work in-progress (Ref. [75] of this thesis) in collaboration with Tolga Altinoluk, Nestor Armesto and Guillaume Beuf. My contribution to this material can be summarized as follows. I have contributed to computation of the quark propagator from before to inside the medium at NEik accuracy. I have also contributed in the computation of the production cross section of photon+(quark jet) at partonic level. I have presented these results in the “DIS2023: XXX International Workshop on Deep-Inelastic Scattering and Related Subjects” (Michigan, USA in March-April 2023).

In this final chapter, we study photon + jet production in forward pA collisions at full next-to-eikonal accuracy in the gluon background field. We first compute the quark propagators that contribute to this process at NEik order.

5.1 Quark propagators at NEik accuracy

In order to compute the photon + jet production at NEik accuracy we need to consider all types of quark propagators contributing to this process and compute them at full NEik accuracy in the gluon background field. The first type of propagator that contributes to this process is the one where the quark traverses through the whole medium. This propagator was computed in the previous chapter (see Eq. (4.17)). In this process, we also need the quark propagator in vacuum as opposed to the previously discussed observables in chapters 3 and 4. Finally, in this process, we also get contribution from the quark propagator with one point inside and one part outside of the target. For this contribution we have two cases: one when the quark propagator starts before the medium and ends inside of it, and the other case where the quark propagator starts inside of the medium and ends after it.¹

The integrated quark propagator in vacuum is

¹Throughout this Chapter we take the following momenta configuration for all possible diagrams: p_0 is the incoming momenta of the quark and p_1 is the final momenta of the quark. The photon emitted has momentum p_2 and, k_0 and k'_0 are the momenta just before and just outside the medium, respectively. For the case of the quark propagating in the vacuum we keep a generic k_1 that we change accordingly to our diagrams later.

$$\tilde{S}_{F0}^q(z)_{\beta\alpha} = (\mathbf{1})_{\beta\alpha} \theta(k_1^+) e^{ik_1 \cdot z} \bar{u}(1) \gamma^+ \frac{(\not{k}_1 + m)}{(2k_1^+)} \quad (5.1)$$

Let us now show the propagator for the case when the quark starts inside the medium and ends after it. This kind of contribution has been derived already in Chapter 4. We can rewrite this propagator inserting our kinematics for this process, where $x^+ > L^+/2$ and $L^+/2 < z^+ < L^+/2$, thus from Eq.(4.26) one can write

$$S_F(x, z) \Big|_{\text{Eik.}}^{\text{IA}, q} = \int \frac{d^3 \underline{k}_1}{(2\pi)^3} \frac{\theta(k_1^+)}{2k_1^+} e^{-ix \cdot \check{k}_1} \times (\not{k}_1 + m) \mathcal{U}_F(x^+, z^+; \mathbf{z}) \left[1 - \frac{\gamma^+ \gamma^i}{2k_1^+} i \overleftrightarrow{\mathcal{D}}_{\mathbf{z}^i} \right] e^{iz^- k_1^+} e^{-iz \cdot \mathbf{k}_1}. \quad (5.2)$$

The second case we consider, is when the quark starts before the medium and ends inside of it. We refer to this contribution as 'before-in'. This corresponds to $y^+ < -L^+/2$ and z^+ belongs to the support $[-L^+/2, L^+/2]$. Therefore, we use Eq. (2.16), where the instantaneous term vanishes and we neglect the phase factor $e^{-iz^+ \check{k}'^-}$. The result is given by

$$S_F(z, y)_{\beta\alpha_0} \Big|_{\text{pure } \mathcal{A}^-, \text{Eik.}}^{\text{BI}, q} = \int \frac{d^3 \underline{k}'}{(2\pi)^3} \int \frac{d^3 \underline{k}}{(2\pi)^3} \int dv^- e^{iv^-(k'^+ - k^+)} e^{iy \cdot \check{k}} e^{-iz^- k'^+ + iz \cdot \mathbf{k}'} \times \frac{(\not{k}' + m)}{2k'^+} \gamma^+ \frac{(\not{k} + m)}{2k^+} \int d^2 \mathbf{v} e^{-iv \cdot (\mathbf{k}' - \mathbf{k})} \times \theta(k'^+) \theta(k^+) \theta(y^+ - z^+) \mathcal{U}_F(z^+, -L^+/2; \mathbf{v}, v^-)_{\beta\alpha_0} \quad (5.3)$$

simplifying and re-expressing the Dirac structure, one obtains

$$S_F(z, y)_{\beta\alpha_0} \Big|_{\text{pure } \mathcal{A}^-, \text{Eik.}}^{\text{BI}, q} = \int \frac{d^3 \underline{k}'}{(2\pi)^3} \int \frac{d^3 \underline{k}}{(2\pi)^3} \frac{\theta(k'^+)}{2k^+} \theta(y^+ - z^+) \int dv^- e^{iv^-(k'^+ - k^+)} \times e^{iy \cdot \check{k}} e^{-iz^- k'^+ + iz \cdot \mathbf{k}'} \int d^2 \mathbf{v} e^{-iv \cdot (\mathbf{k}' - \mathbf{k})} \left[1 + \frac{\gamma^+ \gamma^- i \overleftrightarrow{\partial}_{v^-}}{2k'^+} - \frac{\gamma^+ \gamma^i i \overleftrightarrow{\partial}_{\mathbf{v}^i}}{2k'^+} \right] \times (\not{k} + m) \mathcal{U}_F(z^+, \frac{-L^+}{2}; \mathbf{v}, v^-)_{\beta\alpha_0} \quad (5.4)$$

Here the v^- dependence of the Wilson line can be dropped and the derivative $\partial_{v^-} \mathcal{U}_F(z^+, \frac{-L^+}{2}; \mathbf{v}, v^-)$ vanishes. It is now possible to perform the integral over v^- in addition to the integral over \mathbf{k}' . We thus get

$$S_F(z, y)_{\beta\alpha_0} \Big|_{\text{pure } \mathcal{A}^-, \text{Eik.}}^{\text{BI}, q} = \int \frac{d^3 \underline{k}}{(2\pi)^3} \frac{\theta(k^+)}{2k^+} \theta(y^+ - z^+) e^{iy \cdot \check{k}} e^{-iz^- k^+} e^{iz \cdot \mathbf{k}} \left[1 - \frac{\gamma^+ \gamma^i i \overleftrightarrow{\partial}_{\mathbf{z}^i}}{2k^+} \right] \times (\not{k} + m) \mathcal{U}_F(z^+, \frac{-L^+}{2}; \mathbf{z})_{\beta\alpha_0} \quad (5.5)$$

In addition to this pure \mathcal{A}^- contribution, the quark propagator in the before-after kinematics also receives a next-to-eikonal contribution from a single interaction with the transverse component of the background field. This contribution takes the following final form:

$$\delta S_F(z, y)_{\beta\alpha_0} \Big|_{\text{single } \mathcal{A}_\perp}^{BI} = \int \frac{d^3k}{(2\pi)^3} \frac{\theta(k^+)}{2k^+} \theta(y^+ - z^+) \frac{\gamma^+ \gamma^j}{2k^+} e^{-ik^+ z^-} [g t \mathcal{A}_j(z)] \times e^{iy \cdot \check{k}} e^{izk} (\check{k} + m) \mathcal{U}_F(z^+, \frac{-L^+}{2}; \mathbf{z}) \quad (5.6)$$

Thus, we get for the quark propagator in the before-inside kinematics

$$S_F(z, y)_{\beta\alpha_0} \Big|_{\text{Eik.}}^{BI, q} = \int \frac{d^3k}{(2\pi)^3} \frac{\theta(k^+)}{2k^+} \theta(y^+ - z^+) e^{iy \cdot \check{k}} e^{-iz^- k^+} e^{izk} \left[1 - \frac{\gamma^+ \gamma^i \vec{D}_{zi}}{2k^+} \right] \times (\check{k} + m) \mathcal{U}_F(z^+, \frac{-L^+}{2}; \mathbf{z})_{\beta\alpha_0} \quad (5.7)$$

5.2 S-matrix element

In the previous section we computed the missing propagator corresponding to the before-inside kinematics, as well as we re-derived the quark propagator for inside-after in order to have all propagators with the same notation. We now have all propagators that are needed in order to compute the photon-jet production at NEik order. The next step is computing the S-matrix elements and amplitude for each case. We use the general expression for the S-matrix element in this process

$$S_{q_1 \gamma_2 \leftarrow q_0} = \lim_{y^+ \rightarrow -\infty} \int d^2\mathbf{y} \int dy^- e^{-iy \cdot \check{p}_0} \lim_{x^+ \rightarrow +\infty} \int d^2\mathbf{x} \int dx^- e^{+ix \cdot \check{p}_1} \times (-i) e e_f \int d^4z e^{+iz \cdot \check{p}_2} \bar{u}(1) \gamma^+ [S_F(x, z)]_{\alpha_1\beta} \not{\epsilon}_\lambda(\underline{p}_2)^* [S_F(z, y)]_{\beta\alpha_0} \gamma^+ u(0) \quad (5.8)$$

5.2.1 Photon emission after the medium

In this case, the propagator $[S_F(x, z)]_{\alpha_1\beta}$ is the free propagator of the quark with no interaction with the medium, and $[S_F(z, y)]_{\beta\alpha_0}$ is the full NEik quark propagator traversing through the whole medium (see Fig .5.1). Introducing both expressions into Eq.(5.8) we get:

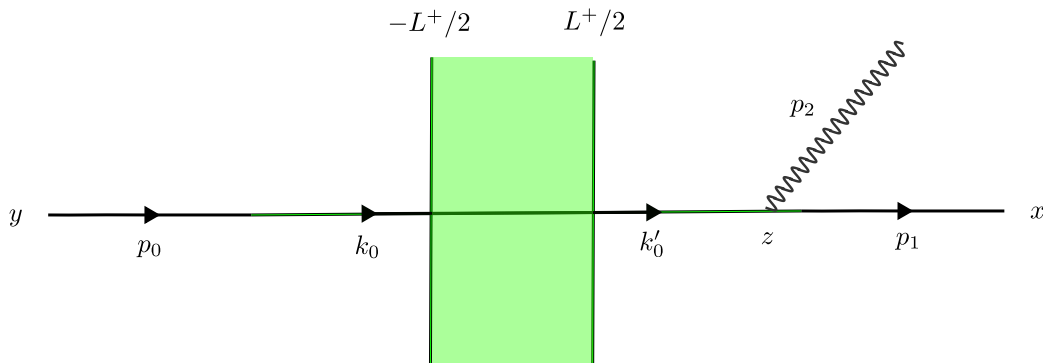


FIGURE 5.1: Diagrammatical representation of the photon emission after the medium

$$\begin{aligned}
S_{q_1 \gamma_2 \leftarrow q_0}^{\text{aft}} &= \lim_{y^+ \rightarrow -\infty} (-i) e e_f \epsilon_\mu^\lambda(p_2)^* \int d^2\mathbf{y} \int dy^- \int d^4z \int \frac{d^3\mathbf{k}_0}{(2\pi)^3} \frac{d^3\mathbf{k}'_0}{(2\pi)^3} (\mathbf{1})_{\alpha_1\beta} \theta(p_1^+) \\
&\times \theta(k_0^+) \theta(k_0'^+) e^{iz \cdot \check{p}_2} e^{-iz \cdot \check{k}'_0} e^{i\check{p}_1 \cdot z} \int dv^- e^{iv^-(k_0^+ - k_0'^+)} \int d^2\mathbf{v} e^{-iv \cdot (\mathbf{k}'_0 - \mathbf{k}_0)} e^{-iy^-(p_0^+ - k_0^+)} e^{iy \cdot (\mathbf{p}_0 - \mathbf{k}_0)} \\
&\times e^{-iy^+(\check{p}_0^- - \check{k}_0^-)} \bar{u}(1) \gamma^+ \frac{(\check{p}_1 + m)}{(2p_1^+)} \gamma^\mu \frac{(\check{k}'_0 + m)}{2k_0'^+} \gamma^+ \left\{ \mathcal{U}_F\left(\frac{L^+}{2}, -\frac{L^+}{2}; \mathbf{v}, v^-\right) \right. \\
&- \frac{(\mathbf{k}'_0^j + \mathbf{k}_0^j)}{2(k_0'^+ + k_0^+)} \int_{-\frac{L^+}{2}}^{\frac{L^+}{2}} dv^+ \left[\mathcal{U}_F\left(\frac{L^+}{2}, v^+; \mathbf{v}, v^-\right) \overleftarrow{\mathcal{D}}_{\mathbf{v}j} \mathcal{U}_F\left(v^+, -\frac{L^+}{2}; \mathbf{v}, v^-\right) \right] \\
&- \frac{i}{(k_0^+ + k_0'^+)} \int_{-\frac{L^+}{2}}^{\frac{L^+}{2}} dv^+ \left[\mathcal{U}_F\left(\frac{L^+}{2}, v^+; \mathbf{v}, v^-\right) \overleftarrow{\mathcal{D}}_{\mathbf{v}j} \overrightarrow{\mathcal{D}}_{\mathbf{v}j} \mathcal{U}_F\left(v^+, -\frac{L^+}{2}; \mathbf{v}, v^-\right) \right] \\
&\left. + \frac{[\gamma^i, \gamma^j]}{4(k_0^+ + k_0'^+)} \int_{-\frac{L^+}{2}}^{\frac{L^+}{2}} dv^+ \mathcal{U}_F\left(\frac{L^+}{2}, v^+; \mathbf{v}, v^-\right) g t \cdot \mathcal{F}_{ij}(v) \mathcal{U}_F\left(v^+, -\frac{L^+}{2}; \mathbf{v}, v^-\right) \right\}_{\beta\alpha_0} \\
&\times \frac{(\check{k}'_0 + m)}{2k_0'^+} \gamma^+ u(0) \tag{5.9}
\end{aligned}$$

Simplifying the Dirac algebra with

$$\begin{aligned}
\bar{u}(1) \gamma^+ (\check{p}_1 + m) &= \bar{u}(1) 2p_1^+ \\
\gamma^+ (\check{k}'_0 + m) \gamma^+ &= 2k_0'^+ \gamma^+ \tag{5.10}
\end{aligned}$$

and integrating over y^- and \mathbf{y} first, then over k_0 and finally performing the integrals over \mathbf{z}, z^- , we arrive to

$$\begin{aligned}
S_{q_1 \gamma_2 \leftarrow q_0}^{\text{aft}} &= (-i) e e_f \epsilon_\mu^\lambda(p_2)^* \int_{L^+/2}^{+\infty} dz^+ \int \frac{d^3\mathbf{k}'_0}{(2\pi)^3} (\mathbf{1})_{\alpha_1\beta} \theta(p_1^+) \theta(k_0'^+) \theta(p_0^+) \\
&\times (2\pi)^2 \delta^2(\mathbf{p}_1 + \mathbf{p}_2 - \mathbf{k}'_0) (2\pi) \delta(p_1^+ + p_2^+ - k_0'^+) \int dv^- e^{iv^-(k_0'^+ - p_0^+)} \int d^2\mathbf{v} e^{-iv \cdot (\mathbf{k}'_0 - \mathbf{p}_0)} \\
&\times e^{iz^+ \cdot (\check{p}_1^- + \check{p}_2^- - \check{k}'_0^-)} \bar{u}(1) \gamma^\mu \frac{(\check{k}'_0 + m)}{2k_0'^+} \gamma^+ \left\{ \mathcal{U}_F\left(\frac{L^+}{2}, -\frac{L^+}{2}; \mathbf{v}, v^-\right) + \frac{1}{(p_0^+ + k_0'^+)} \right. \\
&\times \int_{-\frac{L^+}{2}}^{\frac{L^+}{2}} dv^+ \mathcal{U}_F\left(\frac{L^+}{2}, v^+; \mathbf{v}, v^-\right) \left[\frac{[\gamma^i, \gamma^j]}{4} g t \cdot \mathcal{F}_{ij}(v) - \frac{(\mathbf{p}_0^j + \mathbf{k}'_0^j)}{2} \overleftarrow{\mathcal{D}}_{\mathbf{v}j} - i \overleftarrow{\mathcal{D}}_{\mathbf{v}j} \overrightarrow{\mathcal{D}}_{\mathbf{v}j} \right] \\
&\left. \times \mathcal{U}_F\left(v^+, -\frac{L^+}{2}; \mathbf{v}, v^-\right) \right\}_{\beta\alpha_0} u(0) \tag{5.11}
\end{aligned}$$

Upon integration over k_0' using the delta functions and we can perform the z^+ integral

$$\int_{L^+/2}^{+\infty} dz^+ e^{iz^+ \cdot \left(\check{p}_1^- + \check{p}_2^- - \frac{(\mathbf{p}_1 + \mathbf{p}_2)^2 + m^2}{2(p_1^+ + p_2^+)} \right)} = i \left(\check{p}_1^- + \check{p}_2^- - \frac{(\mathbf{p}_1 + \mathbf{p}_2)^2 + m^2}{2(p_1^+ + p_2^+)} \right)^{-1} - \frac{L^+}{2} \tag{5.12}$$

which leads to

$$\begin{aligned}
S_{q_1 \gamma_2 \leftarrow q_0}^{\text{aft}} &= (-i) e e_f \epsilon_\mu^\lambda(p_2)^* (\mathbf{1})_{\alpha_1 \beta} \theta(p_1^+) \theta(p_1^+ + p_2^+) \theta(p_0^+) \\
&\times \left[i \left(\check{p}_1^- + \check{p}_2^- - \frac{(\mathbf{p}_1 + \mathbf{p}_2)^2 + m^2}{2(p_1^+ + p_2^+)} \right)^{-1} - \frac{L^+}{2} \right] \\
&\int d v^- e^{i v^- (p_1^+ + p_2^+ - p_0^+)} \int d^2 \mathbf{v} e^{-i \mathbf{v} \cdot (\mathbf{p}_1 + \mathbf{p}_2 - \mathbf{p}_0)} \bar{u}(1) \gamma^\mu \frac{(\check{p}_1 + \check{p}_2 + m)}{2(p_1^+ + p_2^+)} \gamma^+ \\
&\times \left\{ \mathcal{U}_F \left(\frac{L^+}{2}, -\frac{L^+}{2}; \mathbf{v}, v^- \right) + \frac{1}{(p_0^+ + p_1^+ + p_2^+)} \right. \\
&\times \int_{-\frac{L^+}{2}}^{\frac{L^+}{2}} d v^+ \mathcal{U}_F \left(\frac{L^+}{2}, v^+; \mathbf{v}, v^- \right) \left[\frac{[\gamma^i, \gamma^j]}{4} g t \cdot \mathcal{F}_{ij}(v) - \frac{(\mathbf{p}_0^j + \mathbf{p}_1^j + \mathbf{p}_2^j)}{2} \overleftrightarrow{\mathcal{D}}_{\mathbf{v}^j} - i \overleftarrow{\mathcal{D}}_{\mathbf{v}^j} \overrightarrow{\mathcal{D}}_{\mathbf{v}^j} \right] \\
&\times \left. \mathcal{U}_F \left(v^+, -\frac{L^+}{2}; \mathbf{v}, v^- \right) \right\} u(0)_{\beta \alpha_0} \quad (5.13)
\end{aligned}$$

The Dirac algebra can be performed in two different manners where we can choose for our convenience that each of the resulting forms multiplies different contributions. First, let us perform the Dirac algebra that will multiply the first term in Eq.(5.12):

$$\begin{aligned}
&\bar{u}(1) \not{\epsilon}_\lambda(p_2) (\check{p}_1 + \check{p}_2 + m) \gamma^+ \\
&= \bar{u}(1) (\{ \not{\epsilon}_\lambda(p_2), \check{p}_1 \} + \{ \not{\epsilon}_\lambda(p_2), \check{p}_2 \} - (\check{p}_1 - m) \not{\epsilon}_\lambda(p_2) - \check{p}_2 \not{\epsilon}_\lambda(p_2)) \gamma^+ \\
&= 2(p_1 \cdot \epsilon_\lambda(p_2)) \bar{u}(1) \gamma^+ - \bar{u}(1) \check{p}_2 \not{\epsilon}_\lambda(p_2) \gamma^+ \\
&= 2(p_1 \cdot \epsilon_\lambda(p_2)) \bar{u}(1) \gamma^+ + \bar{u}(1) \left(\check{p}_2 - \frac{p_2^+}{p_1^+} (\check{p}_1 - m) \right) \gamma^+ \not{\epsilon}_\lambda(p_2) \\
&= 2(p_1 \cdot \epsilon_\lambda(p_2)) \bar{u}(1) \gamma^+ + \bar{u}(1) \left(- \left(p_2^j - \frac{p_2^+}{p_1^+} p_1^j \right) \gamma^j + \frac{p_2^+}{p_1^+} m \right) \gamma^+ \not{\epsilon}_\lambda(p_2) \\
&= \epsilon_\lambda^i(p_2) \bar{u}(1) \gamma^+ \left(\left(p_2^j - \frac{p_2^+}{p_1^+} p_1^j \right) \left(2 \frac{p_1^+}{p_2^+} \delta^{ij} - \gamma^j \gamma^i \right) - \frac{p_2^+}{p_1^+} m \gamma^i \right) \quad (5.14)
\end{aligned}$$

The second form we can find from the Dirac algebra corresponds to the second term in Eq.(5.12). At NEik accuracy, this term $L^+/2$, multiplies only the generalized eikonal term. The corresponding Dirac structure is

$$\begin{aligned}
&\bar{u}(1) \not{\epsilon}_\lambda(p_2) (\check{p}_1 + \check{p}_2 + m) \gamma^+ u(0) \\
&= \bar{u}(1) \not{\epsilon}_\lambda(p_2) (\check{p}_1 + \check{p}_2 - \check{p}_0 + m + \check{p}_0) \gamma^+ u(0) \\
&= \bar{u}(1) \not{\epsilon}_\lambda(p_2) [(p_1^+ + p_2^+ - p_0^+) \gamma^- \gamma^+ - (p_1^i + p_2^i - p_0^i) \gamma^i \gamma^+ + 2p_0^+] u(0) \\
&= \bar{u}(1) \not{\epsilon}_\lambda(p_2) [2p_0^+ + i \overrightarrow{\partial}_{v^-} \gamma^- \gamma^+ + i \overrightarrow{\partial}_{\mathbf{v}} \gamma^i \gamma^+] u(0) \quad (5.15)
\end{aligned}$$

Plugging now both Dirac structures multiplying their corresponding terms that come from the z^+ integration inside Eq. (5.13) and further simplify ignoring the v^- dependence on the NEik terms. When integrating over v^- we get $2\pi \delta(p_1^+ + p_2^+ - p_0^+)$ and we can separate the expression in generalized eikonal and NEik terms as

$$\begin{aligned}
S_{q_1 \gamma_2 \leftarrow q_0}^{\text{aft}} &= (-i) e e_f \epsilon_\lambda^k(p_2) (\mathbf{1})_{\alpha_1 \beta} \theta(p_1^+) \theta(p_0^+) \int d^2 \mathbf{v} e^{-i \mathbf{v} \cdot (\mathbf{p}_1 + \mathbf{p}_2 - \mathbf{p}_0)} \bar{u}(1) \\
&\times \left[i \Delta \gamma^+ \left(\left(p_2^l - \frac{p_2^+}{p_1^+} p_1^l \right) \left(2 \frac{p_1^+}{p_2^+} \delta^{kl} - \gamma^l \gamma^k \right) - \frac{p_2^+}{p_1^+} m \gamma^k \right) \left\{ \frac{1}{2(p_1^+ + p_2^+)} \right. \right. \\
&\times \int d v^- e^{i v^- (p_1^+ + p_2^+ - p_0^+)} \mathcal{U}_F \left(\frac{L^+}{2}, -\frac{L^+}{2}; \mathbf{v}, v^- \right) + \frac{2\pi \delta(p_1^+ + p_2^+ - p_0^+)}{(2p_0^+)^2} \\
&\times \int_{-\frac{L^+}{2}}^{\frac{L^+}{2}} d v^+ \mathcal{U}_F \left(\frac{L^+}{2}, v^+; \mathbf{v} \right) \left[\frac{[\gamma^i, \gamma^j]}{4} g t \cdot \mathcal{F}_{ij}(v) - \frac{(\mathbf{p}_0^j + \mathbf{p}_1^j + \mathbf{p}_2^j)}{2} \overleftrightarrow{\mathcal{D}}_{\mathbf{v}j} - i \overleftrightarrow{\mathcal{D}}_{\mathbf{v}j} \overrightarrow{\mathcal{D}}_{\mathbf{v}j} \right] \\
&\times \left. \mathcal{U}_F \left(v^+, -\frac{L^+}{2}; \mathbf{v} \right) \right\}_{\beta \alpha_0} - 2\pi \delta(p_1^+ + p_2^+ - p_0^+) \gamma^k \left[1 + i \overrightarrow{\partial}_{\mathbf{v}} \frac{\gamma^i \gamma^+}{2p_0^+} \right] \frac{L^+}{2} \mathcal{U}_F \left(\frac{L^+}{2}, -\frac{L^+}{2}; \mathbf{v} \right) \Big] u(0)
\end{aligned} \tag{5.16}$$

Simplifying the notation we introduced $\Delta = \left(\check{p}_1^- + \check{p}_2^- - \frac{(\mathbf{p}_1 + \mathbf{p}_2)^2 + m^2}{2(p_1^+ + p_2^+)} \right)^{-1}$.

5.2.2 Photon emission before the medium

The diagram corresponding to this case is shown in Fig. 5.2 In this case, the propagator $[S_F(z, y)]_{\beta \alpha_0}$ is the free propagator of the quark with no interaction with the medium and $[S_F(x, z)]_{\alpha_1 \beta}$ corresponds to the full NEik expression for a quark going through the whole medium. Introducing both expressions into Eq.(5.8)

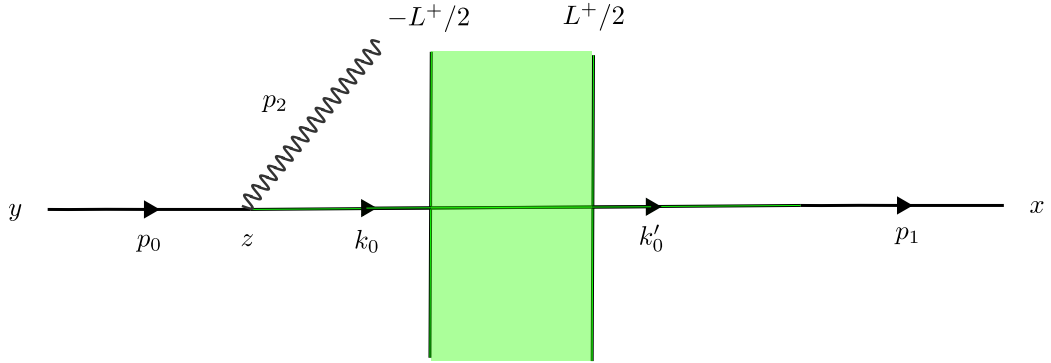


FIGURE 5.2: Diagrammatical representation of the photon emission before the medium

$$\begin{aligned}
S_{q_1 \gamma_2 \leftarrow q_0}^{\text{bef}} &= \lim_{x^+ \rightarrow +\infty} (-i) e e_f \epsilon_\mu^\lambda(p_2)^* \int d^2 \mathbf{x} \int dx^- \int_{-\infty}^{-L/2} dz^+ \int d^2 \mathbf{z} \int dz^- \int \frac{d^3 \underline{k}_0}{(2\pi)^3} \frac{d^3 \underline{k}'_0}{(2\pi)^3} \\
&\times (\mathbf{1})_{\beta\alpha_0} \theta(p_0^+) \theta(k_0^+) \theta(k_0'^+) e^{iz \cdot \check{p}_2} e^{-ix \cdot \check{k}'_0} e^{i\check{p}_1 \cdot x} e^{-iz \cdot \check{p}_0} e^{iz \cdot \check{k}_0} \int d^2 \mathbf{v}^- e^{iv^-(k_0'^+ - k_0^+)} \int d^2 \mathbf{v} e^{-iv \cdot (k_0' - \mathbf{k}_0)} \\
&\times \bar{u}(1) \gamma^+ \frac{(\check{k}'_0 + m)}{2k_0'^+} \gamma^+ \left\{ \mathcal{U}_F \left(\frac{L^+}{2}, -\frac{L^+}{2}; \mathbf{v}, v^- \right) \right. \\
&- \frac{(\mathbf{k}'_0^j + \mathbf{k}_0^j)}{2(k_0'^+ + k_0^+)} \int_{-\frac{L^+}{2}}^{\frac{L^+}{2}} dv^+ \left[\mathcal{U}_F \left(\frac{L^+}{2}, v^+; \mathbf{v}, v^- \right) \overleftarrow{\mathcal{D}}_{\mathbf{v}j} \mathcal{U}_F \left(v^+, -\frac{L^+}{2}; \mathbf{v}, v^- \right) \right] \\
&- \frac{i}{(k_0^+ + k_0'^+)} \int_{-\frac{L^+}{2}}^{\frac{L^+}{2}} dv^+ \left[\mathcal{U}_F \left(\frac{L^+}{2}, v^+; \mathbf{v}, v^- \right) \overleftarrow{\mathcal{D}}_{\mathbf{v}j} \overrightarrow{\mathcal{D}}_{\mathbf{v}j} \mathcal{U}_F \left(v^+, -\frac{L^+}{2}; \mathbf{v}, v^- \right) \right] \\
&+ \left. \frac{[\gamma^i, \gamma^j]}{4(k_0^+ + k_0'^+)} \int_{-\frac{L^+}{2}}^{\frac{L^+}{2}} dv^+ \mathcal{U}_F \left(\frac{L^+}{2}, v^+; \mathbf{v}, v^- \right) g t \cdot \mathcal{F}_{ij}(v) \mathcal{U}_F \left(v^+, -\frac{L^+}{2}; \mathbf{v}, v^- \right) \right\} \\
&\times \frac{(\check{k}'_0 + m)}{(2k_0'^+)} \gamma^\mu \frac{(\check{p}'_0 + m)}{2p_0^+} \gamma^+ u(0) \tag{5.17}
\end{aligned}$$

We integrate over x^- and \mathbf{x} and then over \mathbf{k}'_0 and $k_0'^+$. Integrating also over z^- and \mathbf{z} we arrive at

$$\begin{aligned}
S_{q_1 \gamma_2 \leftarrow q_0}^{\text{bef}} &= (-i) e e_f \epsilon_\mu^\lambda(p_2)^* \int_{-\infty}^{-L/2} dz^+ \int \frac{d^3 \underline{k}_0}{(2\pi)^3} (\mathbf{1})_{\beta\alpha_0} \theta(p_0^+) \theta(p_1^+) \theta(k_0^+) \\
&\times (2\pi)^2 \delta^2(\mathbf{p}_2 - \mathbf{p}_0 + \mathbf{k}_0) 2\pi \delta(p_2^+ - p_0^+ + k_0^+) e^{iz \cdot (\check{k}_0^- + \check{p}_2^- - \check{p}_0^-)} \int d^2 \mathbf{v}^- e^{iv^-(p_1^+ - k_0^+)} \\
&\times \int d^2 \mathbf{v} e^{-iv \cdot (\mathbf{p}_1 - \mathbf{k}_0)} \bar{u}(1) \gamma^+ \left\{ \mathcal{U}_F \left(\frac{L^+}{2}, -\frac{L^+}{2}; \mathbf{v}, v^- \right) + \frac{1}{(p_1^+ + k_0^+)} \right. \\
&\times \int_{-\frac{L^+}{2}}^{\frac{L^+}{2}} dv^+ \mathcal{U}_F \left(\frac{L^+}{2}, v^+; \mathbf{v}, v^- \right) \left[\frac{[\gamma^i, \gamma^j]}{4} g t \cdot \mathcal{F}_{ij}(v) - \frac{(\mathbf{p}_1^j + \mathbf{k}_0^j)}{2} \overleftarrow{\mathcal{D}}_{\mathbf{v}j} - i \overleftarrow{\mathcal{D}}_{\mathbf{v}j} \overrightarrow{\mathcal{D}}_{\mathbf{v}j} \right] \\
&\times \left. \mathcal{U}_F \left(v^+, -\frac{L^+}{2}; \mathbf{v}, v^- \right) \right\}_{\beta\alpha_0} \frac{(\check{k}'_0 + m)}{(2k_0'^+)} \gamma^\mu \frac{(\check{p}'_0 + m)}{2p_0^+} \gamma^+ u(0) \tag{5.18}
\end{aligned}$$

Simplifying the Dirac algebra as

$$(\check{p}'_0 + m) \gamma^+ u(0) = 2p_0^+ u(0) \tag{5.19}$$

performing now the integrals over k_0 we get

$$\begin{aligned}
S_{q_1 \gamma_2 \leftarrow q_0}^{\text{bef}} &= (-i) e e_f \epsilon_\mu^\lambda(p_2)^* \int_{-\infty}^{-L/2} dz^+ (\mathbf{1})_{\beta\alpha_0} \theta(p_0^+) \theta(p_1^+) \theta(p_0^+ - p_2^+) \\
&\times e^{iz^+ \cdot \left(\frac{(\mathbf{p}_0 - \mathbf{p}_2)^2 + m^2}{2(p_0^+ - p_2^+)} + \check{p}_2^- - \check{p}_0^- \right)} \int dv^- e^{iv^-(p_1^+ - p_0^+ + p_2^+)} \int d^2\mathbf{v} e^{-iv \cdot (\mathbf{p}_1 - \mathbf{p}_0 + \mathbf{p}_2)} \bar{u}(1) \\
&\times \left\{ \mathcal{U}_F\left(\frac{L^+}{2}, -\frac{L^+}{2}; \mathbf{v}, v^-\right) + \frac{1}{(p_1^+ + p_0^+ - p_2^+)} \int_{-\frac{L^+}{2}}^{\frac{L^+}{2}} dv^+ \mathcal{U}_F\left(\frac{L^+}{2}, v^+; \mathbf{v}, v^-\right) \right. \\
&\times \left[\frac{[\gamma^i, \gamma^j]}{4} g t \cdot \mathcal{F}_{ij}(v) - \frac{(\mathbf{p}_1^j + \mathbf{p}_0^j - \mathbf{p}_2^j)}{2} \overleftrightarrow{\mathcal{D}}_{\mathbf{v}j} - i \overleftarrow{\mathcal{D}}_{\mathbf{v}j} \overrightarrow{\mathcal{D}}_{\mathbf{v}j} \right] \\
&\times \left. \mathcal{U}_F\left(v^+, -\frac{L^+}{2}; \mathbf{v}, v^-\right) \right\}_{\beta\alpha_0} \gamma^+ \frac{(\check{p}_0 - \check{p}_2 + m)}{2(p_0^+ - p_2^+)} \gamma^\mu u(0) \tag{5.20}
\end{aligned}$$

now the z^+ integral becomes

$$\int_{-\infty}^{-L^+/2} dz^+ e^{iz^+ \cdot \left(\frac{(\mathbf{p}_0 - \mathbf{p}_2)^2 + m^2}{2(p_0^+ - p_2^+)} + \check{p}_2^- - \check{p}_0^- \right)} = i \left(\check{p}_0^- - \check{p}_2^- - \frac{(\mathbf{p}_0 - \mathbf{p}_2)^2 + m^2}{2(p_0^+ - p_2^+)} \right)^{-1} - \frac{L^+}{2} \tag{5.21}$$

We proceed in the same manner as in the previous section, and we rewrite the Dirac structure in two different manners depending on which term they multiply from Eq.(5.21). The Dirac structure that multiplies the first term can be rewritten as:

$$\begin{aligned}
&\gamma^+ (\check{p}_0 - \check{p}_2 + m) \not{\epsilon}_\lambda(p_2) u(0) \\
&= \gamma^+ (\{ \not{\epsilon}_\lambda(p_2), \check{p}_0 \} - \{ \not{\epsilon}_\lambda(p_2), \check{p}_2 \} - \not{\epsilon}_\lambda(p_2) (\check{p}_1 - m) + \not{\epsilon}_\lambda(p_2) \check{p}_2) u(0) \\
&= 2(\epsilon_\lambda(p_2) \cdot p_0) \gamma^+ u(0) + \gamma^+ \not{\epsilon}_\lambda(p_2) \check{p}_2 u(0) \\
&= 2(\epsilon_\lambda(p_2) \cdot p_0) \gamma^+ u(0) + \not{\epsilon}_\lambda(p_2) \gamma^+ \left(-\check{p}_2 + \frac{p_2^+}{p_0^+} (\check{p}_0 - m) \right) u(0) \\
&= 2(\epsilon_\lambda(p_2) \cdot p_0) \gamma^+ u(0) + \not{\epsilon}_\lambda(p_2) \gamma^+ \left(\left(p_2^j - \frac{p_2^+}{p_0^+} p_0^j \right) \gamma^j - \frac{p_2^+}{p_0^+} m \right) u(0) \\
&= \epsilon_\lambda^i(p_2) \gamma^+ \left(\left(p_2^j - \frac{p_2^+}{p_0^+} p_0^j \right) \left(2 \frac{p_0^+}{p_2^+} \delta^{ij} - \gamma^i \gamma^j \right) + \frac{p_2^+}{p_0^+} m \gamma^i \right) u(0) \tag{5.22}
\end{aligned}$$

The second term in Eq.(5.21) will be multiplied by the Dirac structure rewritten in a different, more convenient way for this term. The generalized eikonal term is the only one that gives contribution at NEik accuracy multiplying the $L^+/2$ term. The Dirac structure in this case is written as follows

$$\bar{u}(1) \gamma^+ (\check{p}_0 - \check{p}_2 + m) \not{\epsilon}_\lambda(p_2) u(0) = \bar{u}(1) (2p_1^+ - i \overrightarrow{\partial}_{v^-} \gamma^+ \gamma^- - i \overrightarrow{\partial}_{\mathbf{v}} \gamma^+ \gamma^i) \not{\epsilon}_\lambda(p_2) u(0) \tag{5.23}$$

Ignoring the v^- dependence in all the NEik terms and also simplifying notation with $\Delta' = \left(\check{p}_0^- - \check{p}_2^- - \frac{(\mathbf{p}_0 - \mathbf{p}_2)^2 + m^2}{2(p_0^+ - p_2^+)} \right)^{-1}$ we rewrite

$$\begin{aligned}
S_{q_1 \gamma_2 \leftarrow q_0}^{\text{bef}} &= (-i) e e_f \epsilon_\lambda^k(p_2) (\mathbf{1})_{\beta\alpha_0} \theta(p_0^+) \theta(p_1^+) \int d^2\mathbf{v} e^{-i\mathbf{v}\cdot(\mathbf{p}_1 - \mathbf{p}_0 + \mathbf{p}_2)} \bar{u}(1) \\
&\times \left[i\Delta' \left\{ \frac{1}{2(p_0^+ - p_2^+)} \int dv^- e^{iv^-(p_1^+ - p_0^+ + p_2^+)} \mathcal{U}_F\left(\frac{L^+}{2}, -\frac{L^+}{2}; \mathbf{v}, v^-\right) + \frac{2\pi\delta(p_1^+ - p_0^+ + p_2^+)}{(2p_1^+)^2} \right. \right. \\
&\times \int_{-\frac{L^+}{2}}^{\frac{L^+}{2}} dv^+ \mathcal{U}_F\left(\frac{L^+}{2}, v^+; \mathbf{v}\right) \left[\frac{[\gamma^i, \gamma^j]}{4} g t \cdot \mathcal{F}_{ij}(v) - \frac{(\mathbf{p}_1^j + \mathbf{p}_0^j - \mathbf{p}_2^j)}{2} \overleftrightarrow{\mathcal{D}}_{\mathbf{v}^j} - i \overleftrightarrow{\mathcal{D}}_{\mathbf{v}^j} \overleftrightarrow{\mathcal{D}}_{\mathbf{v}^j} \right] \\
&\times \mathcal{U}_F\left(v^+, -\frac{L^+}{2}; \mathbf{v}\right) \left. \right\} \gamma^+ \left(\left(p_2^l - \frac{p_2^+}{p_0^+} p_0^l \right) \left(2 \frac{p_0^+}{p_2^+} \delta^{kl} - \gamma^k \gamma^l \right) + \frac{p_2^+}{p_0^+} m \gamma^k \right) \\
&- 2\pi\delta(p_1^+ - p_0^+ + p_2^+) \left[1 - i \overleftrightarrow{\partial}_{\mathbf{v}} \frac{\gamma^+ \gamma^i}{2p_1^+} \right] \gamma^k \frac{L^+}{2} \mathcal{U}_F\left(\frac{L^+}{2}, -\frac{L^+}{2}; \mathbf{v}\right) \Big] u(0) \quad (5.24)
\end{aligned}$$

where we used the delta functions to express the common denominator

5.2.3 Photon emission inside the medium

The remaining case is the photon emission inside the medium. This corresponds to the diagram in Fig. 5.3

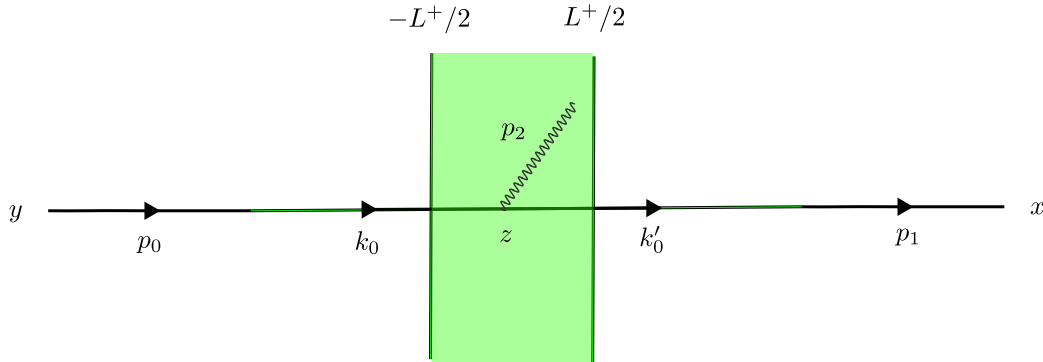


FIGURE 5.3: Diagrammatical representation of the photon emission inside the medium

The case of the integrated propagator coming from before and ending inside the medium reads

$$\begin{aligned}
\tilde{S}_F^{BI}(z)_{\beta\alpha_0} &= \lim_{y^+ \rightarrow -\infty} \int d^2\mathbf{y} \int dy^- e^{-iy\cdot\check{p}_0} \int \frac{d^3\mathbf{k}}{(2\pi)^3} e^{iy\cdot\check{k}} e^{i\mathbf{k}\cdot\mathbf{z}} e^{-ik^+z^-} \theta(k^+) \theta(z^+ - y^+) \\
&\times \left[\mathbf{1} - \frac{1}{2k^+} i\gamma^+ \gamma^i \overleftrightarrow{\mathcal{D}}_{\mathbf{z}^i} \right]_{\beta\beta'} \mathcal{U}_F\left(z^+, -\frac{L^+}{2}; \mathbf{z}\right)_{\beta'\alpha_0} \frac{(\check{k} + m)}{(2k^+)} \gamma^+ u(0). \quad (5.25)
\end{aligned}$$

Computing the integrals over \mathbf{y} and y^- and then over \mathbf{k} , we get

$$\begin{aligned}
\tilde{S}_F^{BI}(z)_{\beta\alpha_0} &= e^{i\mathbf{p}_0\cdot\mathbf{z}} e^{-ip_0^+z^-} \theta(p_0^+) \left[\mathbf{1} - \frac{1}{2p_0^+} i\gamma^+ \gamma^i \overleftrightarrow{\mathcal{D}}_{\mathbf{z}^i} \right]_{\beta\beta'} \\
&\times \mathcal{U}_F\left(z^+, -\frac{L^+}{2}; \mathbf{z}\right)_{\beta'\alpha_0} \frac{(\check{p}_0 + m)}{(2p_0^+)} \gamma^+ u(0). \quad (5.26)
\end{aligned}$$

The Dirac algebra gives $(\not{p}_0 + m)\gamma^+ u(0) = (2p_0^+ - \gamma^+(\not{p}_0 - m))u(0) = 2p_0^+ u(0)$, which leads to

$$\tilde{S}_F^{BI}(z)_{\beta\alpha_0} = e^{i\mathbf{p}_0 \cdot \mathbf{z}} e^{-ip_0^+ z^-} \theta(p_0^+) \left[\mathbf{1} - \frac{1}{2p_0^+} i\gamma^+ \gamma^i \vec{D}_{\mathbf{z}^i} \right]_{\beta\beta'} \mathcal{U}_F\left(z^+, \frac{-L^+}{2}; \mathbf{z}\right)_{\beta'\alpha_0} u(0) \quad (5.27)$$

Following the same procedure, the inside-after propagator can be written

$$\tilde{S}_F^{IA}(z)_{\alpha_1\beta} = \bar{u}(1) e^{-i\mathbf{p}_1 \cdot \mathbf{z}} e^{ip_1^+ z^-} \theta(p_1^+) \mathcal{U}_F\left(\frac{L^+}{2}, z^+; \mathbf{z}\right)_{\alpha_1\alpha'_1} \left(\mathbf{1} - \frac{1}{2p_1^+} i\gamma^+ \gamma^i \overleftarrow{D}_{\mathbf{z}^i} \right)_{\alpha'_1\beta} \quad (5.28)$$

Plugging Eqs.(5.27) and (5.28) in the expression of the S-matrix given in Eq.(5.8), we get

$$\begin{aligned} S_{q_1 \gamma_2 \leftarrow q_0}^{\text{in}} &= (-i) e e_f \epsilon_{\lambda\mu}(\underline{p}_2)^* \int d^4z \theta(p_0^+) \theta(p_1^+) e^{+iz \cdot \not{p}_2} e^{-i\mathbf{p}_1 \cdot \mathbf{z}} e^{ip_1^+ z^-} e^{i\mathbf{p}_0 \cdot \mathbf{z}} e^{-ip_0^+ z^-} \\ &\quad \bar{u}(1) \mathcal{U}_F\left(\frac{L^+}{2}, z^+; \mathbf{z}\right)_{\alpha_1\alpha'_1} \left(\mathbf{1} - \frac{1}{2p_1^+} i\gamma^+ \gamma^j \overleftarrow{D}_{\mathbf{z}^j} \right)_{\alpha'_1\beta} \gamma^\mu \left(\mathbf{1} - \frac{1}{2p_0^+} i\gamma^+ \gamma^i \vec{D}_{\mathbf{z}^i} \right)_{\beta\beta'} \\ &\quad \times \mathcal{U}_F\left(z^+, \frac{-L^+}{2}; \mathbf{z}\right)_{\beta'\alpha_0} u(0) \end{aligned} \quad (5.29)$$

First, we perform the Dirac algebra:

$$\begin{aligned} &\left(\mathbf{1} - \frac{1}{2p_1^+} i\gamma^+ \gamma^j \overleftarrow{D}_{\mathbf{z}^j} \right) \gamma^\mu \left(\mathbf{1} - \frac{1}{2p_0^+} i\gamma^+ \gamma^i \vec{D}_{\mathbf{z}^i} \right) \\ &= \gamma^\mu - \frac{i\gamma^+ \gamma^j \gamma^\mu \overleftarrow{D}_{\mathbf{z}^j}}{2p_1^+} + \frac{i\gamma^\mu \gamma^i \gamma^+ \vec{D}_{\mathbf{z}^i}}{2p_0^+} + \frac{\gamma^+ \gamma^j \gamma^\mu \gamma^i \gamma^+ \overleftarrow{D}_{\mathbf{z}^j} \vec{D}_{\mathbf{z}^i}}{4p_0^+ p_1^+}, \end{aligned} \quad (5.30)$$

to rewrite the S-matrix given in Eq.(5.29) as

$$\begin{aligned} S_{q_1 \gamma_2 \leftarrow q_0}^{\text{in}} &= (-i) e e_f \epsilon_{\lambda\mu}(\underline{p}_2)^* \int d^4z \theta(p_0^+) \theta(p_1^+) e^{+iz \cdot \not{p}_2} e^{-i\mathbf{p}_1 \cdot \mathbf{z}} e^{ip_1^+ z^-} e^{i\mathbf{p}_0 \cdot \mathbf{z}} e^{-ip_0^+ z^-} \\ &\quad \times \bar{u}(1) \mathcal{U}_F\left(\frac{L^+}{2}, z^+; \mathbf{z}\right)_{\alpha_1\alpha'_1} \\ &\quad \left(\gamma^\mu - \frac{i\gamma^+ \gamma^j \gamma^\mu \overleftarrow{D}_{\mathbf{z}^j}}{2p_1^+} + \frac{i\gamma^\mu \gamma^i \gamma^+ \vec{D}_{\mathbf{z}^i}}{2p_0^+} + 2g^{\mu+} \frac{\gamma^j \gamma^+ \gamma^i \overleftarrow{D}_{\mathbf{z}^j} \vec{D}_{\mathbf{z}^i}}{4p_0^+ p_1^+} \right)_{\alpha'_1\beta'} \\ &\quad \times \mathcal{U}_F\left(z^+, \frac{-L^+}{2}; \mathbf{z}\right)_{\beta'\alpha_0} u(0) \end{aligned} \quad (5.31)$$

Upon trivial z^- integration, and using the polarization of the photon as in Eq.(4.36) and setting the phase $e^{iz^+ \cdot \not{p}_2^-} = 1$ to one at NEik accuracy, we finally obtain

$$\begin{aligned} S_{q_1 \gamma_2 \leftarrow q_0}^{\text{in}} &= (-i) e e_f \epsilon_{\lambda k}(\underline{p}_2)^* \int dz^+ \int d^2\mathbf{z} 2\pi\delta(p_1^+ + p_2^+ - p_0^+) \theta(p_0^+) \theta(p_1^+) e^{-iz \cdot (\mathbf{p}_2 + \mathbf{p}_1 - \mathbf{p}_0)} \\ &\quad \times \bar{u}(1) \mathcal{U}_F\left(\frac{L^+}{2}, z^+; \mathbf{z}\right) \left(\gamma^k - \frac{i\gamma^+ \gamma^i \gamma^k \overleftarrow{D}_{\mathbf{z}^i}}{2p_1^+} + \frac{i\gamma^k \gamma^i \gamma^+ \vec{D}_{\mathbf{z}^i}}{2p_0^+} \right) \mathcal{U}_F\left(z^+, \frac{-L^+}{2}; \mathbf{z}\right) u(0). \end{aligned} \quad (5.32)$$

5.2.4 Final expressions for the S-matrix

In Appendix B we computed the final version for the S-matrix elements. There we show that one can get rid of the explicit $L^+/2$ terms that appeared so far in our S-matrix expressions by combining the terms from the different contributions. We have used the notation S' for the final S-matrix, and they read as follows:

$$\begin{aligned}
S'_{q_1 \gamma_2 \leftarrow q_0}{}^{\text{aft}} &= (-i) e e_f \epsilon_\lambda^k(p_2) (\mathbf{1})_{\alpha_1 \beta} \theta(p_1^+) \theta(p_0^+) \int d^2 \mathbf{v} e^{-i \mathbf{v} \cdot (\mathbf{p}_1 + \mathbf{p}_2 - \mathbf{p}_0)} \bar{u}(1) i \bar{\Delta} \gamma^+ \\
&\times \left(\left(p_2^l - \frac{p_2^+}{p_1^+} p_1^l \right) \left(2\delta^{kl} - \frac{p_2^+}{p_1^+} \gamma^l \gamma^k \right) - \left(\frac{p_2^+}{p_1^+} \right)^2 m \gamma^k \right) \\
&\times \left\{ \int d v^- e^{i v^- (p_1^+ + p_2^+ - p_0^+)} \mathcal{U}_F \left(\frac{L^+}{2}, -\frac{L^+}{2}; \mathbf{v}, v^- \right) + \frac{2\pi \delta(p_1^+ + p_2^+ - p_0^+)}{(2p_0^+)} \right. \\
&\times \int_{-\frac{L^+}{2}}^{\frac{L^+}{2}} d v^+ \mathcal{U}_F \left(\frac{L^+}{2}, v^+; \mathbf{v} \right) \left[\frac{[\gamma^i, \gamma^j]}{4} g t \cdot \mathcal{F}_{ij}(v) - \frac{(\mathbf{p}_0^j + \mathbf{p}_1^j + \mathbf{p}_2^j)}{2} \overleftrightarrow{\mathcal{D}}_{\mathbf{v}^j} - i \overleftarrow{\mathcal{D}}_{\mathbf{v}^j} \overrightarrow{\mathcal{D}}_{\mathbf{v}^j} \right] \\
&\times \left. \mathcal{U}_F \left(v^+, -\frac{L^+}{2}; \mathbf{v} \right) \right\}_{\beta \alpha_0} u(0) \tag{5.33}
\end{aligned}$$

,

$$\begin{aligned}
S'_{q_1 \gamma_2 \leftarrow q_0}{}^{\text{bef}} &= (-i) e e_f (\mathbf{1})_{\beta \alpha_0} \theta(p_0^+) \theta(p_1^+) \int d^2 \mathbf{v} e^{-i \mathbf{v} \cdot (\mathbf{p}_1 - \mathbf{p}_0 + \mathbf{p}_2)} \bar{u}(1) (-i \bar{\Delta}') \\
&\times \left\{ \int d v^- e^{i v^- (p_1^+ - p_0^+ + p_2^+)} \mathcal{U}_F \left(\frac{L^+}{2}, -\frac{L^+}{2}; \mathbf{v}, v^- \right) + \frac{2\pi \delta(p_1^+ - p_0^+ + p_2^+)}{2p_1^+} \right. \\
&\times \int_{-\frac{L^+}{2}}^{\frac{L^+}{2}} d v^+ \mathcal{U}_F \left(\frac{L^+}{2}, v^+; \mathbf{v} \right) \left[\frac{[\gamma^i, \gamma^j]}{4} g t \cdot \mathcal{F}_{ij}(v) - \frac{(\mathbf{p}_1^j + \mathbf{p}_0^j - \mathbf{p}_2^j)}{2} \overleftrightarrow{\mathcal{D}}_{\mathbf{v}^j} - i \overleftarrow{\mathcal{D}}_{\mathbf{v}^j} \overrightarrow{\mathcal{D}}_{\mathbf{v}^j} \right] \\
&\times \left. \mathcal{U}_F \left(v^+, -\frac{L^+}{2}; \mathbf{v} \right) \right\} \epsilon_\lambda^k(p_2) \gamma^+ \\
&\times \left(\left(p_2^l - \frac{p_2^+}{p_0^+} p_0^l \right) \left(2\delta^{kl} - \frac{p_2^+}{p_0^+} \gamma^k \gamma^l \right) + \left(\frac{p_2^+}{p_0^+} \right)^2 m \gamma^k \right) u(0) \tag{5.34}
\end{aligned}$$

and

$$\begin{aligned}
S'_{q_1 \gamma_2 \leftarrow q_0}{}^{\text{in}} &= (-i) e e_f \epsilon_{\lambda k}(p_2)^* \int d^2 \mathbf{z} 2\pi \delta(p_1^+ + p_2^+ - p_0^+) \theta(p_0^+) \theta(p_1^+) e^{-i \mathbf{z} \cdot (\mathbf{p}_1 + \mathbf{p}_2 - \mathbf{p}_0)} \\
&\times \bar{u}(1) \int_{-L^+/2}^{L^+/2} d z^+ \mathcal{U}_F \left(\frac{L^+}{2}, z^+; \mathbf{z} \right) \left[\frac{i \gamma^+ \gamma^i \gamma^k}{2p_1^+} + \frac{i \gamma^k \gamma^i \gamma^+}{2p_0^+} \right] \frac{1}{2} \overleftrightarrow{\mathcal{D}}_{\mathbf{z}^i} \mathcal{U}_F \left(z^+, \frac{-L^+}{2}; \mathbf{z} \right) u(0) \tag{5.35}
\end{aligned}$$

Where in Appendix B we have introduced also:

$$\frac{1}{\left((\mathbf{p}_2 - \mathbf{p}_1 \frac{p_2^+}{p_1^+})^2 + m^2 \left(\frac{p_2^+}{p_1^+} \right)^2 \right)} = \bar{\Delta} \tag{5.36}$$

and

$$\frac{1}{\left(\left(\mathbf{p}_2 - \mathbf{p}_0 \frac{p_2^+}{p_0^+} \right)^2 + m^2 \left(\frac{p_2^+}{p_0^+} \right)^2 \right)} = \bar{\Delta}' \quad (5.37)$$

5.3 Photon + jet partonic cross-section

In this section we compute the cross-section for the photon+jet production using the S-matrix elements that are computed for the three types of diagrams contributing to this process. We separate the cross section into two parts. A generalized eikonal contribution and a part with the explicit NEik corrections. The general form to compute the cross-section reads

$$\frac{d\sigma_{q_1 \gamma_2 \leftarrow q_0}}{d\text{P.S.}} \simeq S'_{q_1 \gamma_2 \leftarrow q_0} \left(S'_{q_1 \gamma_2 \leftarrow q_0} \right)^\dagger. \quad (5.38)$$

where S' is the effective S-matrix computed in Appendix B after getting rid of the explicit L^+ terms.

5.3.1 Generalized eikonal contribution to the cross-section

The first contribution to the cross-section is the generalized eikonal cross-section where the v^-, w^- dependence are kept in the Wilson lines. If one sets these coordinates to be zero, one can perform the trivial integration over v^- and w^- and obtain the "+" momentum conservation, recovering the standard eikonal result. The explicit expression for this contribution reads

$$\begin{aligned}
\left. \frac{d\sigma_{q_1 \gamma_2 \leftarrow q_0}}{d\text{P.S.}} \right|_{\text{Gen.Eik}} &= \left[S'_{q_1 \gamma_2 \leftarrow q_0}{}^{\text{aft}} \left(S'_{q_1 \gamma_2 \leftarrow q_0}{}^{\text{aft}} \right)^\dagger + S'_{q_1 \gamma_2 \leftarrow q_0}{}^{\text{bef}} \left(S'_{q_1 \gamma_2 \leftarrow q_0}{}^{\text{bef}} \right)^\dagger \right. \\
&\quad \left. + S'_{q_1 \gamma_2 \leftarrow q_0}{}^{\text{aft}} \left(S'_{q_1 \gamma_2 \leftarrow q_0}{}^{\text{bef}} \right)^\dagger + S'_{q_1 \gamma_2 \leftarrow q_0}{}^{\text{bef}} \left(S'_{q_1 \gamma_2 \leftarrow q_0}{}^{\text{aft}} \right)^\dagger \right]_{G-Eik} \\
&= (e e_f)^2 \epsilon_\lambda^k(p_2) \epsilon_\lambda^r(p_2) \int d^2\mathbf{v} \int d^2\mathbf{w} \int dv^- \int dw^- e^{-i(\mathbf{v}-\mathbf{w}) \cdot (\mathbf{p}_1 + \mathbf{p}_2 - \mathbf{p}_0)} e^{i(v^- - w^-)(p_1^+ + p_2^+ - p_0^+)} \\
&\quad \times \theta(p_1^+) \theta(p_0^+) \bar{u}(1) \left[\theta(p_1^+ + p_2^+) (\bar{\Delta})^2 \gamma^+ \left(\left(p_2^l - \frac{p_2^+}{p_1^+} p_1^l \right) \left(2\delta^{kl} - \frac{p_2^+}{p_1^+} \gamma^l \gamma^k \right) - \left(\frac{p_2^+}{p_1^+} \right)^2 m \gamma^k \right) \right. \\
&\quad \times u(0) \bar{u}(0) \left(\left(p_2^s - \frac{p_2^+}{p_1^+} p_1^s \right) \left(2\delta^{rs} - \frac{p_2^+}{p_1^+} \gamma^r \gamma^s \right) - \left(\frac{p_2^+}{p_1^+} \right)^2 m \gamma^r \right) \gamma^+ \\
&\quad + \theta(p_0^+ - p_2^+) (\bar{\Delta}')^2 \gamma^+ \left(\left(p_2^l - \frac{p_2^+}{p_0^+} p_0^l \right) \left(2\delta^{kl} - \frac{p_2^+}{p_0^+} \gamma^k \gamma^l \right) + \left(\frac{p_2^+}{p_0^+} \right)^2 m \gamma^k \right) \\
&\quad \times u(0) \bar{u}(0) \left(\left(p_2^s - \frac{p_2^+}{p_0^+} p_0^s \right) \left(2\delta^{rs} - \frac{p_2^+}{p_0^+} \gamma^s \gamma^r \right) + \left(\frac{p_2^+}{p_0^+} \right)^2 m \gamma^r \right) \gamma^+ \\
&\quad - 2\theta(p_1^+ + p_2^+) \theta(p_0^+ - p_2^+) \bar{\Delta}' \bar{\Delta} \gamma^+ \left(\left(p_2^l - \frac{p_2^+}{p_0^+} p_0^l \right) \left(2\delta^{kl} - \frac{p_2^+}{p_0^+} \gamma^k \gamma^l \right) + \left(\frac{p_2^+}{p_0^+} \right)^2 m \gamma^k \right) \\
&\quad \times u(0) \bar{u}(0) \left(\left(p_2^s - \frac{p_2^+}{p_1^+} p_1^s \right) \left(2\delta^{rs} - \frac{p_2^+}{p_1^+} \gamma^r \gamma^s \right) - \left(\frac{p_2^+}{p_1^+} \right)^2 m \gamma^r \right) \gamma^+ \left. \right] \\
&\quad \times \mathcal{U}_F \left(\frac{L^+}{2}, -\frac{L^+}{2}; \mathbf{v}, v^- \right) \mathcal{U}_F^\dagger \left(\frac{L^+}{2}, -\frac{L^+}{2}; \mathbf{w}, w^- \right) u(1) \tag{5.39}
\end{aligned}$$

One can now sum over the polarization taking into account $\sum \epsilon_\lambda^k(p_2) \epsilon_\lambda^r(p_2) = \delta^{rk}$ and after performing the Dirac algebra on all possible γ -structures and setting $\mathbf{p}_0 = 0$, we get the following generalized eikonal contribution

$$\begin{aligned}
\left. \frac{d\sigma_{q_1 \gamma_2 \leftarrow q_0}}{d\text{P.S.}} \right|_{\text{Gen.Eik}} &= (e e_f)^2 \int d^2\mathbf{v} \int d^2\mathbf{w} \int dv^- \int dw^- e^{-i(\mathbf{v}-\mathbf{w}) \cdot (\mathbf{p}_1 + \mathbf{p}_2)} e^{i(v^- - w^-)(p_1^+ + p_2^+ - p_0^+)} \theta(p_1^+) \theta(p_0^+) \\
&\quad \times \left\{ \theta(p_1^+ + p_2^+) (\bar{\Delta})^2 \left[16 \left(\mathbf{p}_2 - \frac{p_2^+}{p_1^+} \mathbf{p}_1 \right)^2 p_0^+ \left(2p_1^+ + 2p_2^+ + \left(\frac{p_2^+}{p_1^+} \right)^2 p_1^+ \right) \right. \right. \\
&\quad + 16 \left(\frac{p_2^+}{p_1^+} \right)^4 m^2 p_1^+ p_0^+ \left. \right] + \theta(p_0^+ - p_2^+) (\bar{\Delta}')^2 \left[16 (\mathbf{p}_2)^2 p_1^+ \left(2p_0^+ + 2p_2^+ + \left(\frac{p_2^+}{p_0^+} \right)^2 p_0^+ \right) \right. \\
&\quad + 16 \left(\frac{p_2^+}{p_0^+} \right)^4 m^2 p_1^+ p_0^+ \left. \right] - 2\theta(p_1^+ + p_2^+) \theta(p_0^+ - p_2^+) \bar{\Delta} \bar{\Delta}' \left[16 \left(\mathbf{p}_2 - \frac{p_2^+}{p_1^+} \mathbf{p}_1 \right) \cdot (\mathbf{p}_2) \right. \\
&\quad \times \left. \left. \left(2p_1^+ p_0^+ + p_1^+ p_2^+ + p_0^+ p_2^+ \right) - 16 \left(\frac{p_2^+}{p_1^+} \right)^2 \left(\frac{p_2^+}{p_0^+} \right)^2 m^2 p_1^+ \cdot p_0^+ \right] \right\} \\
&\quad \times \mathcal{U}_F \left(\frac{L^+}{2}, -\frac{L^+}{2}; \mathbf{v}, v^- \right) \mathcal{U}_F^\dagger \left(\frac{L^+}{2}, -\frac{L^+}{2}; \mathbf{w}, w^- \right) \tag{5.40}
\end{aligned}$$

5.3.2 Explicit NEik contribution to the cross-section

For the NEik terms we take the generalized eikonal terms but we ignore the v^- -dependence so that we recover the "+" momentum conservation. As in the generalized eikonal contribution, we set $\mathbf{p}_0 = 0$.

The explicit NEik corrections to the cross-section is the sum of the following contributions:

$$\begin{aligned} \frac{d\sigma_{q_1 \gamma_2 \leftarrow q_0}}{d\text{P.S.}} \Big|_{\text{NEik}} &= \frac{d\sigma_{q_1 \gamma_2 \leftarrow q_0}}{d\text{P.S.}} \Big|_{\text{aft-aft.}} + \frac{d\sigma_{q_1 \gamma_2 \leftarrow q_0}}{d\text{P.S.}} \Big|_{\text{bef-bef}} + \frac{d\sigma_{q_1 \gamma_2 \leftarrow q_0}}{d\text{P.S.}} \Big|_{\text{aft-bef Hel.Dep.}} \\ &+ \frac{d\sigma_{q_1 \gamma_2 \leftarrow q_0}}{d\text{P.S.}} \Big|_{\text{aft-bef Hel.Ind.}} + \frac{d\sigma_{q_1 \gamma_2 \leftarrow q_0}}{d\text{P.S.}} \Big|_{\text{in-(aft+bef)}} + O(\text{NNEik}). \end{aligned} \quad (5.41)$$

in order to simplify notation here we have used $\mathcal{U}_F\left(\frac{L^+}{2}, -\frac{L^+}{2}; \mathbf{v}\right) = \mathcal{U}_F(\mathbf{v})$. Then, each of the above contributions to the cross-section can be computed leading to the following results:

$$\begin{aligned} \frac{d\sigma_{q_1 \gamma_2 \leftarrow q_0}}{d\text{P.S.}} \Big|_{\text{aft-aft.}} &= \left[\mathcal{S}_{q_1 \gamma_2 \leftarrow q_0}^{\text{aft}} \left(\mathcal{S}_{q_1 \gamma_2 \leftarrow q_0}^{\text{aft}} \right)^\dagger \right]_{\text{NEik}} \\ &= (e e_f)^2 \theta(p_1^+) \theta(p_1^+ + p_2^+) \theta(p_0^+) \int d^2 \mathbf{v} \int d^2 \mathbf{w} \\ &\times e^{-i(\mathbf{v}-\mathbf{w}) \cdot (\mathbf{p}_1 + \mathbf{p}_2)} (\bar{\Delta})^2 2\pi \delta(p_1^+ + p_2^+ - p_0^+) \\ &\times \left[16 \left(\mathbf{p}_2 - \frac{p_2^+}{p_1^+} \mathbf{p}_1 \right)^2 p_0^+ \left(2p_1^+ + 2p_2^+ + \left(\frac{p_2^+}{p_1^+} \right)^2 p_1^+ \right) + 16 \left(\frac{p_2^+}{p_1^+} \right)^4 m^2 p_1^+ p_0^+ \right] \frac{1}{2p_0^+} \\ &\times \left[\int_{-\frac{L^+}{2}}^{\frac{L^+}{2}} dw^+ \mathcal{U}_F(\mathbf{v}) \mathcal{U}_F^\dagger \left(w^+, -\frac{L^+}{2}; \mathbf{w} \right) \left(\frac{(\mathbf{p}_1^n + \mathbf{p}_2^n)}{2} \overleftrightarrow{\mathcal{D}}_{\mathbf{w}^n} + i \overleftrightarrow{\mathcal{D}}_{\mathbf{w}^n} \overleftrightarrow{\mathcal{D}}_{\mathbf{w}^n} \right) \right. \\ &\times \mathcal{U}_F^\dagger \left(\frac{L^+}{2}, w^+; \mathbf{w} \right) + \int_{-\frac{L^+}{2}}^{\frac{L^+}{2}} dv^+ \mathcal{U}_F \left(\frac{L^+}{2}, v^+; \mathbf{v} \right) \\ &\left. \times \left(-\frac{(\mathbf{p}_1^j + \mathbf{p}_2^j)}{2} \overleftrightarrow{\mathcal{D}}_{\mathbf{v}^j} - i \overleftrightarrow{\mathcal{D}}_{\mathbf{v}^j} \overleftrightarrow{\mathcal{D}}_{\mathbf{v}^j} \right) \mathcal{U}_F \left(v^+, -\frac{L^+}{2}; \mathbf{v} \right) \mathcal{U}_F^\dagger(\mathbf{w}) \right], \end{aligned} \quad (5.42)$$

$$\begin{aligned}
\left. \frac{d\sigma_{q_1 \gamma_2 \leftarrow q_0}}{d\text{P.S.}} \right|_{\text{bef-bef}} &= \left[S_{q_1 \gamma_2 \leftarrow q_0}^{\text{bef}} \left(S_{q_1 \gamma_2 \leftarrow q_0}^{\text{bef}} \right)^\dagger \right]_{\text{NEik}} \\
&= (e e_f)^2 \theta(p_0^+) \theta(p_1^+) \theta(p_0^+ - p_2^+) \int d^2\mathbf{v} \int d^2\mathbf{w} \\
&\times e^{-i(\mathbf{v}-\mathbf{w}) \cdot (\mathbf{p}_1 + \mathbf{p}_2)} (\bar{\Delta}')^2 2\pi \delta(p_1^+ - p_0^+ + p_2^+) \frac{1}{2p_1^+} \\
&\times \left[16 (\mathbf{p}_2)^2 p_1^+ \left(2p_0^+ + 2p_2^+ + \left(\frac{p_2^+}{p_0^+} \right)^2 p_0^+ \right) + 16 \left(\frac{p_2^+}{p_0^+} \right)^4 m^2 p_1^+ p_0^+ \right] \\
&\times \left[\mathcal{U}_F(\mathbf{v}) \int_{-\frac{L^+}{2}}^{\frac{L^+}{2}} dw^+ \mathcal{U}_F^\dagger \left(w^+, -\frac{L^+}{2}; \mathbf{w} \right) \left(\frac{(\mathbf{p}_1^n - \mathbf{p}_2^n)}{2} \overleftarrow{\mathcal{D}}_{\mathbf{w}^n} + i \overleftarrow{\mathcal{D}}_{\mathbf{w}^n} \overrightarrow{\mathcal{D}}_{\mathbf{w}^n} \right) \right. \\
&\times \mathcal{U}_F^\dagger \left(\frac{L^+}{2}, w^+; \mathbf{w} \right) + \int_{-\frac{L^+}{2}}^{\frac{L^+}{2}} dv^+ \mathcal{U}_F \left(\frac{L^+}{2}, v^+; \mathbf{v} \right) \\
&\left. \times \left(-\frac{(\mathbf{p}_1^j - \mathbf{p}_2^j)}{2} \overleftarrow{\mathcal{D}}_{\mathbf{v}^j} - i \overleftarrow{\mathcal{D}}_{\mathbf{v}^j} \overrightarrow{\mathcal{D}}_{\mathbf{v}^j} \right) \mathcal{U}_F \left(v^+, -\frac{L^+}{2}; \mathbf{v} \right) \mathcal{U}_F^\dagger(\mathbf{w}) \right] \quad (5.43)
\end{aligned}$$

$$\begin{aligned}
\left. \frac{d\sigma_{q_1 \gamma_2 \leftarrow q_0}}{d\text{P.S.}} \right|_{\text{aft-bef Hel.Dep.}} &= \left[S_{q_1 \gamma_2 \leftarrow q_0}^{\text{aft}} \left(S_{q_1 \gamma_2 \leftarrow q_0}^{\text{bef}} \right)^\dagger + S_{q_1 \gamma_2 \leftarrow q_0}^{\text{bef}} \left(S_{q_1 \gamma_2 \leftarrow q_0}^{\text{aft}} \right)^\dagger \right]_{\text{NEik-Hel.Dep.}} \\
&= (e e_f)^2 \theta(p_1^+) \theta(p_0^+) \theta(p_0^+ - p_2^+) \theta(p_1^+ + p_2^+) \int d^2\mathbf{v} d^2\mathbf{w} e^{-i(\mathbf{v}-\mathbf{w}) \cdot (\mathbf{p}_1 + \mathbf{p}_2)} \\
&\times (8\bar{\Delta}\bar{\Delta}') (2\pi)^2 \delta(p_1^+ + p_2^+ - p_0^+) \left[-\frac{p_2^+ p_0^+}{p_1^+} + 2p_2^+ - \frac{p_1^+ p_2^+}{p_0^+} \right] \\
&\times \int_{-\frac{L^+}{2}}^{\frac{L^+}{2}} dv^+ \mathcal{U}_F \left(\frac{L^+}{2}, v^+; \mathbf{v} \right) (p_2^j) \left(p_2^j - \frac{p_2^+}{p_1^+} p_1^j \right) \text{gt}\mathcal{F}_{ij}(v) \mathcal{U}_F \left(v^+, -\frac{L^+}{2}; \mathbf{v} \right) \\
&\times \mathcal{U}_F^\dagger(\mathbf{w}) + \text{CC}. \quad (5.44)
\end{aligned}$$

and

$$\begin{aligned}
\left. \frac{d\sigma_{q_1 \gamma_2 \leftarrow q_0}}{d\text{P.S.}} \right|_{\text{aft-bef Hel.Ind.}} &= \left[S_{q_1 \gamma_2 \leftarrow q_0}^{\text{aft}} \left(S_{q_1 \gamma_2 \leftarrow q_0}^{\text{bef}} \right)^\dagger + S_{q_1 \gamma_2 \leftarrow q_0}^{\text{bef}} \left(S_{q_1 \gamma_2 \leftarrow q_0}^{\text{aft}} \right)^\dagger \right]_{\text{NEik-Hel.Ind.}} \\
&= (e e_f)^2 \theta(p_1^+) \theta(p_0^+) \theta(p_0^+ - p_2^+) \theta(p_1^+ + p_2^+) \\
&\times \int d^2 \mathbf{v} d^2 \mathbf{w} e^{-i(\mathbf{v}-\mathbf{w}) \cdot (\mathbf{p}_1 + \mathbf{p}_2)} (-\bar{\Delta} \bar{\Delta}') (2\pi)^2 \delta(p_1^+ + p_2^+ - p_0^+) \\
&\times \left(16 \left(\mathbf{p}_2 - \frac{p_2^+}{p_1^+} \mathbf{p}_1 \right) \cdot (\mathbf{p}_2) (2p_1^+ p_0^+ + p_1^+ p_2^+ + p_0^+ p_2^+) \right. \\
&- 16 \left(\frac{p_2^+}{p_1^+} \right)^2 \left(\frac{p_2^+}{p_0^+} \right)^2 m^2 p_1^+ \cdot p_0^+ \left[\frac{1}{2p_1^+} \int_{-\frac{L^+}{2}}^{\frac{L^+}{2}} dw^+ \mathcal{U}_F(\mathbf{v}) \mathcal{U}_F^\dagger(w^+, -\frac{L^+}{2}; \mathbf{w}) \right. \\
&\times \left[\frac{(\mathbf{p}_1^n - \mathbf{p}_2^n)}{2} \overleftrightarrow{\mathcal{D}}_{\mathbf{w}^n} + i \overleftrightarrow{\mathcal{D}}_{\mathbf{w}^n} \overrightarrow{\mathcal{D}}_{\mathbf{w}^n} \right] \mathcal{U}_F^\dagger\left(\frac{L^+}{2}, w^+; \mathbf{w}\right) \\
&+ \frac{1}{2p_0^+} \int_{-\frac{L^+}{2}}^{\frac{L^+}{2}} dv^+ \mathcal{U}_F\left(\frac{L^+}{2}, v^+; \mathbf{v}\right) \left[-\frac{(\mathbf{p}_1^j + \mathbf{p}_2^j)}{2} \overleftrightarrow{\mathcal{D}}_{\mathbf{v}^j} - i \overleftrightarrow{\mathcal{D}}_{\mathbf{v}^j} \overrightarrow{\mathcal{D}}_{\mathbf{v}^j} \right] \\
&\times \left. \mathcal{U}_F\left(v^+, -\frac{L^+}{2}; \mathbf{v}\right) \mathcal{U}_F^\dagger(\mathbf{w}) \right] + \text{CC.} \tag{5.45}
\end{aligned}$$

for the interferences with the inside terms

$$\begin{aligned}
\left. \frac{d\sigma_{q_1 \gamma_2 \leftarrow q_0}}{d\text{P.S.}} \right|_{\text{in- (aft+bef)}} &= \\
&S_{q_1 \gamma_2 \leftarrow q_0}^{\text{in}} \left(S_{q_1 \gamma_2 \leftarrow q_0}^{\text{aft}} + S_{q_1 \gamma_2 \leftarrow q_0}^{\text{bef}} \right)^\dagger + \left(S_{q_1 \gamma_2 \leftarrow q_0}^{\text{aft}} + S_{q_1 \gamma_2 \leftarrow q_0}^{\text{bef}} \right) \left(S_{q_1 \gamma_2 \leftarrow q_0}^{\text{in}} \right)^\dagger \\
&= 8(e e_f)^2 \theta(p_0^+) \theta(p_1^+) \int dv^+ \int d^2 \mathbf{v} \int d^2 \mathbf{w} \\
&\times e^{-i(\mathbf{v}-\mathbf{w}) \cdot (\mathbf{p}_2 + \mathbf{p}_1)} (2\pi)^2 \delta(p_1^+ + p_2^+ - p_0^+) \mathcal{U}_F\left(\frac{L^+}{2}, v^+; \mathbf{v}\right) \\
&\times \left[\theta(p_0^+ - p_2^+) \bar{\Delta}' \left(p_2^i \right) \left(\frac{p_1^+}{p_0^+} (p_0^+ + p_2^+) + p_0^+ \right) \right. \\
&- \theta(p_1^+ + p_2^+) \bar{\Delta} \left(p_2^j - \frac{p_2^+}{p_1^+} p_1^j \right) \left(\frac{p_0^+}{p_1^+} (p_1^+ + p_2^+) + p_1^+ \right) \left. \right] \\
&\times \frac{\overleftrightarrow{\mathcal{D}}_{\mathbf{v}^i}}{2} \mathcal{U}_F\left(v^+, -\frac{L^+}{2}; \mathbf{v}\right) \mathcal{U}_F^\dagger(\mathbf{w}) + \text{CC.} \tag{5.46}
\end{aligned}$$

Let us now simplify the expressions above by introducing the decorated Wilson lines, defined in Eqs. (4.64) (4.65), (4.66), (4.67), (4.68) and (4.69)

$$\begin{aligned}
\left. \frac{d\sigma_{q_1 \gamma_2 \leftarrow q_0}}{d\text{P.S.}} \right|_{\text{aft- aft.}} &= (e e_f)^2 \theta(p_1^+) \theta(p_1^+ + p_2^+) \theta(p_0^+) \\
&\times \int d^2\mathbf{v} \int d^2\mathbf{w} e^{-i(\mathbf{v}-\mathbf{w}) \cdot (\mathbf{p}_1 + \mathbf{p}_2)} (\bar{\Delta})^2 2\pi \delta(p_1^+ + p_2^+ - p_0^+) \\
&\times \frac{1}{2p_0^+} \left[16 \left(\mathbf{p}_2 - \frac{p_2^+}{p_1^+} \mathbf{p}_1 \right)^2 p_0^+ \left(2p_1^+ + 2p_2^+ + \left(\frac{p_2^+}{p_1^+} \right)^2 p_1^+ \right) + 16 \left(\frac{p_2^+}{p_1^+} \right)^4 m^2 p_1^+ p_0^+ \right] \\
&\times \left[\mathcal{U}_F(\mathbf{v}) \left(-\frac{(\mathbf{p}_1^n + \mathbf{p}_2^n)}{2} \mathcal{U}_{F;n}^{(1)\dagger}(\mathbf{w}) + i\mathcal{U}_{F;n}^{(2)\dagger}(\mathbf{w}) \right) - \left(\frac{(\mathbf{p}_1^j + \mathbf{p}_2^j)}{2} \mathcal{U}_{F;j}^{(1)}(\mathbf{v}) + i\mathcal{U}_{F;j}^{(2)}(\mathbf{v}) \right) \mathcal{U}_F^\dagger(\mathbf{w}) \right]
\end{aligned} \tag{5.47}$$

$$\begin{aligned}
\left. \frac{d\sigma_{q_1 \gamma_2 \leftarrow q_0}}{d\text{P.S.}} \right|_{\text{bef- bef.}} &= (e e_f)^2 \theta(p_0^+) \theta(p_1^+) \theta(p_0^+ - p_2^+) \\
&\times \int d^2\mathbf{v} \int d^2\mathbf{w} e^{-i(\mathbf{v}-\mathbf{w}) \cdot (\mathbf{p}_1 + \mathbf{p}_2)} (\bar{\Delta}')^2 2\pi \delta(p_1^+ - p_0^+ + p_2^+) \\
&\times \frac{1}{2p_1^+} \left(16 (\mathbf{p}_2)^2 p_1^+ \left(2p_0^+ + 2p_2^+ + \left(\frac{p_2^+}{p_0^+} \right)^2 p_0^+ \right) + 16 \left(\frac{p_2^+}{p_0^+} \right)^4 m^2 p_1^+ p_0^+ \right) \\
&\times \left[\mathcal{U}_F(\mathbf{v}) \left(-\frac{(\mathbf{p}_1^n - \mathbf{p}_2^n)}{2} \mathcal{U}_{F;j}^{(1)\dagger}(\mathbf{w}) + i\mathcal{U}_{F;j}^{(2)\dagger}(\mathbf{w}) \right) - \left(\frac{(\mathbf{p}_1^j - \mathbf{p}_2^j)}{2} \mathcal{U}_{F;j}^{(1)}(\mathbf{v}) + i\mathcal{U}_{F;j}^{(2)}(\mathbf{v}) \right) \mathcal{U}_F^\dagger(\mathbf{w}) \right]
\end{aligned} \tag{5.48}$$

The Eq. (5.44) can be rewritten as

$$\begin{aligned}
\left. \frac{d\sigma_{q_1 \gamma_2 \leftarrow q_0}}{d\text{P.S.}} \right|_{\text{aft- bef Hel. Dep.}} &= (e e_f)^2 \theta(p_1^+) \theta(p_0^+) \theta(p_0^+ - p_2^+) \theta(p_1^+ + p_2^+) \\
&\times \int d^2\mathbf{v} d^2\mathbf{w} e^{-i(\mathbf{v}-\mathbf{w}) \cdot (\mathbf{p}_1 + \mathbf{p}_2)} (8\bar{\Delta}\bar{\Delta}') (2\pi)^2 \delta(p_1^+ + p_2^+ - p_0^+) \\
&\times \frac{(-1)(p_2^+)^3}{p_0^+ p_1^+} \left(p_2^j \right) \left(p_2^j - \frac{p_2^+}{p_1^+} p_1^j \right) \mathcal{U}_{F;j}^{(3)}(\mathbf{v}) \mathcal{U}_F^\dagger(\mathbf{w}) + \text{CC.}
\end{aligned} \tag{5.49}$$

and

$$\begin{aligned}
& \left. \frac{d\sigma_{q_1 \gamma_2 \leftarrow q_0}}{d\text{P.S.}} \right|_{\text{aft-bef Hel.Ind.}} = (e e_f)^2 \theta(p_1^+) \theta(p_0^+) \theta(p_0^+ - p_2^+) \theta(p_1^+ + p_2^+) \\
& \times \int d^2\mathbf{v} d^2\mathbf{w} e^{-i(\mathbf{v}-\mathbf{w}) \cdot (\mathbf{p}_1 + \mathbf{p}_2)} (-\bar{\Delta} \bar{\Delta}') (2\pi)^2 \delta(p_1^+ + p_2^+ - p_0^+) \\
& \times \left(16 \left(\mathbf{p}_2 - \frac{p_2^+}{p_1^+} \mathbf{p}_1 \right) \cdot (\mathbf{p}_2) (2p_1^+ p_0^+ + p_1^+ p_2^+ + p_0^+ p_2^+) - 16 \left(\frac{p_2^+}{p_1^+} \right)^2 \left(\frac{p_2^+}{p_0^+} \right)^2 m^2 p_1^+ \cdot p_0^+ \right) \\
& \times \left[\frac{1}{2p_1^+} \mathcal{U}_F(\mathbf{v}) \left(-\frac{(\mathbf{p}_1^n - \mathbf{p}_2^n)}{2} \mathcal{U}_{F;n}^{(1)\dagger}(\mathbf{w}) + i \mathcal{U}_{F;n}^{(2)\dagger}(\mathbf{w}) \right) \right. \\
& \left. - \frac{1}{2p_0^+} \left(\frac{(\mathbf{p}_1^j + \mathbf{p}_2^j)}{2} \mathcal{U}_{F;j}^{(1)}(\mathbf{v}) + i \mathcal{U}_{F;j}^{(2)}(\mathbf{v}) \right) \mathcal{U}_F^\dagger(\mathbf{w}) \right] + \text{CC.} \tag{5.50}
\end{aligned}$$

and finally

$$\begin{aligned}
& \left. \frac{d\sigma_{q_1 \gamma_2 \leftarrow q_0}}{d\text{P.S.}} \right|_{\text{in- (aft+bef)}} \\
& = 8(e e_f)^2 \theta(p_0^+) \theta(p_1^+) \int d^2\mathbf{v} \int d^2\mathbf{w} e^{-i(\mathbf{v}-\mathbf{w}) \cdot (\mathbf{p}_2 + \mathbf{p}_1)} \\
& \times (2\pi)^2 \delta(p_1^+ + p_2^+ - p_0^+) \left(\theta(p_0^+ - p_2^+) \bar{\Delta}' \left(p_2^j \right) \left(\frac{p_1^+}{p_0^+} (p_0^+ + p_2^+) + p_0^+ \right) \right. \\
& \left. - \theta(p_1^+ + p_2^+) \bar{\Delta} \left(p_2^j - \frac{p_2^+}{p_1^+} p_1^j \right) \left(\frac{p_0^+}{p_1^+} (p_1^+ + p_2^+) + p_1^+ \right) \right) \frac{\mathcal{U}_{F;i}^{(1)}(\mathbf{v})}{2} \mathcal{U}_F^\dagger(\mathbf{w}) + \text{CC.} \tag{5.51}
\end{aligned}$$

Then we can write the final cross-section as follows:

$$\frac{d\sigma_{q_1 \gamma_2 \leftarrow q_0}}{d\text{P.S.}} = \left. \frac{d\sigma_{q_1 \gamma_2 \leftarrow q_0}}{d\text{P.S.}} \right|_{\text{Gen.Eik}} + \left. \frac{d\sigma_{q_1 \gamma_2 \leftarrow q_0}}{d\text{P.S.}} \right|_{\text{NEik}} \tag{5.52}$$

where the first term corresponds to Eq.(5.40) and the second term is the sum of Eqs. (5.47), (5.48), (5.49), (5.50) and (5.51).

5.4 Conclusions

Thus in this chapter we have derived the photon + jet production at full NEik accuracy in the gluon background field, expressing our final cross-section as two main contributions. One is the generalized eikonal contribution and a sum of explicit NEik corrections. The generalized eikonal contribution does not contain the conservation of the "+" momentum since the Wilson lines are still dependent on the "-" coordinates.

We have expressed the explicit NEik corrections to the cross-section in terms of decorated Wilson lines and we can see from our result that we get contributions that are helicity dependent as well as helicity independent. The helicity dependent terms

vanish for all cross-section terms except for the interference of the quark emission before with the quark emission after the medium.

Finally, we would like to mention that this is an ongoing work. As the next step, we are planning to rewrite our cross-section in terms of total momenta and the momentum imbalance of the produced photon and quark jet which are defined as:

$$\mathbf{k}_\perp = \mathbf{p}_1 + \mathbf{p}_2 \quad (5.53)$$

$$\mathbf{P}_\perp = \frac{p_2^+ \mathbf{p}_1 - p_1^+ \mathbf{p}_2}{p_1^+ + p_2^+}. \quad (5.54)$$

This will allow us to establish the connection between the standard TMD factorisation and the CGC computation for this observable beyond eikonal accuracy. We expect to see the interplay between the NEik corrections and the higher-twist corrections for the dipole TMD.

6

Conclusions

The high energy limit of QCD, corresponding to the Regge-Gribov limit which is also referred to as small- x limit, is conveniently described by the Color Glass Condensate effective theory. The basics of CGC is described in Chapter 1, and all the work presented afterwards in this thesis is performed within this effective theory. In the CGC one of the key approximations that is adopted is the eikonal approximation. As discussed in Chapter 2, this approximation amounts to taking three assumptions that keep contributions only leading in energy, neglecting all energy suppressed corrections. The three assumptions can be expressed as:

$$A_a^\mu(x) \propto \delta(x^+) \quad (6.1)$$

$$A_a^\mu(x) \simeq \delta^{\mu-} A_a^-(x) \quad (6.2)$$

$$A_a^\mu(x) \simeq A_a^\mu(x^+, \mathbf{x}) \quad (6.3)$$

The three assumptions are, to take an infinitely thin "shockwave" as the target medium (shockwave approximation) Eq. (6.1), to account only for the leading component of the background field, \mathcal{A}^- Eq. (6.2), and to neglect the dynamics of the target Eq. (6.3). Therefore, the eikonal approximation amounts to $\mathcal{A}_a^\mu(x^-, x^+, \mathbf{x}) \approx \delta^{\mu-} \delta(x^+) \mathcal{A}_a^-(\mathbf{x})$. This eikonal approximation has been proven to be very reliable, specially in the range of very high energies, such as the ones reached at the LHC experiment. The phenomenological studies performed at the LHC are in very good agreement with the computations performed within the eikonal limit. However, experiments such as RHIC or the future EIC have lower scattering energies compared to the LHC. Therefore, one should take into account power suppressed corrections in order to increase the precision in the calculation of observables that are the focus of these experiments. Computing these corrections was the main focus of this thesis.

In particular, we focus on a quark propagator in a gluon background field. In Chapter 2, we provide the derivation of a quark propagator at Eikonal accuracy and discuss the power counting for eikonal and next-to-eikonal contributions. As a first step towards providing the derivation of a quark propagator at NEik accuracy in a gluon background field, in Chapter 3, we relaxed the first two assumptions of the eikonal approximation to calculate the quark propagator. This amounts to taking a finite width of the target instead of a infinitely thin 'shockwave', thus allowing us to have transverse motion in the medium. Relaxing the second assumption we now take into account the interaction with the transverse component of the background field, and not only with \mathcal{A}^- . With this quark propagator, we studied quark target scattering and computed the production cross-section.

The remaining NEik effect that should be accounted for is the dynamics of the target which amounts to relaxing Eq.(6.3). This effect was first considered in [43] at the level of quark and scalar propagators at NEik accuracy. In Chapter 4, we include the effects of dynamical target in the derivation of the quark propagator. With this effect accounted for, we provide the quark propagator at full NEik accuracy in the gluon background field. In the rest of Chapter 4, we used this propagator to compute DIS dijet production cross-section at NEik accuracy both for transverse and longitudinal polarization of the incoming photon. Since this observable will be studied at the future EIC, and therefore at moderate energies, we hope that the NEik corrections computed in this work will provide a better precision in the future phenomenology studies. The result for the DIS dijet cross-section is shown as two separate contributions. the first one is what we call generalized eikonal contribution, which contains the z^- dependence on the Wilson lines and therefore, does not include the "+" momentum conservation, however we recover the standard eikonal result upon taking $z^- = 0$. The second contribution to the cross-section is the explicit NEik contribution and it is described in terms of decorated Wilson lines.

In Chapter 5, we used the full NEik quark propagator in a gluon background field to study photon+jet production in forward pA collisions. This is still an ongoing work, but the main results for the partonic cross-section at NEik accuracy is provided in Chapter 5. This cross-section is divided into a generalized eikonal contribution and an explicit NEik contribution.

In conclusion, in this thesis, we focused on deriving the next-to-eikonal corrections to the quark propagator in a gluon background field. This was achieved by relaxing all the three assumptions that are taken in the eikonal approximation. The resulting quark propagator at NEik accuracy was used to compute different observables. The cross-sections for these observables are given at NEik accuracy, thus, include first order correction to the high energy limit. These corrections are hoped to provide better precision in the phenomenological studies of future EIC. The main feature of NEik corrections is the appearance of decorated Wilson lines at the amplitude level and decorated dipole/quadrupole operators at the cross-section level. Even though there are no models that can that can define these decorated operators, as opposed to eikonal limit (like GBW or MV models), we expect to obtain these models in the near future.

Bibliography

- [1] D.J. Gross and F. Wilczek. Ultraviolet behavior of non-abelian gauge theories. *Phys. Rev. Lett* 30.1343 (1973).
- [2] H.D. Politzer. Reliable perturbative results for strong interactions. *Phys. Rev. Lett* 30.1346 (1973).
- [3] P.A. Zyla et al. Prog. theor. Exp. Phys. (*Particle Data Group*) 083C01 (2020), p. 30.
- [4] J.D. Bjorken. *Phys. Rev* 179.1547 (1969).
- [5] J. Prentki and J. Steinberger. Proceedings, 14th International Conference on High-Energy Physics(ICHEP 68). *Phys. Rev. Lett* (1968).
- [6] R.P.Feynman. *Phys. Rev. Lett* 23.1415 (Dec,1969).
- [7] R.P.Feynman. The behavior of hadron collisions at extreme energies. *Conf. Proc. C* 690905.237 (1969).
- [8] C.G.Callan and D.J.Gross. High-energy electroproduction and the constitution of the electric current. *Phys. Rev. Lett* 22.156 (1969).
- [9] Particle Data Group collaboration. M. Tanabashi et al. *Phys. Rev.* D98.3030001 (2018), p. 320.
- [10] Y. L. Dokshitzer. Calculation of the Structure Functions for Deep Inelastic Scattering and $e^+ e^-$ Annihilation by Perturbation Theory in Quantum Chromodynamics. *Sov. Phys. JETP* 46.641 (1977).
- [11] V. N. Gribov and L. N. Lipatov. $e^+ e^-$ pair annihilation and deep inelastic $e p$ scattering in perturbation theory. *Sov. J. Nucl. Phys.* 15.675 (1972).
- [12] L.N. Lipatov. The parton model and perturbation theory. *Yad. Fiz.* 20.181 (1974).
- [13] G. Altarelli and G. Parisi. Asymptotic Freedom in Parton Language. *Nucl. Phys. B* 126.298 (1977), pp. 1997–2027.
- [14] Y.V. Kovchegov and E. Levin. Quantum chromodynamics at high energy. *Cambridge University Press* 33.10.1017/CBO9781139022187 (8,2012).
- [15] E.A. Kuraev, L.N. Lipatov, and V.S. Fadin. The Pomeranchuk Singularity in Nonabelian Gauge Theories. *Sov. Phys. JETP* 45.199 (1977).
- [16] I.I. Balitsky and L.N. Lipatov. The Pomeranchuk Singularity in Quantum Chromodynamics. *Sov. J. Nucl. Phys* 28.822 (1978).
- [17] Y.V. Kovchegov and E. Lenvin. *Camb. Monogr. Part. Phys. Nucl. Phys. Cosmol* 33.1 (2012).
- [18] M. Froissart. Asymptotic behavior and subtractions in the mandelstam representation. *Phys. Rev.* 123.1053 (1961).
- [19] L.V. Gribov, E.M. Levin, and M.G. Ryskin. *Phys. Rept.* 100.1 (1983).
- [20] A.M. Stasto, K. Golec-Biernat, and J. Kwiecinski. *Phys. Rev. LEtt* 86.596 (2001).
- [21] F. Gelis, R. Peschanski, L. Schoeffel, and Phys G. Soyez. *Phys. Lett. B* 647.376 (2007).
- [22] H. Kowalski, T. Lappi, and R. Venugopalan. *Phys. Rev. Lett.* 100.022303 (2008).
- [23] L.D. McLerran and R. Venugopalan. *Phys. Rev. D* 49.2233 (1994).
- [24] L.D. McLerran and R. Venugopalan. *Phys. Rev. D* 49.3352 (1994).
- [25] L.D. McLerran and R. Venugopalan. *Phys. Rev. D* 50.2225 (1994).
- [26] J. Jalilian-Marian, A. Kovner, L. McLerran, and H. Weigert. Intrinsic glue distribution at very smallx. *Phys. Rev. D* 55.5414 (1997).

- [27] J. Jalilian-Marian, A. Kovner, A. Leonidov, and H. Weigert. Towards the high density regime. *Phys. Rev. D* 59 (1998).
- [28] E. Iancu, A. Leonidov, and L. McLerran. Nonlinear gluon evolution in the color glass condensate: I. *Nuclear Physics A* 692.583 (2001).
- [29] E. Iancu, A. Leonidov, and L. McLerran. The renormalization group equation for the color glass condensate. *Physics Letters B* 510.133 (2001).
- [30] E. Ferreiro, E. Iancu, A. Leonidov, and L. McLerran. Nonlinear gluon evolution in the color glass condensate. *Nuclear Physics A* 703.489 (2002).
- [31] E. Iancu and R. Venugopalan. Quark Gluon Plasma 3. Eds. R.C. Hwa and X.N. Wang, *World Scientific* (). URL: [hep-ph/0303204](https://doi.org/10.1142/9789812700320_003).
- [32] F. Gelis, E. Iancu, J. Jalilian-Marian, and R. Venugopalan. *Ann. Rev. Part. Nucl. Sci.* 60.463 (2010).
- [33] T. Lappi. *Int. J. Mod. Phys E* 20.1 (2011).
- [34] T. Altinoluk, G. Beuf, A. Czajka, and A. Tymowska. Quarks at next-to-eikonal accuracy in the CGC: Forward quark-nucleus scattering. *Phys. Rev. D* 104.1 (2021). URL: [doi:10.1103/PhysRevD.104.014019](https://doi.org/10.1103/PhysRevD.104.014019).
- [35] T. Altinoluk, G. Beuf, A. Czajka, and A. Tymowska. DIS dijet production at next-to-eikonal accuracy in the CGC. *Phys. Rev. D* 107.074016 (2023). URL: [doi:10.1103/PhysRevD.107.074016](https://doi.org/10.1103/PhysRevD.107.074016).
- [36] T. Altinoluk, N. Armesto, G. Beuf, M. Martinez, and C. A. Salgado. Next-to-eikonal corrections in the CGC: gluon production and spin asymmetries in pA collisions. *JHEP* 1407.068 (2014). URL: [doi:10.1007/JHEP07\(2014\)068](https://doi.org/10.1007/JHEP07(2014)068).
- [37] T. Altinoluk, N. Armesto, G. Beuf, and A. Moscoso. Next-to-next-to-eikonal corrections in the CGC. *JHEP* 1601.114 (2016).
- [38] T. Altinoluk and A. Dumitru. Particle production in high-energy collisions beyond the shockwave limit. *Phys. Rev. D* 94.074032 (2016). URL: [doi:10.1103/PhysRevD.94.074032](https://doi.org/10.1103/PhysRevD.94.074032).
- [39] P. Agostini, T. Altinoluk, and N. Armesto. Non-eikonal corrections to multi-particle production in the Color Glass Condensate. *Eur.Phys.J.C* 79.600 (2019). URL: [doi:10.1140/epjc/s10052-019-7097-5](https://doi.org/10.1140/epjc/s10052-019-7097-5).
- [40] P. Agostini, T. Altinoluk, and N. Armesto. Effect of non-eikonal corrections on azimuthal asymmetries in the Color Glass Condensate. *Eur.Phys.J.C* 79.790 (2019). URL: [doi:10.1140/epjc/s10052-019-7315-1](https://doi.org/10.1140/epjc/s10052-019-7315-1).
- [41] P. Agostini, T. Altinoluk, and N. Armesto. Multiparticle production in proton–nucleus collisions beyond eikonal accuracy. *Eur.Phys.J.C* 82.1001 (2022). URL: [doi:10.1140/epjc/s10052-022-10962-1](https://doi.org/10.1140/epjc/s10052-022-10962-1).
- [42] P. Agostini, T. Altinoluk, and N. Armesto. Finite width effects on the azimuthal asymmetry in proton-nucleus collisions in the Color Glass Condensate (2022). URL: [arXiv:2212.03633\[hep-ph\]](https://arxiv.org/abs/2212.03633).
- [43] T. Altinoluk and G. Beuf. Quark and scalar propagators at next-to-eikonal accuracy in the CGC through a dynamical background gluon field. *Phys. Rev. D* 105.7 (2022). URL: [doi:10.1103/PhysRevD.105.074026](https://doi.org/10.1103/PhysRevD.105.074026).
- [44] Y.V.Kovchegov, D.Pitonyak, and M.D.Sievert. Helicity Evolution at Small-x. *JHEP* 1610.072 (2016). URL: [doi:10.1007/JHEP10\(2016\)072](https://doi.org/10.1007/JHEP10(2016)072), [2010.1007/JHEP10\(2016\)148](https://doi.org/10.1007/JHEP10(2016)148).
- [45] Y.V.Kovchegov and M.G.Santiago. Quark sivers function at small x: spin-dependent odderon and the sub-eikonal evolution. *JHEP* 11.200 (2021). URL: [doi:10.1007/JHEP11\(2021\)200](https://doi.org/10.1007/JHEP11(2021)200).
- [46] F.Cougoulic, Y.V.Kovchegov, A.Tarasov, and Y.Tawabutr. Quark and gluon helicity evolution at small x: revised and updated. *JHEP* 07.095 (2022). URL: [doi:10.1007/JHEP07\(2022\)095](https://doi.org/10.1007/JHEP07(2022)095).

- [47] Y.V.Kovchegov and M.G.Santiago. T-odd leading-twist quark TMDs at small x . *JHEP* 11.098 (2022). URL: [doi:10.1007/JHEP11\(2022\)098](https://doi.org/10.1007/JHEP11(2022)098).
- [48] Y.V.Kovchegov, D.Pitonyak, and M.D.Sievert. Small- x asymptotics of the quark helicity distribution. *Phys. Rev. Lett* 118.052001 (2017). URL: [doi:10.1103/PhysRevLett.118.052001](https://doi.org/10.1103/PhysRevLett.118.052001).
- [49] Y.V.Kovchegov, D.Pitonyak, and M.D.Sievert. Helicity Evolution at Small x : Flavor Singlet and Non-Singlet Observables. *Phys. Rev. D* 95.014033 (2017). URL: [doi:10.1103/PhysRevD.95.014033](https://doi.org/10.1103/PhysRevD.95.014033).
- [50] Y.V.Kovchegov, D.Pitonyak, and M.D.Sievert. Small- x Asymptotics of the Quark Helicity Distribution: Analytic Results. *Phys. Lett. B* 772.136 (2017). URL: [doi:10.1016/j.physletb.2017.06.032](https://doi.org/10.1016/j.physletb.2017.06.032).
- [51] Y.V.Kovchegov, D.Pitonyak, and M.D.Sievert. Small- x Asymptotics of the Gluon Helicity Distribution. *JHEP* 1710.198 (2017). URL: [doi:10.1007/JHEP10\(2017\)198](https://doi.org/10.1007/JHEP10(2017)198).
- [52] Y.V.Kovchegov and M.D.Sievert. Small- x Helicity Evolution: an Operator Treatment. *Phys. Rev. D* 99.054032 (2019). URL: [doi:10.1103/PhysRevD.99.054032](https://doi.org/10.1103/PhysRevD.99.054032).
- [53] Y.V.Kovchegov and Y.Tawabutr. Helicity at Small x : Oscillations Generated by Bringing Back the Quarks. *JHEP* 2008.014 (2020). URL: [doi:10.1007/JHEP08\(2020\)014](https://doi.org/10.1007/JHEP08(2020)014).
- [54] D.Adamiak and et al. First analysis of world polarized DIS data with small- x helicity evolution. *Phys. Rev.D* 104.L031501 (2021). URL: [doi:10.1103/PhysRevD.104.L031501](https://doi.org/10.1103/PhysRevD.104.L031501).
- [55] Y.V.Kovchegov, A.Tarasov, and Y.Tawabutr. Helicity evolution at small x : the single-logarithmic contribution. *Phys. Rev.D* 03.184 (2022). URL: [doi:10.1007/JHEP03\(2022\)184](https://doi.org/10.1007/JHEP03(2022)184).
- [56] F.Cougoulic and Y.V.Kovchegov. Helicity-dependent generalization of the JIMWLK evolution. *Phys.Rev.D* 100.114020 (2019). URL: [doi:10.1103/PhysRevD.100.114020](https://doi.org/10.1103/PhysRevD.100.114020).
- [57] F.Cougoulic and Y.V.Kovchegov. Helicity-dependent extension of the McLerran-Venugopalan model. *Nucl.Phys.A* 1004.122051 (2020). URL: [doi:10.1016/j.nuclphysa.2020.122051](https://doi.org/10.1016/j.nuclphysa.2020.122051).
- [58] G.A.Chirilli. Sub-eikonal corrections to scattering amplitudes at high energy. *JHEP* 1901.118 (2019). URL: [doi:10.1007/JHEP01\(2019\)118](https://doi.org/10.1007/JHEP01(2019)118).
- [59] G.A.Chirilli. High-energy operator product expansion at sub-eikonal level. *JHEP* 06.096 (2021). URL: [doi:10.1007/JHEP06\(2021\)096](https://doi.org/10.1007/JHEP06(2021)096).
- [60] I.Balitsky and A.Tarasov. Rapidity evolution of gluon TMD from low to moderate x . *JHEP* 1510.017 (2015). URL: [doi:10.1007/JHEP10\(2015\)017](https://doi.org/10.1007/JHEP10(2015)017).
- [61] I.Balitsky and A.Tarasov. Gluon TMD in particle production from low to moderate x . *JHEP* 1606.164 (2016). URL: [doi:10.1007/JHEP06\(2016\)164](https://doi.org/10.1007/JHEP06(2016)164).
- [62] I.Balitsky and A.Tarasov. Higher-twist corrections to gluon TMD factorization. *JHEP* 1707.095 (2017). URL: [doi:10.1007/JHEP07\(2017\)095](https://doi.org/10.1007/JHEP07(2017)095).
- [63] I.Balitsky and A.Tarasov. Power corrections to TMD factorization for Z-boson production. *JHEP* 1805.150 (2018). URL: [doi:10.1007/JHEP05\(2018\)150](https://doi.org/10.1007/JHEP05(2018)150).
- [64] I.Balitsky and G.A.Chirilli. Conformal invariance of transverse-momentum dependent parton distributions rapidity evolution. *Phys. Rev. D* 100.051504 (2019). URL: [doi:10.1103/PhysRevD.100.051504](https://doi.org/10.1103/PhysRevD.100.051504).
- [65] R.Boussarie and Y.Mehtar-Tani. A novel formulation of the unintegrated gluon distribution for DIS. *Phys. Lett. B* 831.137125 (2022). URL: [doi:10.1016/j.physletb.2022.137125](https://doi.org/10.1016/j.physletb.2022.137125).

- [66] R.Boussarie and Y.Mehtar-Tani. Gluon-mediated inclusive Deep Inelastic Scattering from Regge to Bjorken kinematics. *JHEP* 07.080 (2022). URL: [doi:10.1007/JHEP07\(2022\)080](https://doi.org/10.1007/JHEP07(2022)080).
- [67] J.Jalilian-Marian. Elastic scattering of a quark from a color field: longitudinal momentum exchange. *Phys. Rev. D* 96.074020 (2017). URL: [doi:10.1103/PhysRevD.96.074020](https://doi.org/10.1103/PhysRevD.96.074020).
- [68] J.Jalilian-Marian. Quark jets scattering from a gluon field: from saturation to high p_t . *Phys. Rev. D* 99.014043 (2019). URL: [doi:10.1103/PhysRevD.99.014043](https://doi.org/10.1103/PhysRevD.99.014043).
- [69] J.Jalilian-Marian. Rapidity loss, spin, and angular asymmetries in the scattering of a quark from the color field of a proton or nucleus. *Phys. Rev. D* 102.014008 (2020). URL: [doi:10.1103/PhysRevD.102.014008](https://doi.org/10.1103/PhysRevD.102.014008).
- [70] Y.Hatta, Y.Nakagawa, F.Yuan, Y.Zhao, and B.Xiao. Gluon orbital angular momentum at small- x . *Phys. Rev. D* 95.114032 (2017). URL: [doi:10.1103/PhysRevD.95.114032](https://doi.org/10.1103/PhysRevD.95.114032).
- [71] R.Boussarie, Y.Hatta, and F.Yuan. Proton Spin Structure at Small- x . *Phys. Lett. B* 797.134817 (2019). URL: [doi:10.1016/j.physletb.2019.134817](https://doi.org/10.1016/j.physletb.2019.134817).
- [72] A.Dumitru, A.Hayashigaki, and J.Jalilian-Marian. The Color glass condensate and hadron production in the forward region. *Nucl.Phys.* 765.464 (2006). URL: [doi:10.1016/j.nuclphysa.2005.11.014](https://doi.org/10.1016/j.nuclphysa.2005.11.014).
- [73] T.Altinoluk, C.Contreras, A.Kovner, E.Levin, M.Lublinsky, and A.Shulkin. QCD Reggeon Calculus From KLWMIJ/JIMWLK Evolution: Vertices, Reggeization and All. *JHEP* 1309.115 (2013). URL: [doi:10.1007/JHEP09\(2013\)115](https://doi.org/10.1007/JHEP09(2013)115).
- [74] T.Altinoluk, N.Armesto, A.Kovner, E.Levin, and M.Lublinsky. KLWMIJ Reggeon field theory beyond the large N_c limit. *JHEP* 1408.007 (2014). URL: [doi:10.1007/JHEP08\(2014\)007](https://doi.org/10.1007/JHEP08(2014)007).
- [75] T. Altinoluk, N. Armesto, G. Beuf, and A. Tymowska. Photon + jet production at next-to-eikonal accuracy in pA collisions. *In preparation* (2023).

A

Light-Cone coordinates

In this appendix we introduce the so-called *light-cone coordinates*. These coordinates are introduced by Dirac and simplify greatly the dynamics in high energy collisions. Throughout this whole thesis we use these coordinates, hence we dedicate this appendix to define them more carefully. Let $x^\mu = (x^0, x^1, x^2, x^3) \equiv (x^0, \mathbf{x}, x^3)$ be the 4-vector in Cartesian a representation of the Minkowski metric $g_{\mu\nu} = \text{diag}(1, -1, -1, -1)$. The light-cone coordinates are thus defined as follows:

$$x^+ = \frac{x^0 + x^3}{\sqrt{2}} \quad (\text{A.1})$$

$$x^- = \frac{x^0 - x^3}{\sqrt{2}} \quad (\text{A.2})$$

where the transverse coordinates are left unchanged, $\mathbf{x} = (x^1, x^2)$. This change is equivalent to rotate the Cartesian system by 45° , placing the axis x^0, x^3 on top of the light-cone. the four-momentum k^μ follows the same convention for its components. The product of two 4-vectors in this notation is

$$x^\mu y_\mu = x^+ y^- + x^- y^+ - \mathbf{x} \cdot \mathbf{y}. \quad (\text{A.3})$$

The complete metric in this light-cone frame is

$$g_{\mu\nu} = \begin{pmatrix} 0 & 1 & 0 & 0 \\ 1 & 0 & 0 & 0 \\ 0 & 0 & -1 & 0 \\ 0 & 0 & 0 & -1 \end{pmatrix} \quad (\text{A.4})$$

this implies that

$$x^+ = x_- \quad (\text{A.5})$$

$$x^- = x_+ \quad (\text{A.6})$$

The derivatives are given by

$$\partial^- \equiv \frac{\partial}{\partial x^+} = \frac{1}{\sqrt{2}} \left(\frac{\partial}{\partial x^0} + \frac{\partial}{\partial x^3} \right) \quad (\text{A.7})$$

$$\partial^+ \equiv \frac{\partial}{\partial x^-} = \frac{1}{\sqrt{2}} \left(\frac{\partial}{\partial x^0} - \frac{\partial}{\partial x^3} \right) \quad (\text{A.8})$$

Furthermore, throughout the calculations in this thesis from section 2.3 on, we have used the following notation

$$\underline{x} = (x^+, \mathbf{x}) \quad (\text{A.9})$$

and

$$\check{k}^\mu = (k^+, \mathbf{k}, \check{k}^-) \quad (\text{A.10})$$

where \check{k}^- is on-shell,

$$\check{k}^- = \frac{\mathbf{k}^2 + m^2}{2k^+} \quad (\text{A.11})$$

B

Derivation of final expressions for the S-matrix in Photon+jet production

In this appendix we derive the final expressions for the S-matrix element that contribute to the photon + jet production at NEik accuracy presented in chapter 5.

Let us focus first on the terms that contain the L^+ explicitly in Eqs. (5.16), (5.24) and the contribution from the inside term with γ^k .

$$\begin{aligned}
& (-i)e e_f \epsilon_k^\lambda (p_2)^* (\mathbf{1})_{\beta\alpha_0} \int d^2\mathbf{v} e^{-i\mathbf{v}\cdot(\mathbf{p}_1+\mathbf{p}_2-\mathbf{p}_0)} \bar{u}(1) \left[\left(2\pi\delta(p_1^+ - p_0^+ + p_2^+) \left(-\frac{L^+}{2} \right) \right. \right. \\
& \left. \left. + 2\pi\delta(p_1^+ + p_2^+ - p_0^+) \left(-\frac{L^+}{2} \right) \right) \mathcal{U}_F\left(\frac{L^+}{2}, -\frac{L^+}{2}; \mathbf{v}\right) \right. \\
& \left. + 2\pi\delta(p_1^+ + p_2^+ - p_0^+) \int_{-L^+/2}^{L^+/2} dv^+ \mathcal{U}_F\left(\frac{L^+}{2}, v^+; \mathbf{v}\right) \mathcal{U}_F\left(v^+, -\frac{L^+}{2}; \mathbf{v}\right) \right] \gamma^k u(0) \\
& = (-i)e e_f \epsilon_k^\lambda (p_2)^* (\mathbf{1})_{\beta\alpha_0} \int d^2\mathbf{v} e^{-i\mathbf{v}\cdot(\mathbf{p}_1+\mathbf{p}_2-\mathbf{p}_0)} 2\pi\delta(p_1^+ + p_2^+ - p_0^+) \bar{u}(1) \\
& \times \left[-\frac{L^+}{2} - \frac{L^+}{2} + L^+ \right] \mathcal{U}_F\left(\frac{L^+}{2}, -\frac{L^+}{2}; \mathbf{v}\right) \gamma^k u(0) = 0
\end{aligned} \tag{B.1}$$

We also rewrite

$$\begin{aligned}
\frac{1}{2(p_1^+ + p_2^+)} \left(\check{p}_1^- + \check{p}_2^- - \frac{(\mathbf{p}_1 + \mathbf{p}_2)^2 + m^2}{2(p_1^+ + p_2^+)} \right)^{-1} &= \frac{1}{\left(2(p_1^+ + p_2^+) \left(\frac{p_1^2 + m^2}{2p_1^+} + \frac{p_2^2}{2p_2^+} \right) - (\mathbf{p}_1 + \mathbf{p}_2)^2 - m^2 \right)} \\
&= \frac{1}{\left(\mathbf{p}_2^2 \left(\frac{p_1^+}{p_2^+} + 1 - 1 \right) - 2\mathbf{p}_1 \mathbf{p}_2 + \mathbf{p}_1^2 \left(1 + \frac{p_2^+}{p_1^+} - 1 \right) + m^2 \frac{p_2^+}{p_1^+} \right)} \\
&= \frac{1}{\left(\left(\mathbf{p}_2 \sqrt{\frac{p_1^+}{p_2^+}} - \mathbf{p}_1 \sqrt{\frac{p_2^+}{p_1^+}} \right)^2 + m^2 \frac{p_2^+}{p_1^+} \right)} \\
&= \frac{1}{\frac{p_1^+}{p_2^+} \left(\left(\mathbf{p}_2 - \mathbf{p}_1 \frac{p_2^+}{p_1^+} \right)^2 + m^2 \left(\frac{p_2^+}{p_1^+} \right)^2 \right)} = \bar{\Delta} \frac{p_2^+}{p_1^+}
\end{aligned} \tag{B.2}$$

and

$$\begin{aligned}
\frac{1}{2(p_0^+ - p_2^+)} \left(\check{p}_0^- - \check{p}_2^- - \frac{(\mathbf{p}_0 - \mathbf{p}_2)^2 + m^2}{2(p_0^+ - p_2^+)} \right)^{-1} &= \frac{1}{\left(2(p_0^+ - p_2^+) \left(\frac{p_0^2 + m^2}{2p_0^+} - \frac{p_2^2}{2p_2^+} \right) - (\mathbf{p}_0 - \mathbf{p}_2)^2 - m^2 \right)} \\
&= \frac{1}{\left(\mathbf{p}_2^2 \left(-\frac{p_0^+}{p_2^+} + 1 - 1 \right) + 2\mathbf{p}_0 \mathbf{p}_2 + \mathbf{p}_0^2 \left(1 - \frac{p_2^+}{p_0^+} - 1 \right) - m^2 \frac{p_2^+}{p_0^+} \right)} \\
&= \frac{1}{\left(-\left(\mathbf{p}_2 \sqrt{\frac{p_0^+}{p_2^+}} - \mathbf{p}_0 \sqrt{\frac{p_2^+}{p_0^+}} \right)^2 - m^2 \frac{p_2^+}{p_0^+} \right)} \\
&= \frac{1}{\frac{p_0^+}{p_2^+} \left(-\left(\mathbf{p}_2 - \mathbf{p}_0 \frac{p_2^+}{p_0^+} \right)^2 - m^2 \left(\frac{p_2^+}{p_0^+} \right)^2 \right)} = -\bar{\Delta}' \frac{p_2^+}{p_0^+}
\end{aligned} \tag{B.3}$$

Now taking into account the vanishing of the L^+ terms discussed before and the new expressions for $\bar{\Delta}$ and $\bar{\Delta}'$ we get the new S-matrix elements for the cases of splitting before and after the medium

$$\begin{aligned}
S'_{q_1 \gamma_2 \leftarrow q_0}{}^{\text{aft}} &= (-i) e e_f \epsilon_\lambda^k(p_2) (\mathbf{1})_{\alpha_1 \beta} \theta(p_1^+) \theta(p_0^+) \int d^2 \mathbf{v} e^{-i\mathbf{v} \cdot (\mathbf{p}_1 + \mathbf{p}_2 - \mathbf{p}_0)} \bar{u}(1) \left[i \bar{\Delta} \gamma^+ \right. \\
&\times \left(\left(p_2^l - \frac{p_2^+}{p_1^+} p_1^l \right) \left(2\delta^{kl} - \frac{p_2^+}{p_1^+} \gamma^l \gamma^k \right) - \left(\frac{p_2^+}{p_1^+} \right)^2 m \gamma^k \right) \\
&\times \left\{ \int dv^- e^{i v^- (p_1^+ + p_2^+ - p_0^+)} \mathcal{U}_F \left(\frac{L^+}{2}, -\frac{L^+}{2}; \mathbf{v}, v^- \right) + \frac{2\pi \delta(p_1^+ + p_2^+ - p_0^+)}{(2p_0^+)} \right. \\
&\times \int_{-\frac{L^+}{2}}^{\frac{L^+}{2}} dv^+ \mathcal{U}_F \left(\frac{L^+}{2}, v^+; \mathbf{v} \right) \left[\frac{[\gamma^i, \gamma^j]}{4} g t \cdot \mathcal{F}_{ij}(v) - \frac{(\mathbf{p}_0^j + \mathbf{p}_1^j + \mathbf{p}_2^j)}{2} \overleftrightarrow{\mathcal{D}}_{\mathbf{v}j} - i \overleftarrow{\mathcal{D}}_{\mathbf{v}j} \overrightarrow{\mathcal{D}}_{\mathbf{v}j} \right] \\
&\times \left. \mathcal{U}_F \left(v^+, -\frac{L^+}{2}; \mathbf{v} \right) \right\}_{\beta \alpha_0} - 2\pi \delta(p_1^+ + p_2^+ - p_0^+) \gamma^k i \overrightarrow{\partial}_{\mathbf{v}} \gamma^i \gamma^+ \frac{L^+}{2p_0^+} \frac{L^+}{2} \mathcal{U}_F \left(\frac{L^+}{2}, -\frac{L^+}{2}; \mathbf{v} \right) \left. \right] u(0)
\end{aligned} \tag{B.4}$$

and

$$\begin{aligned}
 S_{q_1 \gamma_2 \leftarrow q_0}^{\text{bef}} &= (-i)e e_f(\mathbf{1})_{\beta\alpha_0} \theta(p_0^+) \theta(p_1^+) \int d^2\mathbf{v} e^{-i\mathbf{v}\cdot(\mathbf{p}_1-\mathbf{p}_0+\mathbf{p}_2)} \bar{u}(1) \left[(-i\bar{\Delta}') \right. \\
 &\times \left\{ \int dv^- e^{iv^-(p_1^+-p_0^++p_2^+)} \mathcal{U}_F\left(\frac{L^+}{2}, -\frac{L^+}{2}; \mathbf{v}, v^-\right) + \frac{2\pi\delta(p_1^+-p_0^++p_2^+)}{2p_1^+} \right. \\
 &\times \int_{-\frac{L^+}{2}}^{\frac{L^+}{2}} dv^+ \mathcal{U}_F\left(\frac{L^+}{2}, v^+; \mathbf{v}\right) \left[\frac{[\gamma^i, \gamma^j]}{4} g^t \cdot \mathcal{F}_{ij}(v) - \frac{(\mathbf{p}_1^j + \mathbf{p}_0^j - \mathbf{p}_2^j)}{2} \overleftrightarrow{\mathcal{D}}_{\mathbf{v}^j} - i \overleftrightarrow{\mathcal{D}}_{\mathbf{v}^j} \overrightarrow{\mathcal{D}}_{\mathbf{v}^j} \right] \\
 &\times \mathcal{U}_F\left(v^+, -\frac{L^+}{2}; \mathbf{v}\right) \left. \right\} \epsilon_\lambda^k(p_2) \gamma^+ \left(\left(p_2^l - \frac{p_2^+}{p_0^+} p_0^l \right) \left(2\delta^{kl} - \frac{p_2^+}{p_0^+} \gamma^k \gamma^l \right) + \left(\frac{p_2^+}{p_0^+} \right)^2 m \gamma^k \right) \\
 &+ 2\pi\delta(p_1^+-p_0^++p_2^+) i \overrightarrow{\partial}_{\mathbf{v}} \frac{\gamma^+ \gamma^i}{2p_1^+} \gamma^k \frac{L^+}{2} \mathcal{U}_F\left(\frac{L^+}{2}, -\frac{L^+}{2}; \mathbf{v}\right) \left. \right] u(0) \tag{B.5}
 \end{aligned}$$

At this point we try to put together the terms that still contain the $L^+/2$ explicitly with the inside terms. One can thus change the inside terms as

$$\begin{aligned}
 &\int_{-L^+/2}^{L^+/2} dz^+ \int d^2\mathbf{z} e^{-i\mathbf{z}\cdot(\mathbf{p}_1+\mathbf{p}_2-\mathbf{p}_0)} \mathcal{U}_F\left(\frac{L^+}{2}, z^+; \mathbf{z}\right) \\
 &\times \left(-\frac{i\gamma^+ \gamma^i \gamma^k}{2p_1^+} \overleftarrow{\mathcal{D}}_{\mathbf{z}^i} + \frac{i\gamma^k \gamma^i \gamma^+}{2p_0^+} \overrightarrow{\mathcal{D}}_{\mathbf{z}^i} \right) \mathcal{U}_F\left(z^+, -\frac{L^+}{2}; \mathbf{z}\right) \\
 &= \int_{-L^+/2}^{L^+/2} dz^+ \int d^2\mathbf{z} e^{-i\mathbf{z}\cdot(\mathbf{p}_1+\mathbf{p}_2-\mathbf{p}_0)} \mathcal{U}_F\left(\frac{L^+}{2}, z^+; \mathbf{z}\right) \\
 &\times \left\{ -\frac{i\gamma^+ \gamma^i \gamma^k}{2p_1^+} \left[\frac{1}{2} (\overleftarrow{\mathcal{D}}_{\mathbf{z}^i} - \overrightarrow{\mathcal{D}}_{\mathbf{z}^i}) + \frac{1}{2} (\overleftarrow{\mathcal{D}}_{\mathbf{z}^i} + \overrightarrow{\mathcal{D}}_{\mathbf{z}^i}) \right] \right. \\
 &+ \left. \frac{i\gamma^k \gamma^i \gamma^+}{2p_0^+} \left[\frac{1}{2} (\overrightarrow{\mathcal{D}}_{\mathbf{z}^i} - \overleftarrow{\mathcal{D}}_{\mathbf{z}^i}) + \frac{1}{2} (\overrightarrow{\mathcal{D}}_{\mathbf{z}^i} + \overleftarrow{\mathcal{D}}_{\mathbf{z}^i}) \right] \right\} \mathcal{U}_F\left(z^+, -\frac{L^+}{2}; \mathbf{z}\right) \\
 &= \int_{-L^+/2}^{L^+/2} dz^+ \int d^2\mathbf{z} e^{-i\mathbf{z}\cdot(\mathbf{p}_1+\mathbf{p}_2-\mathbf{p}_0)} \left\{ \mathcal{U}_F\left(\frac{L^+}{2}, z^+; \mathbf{z}\right) \left[\frac{1}{2} \frac{i\gamma^+ \gamma^i \gamma^k}{2p_1^+} \overleftarrow{\mathcal{D}}_{\mathbf{z}^i} + \frac{1}{2} \frac{i\gamma^k \gamma^i \gamma^+}{2p_0^+} \overleftarrow{\mathcal{D}}_{\mathbf{z}^i} \right] \right. \\
 &\times \left. \mathcal{U}_F\left(z^+, -\frac{L^+}{2}; \mathbf{z}\right) - \frac{1}{2} \frac{i\gamma^+ \gamma^i \gamma^k}{2p_1^+} \overrightarrow{\partial}_{\mathbf{z}} \mathcal{U}_F\left(\frac{L^+}{2}, -\frac{L^+}{2}; \mathbf{z}\right) + \frac{1}{2} \frac{i\gamma^k \gamma^i \gamma^+}{2p_0^+} \overrightarrow{\partial}_{\mathbf{z}} \mathcal{U}_F\left(\frac{L^+}{2}, -\frac{L^+}{2}; \mathbf{z}\right) \right\} \\
 &= \int d^2\mathbf{z} e^{-i\mathbf{z}\cdot(\mathbf{p}_1+\mathbf{p}_2-\mathbf{p}_0)} \left\{ \int_{-L^+/2}^{L^+/2} dz^+ \mathcal{U}_F\left(\frac{L^+}{2}, z^+; \mathbf{z}\right) \left[\frac{1}{2} \frac{i\gamma^+ \gamma^i \gamma^k}{2p_1^+} \overleftarrow{\mathcal{D}}_{\mathbf{z}^i} + \frac{1}{2} \frac{i\gamma^k \gamma^i \gamma^+}{2p_0^+} \overleftarrow{\mathcal{D}}_{\mathbf{z}^i} \right] \right. \\
 &\times \left. \mathcal{U}_F\left(z^+, -\frac{L^+}{2}; \mathbf{z}\right) - \frac{L^+}{2} \frac{i\gamma^+ \gamma^i \gamma^k}{2p_1^+} \overrightarrow{\partial}_{\mathbf{z}} \mathcal{U}_F\left(\frac{L^+}{2}, -\frac{L^+}{2}; \mathbf{z}\right) + \frac{L^+}{2} \frac{i\gamma^k \gamma^i \gamma^+}{2p_0^+} \overrightarrow{\partial}_{\mathbf{z}} \mathcal{U}_F\left(\frac{L^+}{2}, -\frac{L^+}{2}; \mathbf{z}\right) \right\} \tag{B.6}
 \end{aligned}$$

so that in the full inside contribution is

$$\begin{aligned}
S'_{q_1 \gamma_2 \leftarrow q_0}{}^{\text{in}} &= (-i) e e_f \epsilon_{\lambda k} (p_2)^* \int d^2 \mathbf{z} 2\pi \delta(p_1^+ + p_2^+ - p_0^+) \theta(p_0^+) \theta(p_1^+) e^{-i\mathbf{z} \cdot (\mathbf{p}_1 + \mathbf{p}_2 - \mathbf{p}_0)} \bar{u}(1) \\
&\times \left\{ \int_{-L^+/2}^{L^+/2} dz^+ \mathcal{U}_F\left(\frac{L^+}{2}, z^+; \mathbf{z}\right) \left[\frac{1}{2} \frac{i\gamma^+ \gamma^i \gamma^k}{2p_1^+} \overleftrightarrow{\mathcal{D}}_{z^i} + \frac{1}{2} \frac{i\gamma^k \gamma^i \gamma^+}{2p_0^+} \overleftrightarrow{\mathcal{D}}_{z^i} \right] \mathcal{U}_F\left(z^+, -\frac{L^+}{2}; \mathbf{z}\right) \right. \\
&\left. - \frac{L^+}{2} \frac{i\gamma^+ \gamma^i \gamma^k}{2p_1^+} \overrightarrow{\partial}_z \mathcal{U}_F\left(\frac{L^+}{2}, -\frac{L^+}{2}; \mathbf{z}\right) + \frac{L^+}{2} \frac{i\gamma^k \gamma^i \gamma^+}{2p_0^+} \overrightarrow{\partial}_z \mathcal{U}_F\left(\frac{L^+}{2}, -\frac{L^+}{2}; \mathbf{z}\right) \right\} u(0)
\end{aligned} \tag{B.7}$$

now we can compare the last line of this inside contribution with the contributions with splitting before and after the medium, the explicit $L^+/2$ terms in the last lines of both Eqs.(B.4) and (B.5) and we see that they cancel exactly so we are left with the following three final contributions

$$\begin{aligned}
S'_{q_1 \gamma_2 \leftarrow q_0}{}^{\text{aft}} &= (-i) e e_f \epsilon_{\lambda}^k (p_2) (\mathbf{1})_{\alpha_1 \beta} \theta(p_1^+) \theta(p_0^+) \int d^2 \mathbf{v} e^{-i\mathbf{v} \cdot (\mathbf{p}_1 + \mathbf{p}_2 - \mathbf{p}_0)} \bar{u}(1) i \bar{\Delta} \gamma^+ \\
&\times \left(\left(p_2^l - \frac{p_2^+}{p_1^+} p_1^l \right) \left(2\delta^{kl} - \frac{p_2^+}{p_1^+} \gamma^l \gamma^k \right) - \left(\frac{p_2^+}{p_1^+} \right)^2 m \gamma^k \right) \\
&\times \left\{ \int dv^- e^{iv^-(p_1^+ + p_2^+ - p_0^+)} \mathcal{U}_F\left(\frac{L^+}{2}, -\frac{L^+}{2}; \mathbf{v}, v^-\right) + \frac{2\pi \delta(p_1^+ + p_2^+ - p_0^+)}{(2p_0^+)} \right. \\
&\times \int_{-\frac{L^+}{2}}^{\frac{L^+}{2}} dv^+ \mathcal{U}_F\left(\frac{L^+}{2}, v^+; \mathbf{v}\right) \left[\frac{[\gamma^i, \gamma^j]}{4} g t \cdot \mathcal{F}_{ij}(v) - \frac{(\mathbf{p}_0^j + \mathbf{p}_1^j + \mathbf{p}_2^j)}{2} \overleftrightarrow{\mathcal{D}}_{\mathbf{v}^j} - i \overleftrightarrow{\mathcal{D}}_{\mathbf{v}^j} \overrightarrow{\mathcal{D}}_{\mathbf{v}^j} \right] \\
&\left. \times \mathcal{U}_F\left(v^+, -\frac{L^+}{2}; \mathbf{v}\right) \right\}_{\beta \alpha_0} u(0)
\end{aligned} \tag{B.8}$$

$$\begin{aligned}
S'_{q_1 \gamma_2 \leftarrow q_0}{}^{\text{bef}} &= (-i) e e_f (\mathbf{1})_{\beta \alpha_0} \theta(p_0^+) \theta(p_1^+) \int d^2 \mathbf{v} e^{-i\mathbf{v} \cdot (\mathbf{p}_1 - \mathbf{p}_0 + \mathbf{p}_2)} \bar{u}(1) (-i \bar{\Delta}') \\
&\times \left\{ \int dv^- e^{iv^-(p_1^+ - p_0^+ + p_2^+)} \mathcal{U}_F\left(\frac{L^+}{2}, -\frac{L^+}{2}; \mathbf{v}, v^-\right) + \frac{2\pi \delta(p_1^+ - p_0^+ + p_2^+)}{2p_1^+} \right. \\
&\times \int_{-\frac{L^+}{2}}^{\frac{L^+}{2}} dv^+ \mathcal{U}_F\left(\frac{L^+}{2}, v^+; \mathbf{v}\right) \left[\frac{[\gamma^i, \gamma^j]}{4} g t \cdot \mathcal{F}_{ij}(v) - \frac{(\mathbf{p}_1^j + \mathbf{p}_0^j - \mathbf{p}_2^j)}{2} \overleftrightarrow{\mathcal{D}}_{\mathbf{v}^j} - i \overleftrightarrow{\mathcal{D}}_{\mathbf{v}^j} \overrightarrow{\mathcal{D}}_{\mathbf{v}^j} \right] \\
&\left. \times \mathcal{U}_F\left(v^+, -\frac{L^+}{2}; \mathbf{v}\right) \right\} \epsilon_{\lambda}^k (p_2) \gamma^+ \left(\left(p_2^l - \frac{p_2^+}{p_0^+} p_0^l \right) \left(2\delta^{kl} - \frac{p_2^+}{p_0^+} \gamma^k \gamma^l \right) + \left(\frac{p_2^+}{p_0^+} \right)^2 m \gamma^k \right) u(0)
\end{aligned} \tag{B.9}$$

and

$$\begin{aligned}
 S'_{q_1 \gamma_2 \leftarrow q_0}{}^{\text{in}} &= (-i) e e_f \epsilon_{\lambda k} (p_2)^* \int d^2 \mathbf{z} 2\pi \delta(p_1^+ + p_2^+ - p_0^+) \theta(p_0^+) \theta(p_1^+) e^{-i\mathbf{z} \cdot (\mathbf{p}_1 + \mathbf{p}_2 - \mathbf{p}_0)} \\
 &\times \bar{u}(1) \int_{-L^+/2}^{L^+/2} dz^+ \mathcal{U}_F \left(\frac{L^+}{2}, z^+; \mathbf{z} \right) \left[\frac{i\gamma^+ \gamma^i \gamma^k}{2p_1^+} + \frac{i\gamma^k \gamma^i \gamma^+}{2p_0^+} \right] \frac{1}{2} \overleftrightarrow{\mathcal{D}}_{\mathbf{z}} \mathcal{U}_F \left(z^+, \frac{-L^+}{2}; \mathbf{z} \right) u(0)
 \end{aligned} \tag{B.10}$$

the corresponding conjugate amplitudes read

$$\begin{aligned}
 \left(S_{q_1 \gamma_2 \leftarrow q_0}^{\text{LO-aft}} \right)^\dagger &= ie e_f \epsilon_{\lambda}^r (p_2) (\mathbf{1})_{\alpha_1 \beta} \theta(p_1^+) \theta(p_0^+) \int d^2 \mathbf{w} e^{i\mathbf{w} \cdot (\mathbf{p}_1 + \mathbf{p}_2 - \mathbf{p}_0)} \bar{u}(0) (-i) \bar{\Delta} \\
 &\times \left\{ \int dw^- e^{-iw^-(p_1^+ + p_2^+ - p_0^+)} \mathcal{U}_F^\dagger \left(\frac{L^+}{2}, -\frac{L^+}{2}; \mathbf{w}, w^- \right) + \frac{2\pi \delta(p_1^+ + p_2^+ - p_0^+)}{2p_0^+} \int_{-\frac{L^+}{2}}^{\frac{L^+}{2}} dw^+ \right. \\
 &\times \mathcal{U}_F^\dagger \left(w^+, -\frac{L^+}{2}; \mathbf{w} \right) \left[\frac{[\gamma^n, \gamma^m]}{4} g t \cdot \mathcal{F}_{mn}(w) + \frac{(\mathbf{p}_0^n + \mathbf{p}_1^n + \mathbf{p}_2^n)}{2} \overleftrightarrow{\mathcal{D}}_{\mathbf{w}^n} + i \overleftarrow{\mathcal{D}}_{\mathbf{w}^n} \overrightarrow{\mathcal{D}}_{\mathbf{w}^n} \right] \\
 &\times \left. \mathcal{U}_F^\dagger \left(\frac{L^+}{2}, w^+; \mathbf{w} \right) \right\}_{\beta \alpha_0} \left(\left(p_2^s - \frac{p_2^+}{p_1^+} p_1^s \right) \left(2\delta^{rs} - \frac{p_2^+}{p_1^+} \gamma^r \gamma^s \right) - \left(\frac{p_2^+}{p_1^+} \right)^2 m \gamma^r \right) \gamma^+ u(1)
 \end{aligned} \tag{B.11}$$

$$\begin{aligned}
 \left(S_{q_1 \gamma_2 \leftarrow q_0}^{\text{LO-bef}} \right)^\dagger &= ie e_f \epsilon_{\lambda}^r (p_2) (\mathbf{1})_{\beta \alpha_0} \theta(p_0^+) \theta(p_1^+) \int d^2 \mathbf{w} e^{i\mathbf{w} \cdot (\mathbf{p}_1 - \mathbf{p}_0 + \mathbf{p}_2)} \bar{u}(0) i \bar{\Delta}' \\
 &\times \left(\left(p_2^s - \frac{p_2^+}{p_0^+} p_0^s \right) \left(2\delta^{rs} - \frac{p_2^+}{p_0^+} \gamma^r \gamma^s \right) + \left(\frac{p_2^+}{p_0^+} \right)^2 m \gamma^r \right) \gamma^+ \left\{ \right. \\
 &\times \int dw^- e^{-iw^-(p_1^+ - p_0^+ + p_2^+)} \mathcal{U}_F^\dagger \left(\frac{L^+}{2}, -\frac{L^+}{2}; \mathbf{w}, w^- \right) + \frac{2\pi \delta(p_1^+ - p_0^+ + p_2^+)}{2p_1^+} \\
 &\times \int_{-\frac{L^+}{2}}^{\frac{L^+}{2}} dw^+ \mathcal{U}_F^\dagger \left(w^+, -\frac{L^+}{2}; \mathbf{w} \right), \left[\frac{[\gamma^n, \gamma^m]}{4} g t \cdot \mathcal{F}_{mn}(w) + \frac{(\mathbf{p}_1^n + \mathbf{p}_0^n - \mathbf{p}_2^n)}{2} \overleftrightarrow{\mathcal{D}}_{\mathbf{w}^n} + i \overleftarrow{\mathcal{D}}_{\mathbf{w}^n} \overrightarrow{\mathcal{D}}_{\mathbf{w}^n} \right] \\
 &\times \left. \mathcal{U}_F^\dagger \left(\frac{L^+}{2}, w^+; \mathbf{w} \right) \right\} u(1)
 \end{aligned} \tag{B.12}$$

and

$$\begin{aligned}
 \left(S'_{q_1 \gamma_2 \leftarrow q_0}{}^{\text{LO-in}} \right)^\dagger &= ie e_f \epsilon_{\lambda r} (p_2) \int d^2 \mathbf{v} 2\pi \delta(p_1^+ + p_2^+ - p_0^+) \theta(p_0^+) \theta(p_1^+) e^{i\mathbf{v} \cdot (\mathbf{p}_1 + \mathbf{p}_2 - \mathbf{p}_0)} \bar{u}(0) \\
 &\times \int_{-L^+/2}^{L^+/2} dv^+ \mathcal{U}_F^\dagger \left(v^+, \frac{-L^+}{2}; \mathbf{v} \right) \left[\frac{i\gamma^r \gamma^l \gamma^+}{2p_1^+} + \frac{i\gamma^+ \gamma^l \gamma^r}{2p_0^+} \right] \mathcal{U}_F^\dagger \left(\frac{L^+}{2}, v^+; \mathbf{v} \right) \frac{1}{2} \overleftrightarrow{\mathcal{D}}_{\mathbf{v}^l} u(1)
 \end{aligned} \tag{B.13}$$